Aerobic Granulation in Sequencing Batch Reactors for Treating Wastewater Laden with Phenol, Thiocyanate, Ammonium and Nitrogenous Heterocyclic Compounds

A Thesis

Submitted in partial fulfilment of the requirements

for the degree of

Doctor of Philosophy

by

Sachin Kumar Tomar

Department of Civil Engineering
Indian Institute of Technology Guwahati
Guwahati-781039, Assam, India

August, 2020

"Family is a life jacket in the stormy sea of life."

J. K. Rowling (1965-)
British novelist

Dedicated
to
My Family

भारतीय प्रौद्योगिकी संस्थान गुवाहाटी
INDIAN INSTITUTE OF TECHNOLOGY GUWAHATI
DEPARTMENT OF CIVIL ENGINEERING

Statement

I hereby declare that the work embodied in this thesis entitled **Aerobic Granulation in Sequencing Batch Reactors for Treating Wastewater Laden with Phenol, Thiocyanate, Ammonium and Nitrogenous Heterocyclic Compounds** carried out by me in the Department of Civil Engineering, Indian Institute of Technology Guwahati, Assam, India, under the supervision of **Prof. Saswati Chakraborty**. Wherever I have consulted the research findings of others in the creation of this work, I have given due credit by citing them in the text of the thesis and giving their details in the references.

Date : August 20, 2020
Place: Guwahati

Sachin Kumar Tomar
Roll No.11610419
Department of Civil Engineering
Indian Institute of Technology Guwahati
Guwahati - 781039, Assam, India

भारतीय प्रौद्योगिकी संस्थान गुवाहाटी
INDIAN INSTITUTE OF TECHNOLOGY GUWAHATI
DEPARTMENT OF CIVIL ENGINEERING

Certificate

This is to certify that work described in this thesis entitled **Aerobic Granulation in Sequencing Batch Reactors for Treating Wastewater Laden with Phenol, Thiocyanate, Ammonium and Nitrogenous Heterocyclic Compounds** by **Sachin Kumar Tomar** (Roll No. 11610419) is an authentic record of the results obtained from the research work carried out under my supervision in the Department of Civil Engineering, Indian Institute of Technology Guwahati, Assam, India. I certify that he has fulfilled all the requirements according to the rules of this institute regarding the investigations embodied in his thesis and this work has not been submitted elsewhere for a degree.

24/08/20

Date : August 20, 2020
Place: Guwahati

Dr. Saswati Chakraborty
Professor
Department of Civil Engineering
Indian Institute of Technology Guwahati
Guwahati - 781039, Assam, India

Acknowledgements

As the time draws near to bid adieu to the beautiful campus of **Indian Institute of Technology Guwahati**, this is a righteous opportunity to mention the name of those wonderful and supportive persons, who have shown me the right path and made conspicuous contributions for the completion of my research work. Without these supporters, I may not have gotten to where I am today, at least not sanely.

Words in my lexicon, fail to elucidate my profound sense of veneration and indebtedness to my thesis supervisor, **Prof. Saswati Chakraborty**, for her excellent guidance throughout my research work. Her kindness, dedication, hard work, patience and attention to minute details have been a great inspiration to me. Her deep knowledge of the subjects is commendable and guidance on the moral principles of high quality research is exemplary. Her competence to deal with difficult situations is tremendous and always have helped me to tackle complicated situations. Her commitment and diligent encouragement during each phase of the research work have been truly admirable. She has always motivated me to be an independent thinker and contemplate the logics that lead to reasons, which is the biggest takeaway of her supervision.

I express my sincere gratitude to the Chairman of my Doctoral Committee, **Prof. Mohammad Jawed**, and the members of my Doctoral Committee, **Prof. Sharad Gokhale** and **Prof. Animesh Kr. Golder**, for their valuable time and insightful suggestions provided at various stages of my study to improve the quality of my research work. I owe my thanks to **Prof. Pranab K. Ghosh**, **Prof. Ajay Kalamdhad**, **Prof. Chandan Mahanta** and **Prof. Mohammad Jawed** for delivering the in-depth knowledge of the subjects taught by them during my Ph.D. course work. I also express my sincere thanks to the current head, **Prof. Chandan Mahanta** and former heads, **Prof. Sajal K. Deb**, **Prof. Arup Kumar Sarma** and **Prof. Subashisa Dutta** of Department of Civil Engineering, IIT Guwahati, for providing the necessary facilities. I am also grateful to the current Lab Incharge, **Prof. Pranab Kumar Ghosh** and former Lab Incharges, **Prof. Ajay Kalamdhad** and **Dr. Sri Harsha Kota** of Environmental Engineering Laboratory of Department of Civil Engineering, IIT Guwahati, for their constant support and help and for providing me all the necessary facilities for the advance research.

I would like to thank **Dr. Nitin Chaudhary**, Department of Biosciences and Bioengineering, IIT Guwahati, for all the concern, valuable advice, and encouragement.

I sincerely want to express my regards for my doctors (not academician), **Dr. Debashish Chowdhury**, **Dr. N. P. Singh** and **Dr. Rohit Kamboj**, without their medical prescription and personal support I could not have been able to complete my Ph.D. I gratefully acknowledge the unstinted help provided by **Ms. Jonali Saikia**, **Mr. Payodhar Pathak** and **Mr. Chitta Ranjan Medhi** during all phases of my research work. I extend my thanks to former and current office staff members of Department of Civil Engineering, IIT Guwahati, **Mr. Rajib L. Gogoi**, **Mr. Kumud Deka**, **Mr. Dipak Deka**, **Mr. Hemota Patir**, **Mr. Susant Kumar Sarma**, **Ms. Juri J. Hazarika**, **Mr. Bhrigu Kalita** and **Mr. Soroj Patowary**, for their kind co-operation in smooth and rapid execution of office related works.

I am thankful to **Central Instruments Facility** and **Centre for the Environment**, IIT Guwahati for the allowance of sample analysis to accomplish my Ph.D. thesis objectives. I also wish to

acknowledge the **Ministry of Human Resource Development, India** for providing me the fellowship for pursuing my Ph.D.

I am very much grateful to **Ms. Monika Das**, **Ms. Gayatri Laskar**, **Mr. P. K. Saloi**, **Mr. Shekhar Shakya, Mr. Hasim Ahamad**, and **Mr. Shah Alam Siddique** of Indian Oil Corporation Limited, Guwahati and **Mr. Girish Chandra** of Master India Brewing Company, Guwahati for providing me sludge to carry out my research work. I am also thankful to **Dr. Bula Choudhury** for helping me in CLSM analysis.

I wish to thank **Mr. Soumya Ranjan Sahoo** for smooth running and repairing of ion chromatography on time, **Mr. Dipak Sarkar** for being available every time for servicing and repairing the general instruments and **Mr. Amit Thakur** for providing me chemicals and reagents on a phone call itself.

Its a great pleasure for me to acknowledge **Mr. Tapan Das** and **Mr. Tinku Biswas** for maintaining cleanliness in the lab and near my work place.

I wish to put on record my gratitude to the Editors and Reviewers of all my manuscripts published in the respective Journals and Conference proceedings for their valuable comments on upgrading my research study.

In the flow of my research life, I came across certain people who got adhered to my life as best mates with whom I could share my feelings, thoughts, ups, downs and research ideas.

My vocabulary utterly fails to express my extended thanks to **Mr. Rajneesh Kumar** for being a pillar of my strength and for his support, concern, respect and encouragement as a junior, friend and younger brother.

I would like to extend my sincere thanks to **Mr. Rajhans Negi, Mr. Girish Vyas, Mr. Barun Kanoo, Mr. Ankit soni** and **Mr. Vishnu Kumar** for unconditional support and respect you all gave to me as an elder brother. I will always cherish the group tea at 10.30 am and 4.30 pm that I used to have with **Mr. Rajneesh Kumar, Mr. Rajhans Negi,** and **Mr. Girish Vyas** as core members. I really appreciate the time you all spent with me in this campus.

I am very much indebted to my seniors, **Dr. Biju Prava Sahariah, Dr. Bharati Brahmacharimayum and Dr. Ravindra Patil** for the help during my initial phase of this research work. I take this opportunity to thank my lab group members, **Dr. Subrat Kumar Mallick, Dr. Praisy Terangpi, Ms. Sayanti Ghosh, Ms. Jinat Aktar** and **Ms. Shweta Singh** for their selfless love, care and support during my research work and for making congenital atmosphere in the lab for working.

My deepest thanks to my friends, **Dr. Susant Kumar Padhi, Dr. V. Sudharsan Varma, Dr. K. Dhamodharan, Dr. Veluchamy C., Mr. Laveti N V Satish, Dr. Lalit Goswami, Dr. Vihangraj Vijaykumar Kulkarni, Dr. Kunwar Raghvendra Singh, Ms. Juna Probha Devi, Ms. Payal Mazumder** and **Mr. Chandrabhanu Gupt** to whom I met during my Ph.D. for their pleasant company, friendship, uncountable suggestions and unconditional help all through the study.

My unlimited thanks to **Dr. Jiwan Singh, Dr. Mothe Gopi Kiran, Ms. Ruchira Bajpai, Dr. Isha Vishan, Mr. Ravi Prasad, Dr. Ranganadha Gopalarao, Dr. Vanaparthi Satheesh, Dr. Pritam Kumar Dikshit, Dr. Arti Choudhary, Dr. Nongthombam Premananda Singh, Ms. Mitali Sahu, Dr. Gaurav Goel, Dr. Sandip Sathe, Dr. Rakhee Das, Dr. Rajya Lakshmi Garaga, Dr. Mayur Shirish**

Jain and **Dr. Nilesh Agarchand Patil** for their help and support throughout my research.

Its a pleasure to thank **Mr. Prashant Thaker** and **Mr. Nitin Pandey** for helping me during my Ph.D. course work.

I appreciate the help and support rendered by my juniors, **Mr. Ankit Pratim Goswami, Mr. Siddhant Dash, Mr. Sanjeeb Das, Ms. Leichombam Menan Devi, Ms. Deepa Sachan, Mr. Kiran C. Babu, Mr. Gajala Rajshekar, Mr. Chakka Nagendra Subrahmanyam, Mr. M. Krishna Chaitanya, Mr. Sanjib Das, Mr. Smitom Swapna Borah, Mr. Siddhartha Paul, Mr. Anirban Das** and **Mr. Subhradip Pal** during my research work.

I am very pleased to thank **Mr. Ajeet Kumar, Dr. D Narendra Naik, Mr. Bibhas Kumar Bhunia** and **Mr. Jibrail Ali** for helping me in completing different aspects of my research work. Special thanks to **Mr. Upendra Reddy, Mr. Virendra Kumar Gautam**, **Dr. Shyam Trivedi** and **Mr. Rakesh Jana** for helping me in Latex format of thesis writing.

I register my deep sense of modest regards and thankfulness to **Mr. Babu Ram** because without your support My Ph.D. admission would not have possible.

I would specially like to thank my life-long friends, **Mr. Ravi Kumar, Mr. Krishan Kumar, Mr. Himanshu Chauhan, Dr. Avadh Kumar, Mr. Sumit Kumar, Major Deepanshu Chaudhary, Mr. Pranjal Rai, Mr. Manish Kumar, Mr. Ankur Garg, Mr. Sachin Chauhan, Mr. Deep Sagar Tyagi, Mr. Ashish Raj Seth, Mr. Sanjay Pandey, Mr. Priyanshu Rathi, Dr. Arvind Kumar Shakya, Dr. Nitin kumar, Mr. Anuj Srivastav, Mr. Vipin Kumar, Mrs. Smriti Vats, Dr. Sonam Chawla, Dr. Navodita Jain, Dr. Neha Tyagi, Mr. Vivek Tiwari, Mr. Prem Chand, Mr. Piyush Ratan Sharma** and **Mr. Gurmeet** for being my side unconditionally with immense love and support. They have always helped me in all aspects and stayed with me through thick and thin. I consider myself fortune to have such a helpful and genuine friends.

I take this opportunity to thank my college seniors, **Dr. Sharad Verma, Dr. Dinesh Poswal, Mr. Kavinder Dahiya** and **Mr. Raman Sharma**. They have always encouraged me and have always been supportive.

A deep reverence and warm appreciation goes to my **Mummy, Papa, Bhaiya, Bhabhi** and **Guddu Mama** as well as my family members for their blessings, endless love, unending support and understanding throughout my studies. I am thankful to my two little gems, **Meethi** and **Golu**, for making me feel happy by their innocent and cute activities and bringing smile on my face in every situation.

I will forever be thankful to all those people unnamed for their moral support and those who helped me directly or indirectly in stepping me forward through the completion of my Ph.D. work.

Above all, I owe it all to **Almighty God** for granting me the wisdom, health and strength to undertake this research task and enabling me to its completion.

Date : August 20, 2020

Sachin Kumar Tomar

Abstract

Aerobic granular sludge (AGS) technology is developed in the last two decades for the treatment of wastewater. Aerobic granules are the self-immobilized microorganism which do not require any supporting material to grow and many operational factors and feed characteristics affect the granulation process. Because of having unique properties like high settling behavior, compact structure and ability to withstand high and toxic loading, AGS has been used in the treatment of various kinds of domestic and industrial wastewater. Phenol, thiocyanate (SCN^-), ammonia-nitrogen (NH_4^+-N), pyridine and indole found in many industrial wastewater, such as coal gasification, coke oven and petrochemical industries, requiring an economic and sustainable treatment technology before being disposed to surface water bodies. In this research work, aerobic granules were developed by optimizing operational parameters like cycle time and air flow rate for the treatment of multiple toxic pollutants in sequencing batch reactors (SBRs) and their effects on aerobic granulation along with SBR performance were also evaluated.

The first aim of the current research work was to optimize the cycle time followed by the air flow rate for aerobic granulation using toxic phenol as a carbon source along with SCN^- and NH_4^+-N. For cycle time study, synthetic wastewater containing phenol (400 mg L^{-1}), SCN^- (100 mg L^{-1}) and NH_4^+-N (100 mg L^{-1}) was treated in the three SBRs at different cycle times of 6 h (R1), 12 h (R2) and 24 h (R3) with an air flow rate of 2.0 L min^{-1}. Granule size, biomass concentration and extracellular polymeric substances (EPS) in sludge were inversely related to the cycle time. At a cycle time of 6 h, mean biomass size (D50) and volatile suspended solids (VSS) were 1334.24±30.56 μm and 4.31±0.40 g L^{-1}, as compared to D50 value of 97.93±4.21 μm and 2.28±0.13 g L^{-1} VSS with 24 h cycle time. Sludge EPS in R1 was two-fold more than R3. Pollutant removal performance was independent of cycle time with 94-96% removal of chemical oxygen demand (COD) and 99% removals of phenol, SCN^-, and NH_4^+-N. Up-flow liquid velocity of 2.5 m h^{-1} was found appropriate for better granulation. Subsequently, the impact of the air flow rate on aerobic granulation was evaluated with same synthetic wastewater composition as was with the cycle time study by operating three lab scale SBRs at a cycle time of 6 h with different air flow rates 1.5 (R1), 2.5 (R2) and 3.5 L min^{-1} (R3). Larger granules (average size of 2938.67±64.91 μm) with higher biomass concentration (VSS of 4.17±0.09 g L^{-1}) were observed at optimal air flow rate of 2.5 L min^{-1} (R2). In R2, partial nitrification was achieved. Phenol was completely removed in all the reactors while partial removal of SCN^- and no nitrification were observed with a decrease (1.5 L min^{-1}) and an increase (3.5 L min^{-1}) in air flow rates (R1 and R3, respectively). Granules showed good characteristics and pollutant removal performances at the air flow rates of 2.0 L min^{-1} (cycle time study) and 2.5 L min^{-1} (air flow rate study), therefore an economic air flow rate of 2.0 L min^{-1} with a cycle time of 6 h was opted for rest of the research work.

Furthermore, the investigation on rapid granulation seeded with the refinery sludge with two different substrates (400 mg L^{-1} phenol in R1 and 1220 mg L^{-1} of sodium acetate in R2 to maintain similar COD of around 990 mg L^{-1}) along with 100 mg L^{-1} of NH_4^+-N was carried out in two different SBRs. Faster granulation in just 40 days was observed in R1 because of being operated with phenol to which refinery sludge was already exposed, whereas granules took a longer time to develop in R2 (50 days). Better granular characteristics were observed in R1 with larger granule size (D50 value

of 1123.60±113.55 μm) and higher EPS content (77.26±1.13 mg $gVSS^{-1}$). 94% COD removal was noticed in R1 as compared to 91% in R2. NH_4^+-N was almost completely transformed to nitrite-nitrogen in both of the SBRs. After 75 days of stable operation, granules started to break down in R1, therefore the impact of toxic SCN^- on granule reformation was evaluated in R1. Reformation of disintegrated granules was observed after gradual addition of SCN^- (10-340 mg L^{-1}) with the granules having larger size (1819.87±43.44 μm) and higher EPS (101.45±1.06 mg $gVSS^{-1}$) along with the recovery of nitritation efficiency. A signification impact was observed in granule characteristics because of microbial aggregation caused by sticky EPS secretion. It was found that SCN^- played an important role in the granule reformulation by provoking the secretion of EPS, a very high binding capacity substance.

In addition, two SBRs with two different kinds of industrial sludge; refinery sludge (R1) and brewery sludge (R2), were operated to observe the impact of high loading of phenol (5.71 kg COD m^{-3} day^{-1}) along with SCN^- (100 mg L^{-1}) and NH_4^+-N (100 mg L^{-1}) on the stability and performance of AGS. R2 granules were stable at an organic loading rate (OLR) of 5.71 kg COD m^{-3} day^{-1}, whereas the granules of R1 started to disintegrate at an OLR of more than 3.32 kg COD m^{-3} day^{-1}. At an OLR of 5.71 kg COD m^{-3} day^{-1}, almost complete removal of phenol, SCN^- and NH_4^+-N were observed in R2 while in R1, no removal was observed. Pollutant tolerance limit of AGS developed from brewery sludge (R2) was higher despite of long start-up period of 50 days. In addition, more active biomass was observed in R2 than R1 confirmed through the higher biomass activity values of 16.35 and 3.43 mg COD removed $mgVSS^{-1}$ day^{-1}, respectively, at higher load and also supported through CLSM analysis.

Afterward, the potential of AGS for simultaneous biodegradation of two nitrogenous heterocyclic compounds (NHCs), i.e., pyridine and indole, and NH_4^+-N along with phenol and SCN^- was investigated in three SBRs. R1 and R2 were operated with pyridine and indole, respectively, whereas R3 was operated with a mixture of an equimolar concentrations of pyridine and indole. Pyridine did not show any inhibitory effect on characteristics of aerobic granules up to a concentration of 5.0 mM with the removal efficiency of around 74% and >98% for other pollutants (phenol, SCN^- and NH_4^+-N) in R1. However, Indole was having a profound adverse impact on the granular characteristics and other pollutants removal with a concentration of more than 1.0 mM individually as well as when combined with pyridine in reactor R2 and R3, respectively.

Keywords: Aerobic granular sludge, Cycle time, Air flow rate, Rapid cultivation, Reformation, Nitrogenous Heterocyclic compounds.

Contents

List of Figures

List of Tables

List of Abbreviations

Syntax	Abbreviation
AFR	Air flow rate
AGR	Aerobic granular reactor
AGS	Aerobic granular sludge
AHLs	N-acyl homoserine lactones
AOB	Ammonia-oxidizing bacteria
AR	Analytical grade
BPA	Bisphenol A
BSA	Bovine serum albumin
BWTP	Beer wastewater treatment plant
CLSM	Confocal laser scanning microscopy
COD	Chemical oxygen demand
Con A	Concanavalin A
CPCB	Central Pollution Control Board
CSTR	Continuous stirred tank reactor
DGGE	Denaturing gradient gel electrophoresis
DO	Dissolved oxygen
DWRR	Domestic water resource recovery
EPS	Extracellular polymeric substances
FA	Free ammonia
F/M ratio	Food to microorganism ratio
FESEM	Field emission scanning electron microscope
FISH	Fluorescence in situ hybridization
FITC	Fluorescein isothiocyanate
FNA	Free nitrous acid
GAC	Granular activated carbon
GBA	Granular biomass activity
GSV	Granule settling velocity
HPLC	High performance liquid chromatography
HRT	Hydraulic retention time
IC	Integrity coefficient/Ion chromatography
IOCL	Indian Oil Corporation Limited
IWA	International Water Association
LDH	Layered double hydroxide
LPSA	Laser particle size analyser
LR	Laboratory grade
MAS	Municipal activated sludge
MLVSS	Mixed liquor volatile suspended solids
mM	Millimolar
MWTP	Municipal wastewater treatment plant
NHC	Nitrogenous heterocyclic compounds
NLR	Nitrogen loading rate
NOB	Nitrite-oxidizing bacteria
NPs	Nanoparticles
OLR	Organic loading rate
OUR	Oxygen uptake rate
PAC	Poly aluminum chloride

PBS	Phosphate buffered saline
PN	Proteins
POME	Palm oil mill effluent
PS	Polysaccharides
rpm	Revolution per minute
RWTP	Refinery wastewater treatment plant
SBR	Sequencing batch reactor
SEM	Scanning electron microscopy
SND	Simultaneous nitrification/denitrification
SRR	Solvent recovery raffinate
SRT	Solid retention time
SS	Suspended solids
STP	Sewage treatment plant
SUAV	Superficial upflow air velocity
SVI	Sludge volume index
TEM	Transmission electron microscopy
TN	Total nitrogen
TP	Total phosphorous
TOC	Total organic carbon
TSS	Total suspended solids
UASB	Upflow anaerobic sludge blanket
ULV	Up flow liquid velocity
USEPA	United States Environmental Protection Agency
VER	Volume exchange ratio
VSS	Volatile suspended solids
WTP	Wastewater treatment plant

List of Symbols

Symbol	Description
%	Percentage
μm	Micrometre
μM	Micromolar
μS	Microsiemens
cm	Centimetre
d	Day
D	Diameter
D50	Average granule size
g	Gram
h	Hour
H	Height
kg	Kilogram
L	Litre
m	Metre
mg	Milligram
nm	Nanometre
s	Second

There is nothing more difficult to take in hand, more perilous to conduct, or more uncertain in its success, than to take the lead in the introduction of a new order of things.

Niccolo Machiavelli (1469-1527)
Italian writer

1

Introduction and Literature Review

This chapter contains a brief discussion about aerobic granulation and describes the extensive literature survey on aerobic granular sludge (AGS) including properties, advantages over conventional activated sludge process, factors affecting and problems associated with AGS, and its application in wastewater treatment technology. This chapter also focuses on the type of wastewater and pollutants used in the current research along with the objectives of current study based on lacunae in the literature.

1.1 Introduction

The economic and satisfactory treatments of industrial wastewater like from coal gasification, coking plants, petrochemicals and pharmaceuticals, etc., are a great challenge since they are comprised of complex matter having several toxic organic compounds (like aromatic compounds), nitrogenous heterocyclic compounds (NHCs), inorganic compounds and ammonia (Ramos et al., 2016b). The complex and toxic matters can be treated using biological process which is cost-effective, safe and more efficient when compared to physicochemical processes, which are expensive and generate toxic byproducts (Rajasulochana and Preethy, 2016; Zhu et al., 2018). Nevertheless, the aromatic compounds can cause inhibition to the biological processes (Al Khalid and El Naas, 2012). Phenol is accompanied with other toxic and inhibitory compounds like NHCs, thiocyanate (SCN^-) and ammonia-nitrogen (NH_4^+-N) in coal processing wastewater (Li et al., 2011a; Wei et al., 2012a). High levels of SCN^- and NH_4^+-N cause toxicity to the aquatic species and vertebrates (Li et al., 2011a). In addition, NHCs such as pyridine and indole impart an adverse effect on human health and ecosystem because of being toxic, mutagenic and carcinogenic in nature (Shi et al., 2019). Therefore, the treatment of complex toxic wastewater is required before being discharged to the surface water bodies.

The possibility of inhibition phenomenon among the pollutants might have difficulties in removing multiple pollutants concurrently. In wastewater treatment system, removal of ammonia by nitrification step is always considered as the rate-limiting step due to the very slow growth rate of nitrifying bacteria which are very susceptible to several factors like inhibition by aromatic compounds (Ramos et al., 2016a). For example, phenol and SCN^- inhibit the nitrification when present with the NH_4^+-N (Kim et al., 2008). In order to achieve removal of all pollutants and to overcome the toxicity on nitrification, multiple reactor systems are sometimes used, consisting of anoxic-aerobic-anoxic, anaerobic-anoxic-aerobic, etc., which makes treatment system highly cumbersome (Sahariah and Chakraborty, 2011; Zhao et al., 2009). The wastewater treatment system will be highly compact and space-saving, if removal of all pollutants can be achieved in a single reactor. Li et al. (2011a) and Vázquez et al. (2006) adopted a single sludge system with high hydraulic retention time (HRT)

for achieving simultaneous biodegradation/bioconversion of organic and nitrogenous compounds. Organic and inorganic contaminants removal from the industrial wastewater is a complex process and requires an effective treatment technology for removing all the pollutants simultaneously in a shorter time.

Aerobic granulation, a modification of a conventional activated sludge system, has been emerged as a novel technology for treating toxic wastewater using sequencing batch reactors (SBRs). Conventional activated sludge system requires a large surface area during construction because of the necessity of a large settling tank and also retain only lower biomass concentration. The major limitations associated with the conventional activated sludge are the generation of surplus sludge, low volumetric conversion efficiency, sensitivity towards fluctuation in loading. On the other hand, AGS technology does not need any additional settling tank, thus reducing area requirement, eventually reducing the cost of installation and can also retain abundant biomass (Sengar et al., 2018). Aerobic granules are the self-immobilized microbial aggregates which can retain high biomass and possess a regular, denser and stronger microbial structure having good settling property along with the ability to tolerate toxic and high organic loading as compared to conventional activated sludge process (Marques et al., 2013; Tay et al., 2005). Because of above addressed unique properties, AGS has been adopted to treat high loading wastewater containing toxic organics, nitrogen and phosphorous (Corsino et al., 2018; Hamza et al., 2019; Liu et al., 2011). Many factors such as substrate loading, substrate and inoculum type and operational parameters like cycle time, settling time, feeding strategy, feast-famine regime, aeration intensity, etc., affect aerobic granulation (Corsino et al., 2017; Lee et al., 2010).

In the present study, treatment of wastewater containing phenol, SCN^-, NH_4^+-N, pyridine and indole by AGS was studied. The effect of operational parameters and substrate loading along with rapid granulation was also observed.

1.2 Organization of the thesis

This thesis is organized into six chapters. The ongoing **Chapter 1** presents a brief background about the aerobic granulation, widespread scientific findings, lacunae in the literature and objectives of the current research work. **Chapter 2** describes the selection of operational parameters like cycle time and air flow rate for the development of aerobic granules from the multiple toxic pollutants. **Chapter 3** deals with the selection of an appropriate substrate for achieving rapid granulation and also describes the reformation of aerobic granules from the disintegrated one. Tolerance of aerobic granules for high phenol loading is explained in **Chapter 4**. **Chapter 5** focuses on the potential of aerobic granules for concurrent treatment of aromatic (phenol), inorganics (SCN^- and NH_4^+-N) and NHCs (pyridine and indole). **Chapter 6** summarizes the key findings from the current study and also provides some useful recommendations for future research in the field of AGS technology.

1.3 Literature background

1.3.1 History of aerobic granulation

Around a hundred years ago, activated sludge process, a revolutionary wastewater treatment technology, changed the scenario of treatment methods by providing highly efficient biological degradation (Jenkins and Wanner, 2014). Biomass-water separation is a crucial factor in governing the overall operation of the activated sludge process. Therefore, most of the research focused on the separation techniques for activated sludge by improving settling characteristics through the

aggregation of cells (Li and Yang, 2007). Biogranules are compact bacterial aggregates developed by self-immobilization without any supporting material containing millions of organisms per gram of biomass and have good settleability. These biogranules can be aerobic as well as anaerobic (Liu and Tay, 2004).

Anaerobic granules have been globally recognized and were first observed in the upflow anaerobic sludge blanket (UASB) reactor for treating industrial wastewater during late 1970s (Lettinga et al., 1980). Anaerobic granules with relatively high density settled at a faster rate resulting in treated effluent separation from biomass and have demonstrated a potential for efficient high-strength wastewater treatment as well (Liu and Tay, 2004). Long start-up time, relatively high operating temperature, sensitivity for hydraulic and organic loading, incompatibility towards low-strength wastewater and unsuitability in removing nitrogen and phosphorous from wastewater were the major limitations of the anaerobic granulation (Liu and Tay, 2004). To overcome the problems associated with the anaerobic granulation, aerobic granules were developed opening into an interesting arena of research for environmentalists.

Mishima and Nakamura developed the first aerobic granules in the aerobic sludge blanket reactor in 1991 (Mishima and Nakamura, 1991). The aerobic granule formation and its applications using a sequencing batch reactor (SBR) were addressed by Morgenroth et al. (1997) in late 1990s, while the first patent was granted to Heijnen and van Loosdrecht in 1998 (Heijnen and van Loosdrecht, 1998). From the year 2000 onwards, research has been extensively focused on aerobic granulation globally and in last two decades, AGS technology has been regarded as an encouraging technology for wastewater treatment. International Water Association (IWA) clearly defined AGS during the first workshop on AGS at the Technical University of Munich (Germany) in 2004 as *Granules making up aerobic granular activated sludge are to be understood as aggregates of microbial origin, which do not coagulate under reduced hydrodynamic shear, and which settle significantly faster than activated sludge flocs* (de Kreuk et al., 2007).

1.3.2 Formation of aerobic granules

Aerobic granulation is a progressive development resulting from fluffy flocs to compact granules without any supporting materials with a minimum size of 0.2 mm (de Kreuk et al., 2007; Lee et al., 2010). Hailei et al. (2006) classified the aerobic granule formation process into five stages (Fig. 1.1) comprising the microbe multiplication phase followed by floc appearance, floc cohesion and mature floc phases and finally to aerobic granule phase. During the microbe multiplication phase (Fig. 1.1b), microorganisms in sludge and wastewater were proliferated aerobically forming mycelia pellets named as flocs. In floc appearance phase (Fig 1.1c), small flocs started to be in shape with a diameter of 0.3-0.8 mm. Thereafter, formed flocs were enfolded and associated through filamentous microorganisms to form mature flocs in floc the cohesion phase (Fig. 1.1d). Mature flocs of 3.0-6.5 mm diameter developed with improved settling characteristics in the floc maturation phase (Fig. 1.1e). In the last phase of granulation (aerobic granule phase), because of the shear force applied in the reactor, the filamentous structure detached from the boundary of the mature flocs resulting in the formation of compact structure and gradually into aerobic granules (Fig. 1.1f).

1.3.3 Factors affecting aerobic granulation

Granulation is a complex phenomenon affected by a number of parameters, such as seed sludge, substrate composition and organic loading, reactor design, feeding regime, settling time, volume

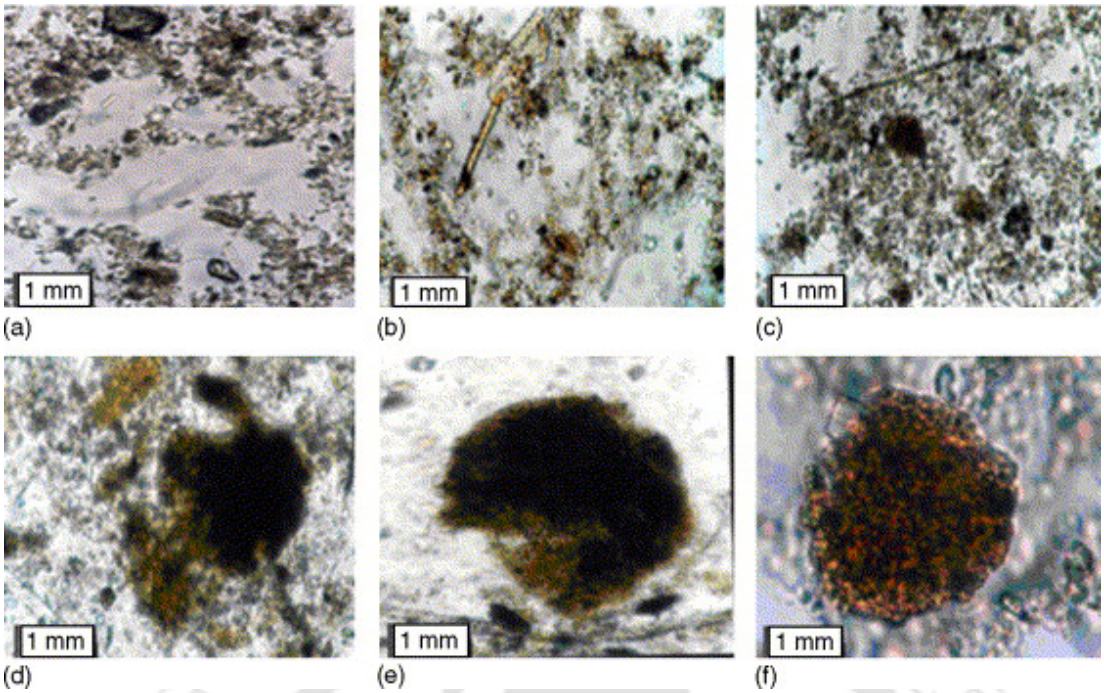

Fig. 1.1. Micrographs of the aerobic granulation process: (a) seed sludge; (b) microbe multiplication phase; (c) floc appearance phase; (d) floc cohesion phase; (e) mature floc phase; (f) aerobic granule phase (Hailei et al., 2006).

exchange ratio, aeration intensity, extracellular polymeric substances (EPS), pH, temperature and augmentation with metal ions and other auxiliary compounds (Winkler et al., 2018). The dominant factor for aerobic granulation is still unknown and thus optimum window of conditions has to be taken into account for achieving the successful cultivation of aerobic granules and for enhancing its stability for long-term operation. The factors affecting aerobic granulation are summarized in Table 1.1 and Table 1.2.

1.3.3.1 Reactor configuration

Reactor design imposes an impact on both the flow pattern of liquid and the microbial aggregates in a reactor (Beun et al., 1999; Liu and Tay, 2002). In an up-flow column type reactor, a high reactor height to diameter (H/D) ratio provides a longer circular flow trajectory resulting in more effective hydraulic attrition to aggregates (Liu and Tay, 2004). Kong et al. (2009) operated four SBRs with four H/D ratios varied from 24 to 4 to evaluate the impact of H/D ratio on granular characteristics and made a conclusion that H/D ratios ranging from 24-4 did not affect the granule formation and its characteristics. However, later in the year 2016, Awang and Shaaban (2016) reported the effect of H/D ratio on aerobic granulation concluding that at a higher H/D ratio of 11.3, rapid granulation with more active granular biomass was observed that that of obtained at lower H/D ratio of 4.4.

1.3.3.2 Seed sludge

In most of the studies, aerobic granules were developed using activated sludge as an inoculum since the bacterial consortia present in activated sludge was important for the granulation (Shi et al., 2019). The higher amount of hydrophobic bacteria than hydrophilic in seed sludge could result in rapid aerobic granulation with better settling properties (Wilén et al., 2008). Sheng et al. (2010a) developed aerobic granules at an organic loading rate (OLR) of 2.0 kg COD m^{-3} day^{-1} using the small-loose and large-compact sludge flocs as an inoculum after being separated from raw activated sludge. Larger

granules (mean size of 2.2±0.4 μm) with good settleability (settling velocity of 33.4±4.6 m h^{-1}) from the large-compact sludge flocs were observed than that of developed from small-loose sludge flocs with mean size and settling velocity of 1.0±0.2 μm and 15.3±4.1 m h^{-1}, respectively. Activated sludge from industrial wastewater treatment plant was found to be more suitable for developing aerobic granules within 35 days with excellent settleability (SVI of 32.75 mL $gTSS^{-1}$) at an OLR of 3.0 kg COD m^{-3} day^{-1} as compared to the sludge from municipal wastewater treatment plant with which granules developed in 56 days (Song et al., 2010).

1.3.3.3 Substrate composition and organic loading rate

Aerobic granules have been successfully developed with various substrates, such as molasses, ethanol, glucose, acetate, sucrose, propionate, starch and other substances (Beun et al., 1999; Jang et al., 2003; Lee et al., 2010; Morgenroth et al., 1997; Tay et al., 2002b; Wu et al., 2012; Zheng et al., 2005). Granulation was also observed with phenol (Adav et al., 2008b; Khan et al., 2009; Wosman et al., 2016) and its derivatives like *p*-nitrophenol, *o*- and *p*-cresol, 2,4-dichlorophenol (Basheer and Farooqi, 2012; Fernández et al., 2013; Wang et al., 2007a), and the mixture of aromatic compounds (*p*-nitrophenol, phenol and *o*-cresol) (Ramos et al., 2016b) as a carbon source. In addition, granulation was achieved efficiently with recalcitrant toxic compounds like pyridine and aniline (Jiang et al., 2019; Liu et al., 2015a). Literature reports on the cultivation of aerobic granules with real wastewater are also available (Cetin et al., 2018; Liu et al., 2010; Zou et al., 2018). Moreover, chemical oxygen demand to nitrogen ratio (COD/N) or N/COD ratio played a vital role in achieving concurrent removal of organic matter and ammonia-nitrogen (Kocaturk and Erguder, 2016; Wei et al., 2013; Yang et al., 2003). Higher N/COD (10/100-30/100) ratio was required to achieve both COD removal and nitrification simultaneously, whereas at a lower N/COD ratio of 5/100, nitrification was absent (Yang et al., 2003). In addition, for achieving nitrogen removal, a higher COD/N ratio of more than 7.0 mg/mg was essential (Wei et al., 2013).

OLR played an indispensable role in the formation of aerobic granules. Aerobic granulation has been reported with an OLR ranging from 1.5 to 15.0 kg COD m^{-3} day^{-1} (Jiang et al., 2004b; Liu et al., 2003a; Liu and Tay, 2015; Moy et al., 2002; Peyong et al., 2012; Zhang et al., 2019a). Glucose fed aerobic granules could be able to tolerate an OLR up to 15.0 kg COD m^{-3} day^{-1}; however, at an organic loading of more than 9.0 kg COD m^{-3} day^{-1}, acetate fed granules disintegrated (Moy et al., 2002). Liu et al. (2003a) reported the independency of aerobic granulation from substrate loading because of being developed with an OLR of 1.5 to 9.0 kg COD m^{-3} day^{-1} using sodium acetate as a carbon source. Despite the finding of substrate-independent aerobic granulation, several studies were performed later reflecting the impact of loading on aerobic granulation. Optimal OLR was reported to enhance the granulation by holding the well-settled biomass resulting in the enhancement of reactor performance in terms of COD removal (Tay et al., 2004a&b). They achieved 99% COD removal efficiency at an OLR of 4.0 kg COD m^{-3} day^{-1} contributed by glucose, peptone and meat extract, whereas reduction (1.0 and 2.0 kg COD m^{-3} day^{-1}) and increment (8.0 kg COD m^{-3} day^{-1}) in OLR caused no granulation and wash out condition, respectively. Long et al. (2015) observed deterioration in granule characteristics at an OLR beyond 15.0 kg COD m^{-3} day^{-1} along with the fall in pollutant removal profiles because of the formation of the anaerobic core by dead cells inside the granules resulting into the rupture of the granules due to instability of the core at an OLR of 18.0 kg COD m^{-3} day^{-1} provided by sodium acetate. The impact of OLR with industrial effluent was also observed. Compact and round granules with clear outline were observed using palm oil mill efuent (POME) wastewater at an OLR of 2.5 kg

Table 1.1. Effect of H/D ratio, seed sludge, substrate composition, substrate loading and F/M ratio on aerobic granulation.

Factor	Activated sludge	Carbon source	Granule maturation (day)	Average granule size (mm)	GSV ($m\ h^{-1}$)	SVI ($mL\ g\ TSS^{-1}$)	OLR[a/b]/ concentration ($mg\ L^{-1}$)[c]	References
H/D ratio	MWTP	Sodium acetate	-	1.6-1.8	39.0-42.0	43.0-57.0	3.0[a]	Kong et al. (2009)
Seed sludge	Large-dense sludge flocs	Sodium acetate	50	2.2±0.4	33.4±4.6	48.1±7.0	2.0[a]	Sheng et al. (2010a)
	BWTP	Glucose	35	-	-	32.8	3.0[a]	Song et al. (2010)
Substrate	MTWP	Molasses	70	2.4	30.0-40.0	-	400.0[c]	Morgenroth et al. (1997)
	Standard SBR	Ethanol	-	3.3	-	-	7.5[a]	Beun et al. (1999)
	STP	Glucose	-	-	35	51.0-85.0	6..0[a]	Tay et al. (2002b)
	MWTP	Acetate	50	1.0±0.4 - 1.3±0.5	25.2 - 28.8	70.0-90.0	2.5[a]	Jang et al. (2003)
	MWTP	Sucrose	60	1.0	18.0-31.0	23.0	830.0[c]	Zheng et al. (2005)
	MWTP	Glucose and 2,4-dichlorophenol	39	1.0-2.0	-	-	2.8[a]	Wang et al. (2007a)
	Digested sludge from paper mill	Phenol	>24	1.0-2.0	-	-	3.9[a]	Khan et al. (2009)
	Real raw domestic wastewater	Real raw domestic wastewater	44	1.5	-	44.0	2.4±0.6[a]	Cetin et al. (2018)
Organic loading rate (OLR)	MAS	Glucose	-	3.3	84.0	31.0	6.0-15.0a	Moy et al. (2002)
	Water reclamation plant	Glucose, peptone and meat extract	52	0.9	-	24.0	1.0-8.0[a]	Tay et al. (2004a&b)
	POME, seed sludge	POME wastewater	60	2.0-4.0	-	24.4	1.5-3.5[a]	Abdullah et al. (2013)
F/M ratio	-	Glucose	15	4.5	148.3	42.5±5.1	2200[c]	Li et al. (2011b)

[a]organic loading rate ($kg\ COD\ m^{-3}day^{-1}$); [b]organic loading rate ($kg\ phenol\ m^{-3}\ day^{-1}$).
MWTP: Municipal wastewater treatment plant; BWTP: Beer wastewater treatment plant; STP: Sewage treatment plant; SBR: Sequencing batch reactor; MAS: Municiple activated sludge; POME: Palm oil mill effluent.

Table 1.2. Effect of operating conditions on aerobic granulation.

Factor	Carbon source	Granule maturation (day)	Average granule size (mm)	GSV ($m\ h^{-1}$)	SVI ($mL\ g\ TSS^{-1}$)	Settling time (min)	HRT (h) /cycle time (h)[a]	AFR[b] /SUAV[c]	OLR[d] / Concentration ($mg\ L^{-1}$)[e]	References
Settling time	Glucose and peptone	20	-	-	47.0±6.0	2, 10	-	4.6[b]	2.4[d]	McSwain et al. (2004)
	Sodium acetate	-	-	-	-	20-5	8	3.0[b]	2560.0[e]	Qin et al. (2004a)
	Sodium acetate	-	1.1-2.2	37.8-44.7	43.3-104.2	10-5	-	4.0[b]	9.0[d]	Adav et al. (2009)
Volume exchange ratio	Sodium acetate	-	0.9-3.7	-	88.0-31.0	5	-	3.0[b]	6.0[d]	Wang et al. (2006)
HRT	Glucose and peptone	-	3.5-0.7	-	44.0-110.0	-	2-24	5.0[b]	4.0[d]	Pan et al. (2004)
	Sodium acetate	-	0.8-0.9	-	80.0-90.0	2	4-8	4.0[b]	8.0[d]	Liu et al. (2016b)
Hydro-dynamic Shear force	Phenol	160	1.0-1.5	26.6±2.0	35.0	-	-	1.0-3.0[b]	-	Adav et al. (2007)
	Sodium acetate	40	0.9	-	14.0±3.0	5	8	3.0-4.0[b]	6.0-15.0[d]	Chen et al. (2008)
Starvation time	Sodium acetate	-	-	-	50-60	2-15	3-16	2.4[c]	1.5-8.0[d]	Liu and Tay (2008)
	-	24-59	3.0-4.0	-	-	5	4-8[a]	1.5[c]	1250-7500[e]	Liu et al. (2016a)

[b]air flow rate ($L\ min^{-1}$); [c]superficial upflow air velocity ($cm\ s^{-1}$); [d]organic loading rate ($kg\ COD\ m^{-3}day^{-1}$).

COD m^{-3} day^{-1}, whereas at an OLR of 1.5 and 3.5 kg COD m^{-3} day^{-1}, porous and loosely bound granules were observed (Abdullah et al., 2013). While treating recalcitrant organics like aromatic compounds, care should be taken while choosing the OLR to avoid the accumulation of intermediates, which can provide more toxicity than the parent wastewater. Accumulation of catechol, a metabolic intermediate compound resulted from the degradation of phenolic compounds, was observed at an OLR of 0.56 kg COD m^{-3} day^{-1}, whereas at an OLR of 0.21 kg COD m^{-3} day^{-1}, almost 100% COD removal was observed without any accumulation of intermediates during simultaneous treatment of phenol, *o*-cresol and *p*-nitrophenol (Ramos et al., 2015). Additionally, cell hydrophobicity (contribute in the aggregation of cells) is affected by OLR. Stable cell hydrophobicity was found in the range of 73-81% at an OLR of 2.5-5.0 kg COD m^{-3} day^{-1} and further increment in OLR upto 15.0 kg COD m^{-3} day^{-1} caused a reduction in cell hydrophobicity with a value of around 50% (Thanh et al., 2009).

1.3.3.4 Food to microorganism (F/M) ratio

F/M ratio is one of the essential operational parameters affecting microbial growth and pollutant removal (Wu et al., 2018). A suitable F/M facilitate the aerobic granulation and also control the granular size (Li et al., 2011b). Nevertheless, the impact of different F/M ratios on the aerobic granulation and optimal range of F/M ratio for the stability of the process is still not well documented (Li et al., 2011b; Wu et al., 2018). Li et al. (2011b) developed aerobic granules at different F/M ratios ranged from 0.3 to 1.1 g COD gSS^{-1} day^{-1} and observed faster granulation (in 15 days) of larger granules (4.5 mm size) at a higher F/M ratio of 1.1 g COD gSS^{-1} day^{-1}, whereas slower granulation (in 40 days) of smaller granules (1.5 mm size) at a lower F/M ratio of 0.3 g COD gSS^{-1} day^{-1}. On the other hand, Wu et al. (2018) reported that aerobic granules with excellent settleability and high pollutant removal efficiency were developed at an F/M ratio of 0.4-0.5 g COD gSS^{-1} day^{-1}. They also stated that the higher F/M ratio (0.9±0.04 g COD gSS^{-1} day^{-1}) was not favourable for the retention of various functional microbial strains. Aerobic granules were also developed at the F/M ratios ranged from 0.3 to 6.0 g COD gSS^{-1} day^{-1} (Li et al., 2008). Tay et al. (2004a) reported that a low F/M ratio (0.33 kg COD $kgMLVSS^{-1}$ day^{-1}) was essential for the stable aerobic granulation. Based on the aforesaid reports mentioning the effect of the F/M ratio on the aerobic granulation, it can be concluded that granules can be developed at different F/M ratios. Therefore the F/M ratio does not significantly affect the aerobic granulation.

1.3.3.5 Free ammonia (FA) and free nitrous acid (FNA)

A small concentration of FA and FNA may affect the granulation and its pollutant removal efficiency. Yang et al. (2004) developed aerobic granules for concurrent removal of organic and ammonium at a FA concentration of less than 23.5 mg L^{-1}. A reduction in both cell hydrophobicity and cell polysaccharides content due to FA was supposed to be the possible reason for granulation failure at high FA concentrations. FA concentration beyond 10 mg L^{-1} inhibited nitrification because of the higher sensitivity of ammonia-oxidizing bacteria (AOB) and nitrite-oxidizing bacteria (NOB) towards FA concentration. However, no inhibitory effect of FA up to a concentration of 36.9 mg NH_3-N L^{-1} was observed on oxygen uptake rate (OUR) of aerobic granules (Peyong et al., 2012), which was quite higher than the study of Yang et al. (2004). On the other hand, FNA started to inhibit the granular activity (measured in terms of OUR) with a concentration of 0.015 mg HNO_2-N L^{-1} and complete inhibition on oxygen utilization was observed at 0.134 mg HNO_2-N L^{-1} (Peyong et al., 2012).

1.3.3.6 Operating conditions

SBR operation

Till now, the successful cultivation of aerobic granules is only reported in SBRs, in which discontinuation in feeding and sedimentation retain only dense granules having excellent settling characteristics (Jahn et al., 2019). Most of the researchers have developed aerobic granulation in SBRs (Adav et al., 2008b; Etterer and Wilderer, 2001; Lee et al., 2010; Liang et al., 2019; Xu et al., 2018) and only a few with continuous mode (Liu et al., 2014a; Ramos et al., 2016b). Treatment of wastewater in SBR is carried out in successive cycles and each cycle comprises filling, aeration (reaction), settling and decanting. SBR offers great advantages, such as ease of operation, relatively economical, flexibility, robustness, single vessel operation and no loss of sludge during the reaction phase (Moussavi et al., 2010).

Settling time, volume exchange ratio (VER) and HRT

The length of setting time and liquid volume exchange ratio at the termination of each SBR cycle are the crucial screening factors in retaining fast-settling granular biomass and in removing the non-granular slow-settling biomass from the SBR (Lee et al., 2010; Winkler et al., 2018). Short settling time favors the selection of high settling velocity bearing biomass (Beun et al., 1999). Effect of settling time on aerobic granulation has been discussed to a great extent (Gómez-Acata et al., 2018; Liu and Tay, 2015; Lochmatter and Holliger, 2014; Qin et al., 2004a; Szabó et al., 2016). At a 2 min settling time, complete granules were found as compared to 10 min settling time with COD removal of 96±1% at both settling times (McSwain et al., 2004). For effective aerobic granulation, settling time should not be more than 5 min. At 5 min settling time, dominant aerobic granules were formed, while at higher settling time (10, 15, 20 min), a mixture of aerobic granules with suspended sludge was observed (Qin et al., 2004a). Adav et al. (2009) also noticed early granulation after two weeks of reactor run at a settling time of 5 min with better granular characteristics as compared to 10 and 7 min settling time, although COD removal (94-96%) remained unaffected by settling time. 1 min settling time was also enough to achieve rapid granulation with better characteristics (Gao et al., 2011). Higher VER favors rapid granulation as better granular characteristics were observed at a VER of 80% as compared to achieved with 20-60% (Wang et al., 2006).

Both short settling time and HRT impart a strong hydraulic selection pressure on sludge granulation (Liu et al., 2016b). Short HRT resulted from the short cycle time is desirable for achieving rapid granulation (Liu and Tay, 2007). Pan et al. (2004) achieved stable granules with an HRT value ranging from 2-12 h, whereas higher HRT of 24, encouraged the suspended biomass growth. The range of HRT between 2-12 h was optimum enough for suppressing the suspended biomass growth and for avoiding sludge loss resulted from the hydraulic washout conditions. Liu et al. (2016b) observed granular appearance within 24 h at all HRTs (4, 6 and 8 h) used in his study after being acclimatized for four days with sodium acetate as a carbon source but granules achieved at HRT of 4 h was bigger in size.

However, in case of continuous stirred tank reactor (CSTR), aerobic granules were achieved only at an HRT of 1 h and at an HRT of 3 and 6 h, dominancy of filamentous bacteria was observed (Morales et al., 2012). Cycle time in SBR is directly related to the HRT of SBR. Optimum cycle time for achieving nitrifying granules was 6 and 12 h because at a shorter cycle time of 3 h sludge loss occurred because of hydraulic washout, whereas at a higher cycle time of 24 h, no nitrifying granules were observed because of lowest selection pressure (Tay et al., 2002a). Later in the year 2006, at a

cycle time of 3 h, rapid granulation within 15 days with a granule size of 1.5 mm was observed as compared to the granules developed at a cycle time of 12 h in 36 days with a granule size of 0.5-1.0 mm (Wang et al., 2005).

Aeration and hydrodynamic shear force

The hydrodynamic shear force contributed by aeration is one of the crucial operational parameters in achieving compact and denser granulation and is measured by means of superficial upflow air velocity (Adav et al., 2007; Chen et al., 2008; Gao et al., 2011; Liu and Tay, 2002). High shear force triggers the secretion of EPS, which contribute to the agglomeration of cells and maintain the granular structural integrity (Feng et al., 2016; Zhu et al., 2012). In addition, higher shear force not only supplies enough oxygen to suppress the growth of filamentous microbes but also generates sufficient force to form compact granules from the aggregates (Liang et al., 2013). The threshold value to form compact and regular granular biomass was set to 1.2 cm s^{-1} (Tay et al., 2001a). However, compact aerobic granulation was also observed with a lower superficial upflow air velocity of 0.6 cm s^{-1} but with low strength wastewater (0.58 kg COD m^{-3} day^{-1}) in an anaerobic/oxic/anoxic SBR (Zhang et al., 2011). Granules developed at an air flow rate of 3.0 L min^{-1} with recalcitrant phenol were smooth and compact exhibiting 97% COD removal efficiency, whereas granules developed at 2.0 L min^{-1} air flow rate displayed filamentous growth after 60 days of reactor operation with 86% COD removal efficiency (Adav et al., 2007).

Chen et al. (2007) reported the importance of shear force on granule stability. Robust structure and potency of granules for long-term operation were observed with the superficial upflow air velocities of 2.4 and 3.2 cm s^{-1}, whereas granules developed at 0.8 and 1.6 cm s^{-1} air velocities were loose, irregular and filamentous resulting in the operational instability. The impact of air flow rate on aerobic granulation to treat high loading wastewater was also reported. At higher shear force (air flow rate of 4.0 L min^{-1}), compact granules were formed which were able to degrade an OLR up to 15.0 kg COD m^{-3} day^{-1} showing good reactor performance along with better granular characteristics, whereas the granules formed with an air flow rate of 3.0 L min^{-1} could not tolerate an OLR beyond 9.0 kg COD m^{-3} day^{-1} resulting in granule disintegration (Chen et al., 2008). Later optimization of shear force for toxic compounds other than phenol was also carried out. Optimum superficial upflow air velocity was 2.4 cm s^{-1} for treating 4-chloroaniline with a loading of 0.8 kg m^{-3} day^{-1}, whereas at lower air velocity (0.6-1.2 cm s^{-1}) presence of filamentous bacteria was observed and disintegration of granules occurred at higher air velocity (3.2 cm s^{-1}) (Zhu et al., 2015). Though high shear force promotes the granulation, a sole high shear force cannot lead to granulation but other factors such as short settling time and organic loading should be coupled to get granulation (Winkler et al., 2018).

Starvation conditions

The starvation period is one of the important conditions for aerobic granulation and longer starvation time supports the formation of aerobic granules (Corsino et al., 2017; Gao et al., 2011; Li et al., 2006). Aerobic starvation, recognized during sequential cyclic operations, triggers the aggregation of microorganisms to form denser microbial aggregates, which is considered as a vital step in achieving granulation (Tay et al., 2001b). The reaction (aeration) period in SBR comprised two phases: substrate degradation phase in which biodegradation of substrate occurred (feast phase) followed by aerobic starvation phase (famine phase) in which only limited concentration of substrate was present (Corsino et al., 2017; Tay et al., 2001b). Under the starvation condition, hydrophobicity of bacteria increased

facilitating the aggregation of microbes (Kjelleberg and Hermansson, 1984). Tay et al. (2001b) reported an increment in hydrophobicity up to 73% after the aerobic granule formation from the seed sludge with the hydrophobicity of 39% thus showing the affinity of cell surface hydrophobicity in cell aggregation. Though Liu et al. (2007) reported that aerobic starvation was not necessary for aerobic granulation because of observing aerobic granulation with and without starvation characterized by higher effluent COD concentration in both conditions. But later, selection of starvation duration was found beneficial for long-term operation of aerobic granular reactor. Liu and Tay (2008) observed rapid but unstable granulation in 16 days only at a short cycle time of 1.5 h with shorter starvation period resulting in reactor failure after 160 days of operation; however, delayed but stable granulation (day 21) with higher starvation time (cycle time of 8 h) was observed for long-term operation. Therefore, two different starvation periods in combination could be beneficial for faster and stable granulation: short starvation period to accelerate the granulation during the starting period of the reactor and enhanced starvation period once the granulation process is over (Liu et al., 2016a).

Dissolved oxygen (DO), pH and temperature

Aerobic granulation has been reported at a low DO concentration of 0.7-1.0 mg L^{-1} (Dangcong et al., 1999) and at a higher DO concentration of 2.0-7.0 mg L^{-1} (Di Bella and Torregrossa, 2013; Hailei et al., 2006) as well. Therefore, it seems that DO is not a granulation governing factor. In contrast, DO concentration below 2.0 mg L^{-1} caused the filamentous outgrowth in aerobic granules treating pig slurry in a CSTR (Morales et al., 2012). In addition, later in the year 2015, it was reported that DO concentration. in combination with COD loading, influenced granule stability. At a high DO concentration of 5.0 mg L^{-1}, independency of the granular stability from a COD loading of 1.55 kg COD m^{-3} day^{-1} was observed, whereas with a reduction in DO concentration up to 2.5 mg L^{-1} with the same COD load (1.55 kg COD m^{-3} day^{-1}), SVI value increased to 385 mL $gTSS^{-1}$ from a value of 60 mL $gTSS^{-1}$ indicating the granular instability (van den Akker et al., 2015). Reactor liquid pH is a crucial environmental factor for the growth of the microorganism. The dominance of fungal granules was observed at a pH of 3.0 with a loose and fluffy structure having a size of 7.0 mm, whereas compact bacterial granules of size 4.8 mm were formed with a pH of around 8.0 (Yang et al., 2008). The effect of pH on stable granules was also addressed. Granular size reduced from initial size of 660 to 449 μm along with increment in flocculent biomass concentration to 26% from 7.8% at a pH of ≤7.0, whereas at pH of ≤7.5 no significant effect on granular characteristics was observed. Also, nitrogen removal was reduced to 17.7% from 44.4% at ≤7.0 pH, while improved phosphorous removal was achieved at pH ≤7.5 (Kang et al., 2019).

Temperature can cause an impact of aerobic granulation only to some extent. Aerobic granulation could be achieved even at 10°C with a mixture of two carbon sources containing sodium acetate and glucose with a smooth surface and compact structure in spite of inhibition to the activity of NOB confirmed through the accumulation of nitrite (Bao et al., 2009). Compact and stable granulation has been achieved with an average diameter of 0.24 mm formed with wastewater consisting of synthetic organic and ammonium at mesophilic temperature (35°C) (Cui et al., 2014). Better granulation at higher temperatures is also documented. Ab Halim et al. (2015) achieved better granulation for treating domestic wastewater at a quite higher temperature of 50°C with an average diameter of 3.36 mm as compared to obtained at 30 and 40°C temperatures. Granules developed at 50°C also performed well in terms of degrading COD, nitrogen and phosphorous than that of developed at 30 and 40°C.

1.3.4 Aerobic granular characteristics

To study the aerobic granular characteristics, a number of parameters have been investigated and regarded as physical, chemical, and biological parameters.

1.3.4.1 Physical characteristics

Settling velocity, density, sludge volume index (SVI), strength of the granules, diameter, porosity, hydrodynamic properties, etc., contribute to the physical characteristics of granules. The granular settling velocity (GSV) determines the solid-liquid separation efficiency, which is a crucial parameter for wastewater treatment systems. The GSV is linked with the granular size and structure and ranged between 30-70 m h^{-1} (Liu and Tay, 2004). An excellent GSV of more than 91 m h^{-1} was observed for treating brewery wastewater (Wang et al., 2007b); however, aerobic granules with more than 9.5 m h^{-1} settling velocity were also retained for treating seafood industry effluent (Val del Río et al., 2013). High GSV enhanced the biomass retention capacity of the reactor, thus enhancing the capability of degrading organic matter (Adav et al., 2008a). The density of aerobic granules (1.04-1.05 g mL^{-1}) (Etterer and Wilderer, 2001) is quite comparable with the flocs of conventional activated sludge (1.02-1.06 g mL^{-1}) (Dammel and Schroeder, 1991). The settling ability and compactness of activated sludge have been commonly described by SVI. With a shorter settling time, more compact microbial structure can be retained in the reactor. High cell hydrophobicity contributes to low SVI resulting in a compact microbial structure (Qin et al., 2004b). SVI value for granulation is usually found in the range of 10-60 mL $gTSS^{-1}$ (Cui et al., 2014; Liu et al., 2018a; Song et al., 2013). The reported typical range of granular size is 0.2-4.0 mm (de Kreuk et al., 2007; Salmiati et al., 2015; Song et al., 2013). Fractal dimension demonstrates the structural integrity of bio-aggregates (Tijani et al., 2015; Xiao et al., 2008). A lower fractal dimension value represents the loose and highly porous aggregates, whereas a denser and stronger structure is represented by the higher fractal dimension. The fungal granules with a fraction dimension of 2.23 were found more porous; however, stronger bacterial granules were having a fractal dimension of 2.42 (Xiao et al., 2008).

1.3.4.2 Chemical characteristics

The production of an entrapping gel network of EPS, a metabolic product of bacteria, which consists of proteins and polysaccharides as the major constituents, is a prerequisite for facilitating a sustainable granulation (Kong et al., 2015; Zhang et al., 2007). EPS is a glue-like sticky substance causing cell adherence, thus promoting the granulation process (Caudan et al., 2014). Several factors have been identified, which may affect the secretion of EPS, such as substrate composition, nutrient content, growth phase and external conditions (Sheng et al., 2010b). Usually, the application of external force on the microbes is the cause of change in EPS content. Bacteria secrete more EPS for reducing surface charge and for enhancing hydrophobicity to resist the external pressures applied on the granules, such as shear force and short settling time. Because of that, microbial aggregates turn into the denser structure and become heavier enough to retain in the reactor (Liang et al., 2019). The polysaccharides content of EPS was supposed to be responsible for the bacterial adherence and self-immobilization and at higher hydrodynamic shear force, aerobic granules secreted more cellular polysaccharides leading to balanced aerobic granular structure (Liu and Tay, 2002). Though the mechanism of stimulation of polysaccharides production by hydrodynamic shear force is still not clear. Later, the protein content was found essential for aerobic granulation (Zhang et al., 2007; Zhu et al., 2012; Zhu et al., 2008). The importance of extracellular protein was reported for controlling the formation and stability of aerobic

granules and an increase in protein content reduced the cell surface negative charge by reducing electrostatic repulsion between the cells, thus favouring the granulation (Zhang et al., 2007). In spite of all above mentioned information, ESP secretion mechanism in AGS is still ambiguous (Zhang et al., 2019b).

EPS presence on the surface of the bacterial cell could change the physicochemical characteristics of the cell surface including surface hydrophobicity and surface charge (Muda et al., 2014). Higher cell hydrophobicity enhanced the cell-to-cell adhesion, therefore cell surface hydrophobicity was supposed to be a triggering force for achieving bio-granulation and assessed by determining the contact angle and adhesion of microbes to hydrocarbons (Liu et al., 2004). The hydrophobicity of acetate fed granules (73%) was almost two times higher as compared to suspended sludge (39%) (Tay et al., 2002b). Application of suitable selection force like high shear force, starvation condition, etc., enhance the hydrophobicity of bacteria, thus increasing the aggregation of cells (Kjelleberg and Hermansson, 1984; Liu et al., 2003b). Though the mechanism responsible for the effect of hydrophobicity on granulation is still unclear (Adav et al., 2008a).

1.3.4.3 Biological characteristics

A number of techniques including scanning and transmission electron microscopy (SEM and TEM), confocal laser scanning microscopy (CLSM) in combination with fluorescence in situ hybridization (FISH) have been used for demonstrating granular microbial structure (Lemaire et al., 2008). The dominancy of *β-Proteobacteria* among the bacterial diversity in aerobic phenol-degrading granules was revealed by the denaturing gradient gel electrophoresis (DGGE) assays (Jiang et al., 2004a). The presence of a mixture of both heterotrophs (phosphate-accumulating organisms) and autotrophs (nitrifiers) in the outer layer and only phosphate-accumulating organisms in the inner part of granules were demonstrated by FISH (De Kreuk et al., 2005). FISH analysis also revealed the presence of nitrifying population at a depth of 70-100 μm below the surface of the granules (Shi et al., 2009) and the dominance of AOB on the granular surface (Jang et al., 2003).

1.3.5 Mechanism of aerobic granulation

Despite too much research on aerobic granulation, the mechanism responsible for aerobic granulation is still vague and considered as a topic of profound research. Different research scientist proposed different mechanisms (de Bruin et al., 2004; Verawaty et al., 2012; Wu et al., 2012). Beun et al. (1999) suggested an aerobic granulation mechanism without the presence of carrier material based on microscopic observation (Fig. 1.2) and reported the formation of mycelial pellets from the fungi after being inoculated with the bacterial sludge inoculum, which could be retained in the reactor because of high settling. On the other hand, bacterial cells washed out from the reactor because of not having the property to form a mycelium, therefore confirming the dominancy of filamentous mycelial pellets in the reactor during startup. Thereafter, because of the shear applied to the reactor, filaments got detached from the surface of pellets resulting in the formation of more compact pellets of 5-6 mm diameter. After lysis of pellets resulted from the oxygen limitation in the inner part of large pellets, the bacterial colonies could sustain because of being large enough to settle. These colonies further turned into the granules and eventually appeared as a dominating community in the reactor. This proposed strategy was based on the experiments in which the reactor was inoculated with the suspended and non-settling cells in small amount.

Recently, a four-step mechanism for aerobic granulation has been reported (Sarma et al., 2017)

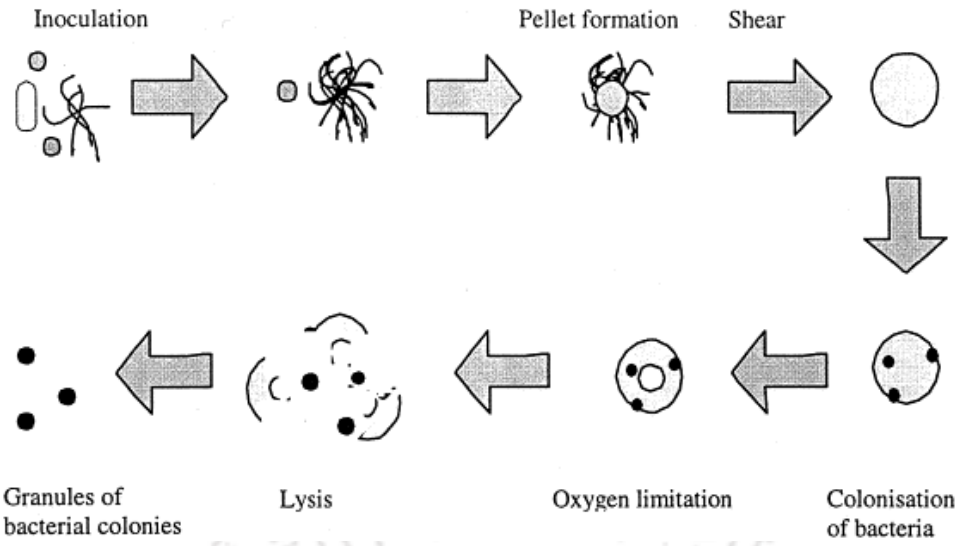

Fig. 1.2. Proposed aerobic granulation mechanism with short settling time in an SBR (Beun et al., 1999).

(Fig. 1.3), which is a slight modification of the mechanism proposed by Liu and Tay (2002). The four steps are as follows:

- Initiation of cell-to-cell adhesion for starting the process.
- Micro-aggregate formation by self-adhered cells. The mechanism responsible for the first two steps can be protoplast translocation, surface charge neutralization, cell surface hydrophobicity and van der Waals force.
- More EPS secretion through agglomerated microbes. The mechanisms behind the third step may be quorum sensing and starvation.
- Maturation of aerobic granules through externally applied hydrodynamic conditions imposed

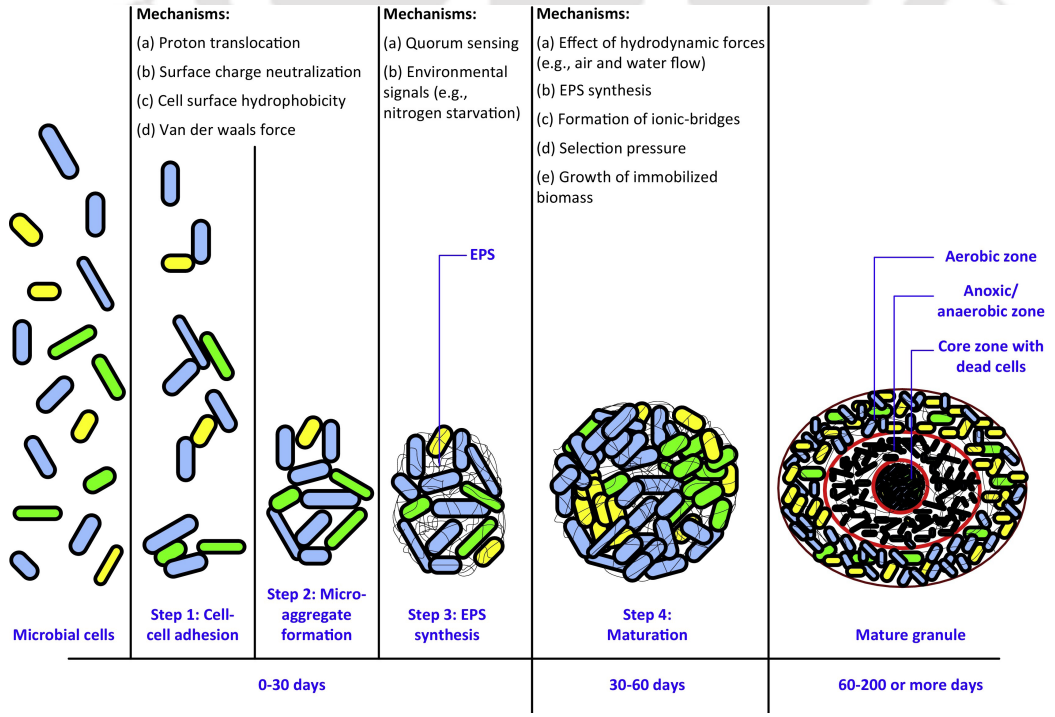

Fig. 1.3. Aerobic granulation process with the mechanisms involved in each step (Sarma et al., 2017).

by the reactor design and operational parameters, such as air and water flow, EPS secretion, selection pressure, etc.

1.3.6 Application of aerobic granules

Application of granules has been reported for treating a variety of wastewater including synthetic, domestic and industrial wastewater and few of them are listed in Table 1.3.

1.3.7 Limitations

Long startup period and loss in granular stability are two major concerns associated with the aerobic granulation and limit its real field application.

1.3.7.1 Long startup period

Despite the several advantages and its application in treating toxic wastewater, the long time required for achieving mature granulation cause reluctance in accepting AGS technology. To overcome this problem, attempts have been made for achieving faster granulation, such as the addition of coagulants, exopolysaccharide and metal ions, fraction of AGS and stored AGS as seed and modification in operating conditions (Gao et al., 2011; Liu et al., 2018b; Liu et al., 2014b; Long et al., 2016). Liu et al. (2014b) observed granular appearance in just 7 days with glucose (1000 mg L^{-1}) as a source of carbon in an SBR supplemented with a coagulant poly aluminum chloride (PAC), as compared to 17 days without the addition of PAC (control); however, granule maturation time was around 30-50 days in PAC supplemented SBR. In addition, 20 days was required to observe the granulation after being supplemented with xanthan gum with sodium acetate (COD of 500-1000 mg L^{-1}), whereas without the addition of xanthan gum, 30 days was required (Liu et al., 2018b).

Addition of Ca^{2+} reduced the granular appearance time from 32 days (without Ca^{2+}) to 16 days with an ethanol and sodium acetate loading of 4.0 kg COD m^{-3} day^{-1}, whereas maturation required 50 days (Jiang et al., 2003). In addition, by augmentation with Mg^{2+} and Al^{3+}, 7 days were required for granule initiation, though granules got matured in 43 days with sodium acetate (Wang et al., 2012a). In order to achieve faster granulation, Long et al. (2014) used 25% AGS as inoculum with sodium acetate (1173 mg L^{-1}) carbon source and observed granular appearance in just 17 days in a pilot-scale SBR. The granular appearance was also observed in only 21 days by using 20% AGS as inoculum with activated sludge for treating solvent recovery raffinate (SRR), though granule maturation required 70 days (Long et al., 2016). Mature granulation in 21 days was also observed by using stored granular sludge as an inoculum with glucose and sodium acetate as substrates (1000 mg L^{-1} COD), whereas granulation required 54 days with activated sludge as seed (Wang et al., 2019).

Gao et al. (2011) observed granular appearance on 11, 11 and 16 days and maturation on 54, 75 and 72 days by applying settling time, starvation and shear force operational strategies, respectively, with glucose (1.0 kg COD m^{-3} day^{-1} load) as a carbon source. Granulation was also achieved in only 3 and 10 days by using well-settled sludge and bulking sludge as an inoculum, respectively, along with a combination of strong hydraulic selection pressure and over-stressed sodium acetate OLR (Liu and Tay, 2015).

1.3.7.2 Granular instability during operation

Loss of granular stability is a major bottleneck for practical applications of aerobic granules for long-term operation. Still, the mechanism of granular instability is not defined, though few mechanisms have been proposed for the loss of granular instability, such as microbial filamentous growth, anaerobic

Table 1.3. Application of aerobic granules.

Wastewater	Carbon source	Average granule size (mm)	SVI	AFL[a]/SUAV[b]	OLR[c]/Concentration (mg L^{-1})[d]	Remarks	References
Soybean processing wastewater	Soybean processing wastewater	1.2	17	-	6.0[c]	Granules with fractal dimension of 1.87±0.34	Su and Yu (2005)
Domestic wastewater	Sewage and synthetic effluent	1.1	38	4.0[a]	1.0[c]	High loading, a vital factor for aerobic granulation	de Kreuk and van Loosdrecht (2006)
Brewery wastewater	Brewery wastewater	2.0-7.0	32	1.8[b]	3.0[c]	AGS with excellent settleability	Wang et al. (2007b)
Synthetic phenolic wastewater	Phenol	-	15-25	-	227-4540[d] (COD)	High COD and phenol removal at phenol concentration of 1000 mg L^{-1}	Moussavi et al. (2010)
NH_4^+-N rich wastewater	Glucose and sodium acetate	2.0	-	1.3[b]	500[d] (COD)	Partial nitrification at a concentration of NH_4^+-N more than 350 mg L^{-1}	Shi et al. (2011)
Landfill leachate	Landfill leachate	0.4-0.6	-	1.7[b]	4298-5992[d] (COD)	Reduction in COD removal rate with an increase in NH_4^+-N	Wei et al. (2012b)
Palm oil mill effluent (POME)	POME	2.0-5.0	19.9	2.5[b]	1.5-3.5[c]	Successful granulation with a POME loadings of 2.5 and 3.5 kg COD m^{-3} day^{-1}	Abdullah et al. (2013)
Pig slurry	Pig slurry	2.0-2.8	<60	-	1.7-6.3[c]	*Nitrosomonas* spp., main nitrifiers	Morales et al. (2013)
Livestock wastewater	Livestock wastewater	3.5-4.1	42	1.0[a]	9.0[c]	Well settled granular biomass with maximum COD, TN and TP removal efficiencies of 74, 73 and 70%	Othman et al. (2013)

Seafood industry	Seafood industry	2.8	35	-	2.0-5.0[c]	Granule disintegration at an OLR > 4.4 kg COD m^{-3} day^{-1}	Val del Río et al. (2013)
Rubber wastewater	Rubber wastewater	2.0	61	1.7[b]	0.9-3.6[c]	Larger and better granular characteristics at 6 h HRT	Rosman et al. (2014)
Slaughter wastewater	Slaughter wastewater	0.6-1.8	-	-	1250±150[d] (COD)	0.6-1.2 and 1.2-1.8 mm granule size favorable for the growth of AOB and NOB, respectively	Liu et al. (2015b)
Pharmace-uticals	Sodium acetate	-	23-51	4.0[a]	3-4 µM fluoxetine	No significant impact of fluoxetine on COD removal	Moreira et al. (2015)
Synthetic bisphenol A (BPA)	BPA, methanol and acetate	-	30-45	4.0[a]	445±79.8[d] (COD)	Highest BPA removal rate at 6 mg BPA L^{-1}	Cydzik-Kwiatkowska et al. (2017)
Solvent recovery raffinate (SRR)	SRR and synthetic wastewater	2.0-4.0	20	1.2-2.0[b]	3.2-4.0[c]	Stable AGS in 55 days for high C/N ratio industrial wastewater treatment	Long et al., (2016)
Piggery wastewater	Piggery wastewater	10-20	25	0.9-1.3[b]	210-832[d] (COD)	Granular appearance on 3rd day	Liu et al. (2017)
Citrus wastewater	Citrus wastewater	1.8	38-135	3.0[a]	3.0-15.0[c]	Around 90% TCOD removal at OLR <7.0 kg TCOD m^{-3} day^{-1}	Corsino et al. (2018)
Synthetic petroleum wastewater	Glucose and Synthetic petroleum wastewater	05-0.9	30	-	600[d] (COD)	Granulation after 35 days with a size of 0.5-0.9 mm	Chen et al. (2019)
Pulp mill wastewater	Pulp mill effluent	20-50	<50	2.2[b]	6700[d] (COD)	79 and 56% removal of COD and tannin/lignin, respectively	Vashi et al. (2019)

[a]air flow rate (L min^{-1}); [b]superficial upflow air velocity (cm s^{-1}); [c]organic loading rate (kg COD m^{-3} day^{-1})

granule core hydrolysis, loss of strains functionality and role of EPS (Lee et al., 2010). To resolve the granular instability demerit, few approaches are suggested including the application of suitable operational parameters, choice of slow-growing microbes, suppressing the activity of anaerobes and granule core strengthening (Lee et al., 2010).

Filamentous outgrowth is usually considered as the failure of AGS systems because of having loose structure resulting in washing out of biomass from the reactor. Control on filamentous outgrowth would enhance the granular stability. Wan et al. (2014) observed aerobic granulation at pH ranged between 4.5-8.0 with acetate or glucose as a carbon source in SBRs and reported that not carbon source, though acidic pH controlled the granulation with filamentous growth. It was also investigated that the granular stability and organic loading were interrelated and high loading was found favorable for the stability of granules (Wang et al., 2009). Extended starvation time favored the long term operation of granules (Liu et al., 2016a; Liu and Tay, 2008). In addition, the role of N-acyl homoserine lactones (AHLs) on granular stability is reported in literature. It was observed that AHLs as being a signal molecule acted as communicating language among the cells and played a substantial role in granular stability. However, the enzyme AHLs-acylase degraded the AHLs and reduced the protein and polysaccharide contents of EPS, thereby eventually deteriorated the granular stability (Li et al., 2014). Later, Li et al. (2015) observed a reduction in stability of granules by algal growth. They also reported the impact of TiO_2 nanoparticles (TiO_2-NPs) with a dose of 10-50 mg L^{-1} on granular stability during reactor operation for 100 days and achieved stable and compact algal-bacterial granules, thereby concluding that TiO_2-NPs could improve the stability of granules. Recently, the interaction between layered double hydroxide (LDH) and EPS was studied for improving granular stability. Addition of LDH stimulated the EPS secretion to enhance granular stability by forming a stable metal ions-EPS-metal ions network because of the presence of functional groups such as hydroxyl, carboxyl and amide (Xu et al., 2019).

1.3.8 Type of wastewater

Toxic and refractory compounds such as phenol, SCN^-, NH_4^+-N and NHCs usually coexist in the wastewater generated from the various industries, such as refinery and coke processing units and may impose severe effects on nature ecology with improper discharge (Pal et al., 2016; Shi et al.,2019). The composition of above mentioned wastewater is complex and differs from one plant to another and provided in Table 1.4. Strict legislation on the discharging of these pollutants to the surface water bodies has been established because of the rising public concern for a clean environment.

Table 1.4. Pollutant composition in industrial wastewater.

Pollutants (mg L^{-1})	Refinery (Pal et al. 2016)	Coke oven (Germany) (Maranon et al. 2008)	Coal gasification (Wang et al. 2012b)	Coal gasification (Ji et al. 2016)
COD	209-5300	4000-6500	2000-4200	-
BOD	61-630	1600-2600	800-1250	-
Phenol	11-200	400-1200	1000-1600	2000
NH_4^+-N	10-82	50-150	110-165	-
SCN^-	-	200-500	22-45	-
Pyridine	-	-	-	120
Indole	-	-	-	50

1.3.9 Pollutants

1.3.9.1 Phenol (C_6H_5OH)

Phenol is an aromatic recalcitrant toxic compound generally exist in the wastewater of several industries, such as coal processing units, petrochemical refineries, paper manufacturing industries, pharmaceutical plants, steel industries, etc. (Al Khalid and El Naas, 2012). Instant skin burns, respiratory problems and eye blisters are the results of short-term exposure of phenolic compounds, whereas long-term exposure may result in exhaustion, lung problems, damage of the immune system and cancer (Raza et al., 2019; Villegas et al., 2016). Phenol is regarded as a priority pollutant and is ranked 11^{th} among the 126 undesirable chemicals according to the United States Environmental Protection Agency (USEPA) (Raza et al., 2019). The range of toxicity levels of phenol is 9-25 mg L^{-1} for humans and aquatic life as well (Villegas et al., 2016). The permissible level of phenol in industrial effluents is 1 and 5 mg L^{-1} for discharging into inland surface water and public sewers according to IS: 2490-1974 and IS: 3306-1974, respectively (Alshabib and Onaizi, 2019; Hussain et al., 2015). In addition, according to the USEPA, phenol level should not be more than 1 part per billion in potable drinking water (Alshabib and Onaizi, 2019).

Physicochemical and biological are the two commonly used methods for treating phenolic wastewater. However, the problems in adopting the physicochemical process is the generation of secondary toxic byproducts and high capital investment. In biological treatment methods, phenol is biodegraded into nontoxic compounds by microbes and aerobic phenol biodegradation is the most commonly used method (Hussain et al., 2015). In the aerobic atmosphere, phenol is biodegraded to CO_2 as a final product (Equation 1.1)(Bajaj et al., 2008). The biodegradation of phenol is a metabolic process governed by enzymatic action in the presence of oxygen. The metabolic route of aerobic phenol biodegradation includes, hydroxylation of aromatic ring to form catechol by phenol hydroxylase followed by transformation of catechol by two alternative pathways; in *o*-pathway, the ring is opened by enzyme catechol 1,2-dioxygenase forming cis, cis muconate, while by enzyme catechol 2,3-dioxygenase to 2-hydroxymuconic semialdehyde in *m*-pathway, and finally both the compounds formed after *o*- and *m*-cleavage metabolize to intermediates of Krebs cycle (Al Khalid and El Naas, 2012; van Schie and Young, 2000). Various microbes, such as *Pseudomonas putida* and *Acinetobacter calcoaceticus* biodegraded phenol by aerobic pathway (Jiang et al., 2013; Lin, 2017).

$$C_6H_5OH + 7\,O_2 \longrightarrow 3\,H_2O + 6\,CO_2 \tag{1.1}$$

1.3.9.2 Thiocyanate (SCN^-)

SCN^- is a sulfur compound and usually found in the effluents of gold mining and coking industries (Gould et al., 2012). The toxicity imparted by SCN^- includes problems associated with respiration and can even aggravate human death by the formation of toxic gases resulting from the reaction with acids (Xi and Shi, 2013). In addition, SCN^- also causes inhibition to several enzymes, particularly Mg^{2+} ATPases (Gould et al., 2012). There is no report available mentioning allowable limit for SCN^-; however in Canada, SCN^- is grouped and categorized as total cyanide (Gould et al., 2012).

The removal of SCN^- cannot be achieved by the extraction, distillation, chemical precipitation and adsorption, nevertheless can be significantly degraded by biological methods because of economic operation, high degradation performance and operability at mild environments (Gould et al., 2012; Pan et al., 2019). Although the mechanism demonstrated SCN^- biodegradation is still not well understood

(Gould et al., 2012). Thiocyanate biotransformation in aerobic conditions was reported by Hung and Pavlostathis (1997). First SCN^- is hydrolyzed to cyanate (OCN^-) and sulfide (S^{-2}); then OCN^- is further hydrolyzed to NH_4^+ and bicarbonate (HCO^{3-}) ions; finally, sulfide is oxidized into sulfate ($SO4^{2-}$). The overall reaction for biotransformation of SCN^- is given in equation (1.2). *Thiobacillus* genus is well known for SCN^- biodegradation (Felföldi et al., 2010).

$$SCN^- + 3\,H_2O + 2\,O_2 \longrightarrow HCO_3^- + NH_4^+ + SO_4^{2-} + H^+ \quad (1.2)$$

1.3.9.3 Ammonia-nitrogen (NH_4^+-N)

NH_4^+-N rich wastewater produced from coking, agricultural and other industries, landfill leachate and urban sewage causes many problems to water bodies including reduction in DO concentration, thus accelerating the eutrophication of water bodies (Peng et al., 2018). According to the Central Pollution Control Board (CPCB), India, the permissible discharge limit for NH_4^+-N is 50 mg L^{-1}. Nitrogen removal by biological methods has been widely accepted because of economical treatment and minimization of secondary pollution (Peng et al., 2018). In the aerobic system, NH_4^+-N is first transformed into nitrite and then into nitrate by autotrophic nitrification. Nitrification involves the conversion of NH_4^+ to NO^{2-} (Equation 1.3a) by AOB (*Nitrosomonas*) and further to NO^{3-} by NOB (*Nitrobacter*) (Equation 1.3b). The overall reaction involved in nitrification is given in equation (1.3c) (Tchobanoglous et al., 2003; Yang et al., 2004). Nitrifiers are very prone to environmental factors and grow at a very slow rate as well (Yang et al., 2004). In addition, a fraction of nitrifiers is beneficial in the systems for nitrogen removal, since the nitrifying bacteria are regarded as a poor contender for oxygen than heterotrophs (Mota et al., 2005).

$$2\,NH_4^+ + 3\,O_2 \longrightarrow 2\,NO_2^- + 4\,H^+ + 2\,H_2O \quad (1.3a)$$

$$2\,NO_2^- + O_2 \longrightarrow 2\,NO_3^- \quad (1.3b)$$

$$NH_4^+ + 2\,O_2 \longrightarrow NO_3^- + 2\,H^+ + H_2O \quad (1.3c)$$

1.3.9.4 Pyridine (C_5H_5N)

Pyridine, a heterocyclic aromatic compound, is a weak organic base with characteristic features like colorless liquid and distinct odor and has been classified as a toxic refractory organic compound because of its severe toxic and teratogenic impacts (Huang et al., 2017; Mathur et al., 2008). Pyridine is recognized as one of the priority pollutants by USEPA (Mathur et al., 2008). Pyridine is generated in the wastewater of various industries including coking, pharmaceuticals, pesticide industries, etc. (Jin et al., 2018).

Physicochemical operations like adsorption, extraction, oxidation, microwave radiation, etc., are limited because of the involvement of high cost and energy consumption. Therefore biological treatment has become a preferred strategy for degrading pyridine rich wastewater because of being ecofriendly and economical (Hou et al., 2018). Aerobic biodegradation of pyridine is activated by many hydroxylation stages followed by the dioxygenolytic cleavage of the aromatic ring. Two most reported strategies for pyridine biodegradation are (i) initially hydroxylation of the ring and later (ii) (aerobic) ring reductive pathway not introduced by hydroxylation. However, the mechanism involving initial hydroxylation for pyridine biodegradation is not clearly established (Fetzner, 1998; Padoley et al., 2008). *Arthrobacter* sp., *Paracoccus* sp., *Pseudomonas* sp., *Rhizobium* sp., etc., have been studied

for aerobic pyridine biodegradation (Fetzner, 1998; Liu et al., 2015a; Mohan et al., 2003; Qiao and Wang, 2010).

1.3.9.5 Indole (C_8H_7N)

Indole is a nitrogen containing heterocyclic aromatic environmental pollutant which is generally found in livestock and coking wastewater (Ma et al., 2019). Indole toxicity can result in animal hemolysis, temporary skin irritation and tumor formation (Ma et al., 2018). Among several treatment methods, biological approach has been considered viable and economical treatment technology for the systems polluted with indole (Ma et al., 2019). Both anaerobic and aerobic biodegradation of indole has been reported. The only difference between them is the initial hydroxylation position. The key step in the aerobic environment was the formation of 2-oxindole resulted from the hydroxylation at C2 position, whereas in the aerobic condition, the common route was the formation of indoxyl or 2,3-dihydroxyindole initiated by the oxygen attack either at C3 position or C2/C3 positions. In general, the anaerobic degradation rate was very slow that that of aerobic degradation rate, which was much faster and efficient (Qu et al., 2015). *Bacillius* spp., *Pseudomonas* and *Cupriavidus* spp. have been characterized for indole biodegradation. However, Ubiquitously accepted bacterial community responsible for aerobic biodegradation of indole has not been reported so far (Ma et al., 2015). Under aerobic conditions, indole degradation is usually started by oxidation followed by the cleavage of heterocyclic ring structure of indole (Arora et al., 2015).

1.3.10 Summary of literature review and lacunae

In the treatment of wastewater, nitrification is usually regarded as rate-limiting because of being inhibited by many factors like aromatic compounds. For achieving multiple pollutants removal along with nitrification, multiple reactor systems have been employed making the treatment process tedious. In addition, the bottlenecks associated with conventional activated sludge systems, such as large area requirement for settling tank, excess sludge production, low volumetric transformation efficacy, sludge bulking and loading fluctuations limit its application in the arena of wastewater treatment technology.

Therefore, AGS technology has been considered as an efficient, space saving and sustainable technology in last two decades for treating high strength and toxic wastewater in a single reactor and to overcome the problems associated with the conventional activated sludge system by owning the unique properties like high biomass retention capacity, high settling behavior, denser structure and potency towards high and toxic loading. The aerobic granulation is influenced by a variety of factors including mainly feed characteristics and operational conditions. The formation of aerobic granules is mostly observed in SBRs because of being operated in cyclic mode, therefore induces starvation condition which is supposed to be responsible for granulation. EPS, a sticky bacterial secretion, facilitates the aggregation of cells by entrapping bacteria in a gel matrix. AGS technology has been employed in treating various kinds of industrial wastewater. Long start-up period and granular stability for the long-term operation are two major factors, which limit the on-field application of AGS.

The development of aerobic granules is generally focused with benign substrates or sole toxic substrate in the research studies reflecting the impact of different factors on granulation. Rapid granulation is also carried out with simple substrates like sodium acetate and glucose and achieved by using either already formed granules or part of it and pure strains, which make the process tedious and expensive. Till now, the prime focus of most of the researchers is to found a sustainable approach to enhance the stability of granules for long-term operation. However, a granule reformation strategy

after its disintegration due to loss in stability without the addition of any supplementary material is scanty and disintegration mechanism is still not well defined. Cultivation of granules has been observed up to the OLRs of 15.0 and 3.0 kg COD m^{-3} day^{-1} with simple carbon source and toxic phenol, respectively. Therefore, aerobic granulation with high phenol loading in SBR is desired. Moreover, the application of granulation for treating recalcitrant phenolic and pyridine rich wastewater is well documented, though the potential of AGS towards NHCs other than pyridine is not reported. Also, the efficacy of AGS for concurrent removal of multiple toxic pollutants, such as aromatics, inorganics and NHCs in an SBR is still a research area requiring exploration. Based on the above mentioned gaps, the following questions need to be considered.

Q1. What is the impact of operational parameters on AGS for treating aromatic (phenol), inorganic (SCN^-) and NH_4^+-N in an SBR?

Q2. What is the role of initial inoculum on rapid granulation and pollutant removals?

Q3. Is granule reformation possible from the disintegrated granules?

Q4. How is granule stability affected by concentrations of aromatics, inorganics and NHCs like phenol, SCN^-, NH_4^+-N, pyridine and indole?

1.3.11 Objectives of the study and methodology

The flow chart of research methodology is given in Fig. 1.4. The main aim of this study was to develop aerobic granules for treating synthetic toxic industrial wastewater containing phenol, thiocyanate,

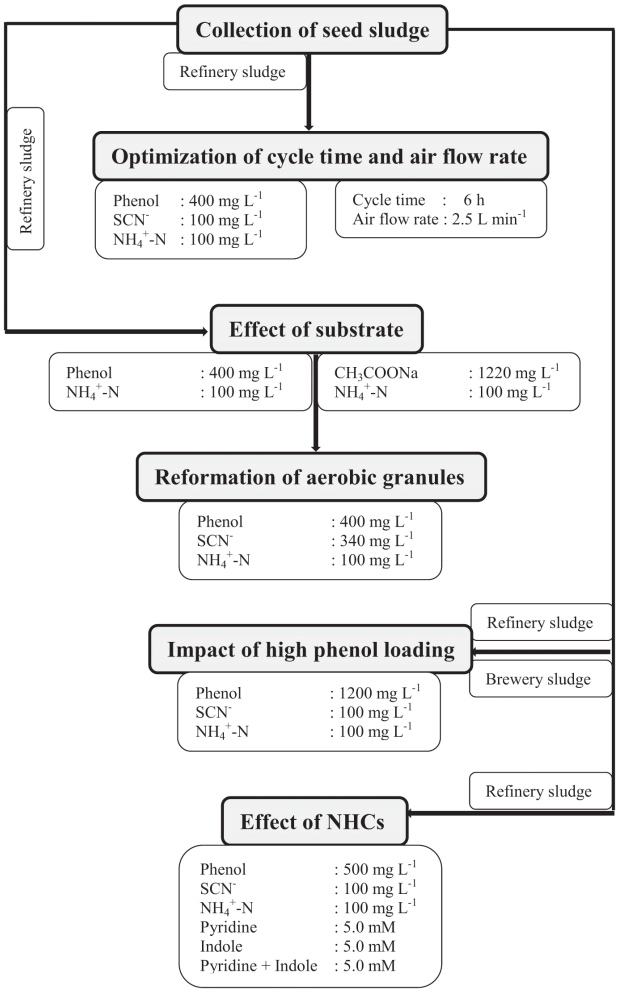

Fig. 1.4. Flow chart of research methodology.

ammonia-nitrogen, pyridine and indole in sequencing batch reactors. Aerobic granules were developed in the acrylic SBRs and the effects of cycle time, air flow rate, thiocyanate, substrate composition and seed sludge were addressed along with pollutant removal profiles. In addition, exposure of aerobic granules to the nitrogenous heterocyclic compounds along with aromatic and inorganics was also investigated.

The following sequences of studies were carried out to achieve the objectives.

- *Assessment of operational parameters, such as cycle time and air flow rate for better granulation with recalcitrant phenol, SCN^- and NH_4^+-N.*
- *Impact of substrates on rapid granulation and evaluation of reformability of granules after being disintegrated.*
- *Study on the effect of high loading of phenol on aerobic granulation.*
- *Evaluation of the potential of aerobic granules for simultaneous biodegradation of aromatic (phenol), inorganics (SCN^- and NH_4^+-N) and NHCs (pyridine and indole).*

References

Ab Halim, M.H., Anuar, A.N., Azmi, S.I., Jamal, N.S.A., Wahab, N.A., Ujang, Z., Shraim, A., Bob, M.M., 2015. Aerobic sludge granulation at high temperatures for domestic wastewater treatment. Bioresource Technology 185, 445-449.

Abdullah, N., Yuzir, A., Curtis, T.P., Yahya, A., Ujang, Z., 2013. Characterization of aerobic granular sludge treating high strength agro-based wastewater at different volumetric loadings. Bioresource Technology 127, 181-187.

Adav, S.S., Lee, D.J., Lai, J.Y., 2009. Aerobic granulation in sequencing batch reactors at different settling times. Bioresource Technology 100, 5359-5361.

Adav, S.S., Lee, D.J., Show, K.Y., Tay, J.H., 2008a. Aerobic granular sludge: Recent advances. Biotechnology Advances 26, 411-423.

Adav, S.S., Lee, D.J., Tay, J.H., 2008b. Extracellular polymeric substances and structural stability of aerobic granule. Water Research 42, 1644-1650.

Adav, S.S., Lee, D.J., Lai, J., 2007. Effects of aeration intensity on formation of phenol-fed aerobic granules and extracellular polymeric substances. Applied Microbiology and Biotechnology 77, 175-182.

Al Khalid, T., El Naas, M.H., 2012. Aerobic biodegradation of phenols: A comprehensive review. Critical Reviews in Environmental Science & Technology 42, 1631-1690.

Alshabib, M., Onaizi, S.A., 2019. A review on phenolic wastewater remediation using homogeneous and heterogeneous enzymatic processes: Current status and potential challenges. Separation and Purification Technology 219, 186-207.

Arora, P.K., Sharma, A., Bae, H., 2015. Microbial degradation of indole and its derivatives. Journal of Chemistry 2015, 13 pages.

Awang, N.A., Shaaban, M.G., 2016. Effect of reactor height/diameter ratio and organic loading rate on formation of aerobic granular sludge in sewage treatment. International Biodeterioration & Biodegradation 112, 1-11.

Bajaj, M., Gallert, C., Winter, J., 2008. Biodegradation of high phenol containing synthetic wastewater by an aerobic fixed bed reactor. Bioresource technology 99, 8376-8381.

Bao, R., Yu, S., Shi, W., Zhang, X., Wang, Y., 2009. Aerobic granules formation and nutrients removal characteristics in sequencing batch airlift reactor (SBAR) at low temperature. Journal of Hazardous Materials 168, 1334-1340.

Basheer, F., Farooqi, I., 2012. Biodegradation of *p*-cresol by aerobic granules in sequencing batch reactor. Journal of Environmental Sciences 24, 2012-2018.

Beun, J.J., Hendriks, A., van Loosdrecht, M.C.M., Morgenroth, E., Wilderer, P.A., Heijnen, J.J., 1999. Aerobic granulation in a sequencing batch reactor. Water Research 33, 2283-2290.

Caudan, C., Filali, A., Spérandio, M., Girbal Neuhauser, E., 2014. Multiple EPS interactions involved in the cohesion and structure of aerobic granules. Chemosphere 117, 262-270.

Cetin, E., Karakas, E., Dulekgurgen, E., Ovez, S., Kolukirik, M., Yilmaz, G., 2018. Effects of high-concentration influent suspended solids on aerobic granulation in pilot-scale sequencing batch reactors treating real domestic wastewater. Water Research 131, 74-89.

Chen, C., Ming, J., Yoza, B.A., Liang, J., Li, Q.X., Guo, H., Liu, Z., Deng, J., Wang, Q., 2019. Characterization of aerobic granular sludge used for the treatment of petroleum wastewater. Bioresource Technology 271, 353-359.

Chen, Y., Jiang, W., Liang, D.T., Tay, J.H., 2007. Structure and stability of aerobic granules cultivated under different shear force in sequencing batch reactors. Applied Microbiology and Biotechnology 76, 1199-1208.

Chen, Y., Jiang, W., Liang, D.T., Tay, J.H., 2008. Aerobic granulation under the combined hydraulic and loading selection pressures. Bioresource Technology 99, 7444-7449.

Corsino, S.F., di Biase, A., Devlin, T.R., Munz, G., Torregrossa, M., Oleszkiewicz, J.A., 2017. Effect of extended famine conditions on aerobic granular sludge stability in the treatment of brewery wastewater. Bioresource Technology 226, 150-157.

Corsino, S.F., Di Trapani, D., Torregrossa, M., Viviani, G., 2018. Aerobic granular sludge treating high strength citrus wastewater: Analysis of pH and organic loading rate effect on kinetics, performance and stability. Journal of Environmental Management 214, 23-35.

Cui, F., Park, S., Kim, M., 2014. Characteristics of aerobic granulation at mesophilic temperatures in wastewater treatment. Bioresource Technology 151, 78-84.

Cydzik Kwiatkowska, A., Bernat, K., Zieliska, M., Bukowska, K., Wojnowska Barya, I., 2017. Aerobic granular sludge for bisphenol A (BPA) removal from wastewater. International Biodeterioration & Biodegradation 122, 1-11.

Dammel, E., Schroeder, E., 1991. Density of activated sludge solids. Water Research 25, 841-846.

Dangcong, P., Bernet, N., Delgenes, J.P., Moletta, R., 1999. Aerobic granular sludgeA case report. Water Research 33, 890-893.

de Bruin, L., de Kreuk, M., van der Roest, H., Uijterlinde, C., van Loosdrecht, M., 2004. Aerobic granular sludge technology: An alternative to activated sludge? Water Science & Technology 49, 11-12.

de Kreuk, M., Heijnen, J., Van Loosdrecht, M., 2005. Simultaneous COD, nitrogen, and phosphate removal by aerobic granular sludge. Biotechnology and Bioengineering 90, 761-769.

de Kreuk, M., Kishida, N., van Loosdrecht, M., 2007. Aerobic granular sludge-state of the art. Water Science and Technology 55, 75-81.

de Kreuk, M.K., van Loosdrecht, M.C., 2006. Formation of aerobic granules with domestic sewage. Journal of Environmental Engineering 132, 694-697.

Di Bella, G., Torregrossa, M., 2013. Simultaneous nitrogen and organic carbon removal in aerobic granular sludge reactors operated with high dissolved oxygen concentration. Bioresource Technology 142, 706-713.

Etterer, T., Wilderer, P., 2001. Generation and properties of aerobic granular sludge. Water Science and Technology 43, 19-26.

Felföldi, T., Székely, A.J., Gorál, R., Barkács, K., Scheirich, G., András, J., Rácz, A., Márialigeti, K., 2010. Polyphasic bacterial community analysis of an aerobic activated sludge removing phenols and thiocyanate from coke plant effluent. Bioresource Technology 101, 3406-3414.

Feng, Q., Xiao, Y., Wang, X., Li, J., Wu, Y., Xue, Z., Cao, J., Oleyiblo, J.O., 2016. The influences of shear stress on extracellular polymeric substances of activated sludge. Desalination and Water Treatment 57, 15835-15842.

Fernández, I., Suárez Ojeda, M.E., Pérez, J., Carrera, J., 2013. Aerobic biodegradation of a mixture of monosubstituted phenols in a sequencing batch reactor. Journal of Hazardous Materials 260, 563-568.

Fetzner, S., 1998. Bacterial degradation of pyridine, indole, quinoline, and their derivatives under

different redox conditions. Applied Microbiology and Biotechnology 49, 237-250.
Gao, D., Liu, L., liang, H., Wu, W.M., 2011. Comparison of four enhancement strategies for aerobic granulation in sequencing batch reactors. Journal of Hazardous Materials 186, 320-327.
Gómez Acata, S., Vital Jácome, M., Pérez Sandoval, M.V., Navarro Noya, Y.E., Thalasso, F., Luna Guido, M., Conde Barajas, E., Dendooven, L., 2018. Microbial community structure in aerobic and fluffy granules formed in a sequencing batch reactor supplied with 4-chlorophenol at different settling times. Journal of Hazardous Materials 342, 606-616.
Gould, W.D., King, M., Mohapatra, B.R., Cameron, R.A., Kapoor, A., Koren, D.W., 2012. A critical review on destruction of thiocyanate in mining effluents. Minerals Engineering 34, 38-47.
Hailei, W., Guangli, Y., Guosheng, L., Feng, P., 2006. A new way to cultivate aerobic granules in the process of papermaking wastewater treatment. Biochemical Engineering Journal 28, 99-103.
Hamza, R.A., Zaghloul, M.S., Iorhemen, O.T., Sheng, Z., Tay, J.H., 2019. Optimization of organics to nutrients (COD: N: P) ratio for aerobic granular sludge treating high-strength organic wastewater. Science of The Total Environment 650, 3168-3179.
Heijnen, J.J., van Loosdrecht, M.C.M., 1998. Method for acquiring grain-shaped growth of a microorganism in a reactor. European Patent Office.
Hou, C., Shen, J., Jiang, X., Zhang, D., Sun, X., Li, J., Han, W., Liu, X., Wang, L., 2018. Enhanced anoxic biodegradation of pyridine coupled to nitrification in an inner loop anoxic/oxic-dynamic membrane bioreactor (A/O-DMBR). Bioresource Technology 267, 626-633.
Huang, D., Liu, W., Wu, Z., Liu, G., Yin, H., Chen, Y., Hu, N., Jia, L., 2017. Removal of pyridine from its wastewater by using a novel foam fractionation column. Chemical Engineering Journal 321, 151-158.
Hung, C.H., Pavlostathis, S.G., 1997. Aerobic biodegradation of thiocyanate. Water Research 31, 2761-2770.
Hussain, A., Dubey, S.K., Kumar, V., 2015. Kinetic study for aerobic treatment of phenolic wastewater. Water Resources and Industry 11, 81-90.
Jahn, L., Svardal, K., Krampe, J., 2019. Comparison of aerobic granulation in SBR and continuous-flow plants. Journal of Environmental Management 231, 953-961.
Jang, A., Yoon, Y.H., Kim, I.S., Kim, K.S., Bishop, P.L., 2003. Characterization and evaluation of aerobic granules in sequencing batch reactor. Journal of Biotechnology 105, 71-82.
Jenkins, D., Wanner, J., 2014. Activated sludge-100 years and counting. IWA publishing.
Ji, Q., Tabassum, S., Hena, S., Silva, C.G., Yu, G., Zhang, Z., 2016. A review on the coal gasification wastewater treatment technologies: past, present and future outlook. Journal of Cleaner Production 126, 38-55.
Jiang, H.L., Tay, J.H., Liu, Y., Tay, S.T.L., 2003. Ca^{2+} augmentation for enhancement of aerobically grown microbial granules in sludge blanket reactors. Biotechnology letters 25, 95-99.
Jiang, H.L., Tay, J.H., Maszenan, A.M., Tay, S.T.L., 2004a. Bacterial diversity and function of aerobic granules engineered in a sequencing batch reactor for phenol degradation. Applied and Environmental Microbiology 70, 6767-6775.
Jiang, H.L., Tay, J.H., Tay, S.L., 2004b. Changes in structure, activity and metabolism of aerobic granules as a microbial response to high phenol loading. Applied Microbiology and Biotechnology 63, 602-608.
Jiang, L., Ruan, Q., Li, R., Li, T., 2013. Biodegradation of phenol by using free and immobilized cells of *Acinetobacter* sp. BS8Y. Journal of Basic Microbiology 53, 224-230.
Jiang, Y., Wei, L., Yang, K., Wang, H., 2019. Investigation of rapid granulation in SBRs treating aniline-rich wastewater with different aniline loading rates. Science of The Total Environment 646, 841-849.
Jin, Y., Yue, Q., Yang, K., Wu, S., Li, S., Gao, B., Gao, Y., 2018. Pre-treatment of pyridine wastewater by new cathodic-anodic-electrolysis packing. Journal of Environmental Sciences 63, 43-49.
Kang, A.J., Munz, G., Yuan, Q., 2019. Influence of pH control on material characteristics, bacterial community composition and BNR performance of mature aerobic granules. Process Safety and Environmental Protection 124, 158-166.
Khan, F., Zain Khan, M., Qamar Usmani, S., Sabir, S., 2009. Biodegradation of phenol by aerobic

granulation technology. Water Science and Technology 59, 273-278.
Kim, Y.M., Park, D., Jeon, C.O., Lee, D.S., Park, J.M., 2008. Effect of HRT on the biological pre-denitrification process for the simultaneous removal of toxic pollutants from cokes wastewater. Bioresource Technology 99, 8824-8832.
Kjelleberg, S., Hermansson, M., 1984. Starvation-induced effects on bacterial surface characteristics. Applied and Environmental Microbiology 48, 497-503.
Kocaturk, I., Erguder, T.H., 2016. Influent COD/TAN ratio affects the carbon and nitrogen removal efficiency and stability of aerobic granules. Ecological Engineering 90, 12-24.
Kong, Q., Wang, Z.B., Shu, L., Miao, M.S., 2015. Characterization of the extracellular polymeric substances and microbial community of aerobic granulation sludge exposed to cefalexin. International Biodeterioration & Biodegradation 102, 375-382.
Kong, Y., Liu, Y.Q., Tay, J.H., Wong, F.S., Zhu, J., 2009. Aerobic granulation in sequencing batch reactors with different reactor height/diameter ratios. Enzyme and Microbial Technology 45, 379-383.
Lee, D.J., Chen, Y.Y., Show, K.Y., Whiteley, C.G., Tay, J.H., 2010. Advances in aerobic granule formation and granule stability in the course of storage and reactor operation. Biotechnology Advances 28, 919-934.
Lemaire, R., Webb, R.I., Yuan, Z., 2008. Micro-scale observations of the structure of aerobic microbial granules used for the treatment of nutrient-rich industrial wastewater. The ISME journal 2, 528-541.
Lettinga, G., Van Velsen, A., Hobma, S.W., De Zeeuw, W., Klapwijk, A., 1980. Use of the upflow sludge blanket (USB) reactor concept for biological wastewater treatment, especially for anaerobic treatment. Biotechnology and Bioengineering 22, 699-734.
Li, A.J., Yang, S.F., Li, X.Y., Gu, J.D., 2008. Microbial population dynamics during aerobic sludge granulation at different organic loading rates. Water Research 42, 3552-3560.
Li, B., Huang, W., Zhang, C., Feng, S., Zhang, Z., Lei, Z., Sugiura, N., 2015. Effect of TiO2 nanoparticles on aerobic granulation of algal-bacterial symbiosis system and nutrients removal from synthetic wastewater. Bioresource Technology 187, 214-220.
Li, H.Q., Han, H.J., Du, M.A., Wang, W., 2011a. Removal of phenols, thiocyanate and ammonium from coal gasification wastewater using moving bed biofilm reactor. Bioresource Technology 102, 4667-4673.
Li, A.J., Li, X.Y., Yu, H.Q., 2011b. Effect of the food-to-microorganism (F/M) ratio on the formation and size of aerobic sludge granules. Process Biochemistry 46, 2269-2276.
Li, X., Yang, S., 2007. Influence of loosely bound extracellular polymeric substances (EPS) on the flocculation, sedimentation and dewaterability of activated sludge. Water Research 41, 1022-1030.
Li, Y., Hao, W., Lv, J., Wang, Y., Zhong, C., Zhu, J., 2014. The role of N-acyl homoserine lactones in maintaining the stability of aerobic granules. Bioresource Technology 159, 305-310.
Li, Z.H., Kuba, T., Kusuda, T., 2006. The influence of starvation phase on the properties and the development of aerobic granules. Enzyme and Microbial Technology 38, 670-674.
Liang, Y.M., Yang, Y.L., Chang, Y.W., Chen, J.Y., Li, C.W., Yu, J.H., Chen, S.S., 2013. Comparison of high pressure and ambient pressure aerobic granulation sequential batch reactor processes. Bioresource Technology 140, 28-35.
Liang, Z., Tu, Q., Su, X., Yang, X., Chen, J., Chen, Y., Liu, C., Li, H., He, Q., 2019. Formation, extracellular polymeric substances and microbial community of aerobic granules enhanced by microbial flocculant compared with poly-aluminum chloride. Journal of Cleaner Production 220, 544-552.
Lin, J., 2017. Stress responses of *Acinetobacter* strain Y during phenol degradation. Archives of Microbiology 199, 365-375.
Liu, H., Xiao, H., Huang, S., Ma, H., Liu, H., 2014a. Aerobic granules cultivated and operated in continuous-flow bioreactor under particle-size selective pressure. Journal of Environmental Sciences 26, 2215-2221.
Liu, J., Li, J., Wang, X., Zhang, Q., Littleton, H., 2017. Rapid aerobic granulation in an SBR treating

piggery wastewater by seeding sludge from a municipal WWTP. Journal of Environmental Sciences 51, 332-341.

Liu, L., Sheng, G.P., Li, W.W., Tong, Z.H., Zeng, R.J., Liu, J.X., Xie, J., Peng, S.C., Yu, H.Q., 2011. Cultivation of aerobic granular sludge with a mixed wastewater rich in toxic organics. Biochemical Engineering Journal 57, 7-12.

Liu, L., Zeng, Z., Bee, M., Gibson, V., Wei, L., Huang, X., Liu, C., 2018a. Characteristics and performance of aerobic algae-bacteria granular consortia in a photo-sequencing batch reactor. Journal of Hazardous Materials 349, 135-142.

Liu, Q., Tay, J., Liu, Y., 2003a. Substrate concentrationindependent aerobic granulation in sequential aerobic sludge blanket reactor. Environmental Technology 24, 1235-1242.

Liu, S., Zhan, H., Xie, Y., Shi, W., Wang, S., 2018b. Rapid cultivation of aerobic granular sludge by xanthan gum in SBR reactors. Water Science and Technology 2017, 360-369.

Liu, X., Chen, Y., Zhang, X., Jiang, X., Wu, S., Shen, J., Sun, X., Li, J., Lu, L., Wang, L., 2015a. Aerobic granulation strategy for bioaugmentation of a sequencing batch reactor (SBR) treating high strength pyridine wastewater. Journal of Hazardous Materials 295, 153-160.

Liu, X., Sun, S., Ma, B., Zhang, C., Wan, C., Lee, D.J., 2016a. Understanding of aerobic granulation enhanced by starvation in the perspective of quorum sensing. Applied Microbiology and Biotechnology 100, 3747-3755.

Liu, Y.Q., Moy, B., Kong, Y.H., Tay, J.H., 2010. Formation, physical characteristics and microbial community structure of aerobic granules in a pilot-scale sequencing batch reactor for real wastewater treatment. Enzyme and Microbial Technology 46, 520-525.

Liu, Y.Q., Tay, J.H., 2008. Influence of starvation time on formation and stability of aerobic granules in sequencing batch reactors. Bioresource Technology 99, 980-985.

Liu, Y.Q., Wu, W.W., Tay, J.H., Wang, J.L., 2007. Starvation is not a prerequisite for the formation of aerobic granules. Applied Microbiology and Biotechnology 76, 211-216.

Liu, Y.Q., Zhang, X., Zhang, R., Liu, W.T., Tay, J.H., 2016b. Effects of hydraulic retention time on aerobic granulation and granule growth kinetics at steady state with a fast start-up strategy. Applied Microbiology and Biotechnology 100, 469-477.

Liu, Y., Kang, X., Li, X., Yuan, Y., 2015b. Performance of aerobic granular sludge in a sequencing batch bioreactor for slaughterhouse wastewater treatment. Bioresource Technology 190, 487-491.

Liu, Y., Tay, J.H., 2004. State of the art of biogranulation technology for wastewater treatment. Biotechnology Advances 22, 533-563.

Liu, Y., Tay, J.H., 2002. The essential role of hydrodynamic shear force in the formation of biofilm and granular sludge. Water Research 36, 1653-1665.

Liu, Y., Yang, S.F., Liu, Q.S., Tay, J.H., 2003b. The role of cell hydrophobicity in the formation of aerobic granules. Current Microbiology 46, 0270-0274.

Liu, Y., Yang, S.F., Tay, J.H., Liu, Q.S., Qin, L., Li, Y., 2004. Cell hydrophobicity is a triggering force of biogranulation. Enzyme and Microbial Technology 34, 371-379.

Liu, Y.Q., Tay, J.H., 2007. Influence of cycle time on kinetic behaviors of steady-state aerobic granules in sequencing batch reactors. Enzyme and Microbial Technology 41, 516-522.

Liu, Y.Q., Tay, J.H., 2015. Fast formation of aerobic granules by combining strong hydraulic selection pressure with overstressed organic loading rate. Water Research 80, 256-266.

Liu, Z., Liu, Y., Zhang, A., Zhang, C., Wang, X., 2014b. Study on the process of aerobic granule sludge rapid formation by using the poly aluminum chloride (PAC). Chemical Engineering Journal 250, 319-325.

Lochmatter, S., Holliger, C., 2014. Optimization of operation conditions for the startup of aerobic granular sludge reactors biologically removing carbon, nitrogen, and phosphorous. Water Research 59, 58-70.

Long, B., Yang, C.z., Pu, W.h., Yang, J.k., Jiang, G.s., Li, C.y., Liu, F.b., Dan, J.f., Zhang, J., Zhang, L., 2016. Rapid cultivation of aerobic granule for the treatment of solvent recovery raffinate in a bench scale sequencing batch reactor. Separation and Purification Technology 160, 1-10.

Long, B., Yang, C.z., Pu, W.z., Yang, J.k., Liu, F.b., Zhang, L., Zhang, J., Cheng, K., 2015. Tolerance to organic loading rate by aerobic granular sludge in a cyclic aerobic granular reactor. Bioresource

Technology 182, 314-322.
Long, B., Yang, C.Z., Pu, W.H., Yang, J.K., Jiang, G.S., Dan, J.F., Li, C.Y., Liu, F.B., 2014. Rapid cultivation of aerobic granular sludge in a pilot scale sequencing batch reactor. Bioresource Technology 166, 57-63.
Ma, Q., Liu, Z., Yang, B., Dai, C., Qu, Y., 2019. Characterization and functional gene analysis of a newly isolated indole-degrading bacterium *Burkholderia* sp. IDO3. Journal of Hazardous Materials 367, 144-151.
Ma, Q., Qu, Y., Zhang, X., Liu, Z., Li, H., Zhang, Z., Wang, J., Shen, W., Zhou, J., 2015. Systematic investigation and microbial community profile of indole degradation processes in two aerobic activated sludge systems. Scientific Reports 5, 17674.
Ma, Q., Zhang, X., Qu, Y., 2018. Biodegradation and biotransformation of indole: Advances and perspectives. Frontiers in Microbiology 9, 2625.
Maranon, E., Vazquez, I., Rodriguez, J., Castrillon, L., Fernandez, Y., Lopez, H., 2008. Treatment of coke wastewater in a sequential batch reactor (SBR) at pilot plant scale. Bioresource Technology 99, 4192-4198.
Marques, A.P., Duque, A.F., Bessa, V.S., Mesquita, R.B., Rangel, A.O., Castro, P.M., 2013. Performance of an aerobic granular sequencing batch reactor fed with wastewaters contaminated with Zn^{2+}. Journal of Environmental Management 128, 877-882.
Mathur, A.K., Majumder, C., Chatterjee, S., Roy, P., 2008. Biodegradation of pyridine by the new bacterial isolates *S. putrefaciens* and *B. sphaericus*. Journal of Hazardous Materials 157, 335-343.
McSwain, B., Irvine, R., Wilderer, P., 2004. The influence of settling time on the formation of aerobic granules. Water Science & Technology 50, 195-202.
Mishima, K., Nakamura, M., 1991. Self-immobilization of aerobic activated sludge-a pilot study of the aerobic upflow sludge blanket process in municipal sewage treatment. Water Science & Technology 23, 981-990.
Mohan, S.V., Sistla, S., Guru, R.K., Prasad, K.K., Kumar, C.S., Ramakrishna, S., Sarma, P., 2003. Microbial degradation of pyridine using *Pseudomonas* sp. and isolation of plasmid responsible for degradation. Waste Management 23, 167-171.
Morales, N., Figueroa, M., Fra Vázquez, A., Val del Río, A., Campos, J., Mosquera-Corral, A., Méndez, R., 2013. Operation of an aerobic granular pilot scale SBR plant to treat swine slurry. Process Biochemistry 48, 1216-1221.
Morales, N., Figueroa, M., Mosquera Corral, A., Campos, J., Mendez, R., 2012. Aerobic granular-type biomass development in a continuous stirred tank reactor. Separation and Purification Technology 89, 199-205.
Moreira, I.S., Amorim, C.L., Ribeiro, A.R., Mesquita, R.B., Rangel, A.O., van Loosdrecht, M.C., Tiritan, M.E., Castro, P.M., 2015. Removal of fluoxetine and its effects in the performance of an aerobic granular sludge sequential batch reactor. Journal of Hazardous Materials 287, 93-101.
Morgenroth, E., Sherden, T., Van Loosdrecht, M.C.M., Heijnen, J.J., Wilderer, P.A., 1997. Aerobic granular sludge in a sequencing batch reactor. Water Research 31, 3191-3194.
Mota, C., Ridenoure, J., Cheng, J., de los Reyes III, F.L., 2005. High levels of nitrifying bacteria in intermittently aerated reactors treating high ammonia wastewater. FEMS Microbiology Ecology 54, 391-400.
Moussavi, G., Barikbin, B., Mahmoudi, M., 2010. The removal of high concentrations of phenol from saline wastewater using aerobic granular SBR. Chemical Engineering Journal 158, 498-504.
Moy, B., Tay, J., Toh, S., Liu, Y., Tay, S., 2002. High organic loading influences the physical characteristics of aerobic sludge granules. Letters in Applied Microbiology 34, 407-412.
Muda, K., Aris, A., Salim, M.R., Ibrahim, Z., van Loosdrecht, M.C., Nawahwi, M.Z., Affam, A.C., 2014. Aggregation and surface hydrophobicity of selected microorganism due to the effect of substrate, pH and temperature. International Biodeterioration & Biodegradation 93, 202-209.
Othman, I., Anuar, A.N., Ujang, Z., Rosman, N.H., Harun, H., Chelliapan, S., 2013. Livestock wastewater treatment using aerobic granular sludge. Bioresource Technology 133, 630-634.
Padoley, K., Mudliar, S., Pandey, R., 2008. Heterocyclic nitrogenous pollutants in the environment and their treatment options-An overview. Bioresource Technology 99, 4029-4043.

Pal, S., Banat, F., Almansoori, A., Abu Haija, M., 2016. Review of technologies for biotreatment of refinery wastewaters: progress, challenges and future opportunities. Environmental Technology Reviews 5, 12-38.

Pan, J., Ma, J., Wu, H., Chen, B., He, M., Liao, C., Wei, C., 2019. Application of metabolic division of labor in simultaneous removal of nitrogen and thiocyanate from wastewater. Water Research 150, 216-224.

Pan, S., Tay, J.H., He, Y.X., Tay, S.T.L., 2004. The effect of hydraulic retention time on the stability of aerobically grown microbial granules. Letters in Applied Microbiology 38, 158-163.

Peng, P., Huang, H., Ren, H., Ma, H., Lin, Y., Geng, J., Xu, K., Zhang, Y., Ding, L., 2018. Exogenous N-acyl homoserine lactones facilitate microbial adhesion of high ammonia nitrogen wastewater on biocarrier surfaces. Science of The Total Environment 624, 1013-1022.

Peyong, Y.N., Zhou, Y., Abdullah, A.Z., Vadivelu, V., 2012. The effect of organic loading rates and nitrogenous compounds on the aerobic granules developed using low strength wastewater. Biochemical Engineering Journal 67, 52-59.

Qiao, L., Wang, J.l., 2010. Microbial degradation of pyridine by Paracoccus sp. isolated from contaminated soil. Journal of Hazardous Materials 176, 220-225.

Qin, L., Liu, Y., Tay, J.H., 2004a. Effect of settling time on aerobic granulation in sequencing batch reactor. Biochemical Engineering Journal 21, 47-52.

Qin, L., Tay, J.H., Liu, Y., 2004b. Selection pressure is a driving force of aerobic granulation in sequencing batch reactors. Process Biochemistry 39, 579-584.

Qu, Y., Shen, E., Ma, Q., Zhang, Z., Liu, Z., Shen, W., Wang, J., Li, D., Li, H., Zhou, J., 2015. Biodegradation of indole by a newly isolated *Cupriavidus* sp. SHE. Journal of Environmental Sciences 34, 126-132.

Rajasulochana, P., Preethy, V., 2016. Comparison on efficiency of various techniques in treatment of waste and sewage water-A comprehensive review. Resource-Efficient Technologies 2, 175-184.

Ramos, C., Suárez-Ojeda, M.E., Carrera, J., 2015. Long-term impact of salinity on the performance and microbial population of an aerobic granular reactor treating a high-strength aromatic wastewater. Bioresource Technology 198, 844-851.

Ramos, C., Suárez Ojeda, M.E., Carrera, J., 2016a. Biodegradation of a high-strength wastewater containing a mixture of ammonium, aromatic compounds and salts with simultaneous nitritation in an aerobic granular reactor. Process Biochemistry 51, 399-407.

Ramos, C., Suárez Ojeda, M.E., Carrera, J., 2016b. Long-term performance and stability of a continuous granular airlift reactor treating a high-strength wastewater containing a mixture of aromatic compounds. Journal of Hazardous Materials 303, 154-161.

Raza, W., Lee, J., Raza, N., Luo, Y., Kim, K.H., Yang, J., 2019. Removal of phenolic compounds from industrial waste water based on membrane-based technologies. Journal of Industrial and Engineering Chemistry 71, 1-18.

Rosman, N.H., Anuar, A.N., Chelliapan, S., Din, M.F.M., Ujang, Z., 2014. Characteristics and performance of aerobic granular sludge treating rubber wastewater at different hydraulic retention time. Bioresource Technology 161, 155-161.

Sahariah, B.P., Chakraborty, S., 2011. Kinetic analysis of phenol, thiocyanate and ammonia-nitrogen removals in an anaerobic-anoxic-aerobic moving bed bioreactor system. Journal of Hazardous Materials 190, 260-267.

Salmiati, Dahalan, F.A., Najib, M.Z.M., Salim, M.R., Ujang, Z., 2015. Characteristics of developed granules containing phototrophic aerobic bacteria for minimizing carbon dioxide emission. International Biodeterioration & Biodegradation 102, 15-23.

Sarma, S.J., Tay, J.H., Chu, A., 2017. Finding Knowledge Gaps in Aerobic Granulation Technology. Trends in Biotechnology 35, 66-78.

Sengar, A., Basheer, F., Aziz, A., Farooqi, I.H., 2018. Aerobic granulation technology: Laboratory studies to full scale practices. Journal of Cleaner Production 197, 616-632.

Sheng, G.P., Li, A.J., Li, X.Y., Yu, H.Q., 2010a. Effects of seed sludge properties and selective biomass discharge on aerobic sludge granulation. Chemical Engineering Journal 160, 108-114.

Sheng, G.P., Yu, H.Q., Li, X.Y., 2010b. Extracellular polymeric substances (EPS) of microbial aggregates

in biological wastewater treatment systems: A review. Biotechnology Advances 28, 882-894.
Shi, J., Xu, C., Han, Y., Han, H., 2019. Enhanced anaerobic biodegradation efficiency and mechanism of quinoline, pyridine, and indole in coal gasification wastewater. Chemical Engineering Journal 361, 1019-1029.
Shi, X.Y., Yu, H.Q., Sun, Y.J., Huang, X., 2009. Characteristics of aerobic granules rich in autotrophic ammonium-oxidizing bacteria in a sequencing batch reactor. Chemical Engineering Journal 147, 102-109.
Shi, Y.J., Wang, X.H., Yu, H.B., Xie, H.J., Teng, S.X., Sun, X.F., Tian, B.H., Wang, S.G., 2011. Aerobic granulation for nitrogen removal via nitrite in a sequencing batch reactor and the emission of nitrous oxide. Bioresource Technology 102, 2536-2541.
Song, Y., Ishii, S., Rathnayake, L., Ito, T., Satoh, H., Okabe, S., 2013. Development and characterization of the partial nitrification aerobic granules in a sequencing batch airlift reactor. Bioresource Technology 139, 285-291.
Song, Z., Pan, Y., Zhang, K., Ren, N., Wang, A., 2010. Effect of seed sludge on characteristics and microbial community of aerobic granular sludge. Journal of Environmental Sciences 22, 1312-1318.
Su, K.Z., Yu, H.Q., 2005. Formation and characterization of aerobic granules in a sequencing batch reactor treating soybean-processing wastewater. Environmental Science & Technology 39, 2818-2827.
Szabó, E., Hermansson, M., Modin, O., Persson, F., Wilén, B.M., 2016. Effects of wash-out dynamics on nitrifying bacteria in aerobic granular sludge during start-up at gradually decreased settling time. Water 8, 172.
Tay, J.H., Pan, S., He, Y., Tay, S.T.L., 2004a. Effect of organic loading rate on aerobic granulation. I: Reactor performance. Journal of Environmental Engineering 130, 1094-1101.
Tay, J.H., Yang, S.F., Liu, Y., 2002a. Hydraulic selection pressure-induced nitrifying granulation in sequencing batch reactors. Applied Microbiology and Biotechnology 59, 332-337.
Tay, J.H., Liu, Q., Liu, Y., 2002b. Characteristics of aerobic granules grown on glucose and acetate in sequential aerobic sludge blanket reactors. Environmental Technology 23, 931-936.
Tay, J.H., Pan, S., He, Y., Tay, S.T.L., 2004b. Effect of organic loading rate on aerobic granulation. II: Characteristics of aerobic granules. Journal of Environmental Engineering 130, 1102-1109.
Tay, J.H., Liu, Q.S., Liu, Y., 2001a. The effects of shear force on the formation, structure and metabolism of aerobic granules. Applied Microbiology and Biotechnology 57, 227-233.
Tay, J.H., Liu, Q.S., Liu, Y., 2001b. Microscopic observation of aerobic granulation in sequential aerobic sludge blanket reactor. Journal of Applied Microbiology 91, 168-175.
Tay, S.T.L., Moy, B.Y.P., Maszenan, A.M., Tay, J.H., 2005. Comparing activated sludge and aerobic granules as microbial inocula for phenol biodegradation. Applied Microbiology and Biotechnology 67, 708-713.
Tchobanoglous, G., Burton, F.L., Stensel, H.D., Metcalf, Eddy, 2003. Wastewater Engineering: Treatment and Reuse, fourth ed. McGraw Hill Education, India.
Thanh, B.X., Visvanathan, C., Aim, R.B., 2009. Characterization of aerobic granular sludge at various organic loading rates. Process Biochemistry 44, 242-245.
Tijani, H., Abdullah, N., Yuzir, A., Ujang, Z., 2015. Rheological and fractal hydrodynamics of aerobic granules. Bioresource Technology 186, 276-285.
Val del Río, A., Figueroa, M., Mosquera Corral, A., Campos, J., Méndez, R., 2013. Stability of aerobic granular biomass treating the effluent from a seafood industry. International Journal of Environmental Research 7, 265-276.
van den Akker, B., Reid, K., Middlemiss, K., Krampe, J., 2015. Evaluation of granular sludge for secondary treatment of saline municipal sewage. Journal of Environmental Management 157, 139-145.
van Schie, P.M., Young, L.Y., 2000. Biodegradation of phenol: Mechanisms and applications. Bioremediation Journal 4, 1-18.
Vashi, H., Iorhemen, O., Tay, J., 2019. Extensive studies on the treatment of pulp mill wastewater using aerobic granular sludge (AGS) technology. Chemical Engineering Journal 359, 1175-1194.

Vázquez, I., Rodríguez, J., Marañón, E., Castrillón, L., Fernández, Y., 2006. Simultaneous removal of phenol, ammonium and thiocyanate from coke wastewater by aerobic biodegradation. Journal of Hazardous Materials 137, 1773-1780.

Verawaty, M., Pijuan, M., Yuan, Z., Bond, P.L., 2012. Determining the mechanisms for aerobic granulation from mixed seed of floccular and crushed granules in activated sludge wastewater treatment. Water Research 46, 761-771.

Villegas, L.G.C., Mashhadi, N., Chen, M., Mukherjee, D., Taylor, K.E., Biswas, N., 2016. A short review of techniques for phenol removal from wastewater. Current Pollution Reports 2, 157-167.

Wan, C., Yang, X., Lee, D.J., Zhang, Q., Li, J., Liu, X., 2014. Formation of filamentous aerobic granules: role of pH and mechanism. Applied Microbiology and Biotechnology 98, 8389-8397.

Wang, F., Lu, S., Wei, Y., Ji, M., 2009. Characteristics of aerobic granule and nitrogen and phosphorus removal in a SBR. Journal of Hazardous Materials 164, 1223-1227.

Wang, F., Yang, F.L., Zhang, X.W., Liu, Y.H., Zhang, H.M., Zhou, J., 2005. Effects of cycle time on properties of aerobic granules in sequencing batch airlift reactors. World Journal of Microbiology and Biotechnology 21, 1379-1384.

Wang, S.G., Liu, X.W., Zhang, H.Y., Gong, W.X., Sun, X.F., Gao, B.Y., 2007a. Aerobic granulation for 2, 4-dichlorophenol biodegradation in a sequencing batch reactor. Chemosphere 69, 769-775.

Wang, S., Shi, W., Yu, S., Yi, X., Yang, X., 2012a. Formation of aerobic granules by Mg^{2+} and Al^{+3} augmentation in sequencing batch airlift reactor at low temperature. Bioprocess and Biosystems Engineering 35, 1049-1055.

Wang, S.G., Liu, X.W., Gong, W.X., Gao, B.Y., Zhang, D.H., Yu, H.Q., 2007b. Aerobic granulation with brewery wastewater in a sequencing batch reactor. Bioresource Technology 98, 2142-2147.

Wang, X.C., Chen, Z.L., Kang, J., Zhao, X., Shen, J.M., Yang, L., 2019. The key role of inoculated sludge in fast start-up of sequencing batch reactor for the domestication of aerobic granular sludge. Journal of Environmental Sciences 78, 127-136.

Wang, Z.W., Liu, Y., Tay, J.H., 2006. The role of SBR mixed liquor volume exchange ratio in aerobic granulation. Chemosphere 62, 767-771.

Wang, Z., Xu, X., Gong, Z., Yang, F., 2012b. Removal of COD, phenols and ammonium from Lurgi coal gasification wastewater using A2O-MBR system. Journal of Hazardous Materials 235, 78-84.

Wei, D., Qiao, Z., Zhang, Y., Hao, L., Si, W., Du, B., Wei, Q., 2013. Effect of COD/N ratio on cultivation of aerobic granular sludge in a pilot-scale sequencing batch reactor. Applied Microbiology and Biotechnology 97, 1745-1753.

Wei, X.X., Zhang, Z.Y., Fan, Q.L., Yuan, X.Y., Guo, D.S., 2012a. The effect of treatment stages on the coking wastewater hazardous compounds and their toxicity. Journal of Hazardous Materials 239, 135-141.

Wei, Y., Ji, M., Li, R., Qin, F., 2012b. Organic and nitrogen removal from landfill leachate in aerobic granular sludge sequencing batch reactors. Waste Management 32, 448-455.

Wilén, B.M., Onuki, M., Hermansson, M., Lumley, D., Mino, T., 2008. Microbial community structure in activated sludge floc analysed by fluorescence in situ hybridization and its relation to floc stability. Water Research 42, 2300-2308.

Winkler, M.K.H., Meunier, C., Henriet, O., Mahillon, J., Suárez Ojeda, M.E., Del Moro, G., De Sanctis, M., Di Iaconi, C., Weissbrodt, D.G., 2018. An integrative review of granular sludge for the biological removal of nutrients and recalcitrant organic matter from wastewater. Chemical Engineering Journal 336, 489-502.

Wosman, A., Lu, Y., Sun, S., Liu, X., Wan, C., Zhang, Y., Lee, D.J., Tay, J., 2016. Effect of operational strategies on activated sludges acclimation to phenol, subsequent aerobic granulation, and accumulation of polyhydroxyalkanoates. Journal of Hazardous Materials 317, 221-228.

Wu, C.Y., Peng, Y.Z., Wang, R.D., Zhou, Y.X., 2012. Understanding the granulation process of activated sludge in a biological phosphorus removal sequencing batch reactor. Chemosphere 86, 767-773.

Wu, D., Zhang, Z., Yu, Z., Zhu, L., 2018. Optimization of F/M ratio for stability of aerobic granular process via quantitative sludge discharge. Bioresource Technology 252, 150-156.

Xi, B., Shi, Q., 2013. Removement of thiocyanate from industrial wastewater by microwave-Fenton oxidation method. Journal of Environmental Sciences 25, S201-S204.

Xiao, F., Yang, S.F., Li, X.Y., 2008. Physical and hydrodynamic properties of aerobic granules produced in sequencing batch reactors. Separation and Purification Technology 63, 634-641.

Xu, J., He, J., Wang, M., Li, L., 2018. Cultivation and stable operation of aerobic granular sludge at low temperature by sieving out the batt-like sludge. Chemosphere 211, 1219-1227.

Xu, X., Liu, J., Sun, H., 2019. Improving granular sludge stability via stimulation of extracellular polymeric substance production by adding layered double hydroxides. International Journal of Environmental Science & Technology 16, 987-994.

Yang, S.F., Tay, J.H., Liu, Y., 2003. A novel granular sludge sequencing batch reactor for removal of organic and nitrogen from wastewater. Journal of Biotechnology 106, 77-86.

Yang, S.F., Tay, J.H., Liu, Y., 2004. Inhibition of free ammonia to the formation of aerobic granules. Biochemical Engineering Journal 17, 41-48.

Yang, S., Li, X., Yu, H., 2008. Formation and characterisation of fungal and bacterial granules under different feeding alkalinity and pH conditions. Process Biochemistry 43, 8-14.

Zhang, H., Dong, F., Jiang, T., Wei, Y., Wang, T., Yang, F., 2011. Aerobic granulation with low strength wastewater at low aeration rate in A/O/A SBR reactor. Enzyme and Microbial Technology 49, 215-222.

Zhang, L., Feng, X., Zhu, N., Chen, J., 2007. Role of extracellular protein in the formation and stability of aerobic granules. Enzyme and Microbial Technology 41, 551-557.

Zhang, Z., Qiu, J., Xiang, R., Yu, H., Xu, X., Zhu, L., 2019a. Organic loading rate (OLR) regulation for enhancement of aerobic sludge granulation: Role of key microorganism and their function. Science of The Total Environment 653, 630-637.

Zhang, Z., Yu, Z., Wang, Z., Ma, K., Xu, X., Alvarezc, P.J., Zhu, L., 2019b. Understanding of aerobic sludge granulation enhanced by sludge retention time in the aspect of quorum sensing. Bioresource Technology 272, 226-234.

Zhao, W.T., Huang, X., Lee, D.J., 2009. Enhanced treatment of coke plant wastewater using an anaerobic-anoxic-oxic membrane bioreactor system. Separation and Purification Technology 66, 279-286.

Zheng, Y.M., Yu, H.Q., Sheng, G.P., 2005. Physical and chemical characteristics of granular activated sludge from a sequencing batch airlift reactor. Process Biochemistry 40, 645-650.

Zhu, H., Han, Y., Xu, C., Han, H., Ma, W., 2018. Overview of the state of the art of processes and technical bottlenecks for coal gasification wastewater treatment. Science of The Total Environment 637, 1108-1126.

Zhu, L., Lv, M.L., Dai, X., Yu, Y.W., Qi, H.Y., Xu, X.Y., 2012. Role and significance of extracellular polymeric substances on the property of aerobic granule. Bioresource Technology 107, 46-54.

Zhu, L., Xu, X., Luo, W., Tian, Z., Lin, H., Zhang, N., 2008. A comparative study on the formation and characterization of aerobic 4-chloroaniline-degrading granules in SBR and SABR. Applied Microbiology and Biotechnology 79, 867-874.

Zhu, L., Zhou, J., Yu, H., Xu, X., 2015. Optimization of hydraulic shear parameters and reactor configuration in the aerobic granular sludge process. Environmental Technology 36, 1605-1611.

Zou, J., Tao, Y., Li, J., Wu, S., Ni, Y., 2018. Cultivating aerobic granular sludge in a developed continuous-flow reactor with two-zone sedimentation tank treating real and low-strength wastewater. Bioresource Technology 247, 776-783.

It is common sense to take a method and try it. If it fails, admit it frankly and try another. But above all, try something.

Franklin D. Roosevelt (1882-1945)
American leader and former US president

2

Optimization of Operational Strategies for Aerobic Granulation

This chapter deals with the impact of operational parameters on the formation of aerobic granules with phenol, thiocyanate and ammonia-nitrogen along with the granule characteristics and pollutant removal efficiencies.

2.1 Introduction

In wastewater treatment, removal of ammonia by nitrification step is always considered as the rate-limiting step due to the very slow growth rate of nitrifying bacteria, which are very susceptible to several factors like inhibition by aromatic compounds (Ramos et al., 2016a). When phenol and thiocyanate are present with ammonia, these compounds inhibit nitrifying bacteria, hence require to be removed prior to nitrification (Jeong and Chung, 2006; Kim et al., 2008b). Aerobic granule based biological treatment systems serve as an alternative approach for treating the complex industrial wastewater (Gao et al., 2011b). Many factors such as substrate loading, substrate type and operational parameters like cycle time, settling time, feeding strategy and aeration intensity affect aerobic granulation (Lee et al., 2010). Aerobic granulation has high potency for the simultaneous removal of both organic and ammonium pollutants in a cost-effective manner (Singh and Srivastava, 2011). Though, very few works of literature are available for the simultaneous removal of recalcitrant phenol with ammonia-nitrogen by aerobic granular reactor (AGR) (Liu et al., 2005; Ramos et al., 2016a&b).

AGR is largely operated in a sequencing batch reactor (SBR) with several phases like the filling of feed, reaction, settling and decanting of supernatant in a cycle. In any SBR, the cycle time is interrelated to hydraulic retention time (HRT) and substrate loading of the reactor and higher cycle time gives longer HRT and lower substrate loading. When cycle time i.e., HRT is too short, microbial growth can be hindered by insufficient reaction time; on the other hand, when cycle time is too high, hydrolysis of biomass may occur by starvation of biomass resulting in a negative impact on biomass aggregation (Liu and Tay, 2015). In addition, in a column type biological reactors, hydraulic turbulence and hydraulic shear force mainly resulted from aeration, are one of the important parameters responsible for granulation and are determined in terms of superficial upflow air velocity (Chen et al., 2008). It enhances the contact possibilities among the flocs by particle-particle collision and maintains the stability and structural integrity of the granules (Liu and Tay, 2002). High air flow rate provides a high shear force that triggers the secretion of bacterial extracellular polymeric substances (EPS), which enhances the microbial aggregation by promoting the stability and communication of cells (Kong et al., 2015). Higher hydraulic shear force contributes to the smoothness of granule by eroding the granule

surface and suppresses the filamentous growth by providing adequate oxygen (Show et al., 2012).

However, previous studies on the parameter optimization in AGR were mainly carried out with acetate and sucrose as feed (Chen et al., 2008; Gao et al., 2011a; Liu and Tay, 2007b; Wang et al., 2005) and a few with toxic carbon sources like phenol (Adav et al., 2007). Therefore, the current study aims to investigate the effect of cycle time and optimal aeration on development and characteristics of granules along with the performance of AGR in removing toxic pollutants like phenol, thiocyanate and achieving nitrification in an economical way in terms of optimal air supply. The feasibility and performance of AGR are also evaluated under the effect of up-flow liquid velocity (ULV).

2.2 Materials and methods

All the instruments used in the entire research work are given in Appendix-I.

2.2.1 Chemicals and reagents

All the chemicals and reagents used in this study were either analytical grade (AR) or laboratory grade (LR). Phenol, potassium thiocyanate, ammonium chloride and sodium acetate used for feeding to the reactor in this study were obtained from Merck (India) and Himedia (India). Potassium dihydrogen phosphate (KH_2PO_4) and dipotassium hydrogen phosphate (K_2HPO_4) used in the phosphate buffer were purchased from Himedia (India) and sodium bicarbonate used for maintaining pH was purchased from Merck, India. $MgSO_4.7H_2O$, $CaCl_2.2H_2O$, $FeCl_3.6H_2O$, $CuCl_2$, $ZnCl_2$, $NiCl_2.6H_2O$ and $CoCl_2$ used in the preparation of trace metal solution were purchased from Merck, India. Ferrous ammonium sulfate, potassium dichromate, mercuric sulfate, silver sulfate, sulfuric acid, ferroin indicator, sodium nitroprusside, tri-sodium citrate, sodium hypochlorite, sodium nitrite, phosphoric acid, sulphanilamide, *N*-(1-naphthyl)-ethylenediamine dihydrochloride, ammonium hydroxide, 4-aminoantipyrine, potassium ferricyanide, ferric nitrate, nitric acid, sodium chloride, glucose, bovine serum albumin (BSA), sodium potassium tartrate, sodium carbonate, copper sulfate, Folin-Ciocalteu reagent, potassium chloride and sodium hydroxide were purchased either from Merck, India or Himedia, India. The dyes used in confocal scanning like SYTO 63, fluorescein isothiocyanate (FITC), concanavalin A (Con A) and SYTOX blue were purchased from Himedia, India. All the reagents and stock/standard solutions were prepared by milli-Q water (Merck Millipore, Germany).

2.2.2 Analytical methods

In general, standard techniques, as mentioned in the Standard Methods (APHA, 2005) have been followed unless otherwise specified. The **size of the granules** was either measured by a laser particle size analyser (LPSA) (Mastersizer 2000, Malvern Instruments, UK) with a 0.02-2000 μm size range or by image analysis software (ImageJ). The sample was analyzed three times by LPSA and average value was produced. The LPSA also produced D50 value, which is the average or median diameter in μm. D50 value represents 50 percentile of the size distribution (Zhang et al., 2011), which means half of the particles above and half of the particles below this value. For image analysis, the collected granules were kept in a glass Petri dish for photo image. From the photo image, the diameters of more than 50 individual granules were analyzed with the help of ImageJ for each SBR. Then the granule size was measured in respect of equivalent diameter from the projected surface area determined by ImageJ (Tijani et al., 2015). The **granule morphology** was determined by the field emission scanning electron microscope (FESEM) (Zeiss, Sigma, Germany). For FESEM analysis, the granules were fixed with 2% glutaraldehyde overnight at 4°C after washing with phosphate buffer (pH 7.0) and then was dehydrated with ethyl alcohol and dried (Wang et al., 2007).

For measuring **total suspended solids (TSS)** and **volatile suspended solids (VSS)**, a known amount of granular sludge was taken during the aeration phase. TSS was measured after drying granular sludge at 105°C in hot air oven (ICT, India) and further ignition at 550°C in the muffle furnace (Multispan, India) provided VSS. **Sludge volume index (SVI_{30})** (mL $gTSS^{-1}$) was determined by collecting one litre of mixed liquor during the aeration phase from the reactor in a graduated cylinder. After 30 min of settling time, the volume of settled sludge was measured. The ratio of settled sludge volume (mL) to the mass of total suspended solids (g) determined the SVI_{30}. **Granule settling velocity (GSV)** (m h^{-1}) was determined by the free settling test as described by Yu et al. (2009). Randomly ten granules were collected from the reactor and taken in one litre graduated cylinder filled with tap water. The average time taken by individual granules to settle in the cylinder was noted and settling velocity was calculated from the distance travelled divided by average settling time of ten granules. **Granular biomass density** was examined by volumetric displacement method of Beun et al. (1999) and performed only in air flow rate study. To know the granular biomass volume through the volume displacement method, water was removed from the known amount of granular biomass by filtration before being added to the known volume of demineralized water. Thereafter, the granular biomass was dried at 105°C in a hot air oven to calculate the dry weight. The biomass density was then determined by dividing the dry weight of granular biomass by the total volume of granular biomass.

EPS of the granules were extracted by a heat extraction procedure (Li and Yang, 2007). 50 mL sludge was taken during the aeration phase from the SBR and centrifuged for 5 min at 4000 rpm. Thereafter, the pellet was washed twice with supernatant and suspended in 0.2% NaCl solution up to 50 mL. The sludge suspension was kept in the water bath for 30 min at 60 °C. Then the sludge was again centrifuged for 15 min at 4000 rpm. The collected supernatant was considered as EPS extract. EPS was the sum of polysaccharides (PS) and proteins (PN). **PS content** was estimated by the phenol-sulphuric acid method (Dubois et al., 1956), whereas **PN content** was analyzed by modified Lowry assay (Lowry et al., 1951). For PS, 2 ml EPS extract was taken and mixed with 1 ml of 5% aqueous phenol solution in a test tube and 5 ml concentrated H_2SO_4 was added rapidly in the mixture. Test tube was allowed to stand for 10 minutes and vortexed using Spinix-vortex-shaker (Tarsons, India) for 30 s. Thereafter, the test tube was placed in a water bath (ICT, India) at room temperature (25-30°C) for 20 min for colour development. Absorbance was measured at 490 nm. Glucose was used as the standard solution. For PN, in 1 ml EPS extract, 0.9 ml of reagent A (consists of 2 g sodium potassium tartrate tetrahydrate and 500 mL of 1N NaOH in 1L distilled water) was added in test tubes and kept in water bath at 50°C for 10 min and allowed to cool to room temperature. Further 0.1 mL of reagent B (consists of 2 g sodium potassium tartrate tetrahydrate, 1 g copper sulfate and 10 mL of 1N NaOH in 100 mL distilled water) was added in test tubes, mixed and tubes were incubated at room temperature for 10 min. Afterward, 3 mL of reagent C (consists of one volume of Folin-Ciocalteau reagent diluted with 15 volumes of distilled water) was added rapidly to the tubes, mixed and incubated at 50°C for 10 min. After cooling to room temperature, the tubes were again incubated at room temperature for 30-60 min and absorbance was measured at 650 nm. For standard curve preparation, BSA was used.

For analysis of pollutant removals, the collected samples were centrifuged using a research centrifuge (REMI CM-8 Plus, India) at 4000 rpm for 5 min and filtered prior to analysis. **pH** was measured by a digital pH meter (μpH System 361, Systronics, India) with 0.01 sensitivity and

temperature correction facility. pH meter was calibrated using standard buffer solutions (pH 4.0 and 7.0) periodically. **Conductivity** was measured by a conductivity meter (VSI-04 Deluxe, VSI Electronics, India) and was calibrated using 0.1N KCl solution at room temperature before any analysis and temperature was measured through a thermometer.

Dissolved oxygen (DO) concentration was analysed by DO meter (LBOD101, Hach, USA). **Chemical oxygen demand (COD)** was analyzed by the closed reflux titrimetric method using ferrous ammonium sulfate as a titrant. **Phenol** was determined by 4-aminonatipyrine method measuring absorbance at 500 nm using 4-aminoantipyrine and potassium ferricyanide. **Ammonia-nitrogen (NH_4^+-N)** was measured at a wavelength of 640 nm by phenate method using sodium nitroprusside, phenol and sodium hypochlorite. **Thiocyanate (SCN^-)** was measured by colorimetric method using ferric nitrate in an acidic medium and absorbance was measured at 460 nm. **Nitrite-nitrogen (NO_2^--N)** was also measured by colorimetric method using phosphoric acid, sulphanilamide and N-(1-naphthyl)-ethylenediamine dihydrochloride at a wavelength of 543 nm. **Nitrate-nitrogen (NO_3^--N)** was analyzed by ion chromatography (792 Basic IC, Metrohm, Switzerland) using an anion column (Metrosep ASupp 5- 250/4.0) and carbonate eluent. The standard curves for all the pollutants are given in Appendix-II.

2.2.3 Granule staining and confocal laser scanning microscopic (CLSM) observation

This CLSM scanning was performed for the granules developed during the air flow rate study. The fully hydrated granules were taken from each reactor for observing the distribution pattern of total cells, dead cells, polysaccharides and proteins in the granules during staining with fluorescent dyes of distinct excitation and emission spectra (Chen et al., 2007). The staining of granules was carried out according to Yu et al. (2009). First of all, SYTO 63 (20 μM, 100 μL) was incubated with the granule samples and kept for shaking for 30 min. For maintaining solution pH 9, $NaHCO_3$ buffer (0.1 M, 100 μL) was added, followed by the addition of fluorescein isothiocyanate FITC solution (10 gL^{-1}, 10 μL) for 1 h. The solution was then immersed for 30 min after adding a Con A solution (250 mg L^{-1}, 100 μL). For removing the excess stain, the granule samples were washed twice with phosphate-buffered saline (PBS) after each of these three staining steps mentioned above and the stained samples were kept at 4°C. Before scanning microscopic observation, a SYTOX Blue solution (2.5 μM, 100 μL) was added to the granule samples for 10 min. After staining, the granule samples were frozen at -20°C after being embedded in paraffin to get 30 μm sections using a manual rotary microtome (RM 2245, Leica, Germany) and were placed on the microscopic slides for CLSM (Leica TCS SP8, Leica, Germany) observations. The stained granule samples were analyzed with LAS X confocal software with 10x or 20x objectives.

2.2.4 Granular biomass activity (GBA) test

This test was carried out only for the air flow rate study. Cumulative COD removal with time was evaluated to analyze biomass activity by collecting the same amount of granular biomass (VSS; 1.30-1.40 g L^{-1}) from each SBR in three different 1 L beakers provided with the same amount of feed (400 mg L^{-1} phenol, 100 mg L^{-1} NH_4^+-N and 100 mg L^{-1} SCN^-) as was given to the SBRs and volume was made up 1 L with tap water. Nutrients were not added in the feed to restrict the biomass growth. All the beakers were aerated with the same air flow rate of 2.5 L min^{-1} throughout the test. COD was measured initially at shorter and later on at longer time interval up to 5 h of feeding. GBA test was performed three times with the same synthetic feed and average was taken to determine the slope

of the linear portion. After completion of each cycle, the supernatant was discarded after 5 min of settling and fresh feed was added to 1 L volume in each beaker. After completion of third feeding, VSS in all the beakers was measured. The granular biomass activity was then estimated by the final VSS and the slope of the linear portion of the cumulative COD removed with time and calculated by modifying the methanogenic activity of Jawed and Tare (1999) (Equation 2.1).

$$\text{Activity}\left(\frac{\text{mg COD removed}}{\text{mg vss day}}\right) = \text{Slope of the graph}\left(\frac{\text{mg of COD removed}}{\text{h}}\right) \times \frac{24\ \text{h}}{\text{day}} \times \frac{1}{\text{mg VSS}} \quad (2.1)$$

2.3 Cycle time study

2.3.1 Experimental set-up

The present study was carried out in three laboratory-scale reactors operated in sequential batch mode. Each reactor had a working volume of 6 L. The working height and inner diameter (ID) of reactors were 212 and 6 cm (H/D ratio of 35), respectively. Aeration was provided by an oil-free compressor at a rate of 2.0 L min^{-1} by air stones kept at the bottom in all three reactors. The influent synthetic wastewater was introduced from the bottom of the reactors with the help of peristaltic pumps. The reactors were maintained at room temperatures (25-30°C). The photographic image of reactor and schematic diagram of reactor are given in Fig. 2.1 and Fig. 2.2, respectively.

2.3.2 Seed sludge characteristics and composition of synthetic wastewater

The inoculum was collected from the activated sludge unit of wastewater treatment plant of Indian Oil Corporation Limited (IOCL), Noonmati, Guwahati, Assam. The TSS and VSS of the sludge obtained from IOCL were 2.42±0.16 and 1.72±0.15 g L^{-1}, respectively. The particle size of sludge was 32.78±0.01 µm along with a SVI_{30} value of 50.13 mL $gTSS^{-1}$. In all three reactors, 3 L sludge was used for working volume of 6 L. The influent synthetic wastewater composition is given in Table

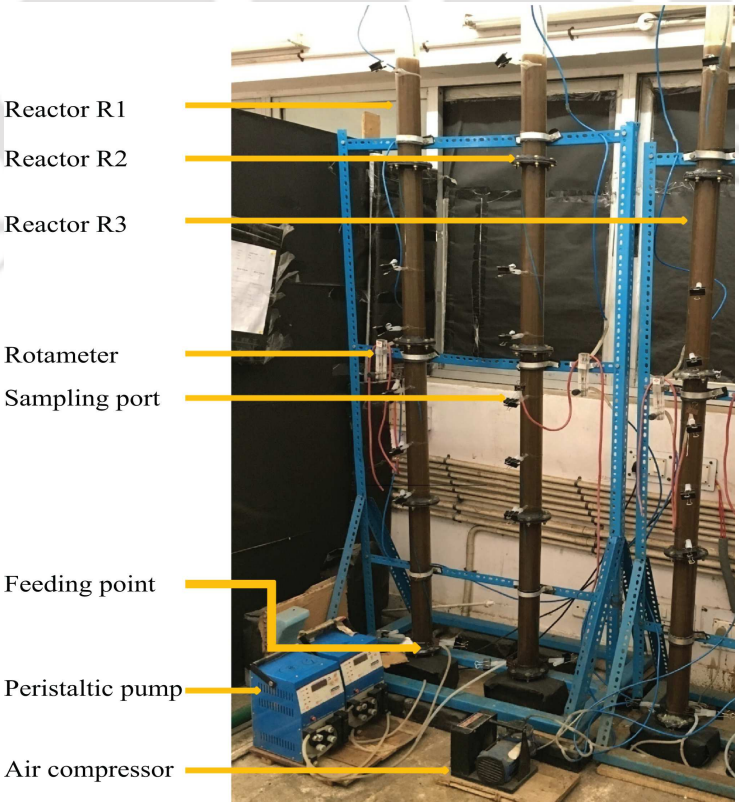

Fig. 2.1. Picture of reactors.

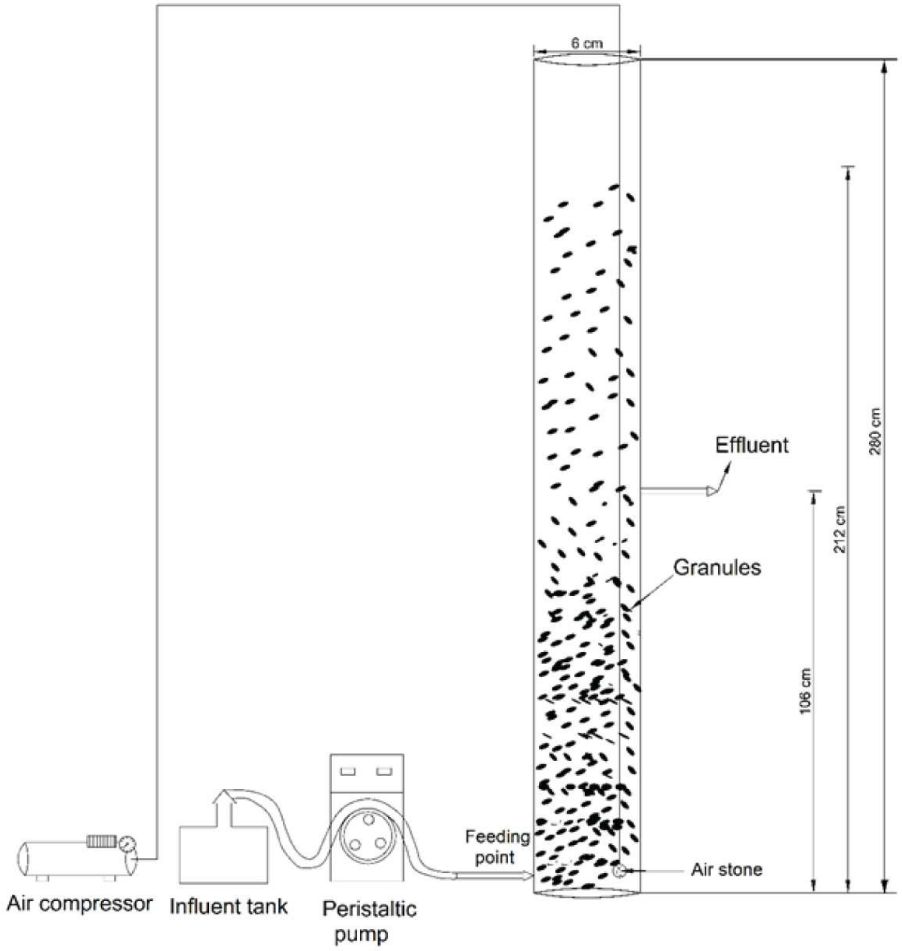

Fig. 2.2. Schematic diagram of SBR.

2.1 and consisted of phenol (400 mg L^{-1}), ammonia-nitrogen (NH_4^+-N as NH_4Cl) (100 mg L^{-1}) and thiocyanate (SCN^- as KSCN) (100 mg L^{-1}). Feed pH was maintained between 7.5-8.0 using sodium bicarbonate and phosphate buffer. This phosphate buffer also worked as a phosphorus source for the growth of microorganisms. The stock trace metal composition was taken from previous literature (Sahariah and Chakraborty, 2011).

Table 2.1. Composition of the influent synthetic wastewater.

Component	Concentration (mg L^{-1})	Component	Concentration (mL L^{-1})
Phenol	400	**Phosphate buffer**[a]	1
NH_4^+-N	100		
SCN^-	100	**Trace metal solution**[b]	1
$NaHCO_3$	added as required		

[a]Phosphate buffer contained (g L^{-1}): 72.3 KH_2PO_4 and 104.5 K_2HPO_4;[b]Trace metal solution contained (mg L^{-1}): 10,000 $MgSO_4.7H_2O$, 10,000 $CaCl_2.2H_2O$, 5000 $FeCl_3.6H_2O$, 1000 $CuCl_2$, 1000 $ZnCl_2$, 500 $NiCl_2.6H_2O$ and 500 $CoCl_2$

2.3.3 Operational strategy

The operational schedule is given in Table 2.2. The reactors were operated in the sequential batch mode with a volume exchange ratio of 50%. i.e., 50% of reactor working volume was decanted in each cycle and a similar amount of fresh feed was added to the reactor. Settling time was kept constant for

5 min in three reactors throughout the study, except for the initial 15 days, when it was 15 min to prevent severe washout of biomass from the reactors. Cycle time was varied as 6 h in R1, 12 h in R2 and 24 h in R3. HRT (day) was calculated using equation 2.2 and HRT values are given in Table 2.2.

$$\text{HRT (day)} = \frac{\text{Reactor volume (L)}}{\text{Volume decanted per cycle (L)} \times \text{No. of cycles per day}} \quad (2.2)$$

ULV is the liquid velocity at which influent feed moves in the upward direction in the reactor during the feeding phase. ULV was kept at 2.0 m h^{-1} in all three reactors during the cycle time study and ULVs of 2.5 and 3.0 m h^{-1} were maintained in reactor R1 for examining the ULV effect on granular sludge characteristics and performance. Equation 2.3 was used for calculating ULV and values of ULVs are given in Table 2.2 with the operation time.

$$\text{ULV (m h}^{-1}) = \frac{\text{Flow rate (m}^3\text{/cycle)}}{\text{Feeding time per cycle (h)} \times \text{Cross sectional area of reactor (m}^2\text{)}} \quad (2.3)$$

During the acclimatization period, concentrations of phenol, thiocyanate and ammonia were increased gradually in the feed. In order to supply suitable carbon source during acclimatization, sodium acetate was added initially in the feed (1000 mg L^{-1}). With the progress of acclimatization, concentrations of feed pollutants were increased and the concentration of sodium acetate was gradually decreased in the feed. After 45 days of acclimatization, there was no sodium acetate in the reactors and phenol, ammonia-nitrogen and thiocyanate concentrations were increased to 400, 100 and 100 mg L^{-1}, respectively. Then reactors were operated for another 27 days with same the feed and operating conditions and steady-state data was collected.

2.3.4 Results and discussion

2.3.4.1 Characteristics of granules

The characteristics of granules are summarized in Table 2.3. Three reactors R1, R2 and R3 were operated at three different cycle times of 6 h, 12 h and 24 h with corresponding HRTs of 12 h, 24 h and 48 h with the organic loading rates (OLRs) of 2.03, 1.02, and 0.51 kg COD m^{-3} day^{-1} and nitrogen loading rates (NLRs) of 0.20, 0.10 and 0.05 kg NH_4^+-N m^{-3} day^{-1}, respectively (Table 2.2). Image of granules in three reactors with time is shown in Fig. 2.3. Seed sludge was of brown colour without any granule. In R1, less number of granules started developing on 7th day onwards, some rod shaped granules were observed on day 15th. On day 45th and 60th, large numbers of granules were present having spherical shape and a few were of rod shaped.

Jiang et al. (2004) observed granulation after 60 days with phenol as a sole carbon source at an organic loading of 1-2 kg phenol m^{-3} day^{-1}. Kong et al. (2009) achieved mature granulation after 91 days of reactor operation by using sodium acetate as a carbon source at an organic loading of 3 kg COD m^{-3} day^{-1}. Najib et al. (2017) used palm oil mill effluent for developing granules with an OLR of 2.75 kg COD m^{-3} day^{-1} and observed the final form of granulation after 100 days of reactor operation (Table 2.4). Therefore, granule formation was found to be faster (45 days) in the present study with multiple toxic pollutants (phenol, thiocyanate and ammonia-nitrogen) at a lower organic load of 2.03 kg COD m^{-3} day^{-1} (0.8 kg phenol m^{-3} day^{-1}) as compared to previous studies observed by Jiang et al. (2004), Kong et al. (2009) and Najib et al. (2017). At a low OLR of 1.50 kg COD m^{-3} day^{-1}, granulation was also achieved by using glucose as a carbon source after 70 days of operation with a granule size of 1000 μm (Gao et al., 2011a) (Table 2.4), which was also higher than the present

Table 2.2. Operational schedule of reactors for cycle time study.

Operational time (day)	Reactor	No of cycles d^{-1}	Cycle time (h)	Distribution of cycle time (min)				HRT (h)	OLR[a]	NLR[b]	ULV[c]
				Feeding	Reaction	Settling	Decanting				
1-75	R1	4	6	30.0	320.0	5.0	5.0	12	2.03	0.20	2.0
	R2	2	12	30.0	680.0	5.0	5.0	24	1.02	0.10	2.0
	R3	1	24	30.0	1400.0	5.0	5.0	48	0.51	0.05	2.0
75-120	R1	4	6	25.5	324.5	5.0	5.0	12	2.03	0.20	2.5
120-155	R1	4	6	21.0	329.0	5.0	5.0	12	2.03	0.20	3.0

[a]Organic loading rate (kg COD $m^{-3}day^{-1}$); [b]Nitrogen loading rate (kg NH_4^+-N m^{-3} day^{-1}); [c]Up-flow liquid velocity (m h^{-1})

Table 2.3. Characteristics of granules at different cycle times.

Characteristics	Cycle time (h)		
	6 (R1)	12 (R2)	24 (R3)
VSS (g L^{-1})	4.31±0.40	2.01±0.22	2.28±0.13
SVI_{30} (mL $gTSS^{-1}$)	67.69±7.13	21.71±4.97	22.98±8.05
GSV (m h^{-1})	35.79±2.20	39.80±2.10	30.00±7.36
Average granule size (μm)	1334.24±30.56	520.94±343.18	97.93±4.21
EPS (mg $gVSS^{-1}$)	79.65±8.42	63.99±3.59	44.36±2.42
SRT (days)	14	6	10
F/M ratio (g COD $gVSS^{-1}$ day^{-1})	0.47	0.51	0.22

Table 2.4. Comparison of characteristics of granules.

Wastewater characteristic	Average granule size (μm)	Average settling velocity (m h^{-1})	SVI (mL g TSS^{-1})	Air flow rate (L min^{-1})	Granulation (days)	OLR[a/b]	References
Synthetic phenol	-	-	40.00-45.00	3.5	60	1.00-2.00[b]	Jiang et al. (2004)
Synthetic phenol	520-1200	-	40.00±5.60 - 60.50±5.00	3.5	30	1.50-2.50[b]	Tay et al. (2004)
Synthetic glucose and acetate	>390.9-1400	-	99.00	1.5	34	2.52[a]	Kim et al. (2008a)
Synthetic sodium acetate	1700	39-42	43.20 - 57.50	3.0	91	3.00[a]	Kong et al. (2009)
Synthetic glucose	1000	34-90	20.00	5.0	70	1.50[a]	Gao et al. (2011a)
Palm oil mill effluent	300-2360	18-103	10.30 - 14.80	4.0	100	2.75[a]	Najib et al. (2017)
Synthetic phenol, thiocyanate, ammonia	1334.24±30.56	35.79±2.20	67.69±7.13	2.0	45	2.03[a]/ 0.80[b]	Present study (R1)

[a]Organic loading rate (kg COD m^{-3} day^{-1});[b]Organic loading rate (kg phenol m^{-3} day^{-1})

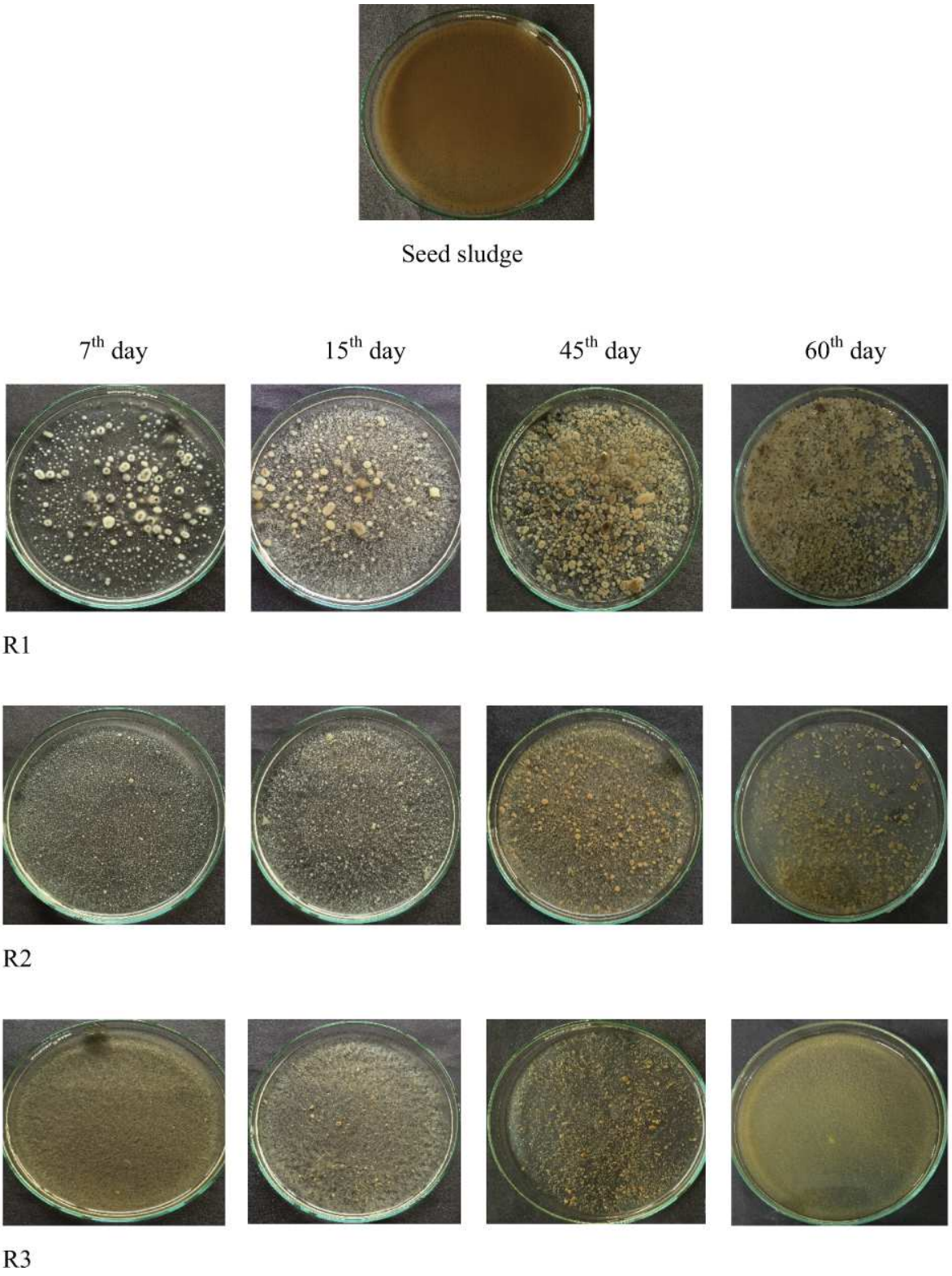

Fig. 2.3. Image of granules with operational time at varying cycle time.

study. In reactor R2, Fig. 2.3 depicts the presence of a single granule on day 7th. The granule's shape was mainly spherical but less in numbers than R1. In reactor R3, small number of granules started appearing on day 15th and increased slightly on day 45th. However, on day 60th, no granule was seen in the image (Fig. 2.4). FESEM images of granules are shown in Fig. 2.4. In R1 and R2, initially, filamentous growth was observed (5th day), which later became compact granule (55th day).

Size distribution of biomass and D50 values in three reactors with operational time is shown

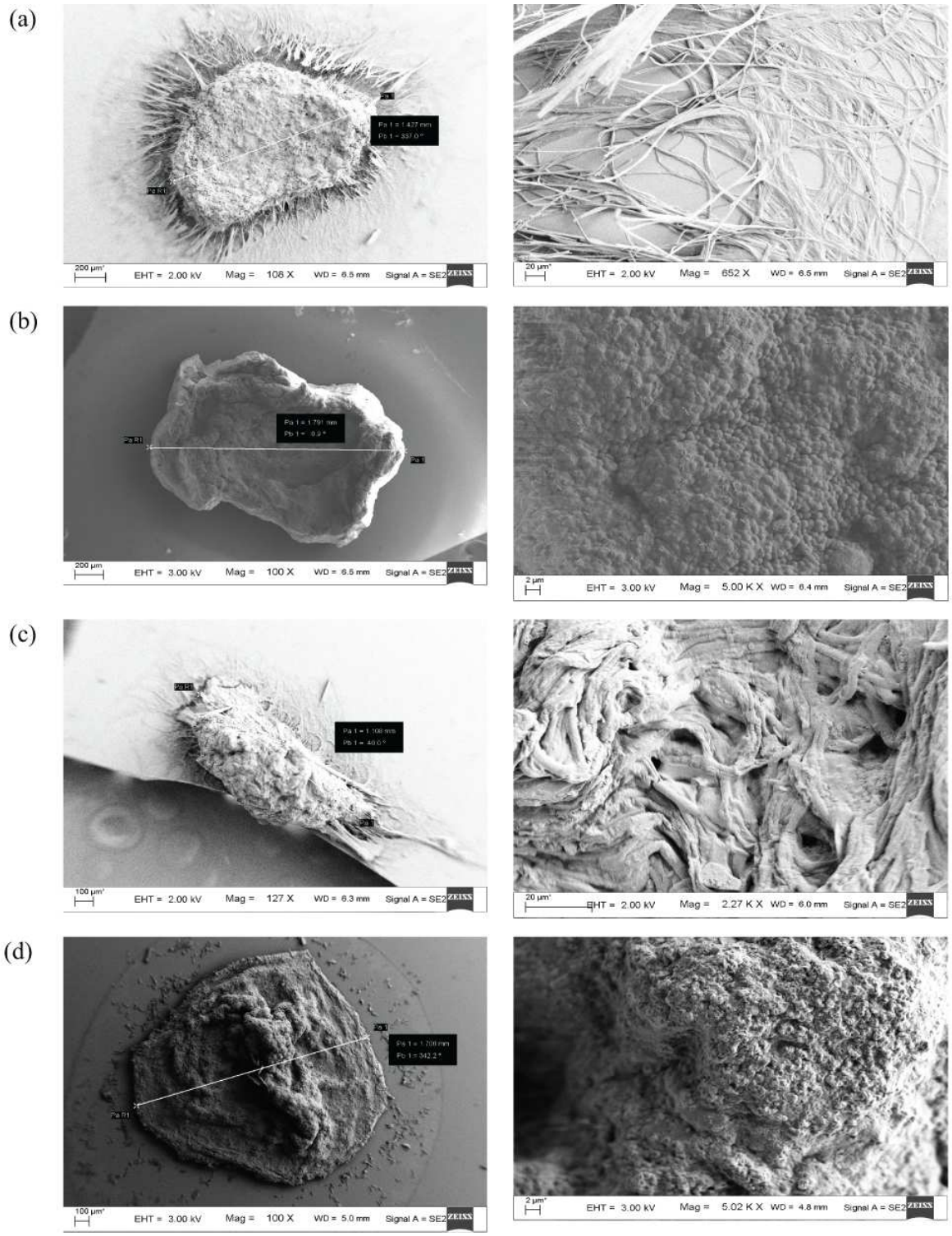

Fig. 2.4. FESEM images of granules of (a) R1 on 5th day, (b) R1 on 55th day, (c) R2 on 5th day and (d) R2 on 55th day for cycle time study.

in Fig. 2.5. The initial size of seed sludge was 34 μm. In R1 and R2, within initial 10 days, mean size increased to 1000-1200 μm and then granule size decreased to 500 μm. In R1, granule size again increased and stabilized to 1200 μm and remained stable throughout the study period. Almost 40% of the granules in R1 were in the size range of 1-1.6 mm (1000-1600 μm). In R2, granules size decreased steadily with operational period and finally, the large fraction was of the size range <0.1 mm (100 μm) and only 20% were in range of 1.0-1.6 mm (1000-1600 μm). In reactor R3, granule development was poor with the maximum size of 360 μm, which further decreased with time. In R3,

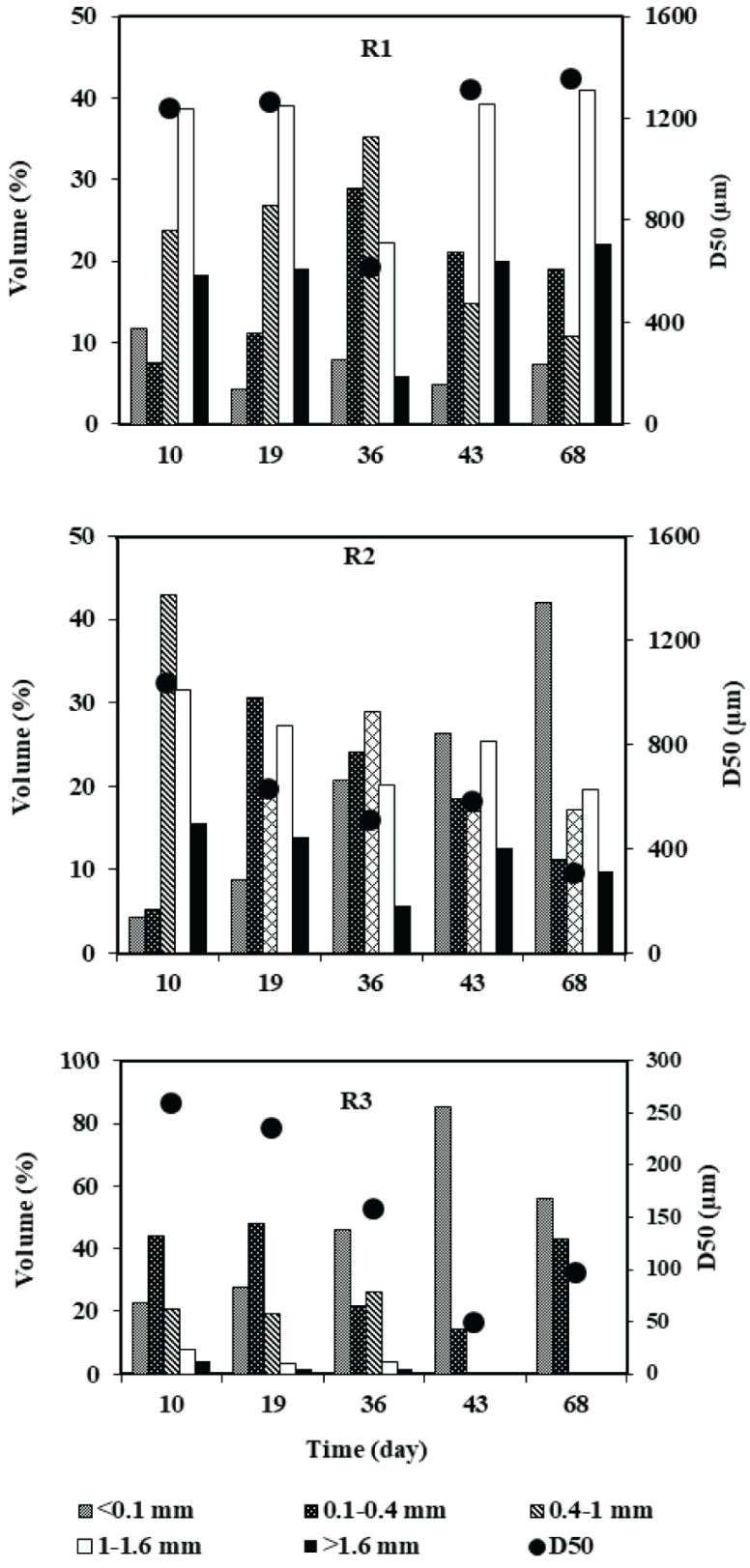

Fig. 2.5. Size distribution of granular biomass for the three reactors for cycle time study.

all granules were less than 0.4 mm (400 µm). During the steady-state period, average granule size in R1, R2, and R3 were 1334.24±30.56, 520.94±343.18 and 97.93±4.21 µm, respectively. It seems that with an increase in the reactor cycle time, substrate loading in the reactor decreased and more was the disintegration of granules resulting in a smaller size, which was similar to other research works

(Chen et al., 2008; Liu and Tay, 2007b). Liu and Tay (2007a) reported that with the increase in cycle time, starvation time increased and granulation reduced in acetate fed AGR. This study showed that with phenol, thiocyanate, and ammonia containing wastewater, a cycle time of 6 h with an OLR of 2.03 kg COD m^{-3} day^{-1} and NLR of 0.20 kg NH_4^+-N m^{-3} day^{-1} is quite adequate to achieve granulation. Tay et al. (2001a) reported biomass size of 370 μm at organic loading of 6 kg COD m^{-3} day^{-1} with an air flow rate of 2.0 L min^{-1} (same air flow rate as in present study). Granule size observed in R1 and R2 were comparable to these findings at much lower organic loading (2.03 and 1.02 kg COD m^{-3} day^{-1}, respectively).

Concentrations of VSS (g L^{-1}) in three reactors are shown in Fig. 2.6a. From initial VSS of 0.8 g L^{-1}, it increased steadily in R1 and after the acclimatization period, VSS concentration increased to 4.08±0.11 g L^{-1}. In steady-state period, average VSS in R1 was 4.31±0.40 g L^{-1}. At the end of the acclimatization phase, VSS increased to 1.33±0.26 g L^{-1} in R2 and 0.99±0.12 g L^{-1} in R3. During steady-state, average VSS concentrations were 2.01±0.22 g L^{-1} and 2.28±0.13 g L^{-1}, respectively, in R2 and R3. Due to the higher load applied in R1, VSS was higher in R1 as compared to R2 and R3. In R1, no steady-state was observed in terms of VSS and it increased as the operation continued, while VSS profile was stable in R2 and R3 (Fig. 2.6a). All three reactors were operated under the same conditions and same operation time except their loadings. Therefore, loading was the reason due to which VSS didnt get stabilized in R1. Liu et al. (2016) also reported that there was no steady-state found in terms of VSS at an HRT of 6 and 8 h with a high OLR of 8 kg COD m^{-3} day^{-1}. In R1, biomass concentration was almost two-fold of R2 and R3.

Initial SVI_{30} of seed sludge was 76.00 mL $gTSS^{-1}$ (Fig. 2.6b). In three reactors, initially, SVI_{30} value increased to 130-270 mL $gTSS^{-1}$ and then decreased gradually. During steady-state, these values were 67.69±7.13, 21.71±4.97, and 22.98±8.05 mL $gTSS^{-1}$ in R1, R2, and R3, respectively. SVI_{30} of R2 and R3 were almost three-fold less than R1. Yang et al. (2005) reported SVI value of 60.00 mL $gTSS^{-1}$ in acetate fed reactor at COD:N ratio of 10 (similar to COD:N ratio of this study). Lower SVI value of 30-60 mL $gTSS^{-1}$ was found to be suitable for shortening the settling phase resulting in the improved and faster sedimentation (Janczukowicz et al., 2001). Tay et al. (2004), achieved granulation with mean size and SVI value of 520-1200 μm and 40.0±5.6-60.5±5.0 mL gTSS -1, respectively, by using phenol at an organic load of 1.5-2.5 kg phenol m^{-3} day^{-1}. Kim et al. (2008a) used glucose and acetate with an organic load of 2.52 kg COD m^{-3} day^{-1} and observed granulation with the size of >390.9 μm, which was rarely more than 1400 μm and SVI value of 99 mL $gTSS^{-1}$ (Table 2.4). As compared to the findings of Tay et al. (2004) and Kim et al. (2008a), the present study was found to be more advantageous in terms of the size of the granules. In R1, bigger granules (1334.24±30.56 μm) were achieved in spite of having the low organic load of 2.03 kg COD m^{-3} day^{-1} (0.8 kg phenol m^{-3} day^{-1}) as compared to their research works and SVI values were found to be nearly similar to a previous study (Tay et al., 2004).

GSV is given in Fig 2.6c. GSV was measured from day 20^{th} onwards. Initial GSV were 22, 30 and 39 m h^{-1} in R1, R2, and R3, respectively. At the end of the acclimatization period, this increased both in R1 and R2 to 37 m $h^{-1}$and 42 m h^{-1}, respectively, but decreased in R3 to 28 m h^{-1}. In the steady-state, average GSV values were 35.79±2.20, 39.80±2.10, and 30±7.36 m h^{-1} in R1, R2 and R3, respectively. Janczukowicz et al. (2001) described the role of settling velocity in wastewater treatment and was found to be important in avoiding sludge bulking. High settling velocity carried out by the aerobic granular sludge allows the granules to prevent from being washed out from the

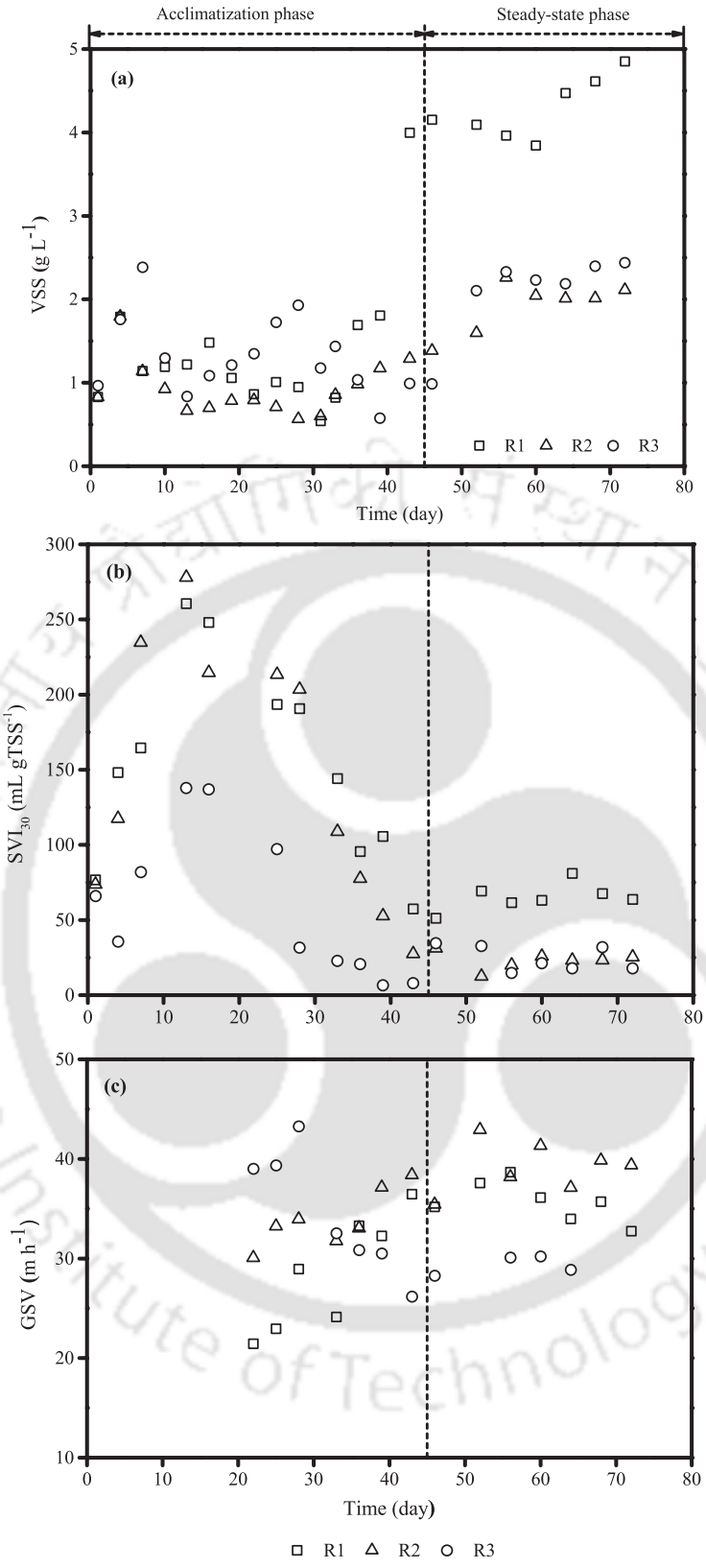

Fig. 2.6. Granule characteristics (a) VSS, (b) SVI_{30} and (c) GSV for the three reactors with different cycle time.

reactor during the withdrawal phase (Salmiati et al., 2015).

Comparing the results of Fig. 2.5 with 2.6b and 2.6c, it can be inferred that R1 sludge was having lower GSV with higher SVI_{30} as compared to R2. The possible reason for this might be higher OLR and NLR applied to the R1 as compared to R2. Though the SVI_{30} values were higher in R1 than

the R2 and R3 but were quite comparable to the previous research works (Tay et al., 2004; Yang et al., 2005). A similar phenomenon was reported by Liu et al. (2016) in acetate fed AGR where higher SVI value of 80.00 mL $gTSS^{-1}$ was observed in more granulated sludge and it was concluded that SVI should not be the only parameter to evaluate granulation in AGR. From the present study, it was observed that only SVI cant be a decisive factor for settling property of granules and settling behaviour was affected by the load applied.

Food to microorganism (F/M) ratios were 0.47, 0.51 and 0.22 g COD $gVSS^{-1}$ day^{-1} in R1, R2 and R3, respectively. F/M was calculated using equation 2.4 (Ben and Semmens, 2003). F/M ratio of 0.4-0.5 g COD gSS^{-1} day^{-1} was suitable for the aerobic granules having excellent settleability along with the high pollutant removal efficiency (Wu et al., 2018). F/M ratio of 0.47 g COD $gVSS^{-1}$ day^{-1} also might be a possible reason for getting granules with excellent characteristics and pollutant removal profiles in R1, which was in the range of the F/M ratio as mentioned by Wu et al. (2018).

$$\frac{F}{M}=\frac{QS_0}{VX} \tag{2.4}$$

Where Q represents the influent flow rate (L day^{-1}), S_0 is the substrate concentration (g L^{-1}), V is the working volume of the reactor (L) and X is the VSS in the reactor (g L^{-1}).

2.3.4.2 Organic and nitrogen removal performance

The OLRs and NLRs were different in all three reactors. The OLRs were 2.03, 1.02, and 0.51 kg COD m^{-3} day^{-1} and the NLRs were 0.20, 0.10 and 0.05 kg NH_4^+-N m^{-3} day^{-1} in R1, R2, and R3, respectively, (Table 2.2), with influent COD: NH_4^+-N ratio of 10.2. The pollutant removal performance at different cycle times during steady-state is provided in Table 2.5. Phenol removal in R1, R2 and R3 was 99% and above during acclimatization and steady-state conditions from influent of 400 mg L^{-1} (Fig. 2.7a). Effluent phenol concentrations were 0.25±0.02, 0.22±0.03 and 0.12±0.01 mg L^{-1}, respectively in R1, R2, and R3. COD removal was 94-96% in three reactors from the influent value of 1015.71±33.83 mg L^{-1} during steady-state (Fig. 2.7b). Effluent COD values were higher in reactor R2 (104.67±1.34 mg L^{-1}) as compared to other two reactors (38.92±2.74 and 42.99±3.75 mg L^{-1} in R1 and R3, respectively). High COD removal confirms mineralization of intermediates formed from phenol oxidation in AGR.

In R1 and R2, SCN^- removal decreased when the influent SCN^- concentration was more than 20 mg L^{-1} and this continued up to feed SCN^- concentration of 90 mg L^{-1} in R1 (from days 13 to

Table 2.5. Pollutant removal performance at different cycle times during steady-state.

Pollutant	R1			R2			R3		
	Influent (mg L^{-1})	Effluent (mg L^{-1})	% removal	Influent (mg L^{-1})	Effluent (mg L^{-1})	% removal	Influent (mg L^{-1})	Effluent (mg L^{-1})	% removal
Phenol	394.85 ±3.07	0.25 ±0.02	99.94 ±0.05	396.28 ±2.42	0.22 ±0.03	99.94 ±0.03	400.26 ±2.19	0.12 ±0.01	99.97 ±0.02
COD	1015.71 ±33.83	38.92 ±2.74	96.16 ±1.68	1015.71 ±33.83	104.67 ±1.34	93.78 ±0.75	1015.71 ±33.83	42.99 ±3.75	95.69 ±2.10
SCN^-	94.89 ±2.90	0.44 ±0.37	99.53 ±0.40	95.36 ±2.38	0.35 ±0.22	99.64 ±0.22	96.88 ±1.06	0.18 ±0.12	99.82 ±0.12
NH_4^+-N	99.18 ±2.40	0.14 ±0.01	99.86 ±0.07	101.83 ±0.61	0.09 ±0.01	99.91 ±0.10	97.95 ±0.88	0.23 ±0.01	99.76 ±0.20

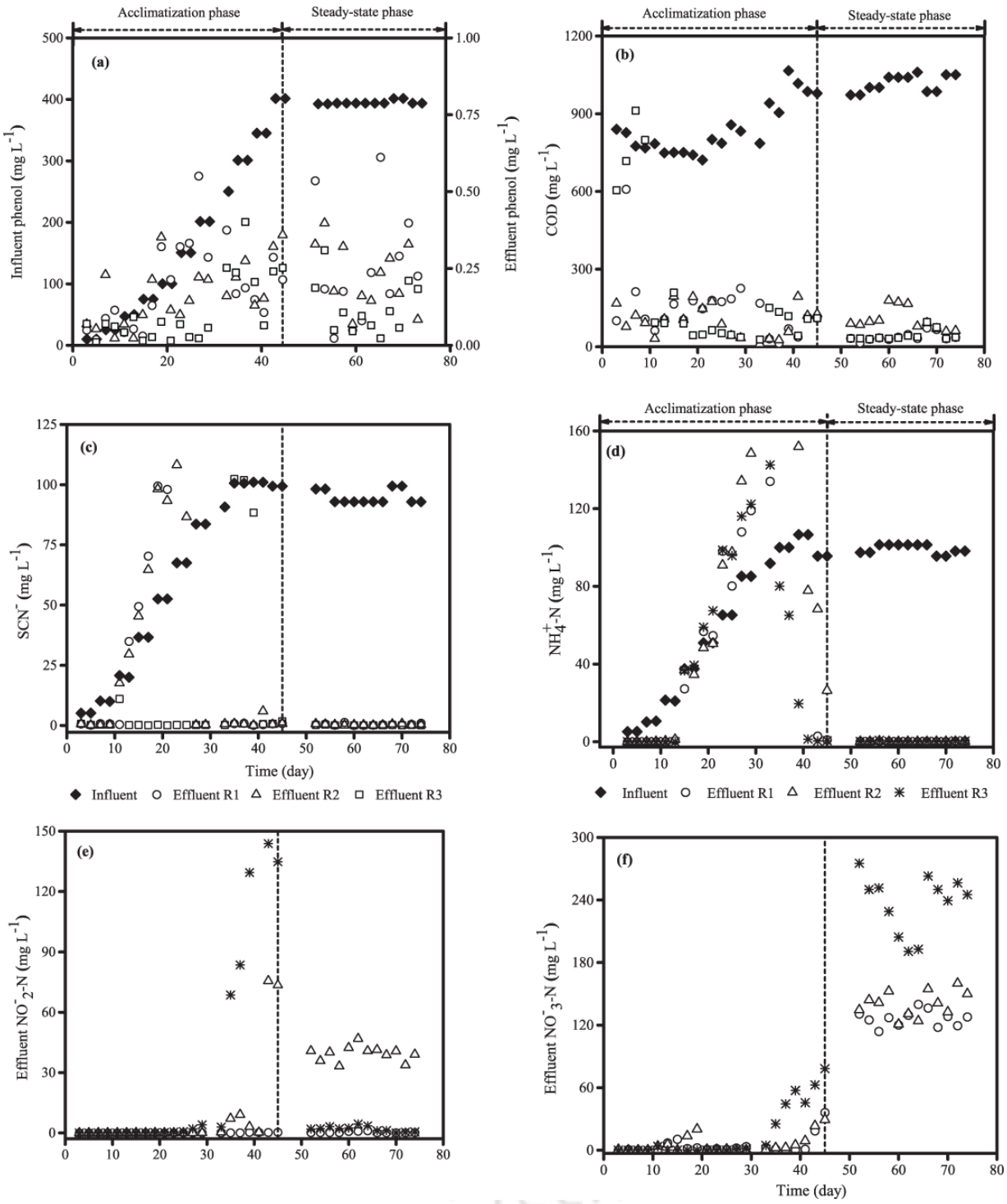

Fig. 2.7. Influent and effluent (a) phenol, (b) COD, (c) thiocyanate, (d) NH_4^+-N, (e) NO_2^--N and (f) NO_3^--N in R1, R2 and R3 at different cycle times.

33) and up to 65 mg L^{-1} feed SCN^- in R2 (from days 13 to 25) (Fig 2.7c). The possible reason for this might be that the granules couldnt get acclimatized with an increase in SCN^- concentration because of not getting enough time to degrade SCN^-, due to the operation of R1 and R2 at lower HRTs. As soon as granules became acclimatized to higher SCN^- concentrations, almost complete removal was observed in R1 and R2 throughout the study (from days 35 and 27 onwards, respectively) (Fig 2.7c). R3 showed more stable performance in removing SCN^- up to the influent concentration of 90 mg L^{-1}, probably due to the availability of longer reaction time to transform thiocyanate. As SCN^- concentration increased to 100 mg L^{-1} (35^{th} day) in R3, no SCN^- removal was observed because of

the inhibition to the granular activity for degrading SCN^- caused by the toxic effect of higher SCN^- concentration (100 mg L^{-1}). After one week of stable operation with SCN^- concentration of 100 mg L^{-1} (from days 34 to 41), granules again became susceptible to degrade SCN^- and continued to exhibit the same performance throughout the study (Fig 2.7c). During the steady-state, effluent SCN^- was less than 1 mg L^{-1} in all three reactors with the removal efficiencies of 99%. Sulfate was present in the reactors, though quantitative estimation was not made, suggesting SCN^- oxidation followed equation 1.2.

NH_4^+-N removal profile shows that during the acclimatization in initial 13 days with influent concentration up to 20 mg L^{-1}, a very low concentration of NH_4^+-N was observed in the effluent of all the reactors (Fig. 2.7d). With the increase of NH_4^+-N in influent above 20 mg L^{-1}, removal efficiency decreased substantially and reactors required an additional 20 days for the start-up of nitrification. This could be due to the time required for the development of nitrifying bacteria in three reactors. In the steady-state, NH_4^+-N removal was 99% in three reactors from the influent of 100 mg L^{-1} with effluent concentrations of 0.14±0.01, 0.09±0.01, and 0.23±0.01 mg L^{-1}, in R1, R2, and R3, respectively. The present study showed that the granulation in AGR was directly related to the loadings (organic and nitrogen) and inversely related to the reactor cycle time; however, phenolic organics removal and nitrification were independent of granulation in AGR.

During steady-state, in R1 and R3, effluent NO_2^--N concentrations were found negligible, but in R2, effluent NO_2^--N was almost 40 mg L^{-1} (Fig. 2.7e). Effluent NO_3^--N concentrations in R1, R2, and R3 were 126.41±7.60, 140.60±12.37, and 237.31±27.57 mg L^{-1}, respectively (Fig. 2.7f). Nitrification was complete to nitrate in R1 and R3 suggesting the presence of both ammonia-oxidizing bacteria (AOB) and nitrite-oxidizing bacteria (NOB) in these two reactors. In R2, nitrification was partial. Previous literature works reported that longer solid retention time (SRT) favors the growth of NOB, whereas shorter SRT inhibits the growth of NOB resulting in the accumulation of nitrite (Pollice et al., 2002; Wan et al., 2013). SRT was calculated using equation 2.5 (Liu and Tay, 2007a).

$$SRT = \frac{X_{VSS}V}{X_e V_e / t_c} \tag{2.5}$$

Where X_{VSS} represents the VSS inside the reactor (g L^{-1}), V is the working volume of the reactor (L), X_e is the VSS in the effluent (g L^{-1}), V_e is the volume of the effluent withdrawal (L), and t_c is the cycle time of the SBR (day). The SRT values were around 14, 6, and 10 days in R1, R2, and R3, respectively (calculated from the effluent VSS of 0.16, 0.32, and 0.44 g L^{-1}, respectively, in R1, R2, and R3). R1 and R3 were having longer SRT as compared to R2, so complete nitrification was achieved, while in R2, the growth of NOB was inhibited due to shorter SRT. The SRT values of R1 and R3 were in the range of the standard values for achieving nitrification (10-30 days) (Tchobanoglous et al., 2003).

Influent nitrogen consisted of feed NH_4^+-N along with nitrogen generated from SCN^- degradation (Equation 2.6) (1 mg of SCN^- yields 0.24 mg of NH_4^+-N, Equation 1.2)

$$\text{Influent nitrogen} = \left(\Sigma \text{influent } NH_4^+\text{-N} + 0.24 \times \text{influent } SCN^-\right) \tag{2.6}$$

Influent nitrogen was 124 mg L^{-1}. Effluent NH_4^+-N in R1, R2, and R3 were 0.14, 0.09, and 0.23 mg L^{-1}, respectively (Fig. 2.7d). Nitrogen used for biomass growth was calculated from SRT of

the reactor (Equation 2.7) and were observed as 19.16, 40.20, and 52.32 mg L^{-1} in R1, R2, and R3, respectively.

$$\text{Nitrogen used for biomass growth} = 0.12\, P_{X,bio}/Q \tag{2.7}$$

Where $P_{X,\,bio}$ represents the biomass wasted daily (mg VSS day^{-1}) and was calculated by equation 2.8 and Q is the influent flow rate (L day^{-1}) (12, 6 and 3 L day^{-1}, respectively, in R1, R2, and R3) (Tchobanoglous et al., 2003).

$$P_{X,bio} = \frac{X_{VSS}V}{SRT} \tag{2.8}$$

Theoretical nitrogen oxidized was 104.70, 83.71 and 71.45 mg L^{-1} in R1, R2, and R3, respectively (Equation 2.9) (Tchobanoglous et al., 2003).

$$\text{Theoretical nitrogen oxidized (mg } L^{-1}) = \left[\begin{array}{l}\text{influent nitrogen (mg}L^{-1}) - \text{effluent } NH_4^+\text{-N (mg } L^{-1}) \\ -\text{nitrogen used for biomass growth (mg } L^{-1})\end{array}\right] \tag{2.9}$$

Actual nitrogen oxidized was obtained from Σ effluent NO_2^--N + NO_3^--N. Actual nitrogen oxidized was 126.81, 179.98 and 239.39 mg L- in R1, R2, and R3, respectively. Higher effluent nitrogen than influent suggested the absence of denitrification. Denitrification was absent because of small granule size (1300 μm). The same phenomenon was also observed by Corsino et al. (2015) with a mature granule size of 1000 μm with the absence of simultaneous nitrification/denitrification (SND). Higher effluent nitrogen than influent nitrogen was due to the accumulation of oxidized nitrogen (NO_2^--N and NO_3^--N) from previous cycles. In every cycle, 50% of supernatant was withdrawn from each reactor. Cycle time in R1 was much lower (6 h) than R2 (12 h) and R3 (24 h) and 50% volume was withdrawn/cycle. Volumes of supernatant withdrawn daily from each 6 L reactor volume were 12 L, 6 L, and 3 L in R1, R2, and R3, respectively. In reactor R3, maximum accumulation of nitrate occurred due to the minimum cycle time of this reactor.

It was clear that phenol and SCN^- concentrations of 400 and 100 mg L^{-1}, respectively, did not inhibit nitrification in any of the three reactors. Liu et al. (2005) demonstrated that microbial granules possessing nitrifying bacteria were found to sustain phenol up to 10 mg L^{-1} with NH_4^+-N concentration up to 150 mg L^{-1}. Kim et al. (2008b) reported that phenol concentration ⩾200 mg L^{-1}, in activated sludge system, strongly inhibited the nitrification process. Yang et al. (2014) reported 60% nitrification efficiency with domestic wastewater from influent concentrations of 167 mg L^{-1} COD and 45 mg L^{-1} NH_4^+-N in a continuous flow granular reactor at reactor HRT of 2 h. Maranon et al. (2008) reported complete phenol and SCN^- removals along with 60-70% COD removal from influent concentrations of 200, 250 and 1500 mg L^{-1}, respectively, in a three-stage anoxic-aerobic suspended growth activated sludge process having a total HRT of 229 h. In the present study, influent COD and NH_4^+-N concentrations were much higher and 99% NH_4^+-N removal efficiency was achieved at a cycle time of 6 h in R1. It is clear that present AGR showed higher COD and comparable phenol and SCN^- removals at much lower HRT. Ramos et al. (2016b) reported aerobic granulation with high strength wastewater containing ammonia and aromatic compounds like phenol, *o*-cresol, quinoline with high NLR of 1.10 kg N m^{-3} day^{-1} and OLR of 0.70 kg COD m^{-3} day^{-1} at HRT of 6.3 to 0.9 days (21.6 h). In the present study, aerobic granulation was achieved with an HRT of 12 h along with OLR and NLR of 2.03 kg COD m^{-3} day^{-1} and 0.20 kg NH_4^+-N m^{-3} day^{-1} respectively. The present study was found to be better in terms of NLR (0.13 kg NH_4^+-N m^{-3} day^{-1}) reported by Kong et al. (2013) with synthetic wastewater at an OLR of 2.09 kg COD m^{-3} day^{-1}, which is nearly same to the present study.

So the present study showed AGR, a possible substitute for simultaneous removals of high phenolics and nitrogen at a lower HRT.

2.3.4.3 Effect of cycle time on EPS

Literature reports mentioned EPS content in sludge is responsible for granule formation and stability in AGR. EPS is a combination of PN and PS. In Fig. 2.8a, PN and PS values in three reactors are shown. Initial PN value was around 27-31 mg $gVSS^{-1}$. The increase in PN value from the acclimatization phase to the steady-state phase was distinct in three reactors. The increase in PS was less profound than PN in three reactors. Total sludge EPS increased with operational time from 45.93±0.87 to 79.65±8.42 mg $gVSS^{-1}$ in R1, 43.84±0.78 to 63.99±3.59 mg $gVSS^{-1}$ in R2 and 37.94±4.05 to 44.36±2.42 mg $gVSS^{-1}$ in R3 (Fig. 2.8b). It can be inferred that with a decrease in reactor cycle time by four-fold, total sludge EPS increased by two-fold and higher EPS was responsible for better granulation in R1. In Fig. 2.8b, change in PN/PS ratio with operational time is also shown. It can be seen that PN/PS

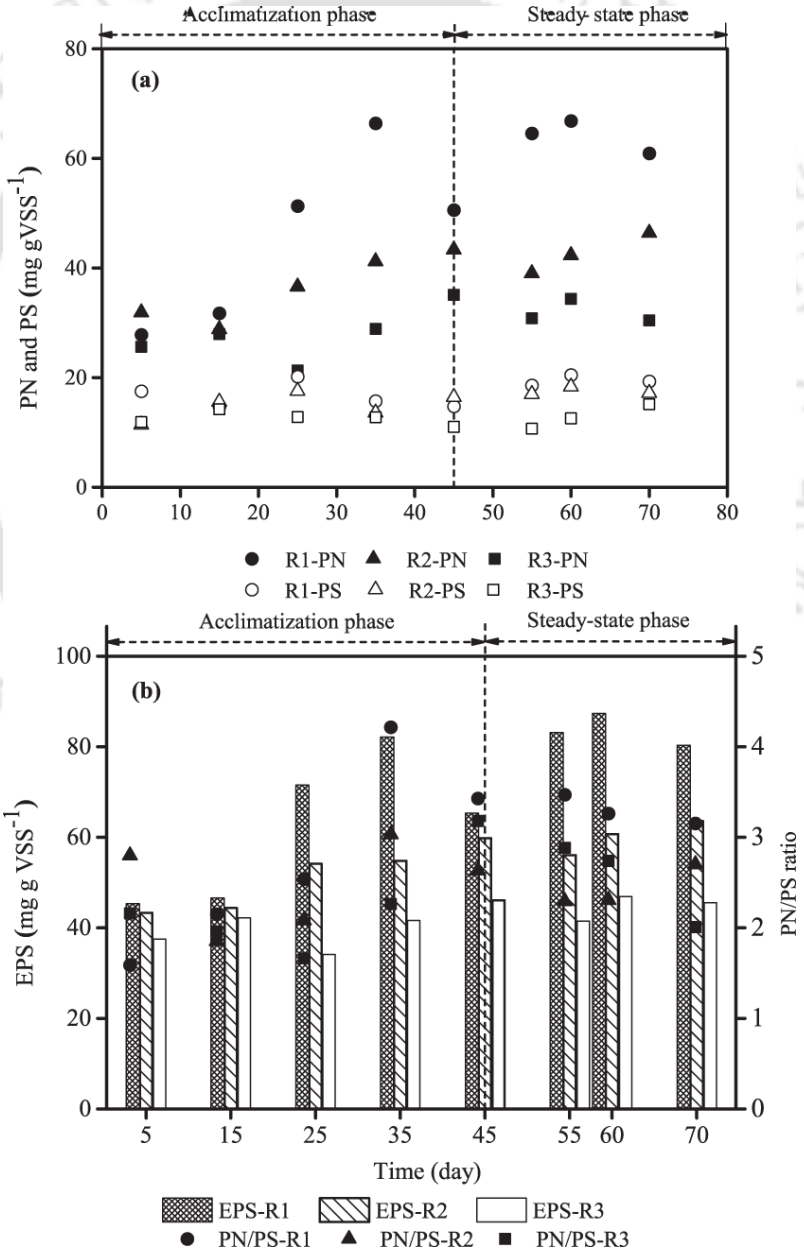

Fig. 2.8. Concentrations of (a) PN and PS in sludge and (b) total EPS and PN/PS ratio in sludge for three reactors at different cycle times.

ratio was maximum in three reactors during 35-45 days. This time period (i.e. 35-45 days) was the end part of the acclimatization period during which influent pollutant concentrations almost achieved the target levels. The PN/PS ratio of 3.33±0.15 was observed in R1 at steady-state corresponding to 2.48±0.21 and 2.01±0.50 in R2 and R3, respectively. Adav et al. (2007) reported PN/PS ratio of 3.4-5.3 in a phenol fed AGR with NH_4^+-N concentration of 106 mg L^{-1}, which was similar to R1 in this study. In the literature, it is documented that PN/PS ratio in aerobic granular sludge (AGS) was dependent on substrate type and operational parameters (McSwain et al., 2005). Jemaat et al. (2014) reported PN/PS ratio of 0.66 in an AGR fed with glucose, sucrose, NH_4^+-N and para-nitrophenol. Zhu et al. (2012) reported PN/PS ratio of 12.5 with 4-chloroaniline and glucose fed AGR. Yang et al. (2005) observed an inverse relationship between PN/PS ratio and feed COD/N ratio. The present study showed that PN/PS ratio was strongly dependent on operational parameters like cycle time at a constant feed COD/N ratio. It is also obvious that PN played a more significant role in granule formation as compared to PS with phenol, thiocyanate and ammonia containing wastewater. Previous research works pointed out a similar role of PN with glucose and acetate containing wastewater (Adav et al., 2007; Gao et al., 2011a; McSwain et al., 2005).The EPS secreted by microorganisms can also clog the pores within the aerobic granules resulting in the decrement in permeation and settling velocities (Basheer and Farooqi, 2014), as observed in the present study (R1 was having low settling ability than R2 and R3).

2.3.5 Conclusion of cycle time study

Aerobic granules were successfully cultivated with phenol, thiocyanate and ammonium at different cycle times and organic and nitrogen loadings. Large granules with higher biomass concentration were observed at 6 h cycle time (OLR of 2.03 kg COD m^{-3} day^{-1} and NLR of 0.20 kg NH_4^+-N m^{-3} day^{-1}). With a decrease in the cycle time by four-fold, EPS in the sludge increased by two-fold. Effect of cycle time was insignificant on reactor performance with more than 99% phenol and thiocyanate removals and 95% reduction of COD. Complete nitrification was observed at different cycle times.

2.4 Effect of ULV on characteristics and performance of reactor R1

The effect of two ULVs, 2.5 and 3.0 m h^{-1}, was investigated in R1 for its impact on granule characteristics and pollutant's degradation profiles. R1 was selected because it showed maximum granules with the highest VSS, EPS and pollutants degradation profile. Up to 75 days, R1 was operated at a ULV of 2.0 m h^{-1}, at which cycle time and loading study was carried out. From day 75 to 89, R1 was acclimatized with ULV of 2.5 m h^{-1} and analyzed from days 90 to 120. The acclimatization period for ULV of 3.0 m h^{-1} was from 121 to 141 days and since then up to 155 days, analysis for characteristics and performance of R1 for ULV 3.0 m h^{-1} was done.

Fig. 2.9a showed that granules were bigger in size at 2.5 m h^{-1} with an average size (D50) of 1353.64±0.02 μm than that of 3.0 m h^{-1} (1138.01±0.03 μm). Biomass concentration was found to be more at ULV of 2.5 (4.72±0.13 g L^{-1}) as compared to 3.0 m h^{-1} (4.55±0.26 g L^{-1}) (Fig. 2.9a). Lower SVI_{30} and higher GSV were observed at ULV of 2.5 (61.53±1.75 mL $gTSS^{-1}$ and 41.83±1.49 m h^{-1}, respectively) as compared to 3.0 m h^{-1} (67.33±1.64 mL $gTSS^{-1}$ and 36.36±0.78 m h^{-1}, respectively) (Fig. 2.9a). Stress conditions are one of the main causes for the production of EPS responded by the cells (Kong et al., 2015). EPS promotes the stability and communication of cells resulting in the enhancement of microbial aggregation (Kong et al., 2014). PN, PS and EPS were found to be less at ULV 3.0 m h^{-1}as compared to ULV of 2.5 m h^{-1} (Fig. 2.9b), confirming that EPS was one of the

parameters responsible for granulation.

Granule characteristics at different ULVs are given in Table 2.6. R1 was operated for 75 days at a ULV of 2.0 m h^{-1} and was compared with ULVs of 2.5 and 3.0 m h^{-1} for better understanding (Table 2.6). From the table values, it was clear that granules were showing better characteristics at ULV of 2.5 than 2.0 and 3.0 m h^{-1}, in terms of higher GSV, size and VSS and lower SVI_{30}. EPS was comparable at ULVs of 2.0 and 2.5 m h^{-1}. F/M ratios for all three ULVs were nearly same. F/M ratios were 0.47, 0.44 and 0.46 g COD $gVSS^{-1}$ day^{-1} at ULVs of 2.0, 2.5 and 3.0 m h^{-1}, respectively.

Pollutants degradation profile wise, there was no distinct difference was found at both ULVs. Phenol, COD, SCN^- and nitrogen profiles are given in Fig. 2.10. Complete nitrification was achieved at two different ULVs. From this study, it was observed that granules were very sensitive to ULVs. Granule characteristics were started to be deteriorated as the ULV was increased from 2.5 to 3.0 m h^{-1}. The possible reason for the disintegration might be that granules were not able to withstand with the

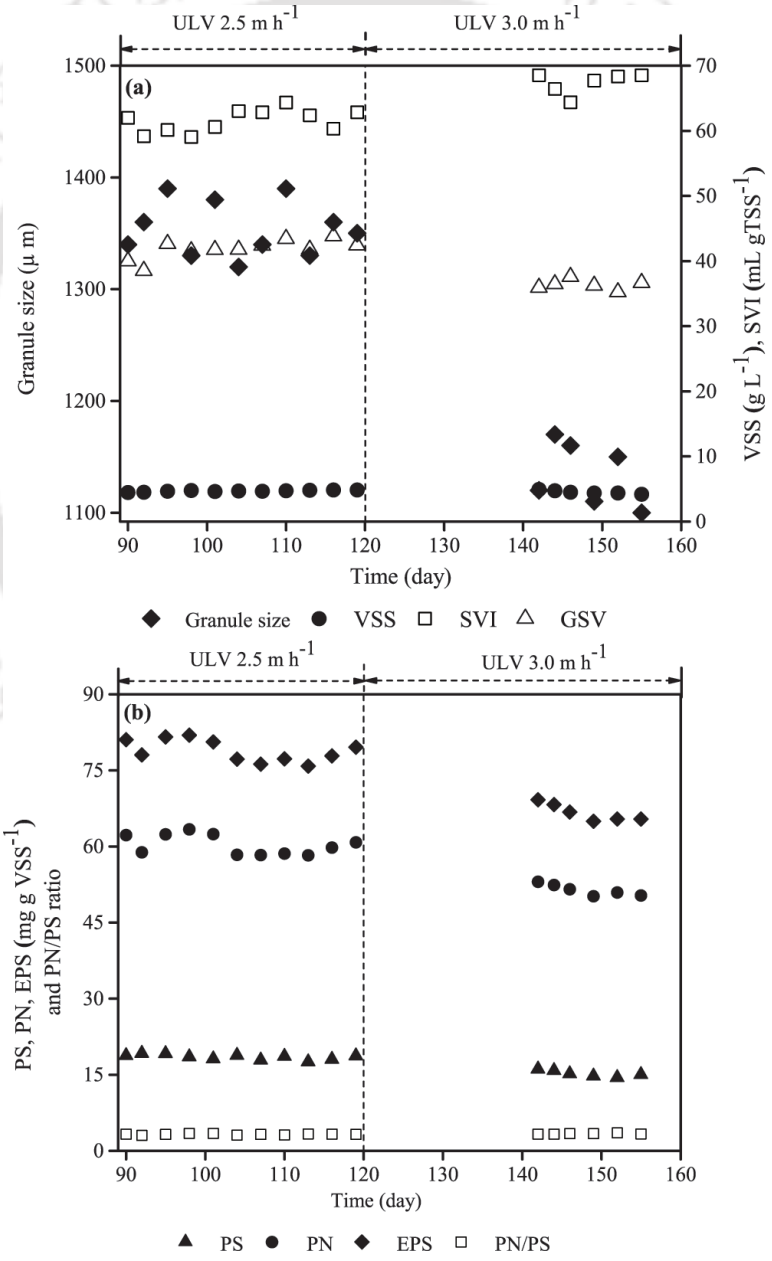

Fig. 2.9. (a) Granule size, VSS, SVI_{30} and GSV and (b) PS, PN, EPS and PN/PS ratio at two ULVs in R1.

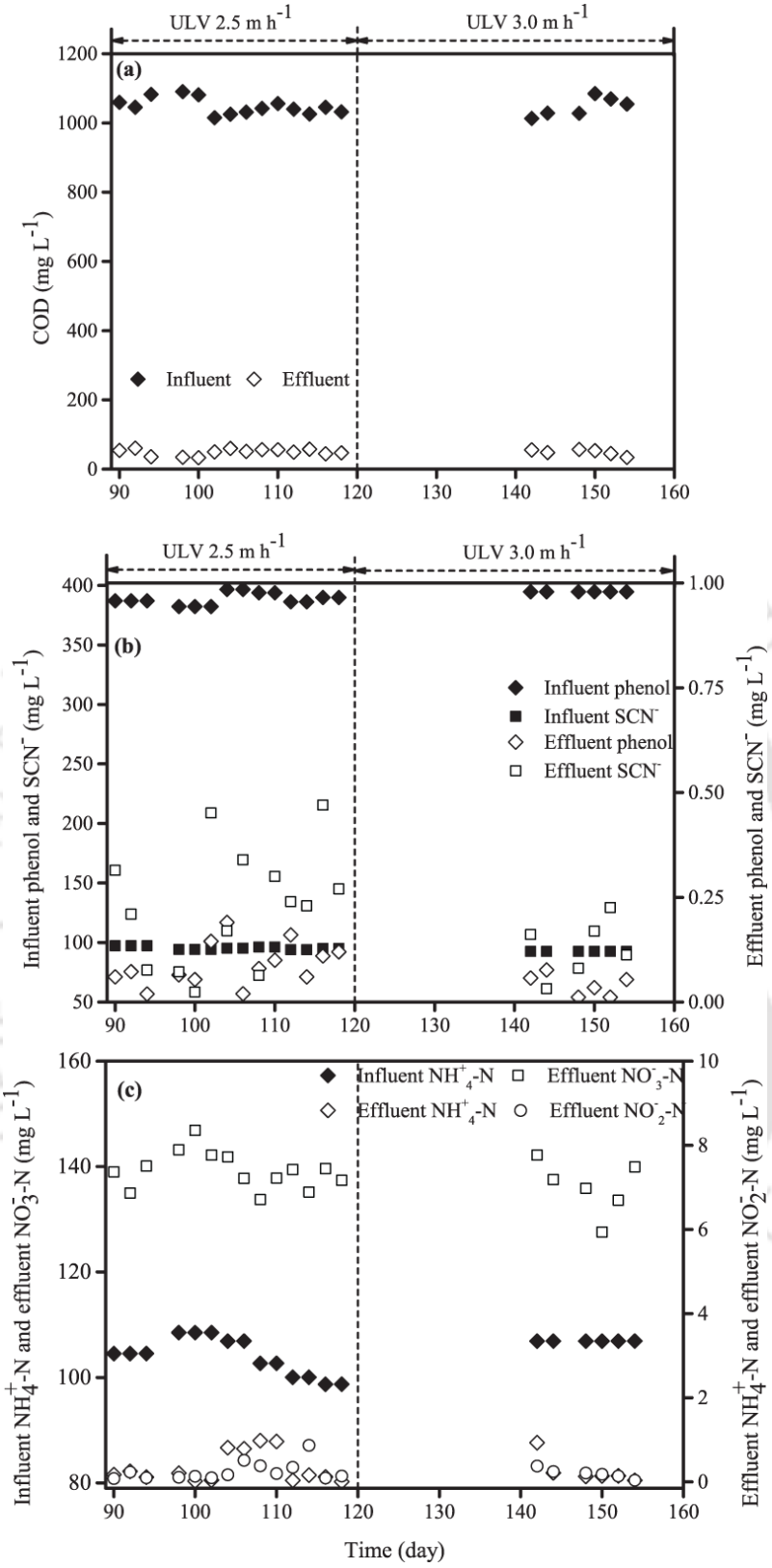

Fig. 2.10. Influent and effluent (a) COD, (b) phenol and thiocyanate and (c) nitrogen profile at two ULVs in R1.

pressure generated at higher ULV resulting in the breakdown of granules. Thus, it can be concluded that ULV can be a selection pressure for better granulation. To the best of the authors knowledge, no study addressed the effect of ULV on aerobic granular characteristics, but literature works are available for evaluating the effect of ULV on anaerobic granulation. Bárcenas Ruiz et al. (2016) investigated

Table 2.6. Characteristics of granules at different ULVs in R1.

Characteristics	ULV (m h^{-1})		
	2.0[a]	**2.5**[b]	**3.0**[c]
VSS (g L^{-1})	4.31±0.40	4.72±0.13	4.55±0.26
SVI_{30} (mL g TSS^{-1})	67.69±7.13	61.53±1.75	67.33±1.64
GSV (m h^{-1})	35.79±2.20	41.83±1.49	36.36±0.78
Average granule size (μm)	1334.24±30.56	1353.64±0.02	1138.01±0.03
PN (mg $gVSS^{-1}$)	61.87±6.73	60.32±1.99	51.44±1.15
PS (mg $gVSS^{-1}$)	17.78±2.43	18.51±0.53	15.24±0.06
EPS (mg $gVSS^{-1}$)	79.65±8.42	78.83±2.19	66.68±1.72
PN/PS ratio	3.33±0.15	3.26±0.12	3.38±0.08
F/M ratio (g COD $gVSS^{-1}$ day^{-1})	0.47	0.44	0.46

Reactor operation time (days): [a]1-75, [b]75-120, [c]120-155

the effect of ULV on the anaerobic granular biomass and observed that anaerobic granules were able to tolerate ULV within the range of 2.5-4.5 m h^{-1}. At a ULV of more than 4.5 m h^{-1}, granules were started to disintegrate resulting in the washout from the reactor. In the present study, granules were very stable at 2.0 and 2.5 m h^{-1} ULVs and started to degrad at the ULV of 3.0 m h^{-1}. ULV of 2.5 m h^{-1} was found to be appropriate for better granulation and can be a selection pressure for granulation.

2.5 Air flow rate study

After achieving better granulation along with pollutants removal in a shorter time, a cycle time of 6 h was opted for the rest of the research work.

2.5.1 Reactor and experimental set-up

Three similar acrylic SBRs as used in the cycle time study were used (Fig. 2.1 and 2.2). Aeration was provided as fine air bubbles through an oil free air compressor by the air stones kept at the reactor bottom with 1.5, 2.5 and 3.5 L min^{-1} air flow rates resulting in hydraulic shear force in terms of superficial upflow air velocities of 0.88, 1.48 and 2.07 cm s^{-1} in R1, R2 and R3, respectively. DO concentration in R1 was 3.0-3.5 mg L^{-1}, while in R2 and R3, it was above 5.0 mg L^{-1}. The superficial upflow air velocity was calculated by using equation 2.10. The reactors were maintained at room temperature (25-30°C).

$$\text{Superficial upflow air velocity (cm } s^{-1}) = \frac{\text{Air flow rate (min } L^{-1})}{\text{Cross sectional area of reactor (m}^2)} \quad (2.10)$$

2.5.2 Characteristics of seed sludge and composition of synthetic wastewater

The seed sludge was taken from the activated sludge unit of wastewater treatment plant of Indian Oil Corporation Limited (IOCL), Noonmati, Guwahati, Assam. TSS and VSS in the seed sludge were 0.26±0.05 and 0.19±0.03 g L^{-1}, respectively. The seed sludge had a particle size of 49.41 μm with an SVI_{30} value of 208.60 mL $gTSS^{-1}$. 3 L sludge was used as inoculum for 6 L working volume in all three reactors. The reactors were fed with the same synthetic wastewater (Table 2.1) as was used for cycle time study with an OLR of 2.06 kg COD m^{-3} day^{-1} (0.80 kg phenol m^{-3} day^{-1}) and NLR of 0.20 kg NH_4^+-N m^{-3} day^{-1}. All the conditions used for the cycle time study were applied in this work except variation in air flow rates with the optimized cycle time of 6 h.

2.5.3 Operational strategy

The operational schedule of all three reactors is given in Table 2.7. Each reactor had a cycle time of 6 h and HRT of 12 h. Each 6 h cycle was comprised of four stages: influent feeding (30 min), aeration (320 min), settling (5 min) and effluent decanting (5 min). The effluent was withdrawn from the midpoint of the reactors maintaining 50% volume exchange ratio. For the initial 15 days, settling time was set to 15 min for preventing biomass washout from the reactor and then reduced to 5 min throughout the study.

Table 2.7. Operational schedule of reactors for air flow rate study.

Reactor	No of cycles d^{-1}	Cycle time (h)	HRT (h)	Air flow rate (L min^{-1})	SUAV (cm s^{-1})	OLR[a]	NLR[b]	ULV[c]
R1	4	6	12	1.5	0.88	2.06	0.20	2
R2	4	6	12	2.5	1.48	2.06	0.20	2
R3	4	6	12	3.5	2.07	2.06	0.20	2

[a]Organic loading rate (kg COD m^{-3} day^{-1}); [b]Nitrogen loading rate (kg NH_4^+-N m^{-3} day^{-1}); [c]Up-flow liquid velocity (m h^{-1}); SUAV: Superficial upflow air velocity.

During acclimatization, phenol, NH_4^+-N and SCN^- concentrations increased gradually in the feed. Sodium acetate with a 1000 mg L^{-1} concentration was added initially in the feed as a suitable carbon source during the acclimatization period. As the acclimatization period progressed, the pollutant concentrations in the feed increased, whereas sodium acetate concentration decreased gradually. After 34 days of the acclimatization, sodium acetate concentration was suspended and phenol, NH_4^+-N and SCN^- concentrations were reached to 400, 100 and 100 mg L^{-1}, respectively. Thereafter, all three reactors were operated for another one month (day 35-65) with the same feed and steady-state data was obtained.

2.5.4 Results and discussion

2.5.4.1 Characteristics of granules

The characteristics of granules developed at different air flow rates are given in Table 2.8. The progression of granule development in R1, R2 and R3 is illustrated in Fig. 2.11. There was no granular appearance in the seed sludge and it was brown in color. After 10 days of inoculation, less in

Table 2.8. Characteristics of granules at different air flow rates.

Characteristics	Air flow rate (L min^{-1})		
	1.5 (R1)	**2.5 (R2)**	**3.5 (R3)**
VSS (g L^{-1})	2.71±0.06	4.17±0.09	2.40±0.08
SVI_{30} (mL g TSS^{-1})	74.15±1.48	35.25±1.71	56.84±1.92
GSV (m h^{-1})	37.17±1.96	55.56±1.36	44.24±1.01
Average granule size (μm)	2433.82±146.37	2938.67±64.91	1791.47±36.24
PN (mg $gVSS^{-1}$)	68.98±0.98	107.43±1.52	76.47±1.14
PS (mg $gVSS^{-1}$)	21.18±1.17	37.65±1.74	27.84±1.43
EPS (mg $gVSS^{-1}$)	90.16±1.71	145.08±2.65	104.31±1.96
PN/PS ratio	3.27±0.18	2.86±0.13	2.75±0.14
SRT (days)	3.0	9.5	2.0
F/M ratio (g COD $gVSS^{-1}$ day^{-1})	0.76	0.49	0.86

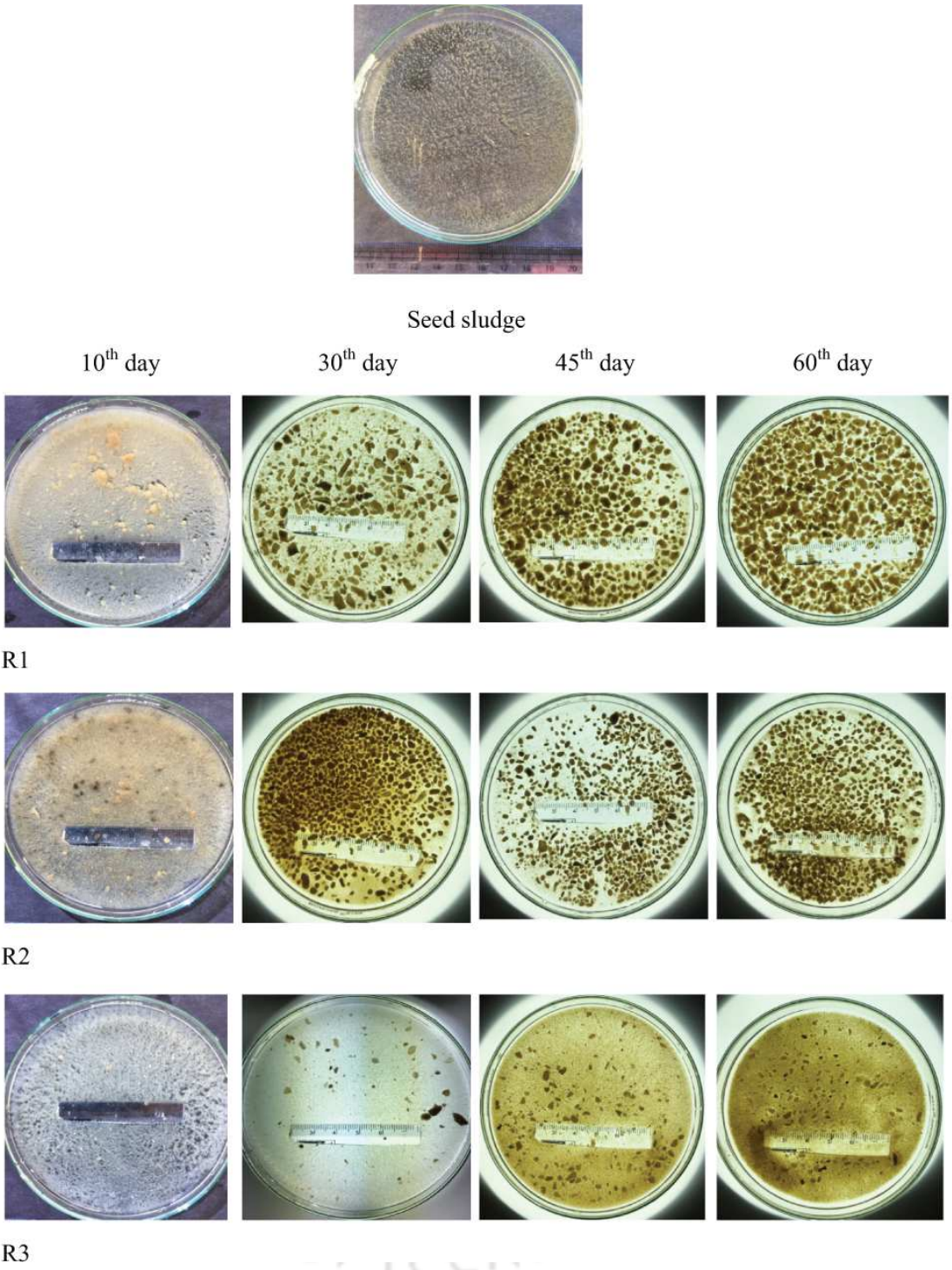

Fig. 2.11. Image of granules with operational time at different air flow rates.

number and irregular shaped granules appeared in R1 and R2 but for R3, granule took longer time to develop because of higher air flow rate (2.07 cm s^{-1} superficial upflow air velocity). The granules were stabilized from day 35 in all the reactors. FESEM images of 50th day granules are depicted in Fig. 2.12. In R1 granules were developed though having a loose structure. The granules of R1 did not possess a clear outline and were not as much compact and denser as were of R2 granules, because of weak shear force (0.88 cm s^{-1} superficial upflow air velocity). The granules of R2 were having a smooth, compact and regular structure because of intensive mixing by adequate aeration (1.48 cm s^{-1} superficial upflow air velocity). In R3, granules were compact but less in number because of biomass washout triggered by stronger hydraulic shear force applied (2.07 cm s^{-1} superficial upflow

air velocity) (Fig. 2.12). Adav et al. (2007) developed granules after 160 days at 3.0 L min^{-1} air flow rate with phenol as a sole carbon source. Ab Halim et al. (2016) observed granule formation after more than 30 days with an acetate based synthetic wastewater at 2.0 cm s^{-1} superficial upflow air velocity with an OLR of 1.60 kg COD m^{-3} day^{-1}. Granules were also developed after 120 days of reactor operation at a higher OLR of 3.60 kg COD m^{-3} day^{-1} with acetate at 2.4 cm s^{-1} superficial upflow air velocity (Corsino et al., 2016).

Deng et al. (2016) achieved granulation after 30-35 days with an OLR of 2.00 kg COD m^{-3} day^{-1} (same as present study) at much higher air flow rate of 5.0 L min^{-1} with acetate as a carbon source (Table 2.9). Therefore, the granulation was found to be faster (35 days) at a lower air flow rate of 2.5 L min^{-1} (1.48 cm s^{-1} superficial upflow air velocity) in the present work with multiple toxicants (phenol, thiocyanate and ammonia-nitrogen) with an OLR of 2.06 kg COD m^{-3} day^{-1} as compared to previous research studies (Table 2.9) (Ab Halim et al., 2016; Adav et al., 2007; Corsino et al., 2016).

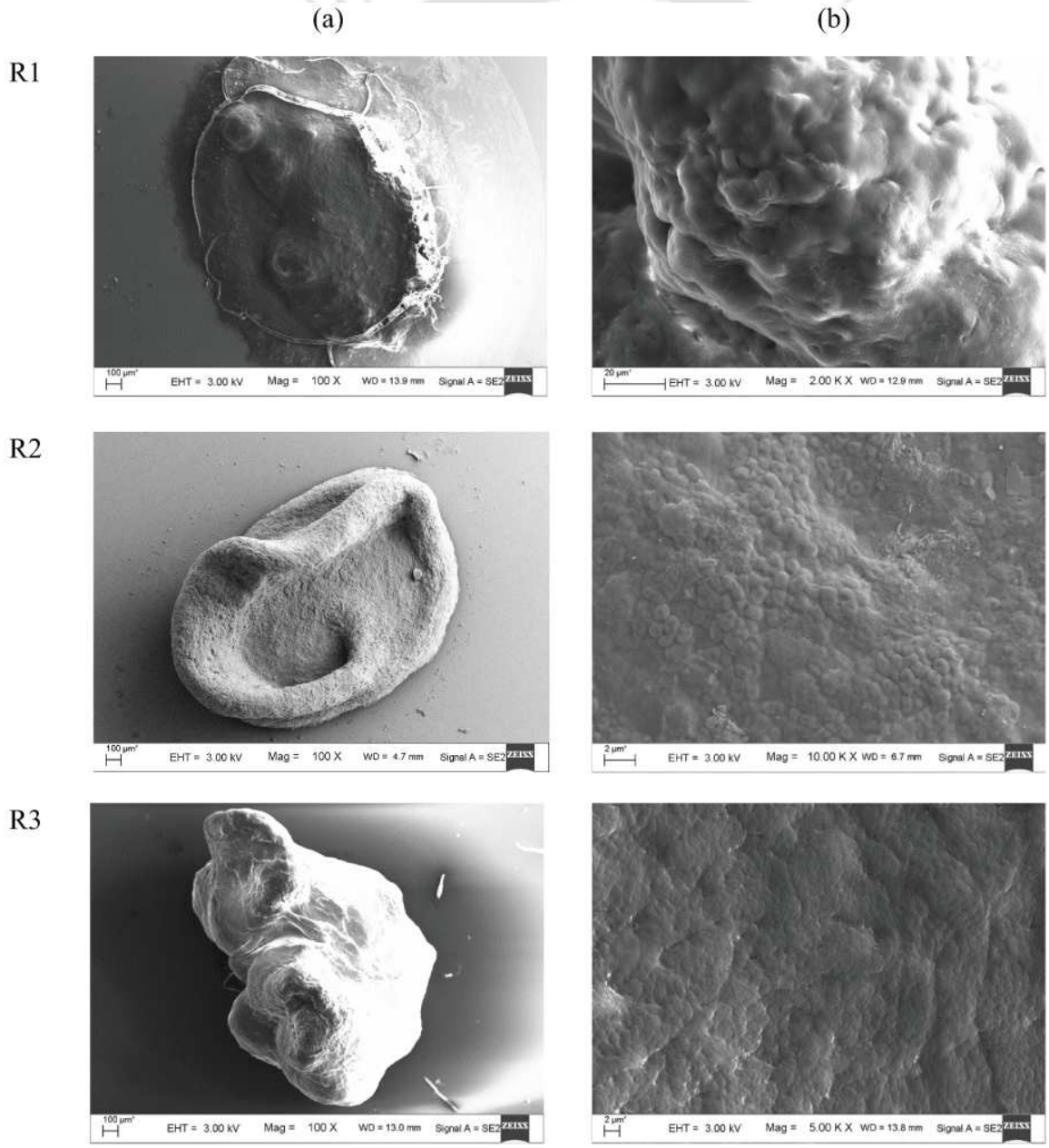

Fig. 2.12. FESEM images of granules of R1, R2 and R3 on 50th day.

Table 2.9. Comparison of characteristics of granules.

Type of waste water	Average granule size (μm)	Average settling velocity (m h^{-1})	SVI (mL g TSS^{-1})	Air flow rate (L min^{-1})	Superficial upflow air velocity (cm s^{-1})	Granulation (days)	OLR[a/b]	References
Phenol based synthetic	520 - 1200	-	40.00±5.60-60.50±5.00	3.5	-	33	1.50 - 2.50[b]	Tay et al. (2004)
Phenol based synthetic	1000 - 1500	26.60±2.00	35.00	3.0	-	160	-	Adav et al. (2007)
Acetate based synthetic domestic	-	-	24.50 - 63.21	-	2.00	>30	1.60[a]	Ab Halim et al. (2016)
Acetate based synthetic	1200 - 2000	-	30.00 - 40.00	3.0	2,40	120	3.60[a]	Corsino et al. (2016)
Acetate based synthetic	800 - 1100	-	30.00	5.0	-	30-35	2.00[a]	Deng et al. (2016)
Phenol, thiocyanate, ammonia based synthetic	2938.67±64.91	55.56±1.36	35.31±1.49	2.5	1.48	35	2.06[a]/0.80[b]	Present study (R2)

[a]Organic loading rate (kg COD m^{-3} day^{-1});[b]Organic loading rate (kg phenol m^{-3} day^{-1})

The CLSM imaging was carried out on 55th day (Fig. 2.13) and showed high fluorescence for Sytox Blue in R1 and R3 as compared to R2 indicating higher portion of dead cells caused by both lower and higher air flow rates. Extended fluorescence was observed for proteins and polysaccharides in R2 as compared to R1 and R3 indicating that air flow rate of 2.5 L min^{-1} was optimal for better granulation treating toxic pollutants.

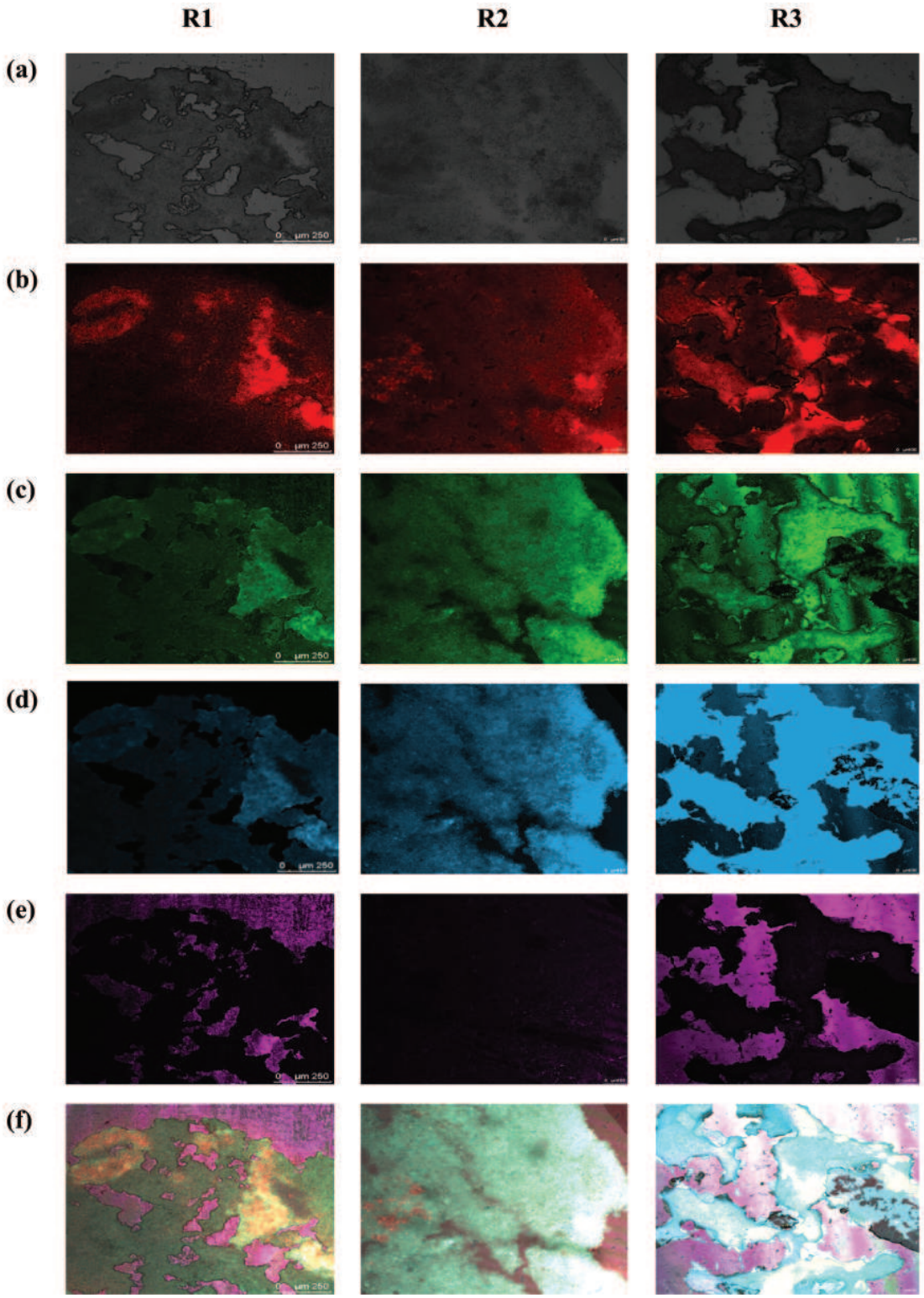

Fig. 2.13. CLSM images of R1 (Bar=250μm) and R2, R3 (Bar=100μm) on 55th day: (a) optical microscopy photograph; (b) total cells (Syto 63); (c) proteins (FITC); (d) polysaccharides (Con A); (e) dead cells (Sytox Blue); (f) combined image of (b)-(e).

Fig. 2.14a illustrates the concentrations of VSS (g L^{-1}) in all three reactors. The VSS in seed sludge was 0.19±0.03 g L^{-1}. VSS concentration increased from an initial value of 0.55, 0.67 and 0.51 to 2.57, 3.79 and 2.41 g L^{-1} after acclimatization period in R1, R2 and R3, respectively. During steady-state, VSS values were stabilized to 2.71±0.06, 4.17±0.09 and 2.40±0.08 g L^{-1}, in R1, R2 and R3, respectively (Table 2.8). VSS was lower in R1 and R3 as compared to R2 because in R1, loose and weaker granules formed, while in R3 biomass washout occurred due to higher shear force resulting in lower VSS in the reactor and higher VSS in the effluent (0.51±0.03 g L^{-1}).

The hydraulic shear force applied as superficial upflow air velocity was imposed for granule development. The seed sludge was having an initial size of 49.41 μm. Within initial 15 days, granule mean size increased to around 1000 μm in all the reactors and stabilized to 2433.82±146.37, 2938.67±64.91 and 1791.47±36.24 μm in steady-state in R1, R2 and R3, respectively (Fig. 2.14b) (Table 2.8). R2 granules were bigger in size as than the granules of R1 and R3. R1 was having a larger size than R3 in spite of having a lower air flow rate (1.5 L min^{-1}). Due to the weak shear force applied as superficial upflow air velocity, granule thickness increased through porous structure and weaker adhesion strengths (Di Iaconi et al., 2005). Though in R3, granules were less in number as compared to R1 and R2 (only based on visual analysis of photographic image; Fig. 2.11), but size (1791.47±36.24 μm) was higher than the previous studies illustrating the effect of aeration on granulation (Chen et al., 2008; Gao et al., 2011a). This study was found to be similar to a previous work in which compact and regular shaped granules were developed at superficial upflow air velocities higher than 1.20 cm s^{-1} (Tay et al., 2001b). Although, granules were developed at less than 1.20 cm s^{-1} superficial upflow air velocity (0.88 cm s^{-1}) in the present study in R1, but those were loosely packed. Granules were successfully developed at a superficial upflow air velocity of more than 2.00 cm s^{-1} with high OLR of 3.60 (Corsino et al., 2016) and 6.00-15.00 kg COD m^{-3} day^{-1} (Chen et al., 2008), but in present study granules could not tolerate high shear force (2.07 cm s^{-1} superficial upflow air velocity), this might be due to lower load applied (2.06 kg COD m^{-3} day^{-1}) with multiple toxic pollutants in R3. During steady-state period (40-65 days), VSS and the size of the granules in all the reactors were changed insignificantly and fell within a certain range (Fig. 2.14a&b).

The seed sludge was having a 208.60 mL $gTSS^{-1}$ SVI_{30}. Initial SVI_{30} values were 36.91, 59.55 and 44.57 mL $gTSS^{-1}$ in R1, R2 and R3, respectively. SVI_{30} initially increased to 86-156 mL $gTSS^{-1}$ and then gradually decreased (Fig. 2.14c). During steady-state, SVI_{30} values were 74.15±1.48, 35.25±1.71 and 56.84±1.92 mL $gTSS^{-1}$ in R1, R2 and R3, respectively (Table 2.8). R2 SVI_{30} was almost two-fold less than R1. SVI_{30} was highest in R1 because of loose and porous structure. Corsino et al. (2016) developed granules with an SVI value of 30.00-40.00 mL $gTSS^{-1}$ in an acetate fed reactor with a granule size of 1200-2000 μm at an air flow rate of 3.0 L min^{-1}. Tay et al. (2004) developed the granules with 520-1200 μm size and an SVI value of 40.00±5.60-60.50±5.00 mL $gTSS^{-1}$ at a phenolic OLR of 1.50-2.50 kg phenol m^{-3} day^{-1} (Table 2.9). As compared to Tay et al. (2004) and Corsino et al. (2016) findings, the present research work (R2) was found to be more advantageous in terms of the SVI and granule size, in spite of having the lower OLR of 2.06 kg COD m^{-3} day^{-1} (0.80 kg phenol m^{-3} day^{-1}).

GSV was analyzed from day 10^{th} onwards (Fig. 2.14c). Initial GSV values were 18.60, 39.70 and 29.21 m h^{-1} and after the acclimatization period, GSV values were 37.40, 53.14 and 44.53 m h^{-1} in R1, R2 and R3, respectively. In the steady state, average GSV values were 37.17±1.96, 55.56±1.36 and 44.24±1.01 m h^{-1} in R1, R2 and R3, respectively (Table 2.8). R2 was having highest GSV because

of the denser and compact granules. GSV was more in R3 than R1 in spite of having lower size and being less in number. It might be due to denser granule formation in R3 (Fig. 2.12). GSV and SVI_{30} values confirmed that R1 was showing poorer settling characteristics as compared to R2 and R3

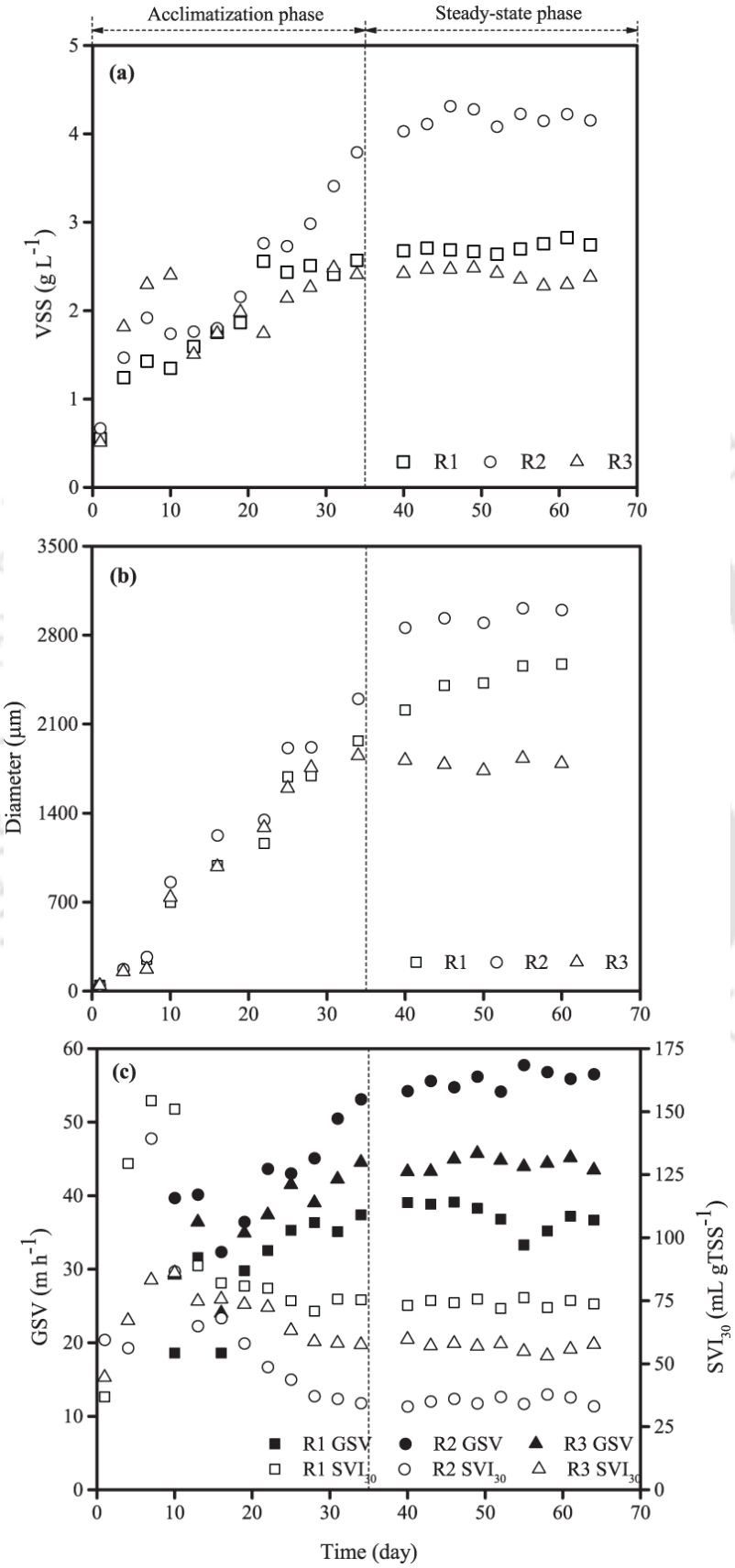

Fig. 2.14. Granule characteristics (a) VSS, (b) Size and (c) GSV and SVI at different air flow rates.

because of the lower detachment force (arising from lower superficial upflow air velocity), which was not enough to remove filamentous outgrowth and resulting in the formation of filamentous granules. From Fig. 2.14c, it was clear that as the operation continued, GSV increased and SVI_{30} decreased gradually except some initial days, indicating granule development.

Density of granular biomass was 25.11, 43.09 and 34.81 g L^{-1} in R1, R2 and R3, respectively. Tay et al. (2001c) observed 41.10 g L^{-1} granular biomass density in a glucose fed reactor with an OLR of 6.00 kg COD m^{-3} day^{-1} at an air flow rate of 3.0 L min^{-1}. So in the present study, slightly higher density was obtained at both lower OLR and air flow rate with phenol, thiocyanate and ammonia-nitrogen.

In R1, due to insufficient hydraulic shear force (<1.20 cm s^{-1} superficial upflow air velocity; Tay et al., 2001b), loose and porous granules formed (supported by higher SVI_{30} and lower GSV and density) resulting in poor settling behaviour causing biomass washout (effluent VSS 0.44±0.03 g L^{-1}) and a shorter SRT of around 3 days (discussed later in *section 2.5.4.3*). The most probable reason for biomass washout in R3 might be the extreme turbulence caused by the higher superficial upflow air velocity resulting in granule disintegration and washing out of the granules from the reactor. That also resulted in a shorter SRT (2 days) because of the higher VSS in the effluent (0.51±0.03 g L^{-1}). Luo et al. (2014) also reported that a reduction in SRT results in granule washout due to granule disintegration. Therefore, optimal aeration is required for efficient reactor operation with phenol, thiocyanate and ammonia-nitrogen without disintegration of granules.

Fig. 2.15 depicts the air flow rate effect on EPS. Initial EPS was around 30.00 mg $gVSS^{-1}$. EPS increased with operation time and stabilized during steady-state with 90.16±1.71, 145.08±2.65 and 104.31±1.96 mg $gVSS^{-1}$ (Table 2.8) in R1, R2 and R3, respectively. PN concentration was more profound than PS in all the reactors, indicating that PN was responsible for granulation than PS. EPS was highest in R2 than R1 and R3. R1 was having loose and porous structure due to which EPS was lowest in R1 and R3 was having lesser granules so EPS was also found to be less. In R2, adequate aeration provided optimum turbulence, which enhanced the contact possibilities between the flocs

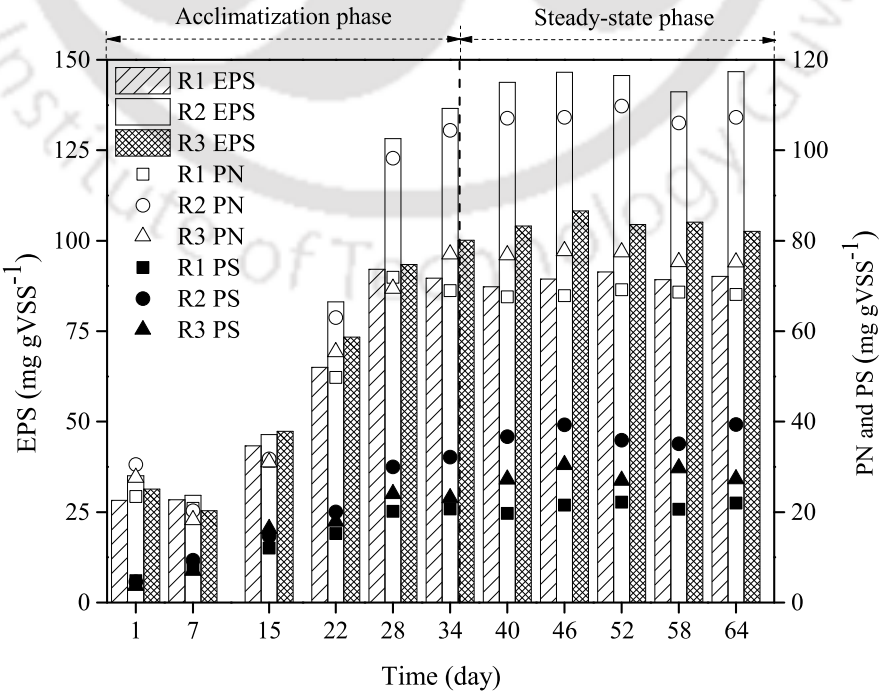

Fig. 2.15. Concentrations of total EPS, PN and PS at different air flow rates.

and stimulated the EPS secretion (sticky substance), which promoted the adhesion between them resulting in the formation of more number of compact granules. During steady-state, PN/PS ratio was 3.27±0.18, 2.86±0.13 and 2.75±0.14 in R1, R2 and R3, respectively.

F/M ratios were 0.76, 0.49 and 0.86 g COD $gVSS^{-1}$ day^{-1}, respectively, in R1, R2 and R3. Li et al. (2008) developed aerobic granules at the F/M ratios of 0.3 to 6.0 g COD gSS^{-1} day^{-1}. F/M ratio of R2 was in the range of F/M ratios for developing aerobic granules, as reported by Li et al. (2008). Higher F/M ratio was not favourable for the retention of various microbial strains (Wu et al., 2018). R1 and R3 had higher F/M ratios resulting in the deterioration of the granular characteristics and absence of ammonia-nitrogen removal.

2.5.4.2 GBA

Fig. 2.16a shows the cumulative COD removal with time and Fig. 2.16b illustrates the biomass activity of all the reactors. In R1, R2 and R3 activity values were 11.22, 14.10 and 12.19 mg COD removed $mgVSS^{-1}$ day^{-1}, respectively. The highest activity was observed in the granular biomass of R2 indicating that granules of R2 were more metabolically active than R1 and R3 because of being operated at an

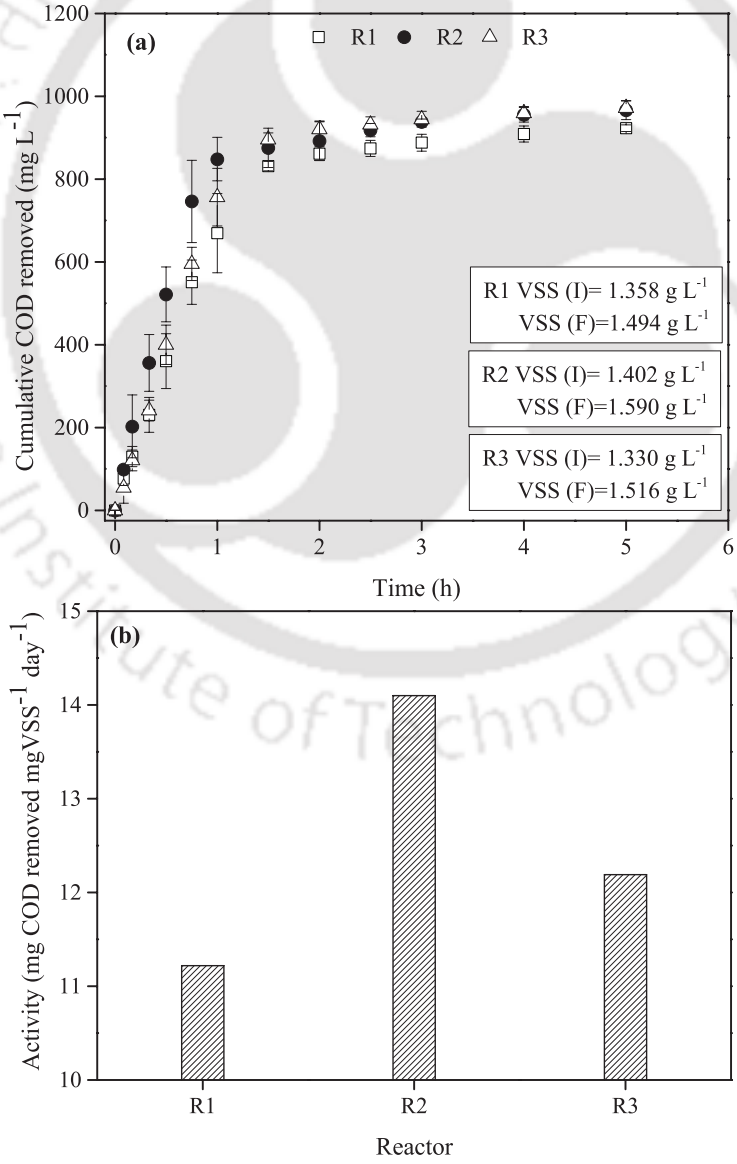

Fig. 2.16. (a) Cumulative COD removed (mg L^{-1}) with time and (b) biomass activity of all reactors.

optimal air flow rate. Biomass activity increased with a rise in hydraulic shear force to an optimal value indicating that rise in shear force can provoke the metabolism of granules in a distinct manner (R2) and also concluded that stronger shear force can trigger the biomass washout resulting in the reduction in biomass activity (R3). Biomass activity was lower for the granules developed at weaker shear force (R1) because of lower air supply for the metabolism of granules.

2.5.4.3 Effect of air flow rate on pollutants degradation

The OLRs and NLRs were same in all three reactors (Table 2.7) with 10.3 influent COD:NH_4^+-N ratio. The pollutant removal performance at different air flow rates during steady-state is given in Table 2.10. Almost complete phenol biodegradation (⩾99%) was observed in all the reactors during both acclimatization and steady-state phases from the influent concentration of 400 mg L^{-1} (Fig. 2.17a). Effluent phenol concentrations were 0.52±0.20, 0.51±0.24 and 0.56±0.18 mg L^{-1}, respectively, in R1, R2 and R3 during the steady-state. During steady-state (Fig. 2.17b), COD reduction was around 89% in R1 and R3, while in R2, it was around 95% from the initial value of 1028.85±13.21 mg L^{-1}. The effluent COD value was lower in R2 (48.18±3.42 mg L^{-1}) as compared to R1 (113.99±7.39 mg L^{-1}) and R3 (112.68±7.17 mg L^{-1}). Air flow rate does not have any significant impact on COD removal and high removal of COD confirms the mineralization of intermediates formed during the oxidation of phenol in AGS.

Table 2.10. Pollutant removal performance at different air flow rates during steady-state.

Pollutant	R1			R2			R3		
	Influent (mg L^{-1})	Effluent (mg L^{-1})	% removal	Influent (mg L^{-1})	Effluent (mg L^{-1})	% removal	Influent (mg L^{-1})	Effluent (mg L^{-1})	% removal
Phenol	397.48 ±3.71	0.52 ±0.20	99.87 ±0.05	399.24 ±4.68	0.51 ±0.24	99.87 ±0.06	396.23 ±4.82	0.56 ±0.18	99.86 ±0.05
COD	1028.92 ±13.19	113.99 ±7.39	88.92 ±0.73	1028.85 ±13.21	48.18 ±3.42	95.32 ±0.31	1024.18 ±12.04	112.68 ±7.17	89.00 ±0.71
SCN^-	99.27 ±1.09	77.77 ±0.92	21.66 ±1.07	99.66 ±1.26	1.33 ±0.40	98.66 ±0.40	98.14 ±0.62	51.26 ±1.06	47.77 ±1.09
NH_4^+-N	99.30 ±1.96	126.41 ±1.71	-27.36 ±3.50	98.42 ±0.94	0.09 ±0.03	99.91 ±0.03	98.57 ±1.21	131.54 ±2.09	-33.47 ±2.42

In R1 and R3, SCN^- removal decreased when the influent SCN^- concentration was more than 10 (day 3) and 60 mg L^{-1} (day 18), respectively, and this continued throughout the study (Fig. 2.17c). The possible reason for the early reduction in SCN^- removal in R1 might be that the granules of R1 were exposed to lower superficial upflow air velocity (0.88 cm s^{-1}), due to which granules couldn't get sufficient oxygen for the complete transformation of SCN^-. In R3, removal decreased because of biomass washout at higher superficial upflow air velocity (2.07 cm s^{-1}). Complete biotransformation of SCN^- was achieved only in R2 throughout the study because of optimal aeration. During the steady-state, the SCN^- removal efficiencies in R1, R2 and R3 were 21.66±1.07, 98.66±0.40 and 47.77±1.09%, respectively, from 100 mg L^{-1} influent SCN^- concentration (Fig. 2.17c). Sulfate was present in the reactors suggesting SCN^- oxidation followed equation 1.2, though quantitative estimation of sulfate was not made.

NH_4^+-N removal profile (Fig. 2.18a) illustrated that very low effluent NH_4^+-N concentration was observed in all three reactors with influent concentrations up to 20 mg L^{-1} during initial 7 days. With an increase in influent NH_4^+-N from 20 to 40 mg L^{-1} (days 9-11), NH_4^+-N removal was observed to some extent in R1 and R3. After increasing concentration more than 40 mg L^{-1} (day 13

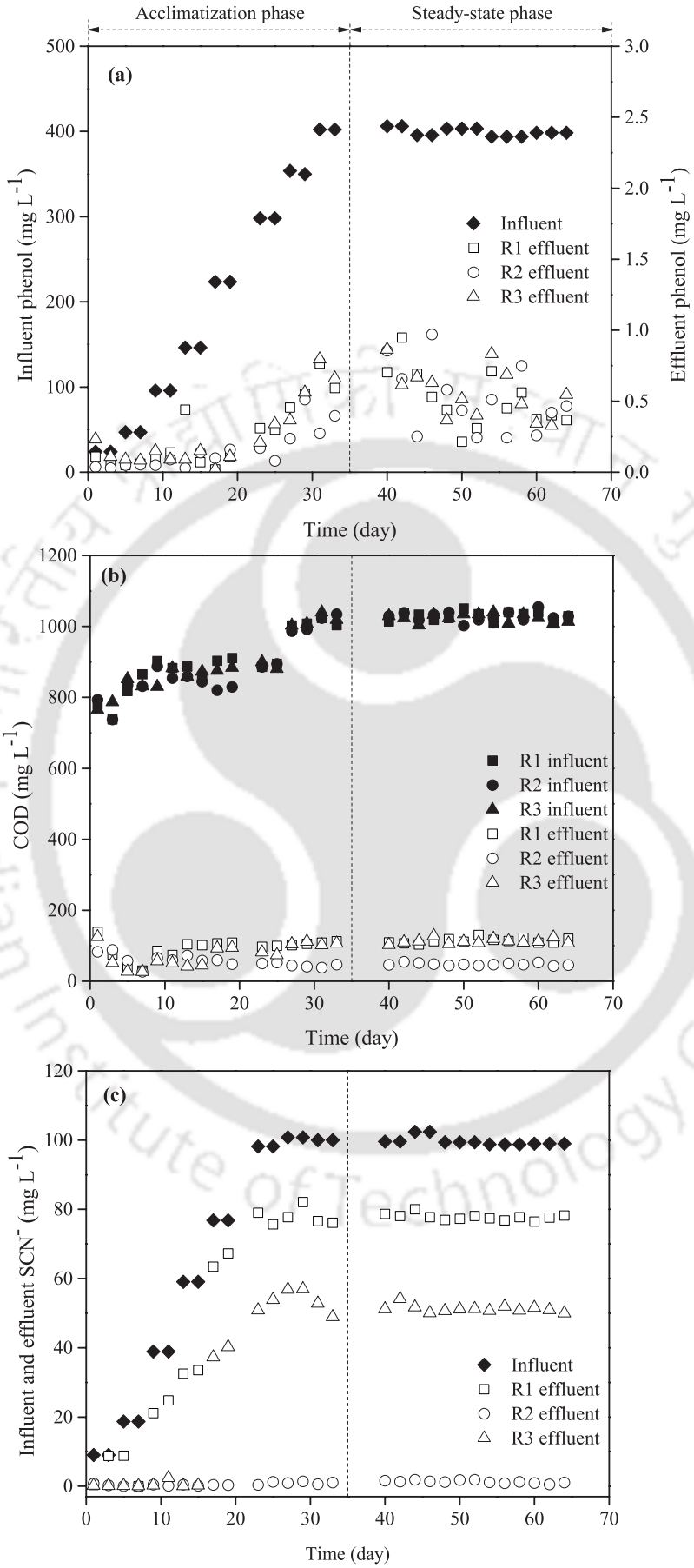

Fig. 2.17. Influent and effluent (a) phenol, (b) COD and (c) SCN^- at different air flow rates.

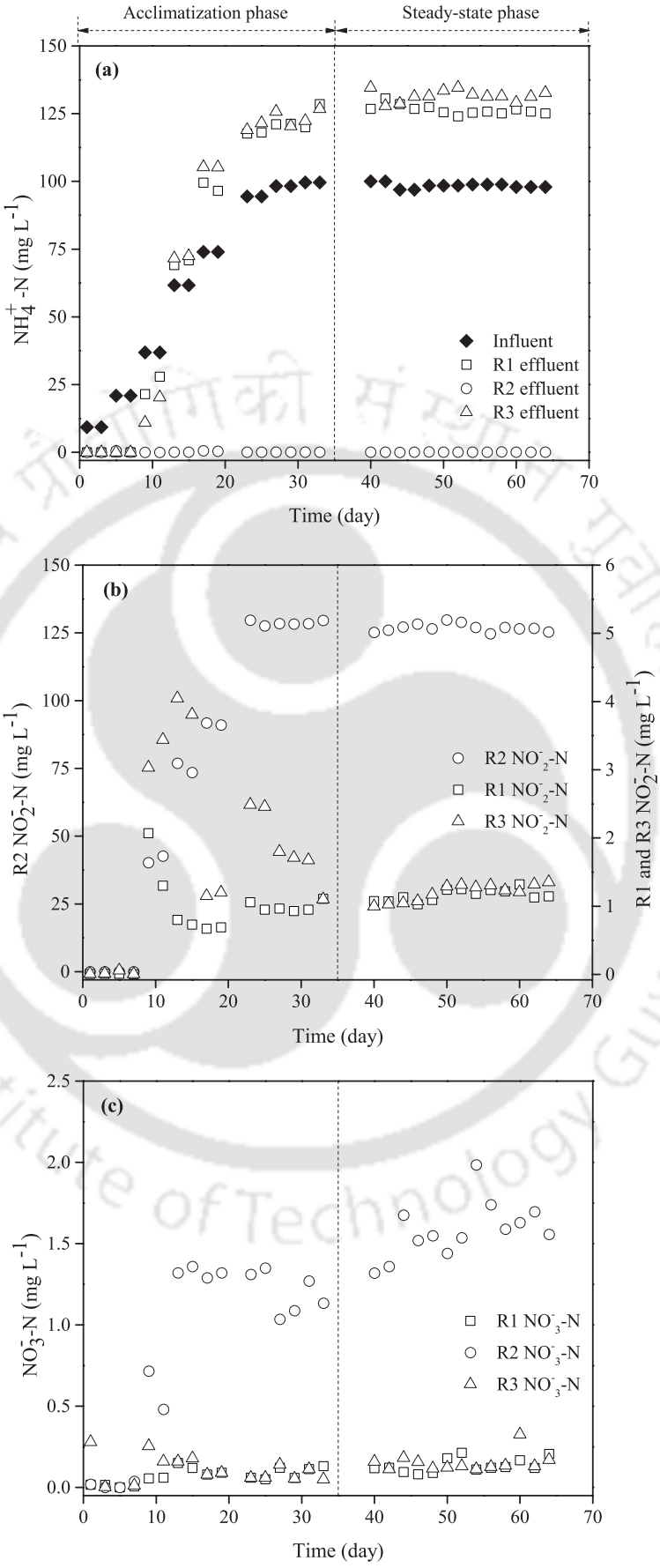

Fig. 2.18. Influent and effluent (a) NH_4^+-N, (b) effluent NO_2^--N and (c) effluent NO_3^--N at different air flow rates.

onwards), no removal was observed in R1 and R3. R2 showed stable performance in removing NH_4^+-N throughout the study from the influent NH_4^+-N concentration of 100 mg L^{-1}. In the steady-state, NH_4^+-N removal was 99% in R2 with effluent concentration of 0.09±0.03 mg L^{-1}. In R1 and R3, effluent NH_4^+-N concentration were 126.41±1.71 and 131.54±2.09 mg L^{-1}, respectively, which was higher than the influent (calculated from equation 2.6) because of the accumulation of NH_4^+-N from the previous cycle. Influent nitrogen comprised of feed NH_4^+-N along with nitrogen evolved from SCN^- biotransformation (Equation 2.6). Influent NH_4^+-N was 100 mg L^{-1}. Nitrogen due to SCN^- transformation varied in all the reactors because in R1, R2 and R3, SCN^- removal efficiencies were 21.66±1.07, 98.66±0.40 and 47.77±1.09%, respectively, from the influent SCN^- concentration of 100 mg L^{-1}. Therefore, nitrogen concentrations generated from SCN^- transformation were 5.28±0.14, 23.84±0.07 and 11.30±0.02 mg L^{-1} in R1, R2 and R3, respectively. Therefore, total influent nitrogen was around 105, 124 and 111 mg L^{-1}, respectively in R1, R2 and R3. During steady-state, in R2, NO_2^--N and NO_3^--N concentrations were 126.48±1.88 and 1.58±0.17 mg L^{-1}, respectively. In R1 and R3, no NH_4^+-N removal was observed, therefore NO_2^--N (1.22±0.22 and 1.20±0.13 mg L^{-1}, respectively) and NO_3^--N concentrations (0.13±0.04 and 0.15±0.06 mg L^{-1}, respectively) were almost negligible (Fig. 2.18b&c).

In R2, nitrification was partial (conversion of NH_4^+ to NO_2^-) suggesting the absence of NOB. The reason for the absence of NOB was SRT (*section 2.3.4.2*). SRT values were around 3.0, 9.5, and 2.0 days, respectively, in R1, R2 and R3 (calculated from the effluent VSS of 0.44±0.03, 0.22±0.01, 0.51±0.03 g L^{-1}, respectively, in R1, R2 and R3). R1 and R3 were having too shorter SRT due to high biomass loss in effluent, so the growth of both AOB and NOB was inhibited because of being washed out from the reactor. Pollice et al. (2002) achieved partial nitrification (oxidation of ammonia to nitrite) at an SRT value of around 10 days, which is nearly similar to the present work (R2). Though in R2, NOB growth was inhibited because of the shorter SRT than the standard values required for achieving nitrification (10-30 days) (Tchobanoglous et al., 2003). Another possible reason for absence of nitrification in R1 might be the lower DO concentration (3.0-3.5 mg L^{-1}). A decrease in air flow rates and therefore DO concentration affects the nitrification efficiency by reducing the oxygen diffusion inside the granules. In the aerobic granules, nitrifying bacteria and heterotrophic organisms lived in the outer layer and the nitrifiers were not able to outcompete with heterotrophs for DO due to slow growth rate, thus effecting nitrification efficiency (Okabe et al., 1995). In spite of having appropriate DO concentrations, nitrification was absent in R3, whereas partial nitrification was observed in R2. Therefore, SRT was the governing parameter for achieving nitrification in the present study.

In all three rectors, phenol was the only available organics and was completely removed by the heterotrophic bacteria (Kim et al., 2008b). Mostly autotrophs (Watts et al., 2017) were found to be responsible for SCN^- biotransformation resulting in partial SCN^- biotransformation in R1 and R3. Autotrophic nitrifiers were the most profoundly affected by the aeration availability and intensity resulting in the absence of nitrification in R1 and R3, whereas partial nitrification in R2.

Chen et al. (2008) reported limited reactor operation at superficial upflow air velocity of 2.40 cm s^{-1} in the OLR range of 6.00 to 9.00 kg COD m^{-3} day^{-1} with sodium acetate. Gao et al. (2011a) developed granules at a higher superficial upflow air velocity of 3.90 cm s^{-1} with glucose at an OLR of 0.75 kg COD m^{-3} day^{-1}. Very few studies addressed the effect of aeration on AGS with toxic substrates like phenol as a carbon source (Adav et al., 2007). So, present research work showed AGS, a possible substitute for granule formation by using multiple toxic pollutants like phenol, thiocyanate

and ammonia-nitrogen at an OLR of 2.06 kg COD m^{-3} day^{-1} in a cost-effective manner in terms of optimal air supply (1.48 cm s^{-1} superficial upflow air velocity).

2.5.5 Conclusion of the air flow rate study

From the air flow rate study, it was concluded that the treatment of toxic wastewater consisting of phenol, thiocyanate and ammonia-nitrogen required optimal aeration for their removal resulting in a low cost operation. Lower air flow rate can cause formation of loosely packed granules, on the other hand, higher air flow rate can cause biomass washout, both resulting in deterioration in granule characteristics and reactor performance. R2 was found to be best than R1 and R3 in terms of both reactor performance and granule characteristics. Performance of the reactor with more than 99% phenol, 98% thiocyanate and 95% COD removal was observed at air flow rate of 2.5 L min^{-1}. Partial nitrification was observed in R2, while in R1 and R3, no NH_4^+-N removal was observed.

Better granule characteristics and reactor performance were observed with a cycle time of 6 h and air flow rate of 2.5 L min^{-1}. For further studies, air flow rate of 2.0 L min^{-1} (used in cycle time study) was opted over 2.5 L min^{-1} because at both air flow rate, 2.0 and 2.5 L min^{-1} granule characteristics were found better, but taking cost-effectiveness into consideration, 2.0 L min air flow rate was opted with a 6 h cycle time.

References

Ab Halim, M.H., Nor Anuar, A., Abdul Jamal, N.S., Azmi, S.I., Ujang, Z., Bob, M.M., 2016. Influence of high temperature on the performance of aerobic granular sludge in biological treatment of wastewater. Journal of Environmental Management 184, 271-280.

Adav, S.S., Lee, D.J., Lai, J., 2007. Effects of aeration intensity on formation of phenol-fed aerobic granules and extracellular polymeric substances. Applied Microbiology and Biotechnology 77, 175-182.

APHA, 2005. Standard methods for the examination of water and wastewater, 21st ed. American Public Health Association, Washington, DC.

Bárcenas Ruiz, C.D., Carrillo Reyes, J., Arellano García, L., Celis, L.B., Alatriste Mondragón, F., Razo Flores, E., 2016. Pretreatment and upward liquid velocity effects over granulation in hydrogen producing EGSB reactors. Biochemical Engineering Journal 107, 75-84.

Basheer, F., Farooqi, I., 2014. Hydrodynamic properties of aerobic granules cultivated on phenol as carbon source. APCBEE Procedia 10, 126-130.

Ben Aim, R. M., Semmens, M. J., 2003. Membrane bioreactors for wastewater treatment and reuse: a success story. Water Science and Technology 47, 1-5.

Beun, J.J., Hendriks, A., van Loosdrecht, M.C.M., Morgenroth, E., Wilderer, P.A., Heijnen, J.J., 1999. Aerobic granulation in a sequencing batch reactor. Water Research 33, 2283-2290.

Chen, M., Lee, D., Tay, J., 2007. Distribution of extracellular polymeric substances in aerobic granules. Applied Microbiology and Biotechnology 73, 1463-1469.

Chen, Y., Jiang, W., Liang, D.T., Tay, J.H., 2008. Aerobic granulation under the combined hydraulic and loading selection pressures. Bioresource Technology 99, 7444-7449.

Corsino, S.F., Campo, R., Di Bella, G., Torregrossa, M., Viviani, G., 2015. Cultivation of granular sludge with hypersaline oily wastewater. International Biodeterioration & Biodegradation 105, 192-202.

Corsino, S.F., Capodici, M., Torregrossa, M., Viviani, G., 2016. Fate of aerobic granular sludge in the long-term: The role of EPSs on the clogging of granular sludge porosity. Journal of Environmental Management 183, 541-550.

Deng, S., Wang, L., Su, H., 2016. Role and influence of extracellular polymeric substances on the preparation of aerobic granular sludge. Journal of Environmental Management 173, 49-54.

Di Iaconi, C., Ramadori, R., Lopez, A., Passino, R., 2005. Hydraulic shear stress calculation in a

sequencing batch biofilm reactor with granular biomass. Environmental Science & Technology 39, 889-894.

Dubois, M., Gilles, K.A., Hamilton, J.K., Rebers, P., Smith, F., 1956. Colorimetric method for determination of sugars and related substances. Analytical Chemistry 28, 350-356.

Gao, D., Liu, L., liang, H., Wu, W.M., 2011a. Comparison of four enhancement strategies for aerobic granulation in sequencing batch reactors. Journal of Hazardous Materials 186, 320-327.

Gao, D., Liu, L., Liang, H., Wu, W.M., 2011b. Aerobic granular sludge: characterization, mechanism of granulation and application to wastewater treatment. Critical Reviews in Biotechnology 31, 137-152.

Janczukowicz, W., Szewczyk, M., Krzemieniewski, M., Pesta, J., 2001. Settling properties of activated sludge from a sequencing batch reactor (SBR). Polish Journal of Environmental Studies 10, 15-20.

Jawed, M., Tare, V., 1999. Microbial composition assessment of anaerobic biomass through methanogenic activity tests. Water SA 25, 345-350.

Jemaat, Z., Suárez Ojeda, M.E., Pérez, J., Carrera, J., 2014. Partial nitritation and *o*-cresol removal with aerobic granular biomass in a continuous airlift reactor. Water Research 48, 354-362.

Jeong, Y.S., Chung, J.S., 2006. Simultaneous removal of COD, thiocyanate, cyanide and nitrogen from coal process wastewater using fluidized biofilm process. Process Biochemistry 41, 1141-1147.

Jiang, H.L., Tay, J.H., Tay, S.L., 2004. Changes in structure, activity and metabolism of aerobic granules as a microbial response to high phenol loading. Applied Microbiology and Biotechnology 63, 602-608.

Kim, I.S., Kim, S.M., Jang, A., 2008a. Characterization of aerobic granules by microbial density at different COD loading rates. Bioresource Technology 99, 18-25.

Kim, Y.M., Park, D., Jeon, C.O., Lee, D.S., Park, J.M., 2008b. Effect of HRT on the biological pre-denitrification process for the simultaneous removal of toxic pollutants from cokes wastewater. Bioresource Technology 99, 8824-8832.

Kong, Q., Ngo, H.H., Shu, L., Fu, R.S., Jiang, C.H., Miao, M.S., 2014. Enhancement of aerobic granulation by zero-valent iron in sequencing batch airlift reactor. Journal of Hazardous Materials 279, 511-517.

Kong, Q., Wang, Z.B., Shu, L., Miao, M.S., 2015. Characterization of the extracellular polymeric substances and microbial community of aerobic granulation sludge exposed to cefalexin. International Biodeterioration & Biodegradation 102, 375-382.

Kong, Q., Zhang, J., Ngo, H.H., Ni, S., Fu, R., Guo, W., Guo, N., Tian, L., 2013. Nitrous oxide emission in an aerobic granulation sequencing batch airlift reactor at ambient temperatures. International Biodeterioration & Biodegradation 85, 533-538.

Kong, Y., Liu, Y.Q., Tay, J.H., Wong, F.S., Zhu, J., 2009. Aerobic granulation in sequencing batch reactors with different reactor height/diameter ratios. Enzyme and Microbial Technology 45, 379-383.

Lee, D.J., Chen, Y.Y., Show, K.Y., Whiteley, C.G., Tay, J.H., 2010. Advances in aerobic granule formation and granule stability in the course of storage and reactor operation. Biotechnology Advances 28, 919-934.

Li, A.J., Yang, S.F., Li, X.Y., Gu, J.D., 2008. Microbial population dynamics during aerobic sludge granulation at different organic loading rates. Water Research 42, 3552-3560.

Li, X., Yang, S., 2007. Influence of loosely bound extracellular polymeric substances (EPS) on the flocculation, sedimentation and dewaterability of activated sludge. Water Research 41, 1022-1030.

Liu, Y.Q., Tay, J.H., 2007a. Influence of cycle time on kinetic behaviors of steady-state aerobic granules in sequencing batch reactors. Enzyme and Microbial Technology 41, 516-522.

Liu, Y.Q., Zhang, X., Zhang, R., Liu, W.T., Tay, J.H., 2016. Effects of hydraulic retention time on aerobic granulation and granule growth kinetics at steady state with a fast start-up strategy. Applied Microbiology and Biotechnology 100, 469-477.

Liu, Y., Tay, J.H., 2002. The essential role of hydrodynamic shear force in the formation of biofilm and granular sludge. Water Research 36, 1653-1665.

Liu, Y.Q., Tay, J.H., 2007b. Characteristics and stability of aerobic granules cultivated with different

starvation time. Applied Microbiology and Biotechnology 75, 205-210.
Liu, Y.Q., Tay, J.H., 2015. Fast formation of aerobic granules by combining strong hydraulic selection pressure with overstressed organic loading rate. Water Research 80, 256-266.
Liu, Y.Q., Tay, J.H., Ivanov, V., Moy, B.Y.P., Yu, L., Tay, S.T.L., 2005. Influence of phenol on nitrification by microbial granules. Process Biochemistry 40, 3285-3289.
Lowry, O.H., Rosebrough, N.J., Farr, A.L., Randall, R.J., 1951. Protein measurement with the Folin phenol reagent. Journal of Biological Chemistry 193, 265-275.
Luo, J., Hao, T., Wei, L., Mackey, H.R., Lin, Z., Chen, G.H., 2014. Impact of influent COD/N ratio on disintegration of aerobic granular sludge. Water research 62, 127-135.
Maranon, E., Vazquez, I., Rodriguez, J., Castrillon, L., Fernandez, Y., 2008. Coke wastewater treatment by a three-step activated sludge system. Water, Air, and Soil Pollution 192, 155-164.
McSwain, B., Irvine, R., Hausner, M., Wilderer, P., 2005. Composition and distribution of extracellular polymeric substances in aerobic flocs and granular sludge. Applied and Environmental Microbiology 71, 1051-1057.
Najib, M., Ujang, Z., Salim, M., Ibrahim, Z., 2017. Developed microbial granules containing photosynthetic pigments for carbon dioxide reduction in palm oil mill effluent. International Biodeterioration & Biodegradation 116, 163-170.
Okabe, S., Hirata, K., Watanabe, Y., 1995. Dynamic changes in spatial microbial distribution in mixed-population biofilms: Experimental results and model simulation. Water Science & Technology 32, 67-74.
Pollice, A., Tandoi, V., Lestingi, C., 2002. Influence of aeration and sludge retention time on ammonium oxidation to nitrite and nitrate. Water Research 36, 2541-2546.
Ramos, C., Suárez-Ojeda, M.E., Carrera, J., 2016a. Biodegradation of a high-strength wastewater containing a mixture of ammonium, aromatic compounds and salts with simultaneous nitritation in an aerobic granular reactor. Process Biochemistry 51, 399-407.
Ramos, C., Suárez Ojeda, M.E., Carrera, J., 2016b. Long-term performance and stability of a continuous granular airlift reactor treating a high-strength wastewater containing a mixture of aromatic compounds. Journal of Hazardous Materials 303, 154-161.
Sahariah, B.P., Chakraborty, S., 2011. Kinetic analysis of phenol, thiocyanate and ammonia-nitrogen removals in an anaerobic-anoxic-aerobic moving bed bioreactor system. Journal of Hazardous Materials 190, 260-267.
Salmiati, Dahalan, F.A., Najib, M.Z.M., Salim, M.R., Ujang, Z., 2015. Characteristics of developed granules containing phototrophic aerobic bacteria for minimizing carbon dioxide emission. International Biodeterioration & Biodegradation 102, 15-23.
Show, K.Y., Lee, D.J., Tay, J.H., 2012. Aerobic Granulation: Advances and Challenges. Applied Biochemistry and Biotechnology 167, 1622-1640.
Singh, M., Srivastava, R., 2011. Sequencing batch reactor technology for biological wastewater treatment: a review. AsiaPacific Journal of Chemical Engineering 6, 3-13.
Tay, J.H., Jiang, H.L., Tay, S.T.L., 2004. High-rate biodegradation of phenol by aerobically grown microbial granules. Journal of Environmental Engineering 130, 1415-1423.
Tay, J.H., Liu, Q.S., Liu, Y., 2001a. The role of cellular polysaccharides in the formation and stability of aerobic granules. Letters in Applied Microbiology 33, 222-226.
Tay, J.H., Liu, Q.S., Liu, Y., 2001b. The effects of shear force on the formation, structure and metabolism of aerobic granules. Applied Microbiology and Biotechnology 57, 227-233.
Tay, J.H., Liu, Q.S., Liu, Y., 2001c. Microscopic observation of aerobic granulation in sequential aerobic sludge blanket reactor. Journal of Applied Microbiology 91, 168-175.
Tchobanoglous, G., Burton, F.L., Stensel, H.D., Metcalf, Eddy, 2003. Wastewater Engineering: Treatment and Reuse, fourth ed. McGraw Hill Education, India.
Tijani, H., Abdullah, N., Yuzir, A., Ujang, Z., 2015. Rheological and fractal hydrodynamics of aerobic granules. Bioresource Technology 186, 276-285.
Wan, C., Sun, S., Lee, D.J., Liu, X., Wang, L., Yang, X., Pan, X., 2013. Partial nitrification using aerobic granules in continuous-flow reactor: Rapid startup. Bioresource Technology 142, 517-522.
Wang, F., Yang, F.L., Zhang, X.W., Liu, Y.H., Zhang, H.M., Zhou, J., 2005. Effects of cycle time on

properties of aerobic granules in sequencing batch airlift reactors. World Journal of Microbiology and Biotechnology 21, 1379-1384.

Wang, S.G., Liu, X.W., Gong, W.X., Gao, B.Y., Zhang, D.H., Yu, H.Q., 2007. Aerobic granulation with brewery wastewater in a sequencing batch reactor. Bioresource Technology 98, 2142-2147.

Watts, M.P., Spurr, L.P., Gan, H.M., Moreau, J.W., 2017. Characterization of an autotrophic bioreactor microbial consortium degrading thiocyanate. Applied Microbiology and Biotechnology 101, 5889-5901.

Wu, D., Zhang, Z., Yu, Z., Zhu, L., 2018. Optimization of F/M ratio for stability of aerobic granular process via quantitative sludge discharge. Bioresource Technology 252, 150-156.

Yang, S.F., Tay, J.H., Liu, Y., 2005. Effect of substrate nitrogen/chemical oxygen demand ratio on the formation of aerobic granules. Journal of Environmental Engineering 131, 86-92.

Yang, Y., Zhou, D., Xu, Z., Li, A., Gao, H., Hou, D., 2014. Enhanced aerobic granulation, stabilization, and nitrification in a continuous-flow bioreactor by inoculating biofilms. Applied Microbiology and Biotechnology 98, 5737-5745.

Yu, G.H., Juang, Y.C., Lee, D.J., He, P.J., Shao, L.M., 2009. Enhanced aerobic granulation with extracellular polymeric substances (EPS)-free pellets. Bioresource Technology 100, 4611-4615.

Zhang, H., He, Y., Jiang, T., Yang, F., 2011. Research on characteristics of aerobic granules treating petrochemical wastewater by acclimation and co-metabolism methods. Desalination 279, 69-74.

Zhu, L., Lv, M.L., Dai, X., Yu, Y.W., Qi, H.Y., Xu, X.Y., 2012. Role and significance of extracellular polymeric substances on the property of aerobic granule. Bioresource Technology 107, 46-54.

Exploring the unknown requires tolerating uncertainty.

Brian Greene (1963-)
American physicist

3

Effect of Substrates on Rapid Aerobic Granulation and Reformation of Aerobic Granules

This chapter aims to develop an efficient and economic strategy for rapid granulation without the addition of any supplementary material and also evaluates the reformation ability of aerobic granules after disintegration by the addition of a toxic compound.

3.1 Introduction

Aerobic granules possess excellent settling behaviour, denser, compact microbial structure and better nutrient and pollutant removal ability as compared to conventional activated sludge (Ou et al., 2018; Xu et al., 2018). However, the long start-up period required for granulation and its maturation and poor granule stability for prolonged reactor operation are the two major issues in adopting aerobic granular sludge (AGS) technology for efficient wastewater treatment (Hamza et al., 2018; Hu et al., 2016; Liu et al., 2018; Long et al., 2019). Therefore, a rapid and prolonged AGS reactor operation is needed, which would significantly improve the wastewater treatment process.

The primary attention of many research works was to investigate the factors which might affect the granulation, viz., inoculum sludge, substrate type and loading, cycle time, settling time, aeration intensity, etc. (Lee et al., 2010). Rapid granulation could be achieved by using better settleability sludge or a part of AGS like crushed AGS (Verawaty et al., 2012), 25% AGS (Long et al., 2014) and stored granular sludge (Wang et al., 2019). In addition, external carrier materials were also used for shortening the granulation time like granular activated carbon (Li et al., 2011a) and poly aluminum chloride (PAC) (Liu et al., 2016). Apart from this, augmentation with metal ions, viz., Ca^{2+}, Mg^{2+} and Al^{3+} has been significantly implemented for reducing granulation period (Gao et al., 2011; Wang et al., 2012). Supplementation of exopolysaccharides or different coagulants significantly decreased the granulation time up to 20-30 days (Liu et al., 2018; Liu et al., 2016).

Even though all above addressed approaches could result in making the granulation process faster to a different extent, but addition of any supplement results in a rise in the operation cost, which limits the application of AGS technology in a real operational field. Furthermore, when a mixture of activated sludge and pure strains isolated from AGS with high self-aggregation and co-aggregation index were used for granule bio-augmentation, 8 days were required to develop the aerobic granules (Ivanov et al., 2006). But culturing and isolation of pure strains are tedious and an expensive process in spite of its ability to shorten up the granulation period. In addition, Usage of either fraction of AGS

or already formed/stored granules as inoculum could result in bringing down the granulation time up to 7-22 days (Long et al., 2014; Tay et al., 2005; Wang et al., 2019). All these methods for achieving rapid granulation require an additional study; first to form granules in a separate reactor or to collect from other sources where granules are already formed then inoculated in the other reactor for quicker granulation, which makes the process tedious and little bit expensive. Therefore, there was no rapid, consolidated and reliable approach for cultivating AGS.

Mechanism of granule disintegration is still not clear, although few mechanisms have been proposed which contribute to granule instability like filamentous outgrowth, anaerobic core hydrolysis, change in extracellular polymeric substances (EPS) composition, etc. (Lee et al., 2010). However, the addition of calcium, magnesium, zinc, PAC were found to accelerate the microbial aggregation process and assisted in sustaining the aerobic granule's stability (Liu et al., 2010; Liu et al., 2014; Wei et al., 2016).

EPS, secreted by microorganisms, plays a key part in governing the granule formation and granule's stability and is supposed to be a glue-like sticky substance which helps in the building a gel like structure for keeping bacteria together in the biofilms (Muñoz-Palazon et al., 2018; Zhang et al., 2007). Substrate type, nutrient content, external conditions like the addition of metal ions or toxic substances can enhance the EPS secretion (Sheng et al., 2010). However, the direct addition of metal ions to the solution can result in washing out condition and also enhances the reactor operational cost, besides this insufficient metal ions cannot stimulate the EPS secretion (Xu et al., 2019). The secretion of EPS is a self-adaptive action of granular biomass against the exposure to the toxic substance for their existence. This bacterial survival action helps in providing strength to the granules (Chen et al., 2017). SCN^- being a toxic substance promotes the anammox granule integrity by enhancing the EPS secretion (Chen et al., 2017). Furthermore, the concentration of toxic substances higher than the threshold value has a lesser significant impact on EPS production (Sheng et al., 2010). Therefore, a suitable toxic substance in an adequate amount is required.

So far, the focus of most of the research works is either on the improvement of the granule stability during the formation of the granules or on the suitable and sustainable granular storage strategy (Hu et al., 2016; Wang et al., 2008). However, an approach to the granule reformulation after its disintegration is still very limited in the literature (Liu et al., 2014).

The current study evaluates the quick start-up of aerobic granules developed from refinery sludge with two different substrates; a recalcitrant organics (phenol) and a simple carbon source (sodium acetate) along with the assessment and comparison of the granule characteristics resulted from two different substrates. The present work also aims to evaluate the impact of toxic SCN^- on granule reformulation from the disintegrated granules along with the investigation on the ability of reformed aerobic granules to transform SCN^-. Furthermore, the removal profiles of phenol, chemical oxygen demand (COD) and ammonia-nitrogen are also analyzed.

3.2 Materials and methods

All the chemicals and reagents used to perform this work are given in *Chapter 2 (section 2.2.1)*.

3.3 Analytical methods

All the analytical techniques used in this study are mentioned in *Chapter 2 (section 2.2.2)*.

3.4 Effect of substrates on aerobic granulation

3.4.1 Experimental set-up

The current work was performed in two similar transparent acrylic SBRs (R1 and R2) (configuration is given in *Chapter 2; section 2.3.1*). The feed was given through the peristaltic pumps from the bottom to the SBRs in an up-flow mode. The photographic image and schematic illustration of SBRs are given in *Chapter 2* (Fig. 2.1 and Fig. 2.2, respectively).

3.4.2 Characteristics of inoculum sludge and synthetic wastewater

The source of inoculum sludge was the wastewater treatment plant of Indian Oil Corporation Limited (IOCL), Guwahati. The inoculum sludge was having the total suspended and volatile suspended solids (TSS and VSS) of 2.05±0.07 and 1.60±0.11 g L^{-1}, respectively. The inoculum sludge was of 45.76±12.06 μm in size and having a sludge volume index (SVI_{30}) of 51.26 mL $gTSS^{-1}$. In refinery sludge, phenol was around 1.15 mg L^{-1} because of the collection from the treatment unit. The inoculum volume was 3 L for 6 L SBRs. The synthetic wastewater composition of R1 and R2 was given in Table 3.1. R1 and R2 were fed with two different carbon sources, phenol, a recalcitrant organics and simple sodium acetate, respectively. The common constituents of R1 and R2 wastewater were:

Table 3.1. Composition of synthetic wastewater for substrate study.

Component	Concentration (mg L^{-1})		Component	Concentration (mL L^{-1})
	Substrate concentration	Corresponding COD concentration		
Phenol (R1)	400	996.62± 24.48	**Phosphate buffer**[a]	1
CH_3COONa (R2)	1220	984.36± 16.83		
NH_4^+-N	100		**Trace metal solution**[b]	1
$NaHCO_3$	added as required			

[a]Phosphate buffer contained (g L^{-1}): 72.3 KH_2PO_4 and 104.5 K_2HPO_4; [b]Trace metal solution contained (mg L^{-1}): 10,000 $MgSO_4.7H_2O$, 10,000 $CaCl_2.2H_2O$, 5000 $FeCl_3.6H_2O$, 1000 $CuCl_2$, 1000 $ZnCl_2$, 500 $NiCl_2.6H_2O$ and 500 $CoCl_2$

ammonia-nitrogen (NH_4^+-N as NH_4Cl), phosphate buffer and trace metal solution. Reactors were operated under an uncontrolled temperature regime. pH was ranged from 7.5 to 8.0 in both of the reactors during steady-state by using phosphate buffer and $NaHCO_3$ (added as required). Phosphorous for microbial growth was also provided from phosphate buffer. Phosphate buffer and trace metal compositions were adopted from Sahariah and Chakraborty (2011).

3.4.3 Operational approach

Each SBR was scheduled with a 6 and 12 h of cycle time and hydraulic retention time (HRT), respectively. Each 6 h cycle was divided into four phases; 30 min for influent feeding, 320 min for reaction, 5 min for each sludge settling and effluent decanting. The volume exchange ratio was maintained at 50%. For first 15 days, 15 min settling time was set in both R1 and R2 to prevent biomass washout from the SBRs. Later on, it was reduced to 5 min and was kept constant throughout the reactor's operation. In R1, 1000 mg L^{-1} of CH_3COONa was supplemented initially as a simple carbon source and was gradually decreased, whereas phenol was gradually increased to 400 mg L^{-1}. After being operated for 43 days, CH_3COONa was suspended and phenol concentration was reached to the maximum level of 400 mg L^{-1} in R1. The concentration fo CH_3COONa fed to R2 throughout the study was 1220 mg L^{-1} to make COD value similar to that obtained from 400 mg L^{-1}

of phenol. NH_4^+-N was also gradually increased to 100 mg L^{-1} in both R1 and R2. After 45 days of the acclimatization, phenol and NH_4^+-N concentrations were reached to the desired levels of 400 and 100 mg L^{-1}, respectively. In both SBRs, the nitrogen loading rate (NLR) was 0.20 kg NH_4^+-N m^{-3} day^{-1}. Whereas the organic loading rates (OLRs) were around 2.00 kg COD m^{-3} day^{-1} (0.80 kg phenol m^{-3} day^{-1}) and 1.97 kg COD m^{-3} day^{-1} in R1 and R2, respectively. For obtaining steady-state data, R1 and R2 were operated for the next 30 days (day 45-74) with the same influent feed.

3.4.4 Results and discussion

3.4.4.1 Granule formation

Fig. 3.1 illustrated the granular development process in both R1 and R2. Inoculum sludge was clear and brown in colour and was not having any granules. More granules started to develop in R1 than

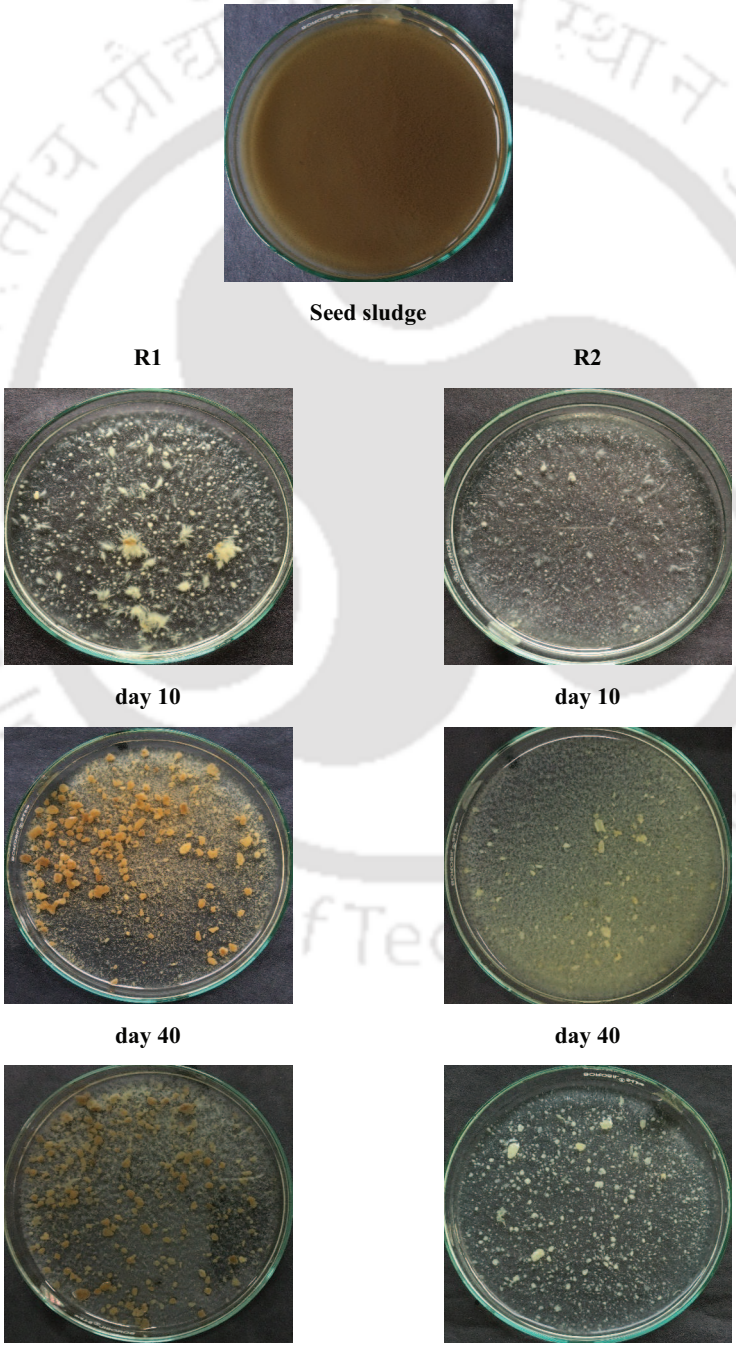

Fig. 3.1. Images of the granules with operational time in R1 and R2.

R2 on day 10. Although granules developed in both R1 and R2 were filamentous on day 10 (Fig. 3.1). The granules got stabilized in R1 with large number of spherical granules on day 40. In contrast, granule maturation process was slow in R2 and granules required 50 days to get stabilized. It might be due to the fact that sodium acetate was a new substrate to the refinery sludge, therefore required more time to get acclimatized along with the delayed granule maturation. On the other hand, refinery sludge was previously exposed to the phenol resulting in rapid granulation. 60 days were required to develop granules with 1-2 kg phenol m^{-3} day^{-1} loading of phenol as a carbon source (Jiang et al., 2004). The current research work was observed to be better in regards to obtaining faster granulation with toxic phenol and ammonia-nitrogen as compared to the work of Jiang et al. (2004). From the FESEM analysis, it was observed that R1 granules were more spherical with a clear outline than the granules of R2 (Fig. 3.2).

Almost all approaches reported till now for achieving rapid granulation is compiled in Table 3.2 (most of the research works have been discussed in the text) in a comparable form in terms of time required for achieving full granulation along with different parameters like the source of seed sludge, wastewater treatment, granule size, SVI, air flow rate, OLR, etc. Research works were carried out to obtain faster granulation by modifying operating conditions. Ca^{2+} augmentation significantly reduced the granule initiation time up to 21 days, but still a longer period (70 days) was required for the granules to be matured (Gao et al., 2011). In addition, mature aerobic granulation time was reduced from 73 days to 43 days by augmenting with Mg^{2+} and Al^{3+} (Wang et al., 2012). Mature granulation was also achieved in 42 days by using pure pyridine degrading strain to treat a recalcitrant organics; pyridine (Liang et al., 2018). By modifying applied shear force, aerobic starvation phase and settling

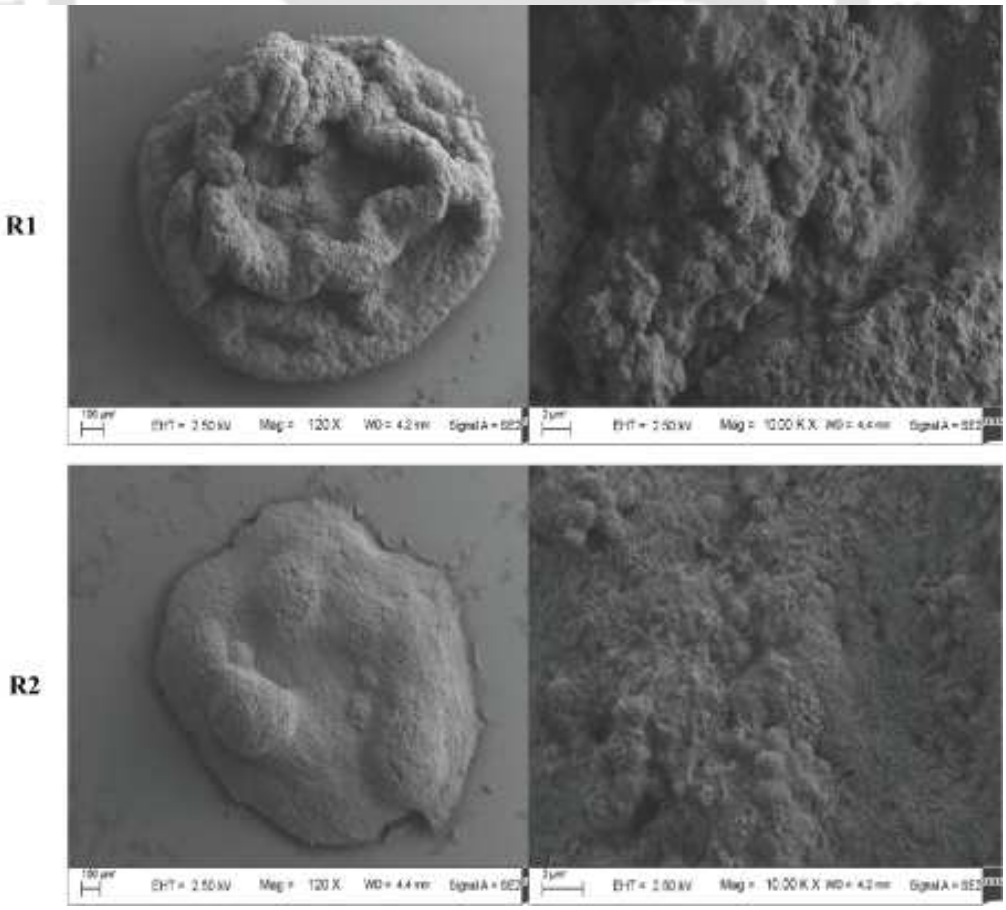

Fig. 3.2. FESEM images of a mature granule on day 70.

Table 3.2. Comparison of various approaches for rapid cultivation of aerobic granules.

Strategy for rapid granulation		Activated seed sludge	Type of wastewater	Wastewater Treatment	Average granule size (μm)	SVI (mL g TSS^{-1})	Air flow rate[a] / superficial gas velocity[b]	Initiation of granulation (days)	Complete granulation (days)	OLR[c/d]	References
Augmentation with metal / metal ions / exopolysaccharide	Ca^{2+}	MWTP	Glucose	COD and N	1000	20	5.00[a]	21	70	0.45-1.5[c]	Gao et al. (2011)
	Mg^{2+} and Al^{3+}	WTP	Sodium acetate	COD, N and P	-	35.8-42	3.33[a]	7	43	-	Wang et al. (2012)
	Zero-valent iron	WTP	Sodium acetate and glucose	COD and N	1500-2500	20-30	3.00[b]	7	43	-	Kong et al. (2014)
	Xanthan gum	DWRR facility	Sodium acetate	COD and N	500-1000	42	2.00[a]	5	20	-	Liu et al. (2018)
Selection of good inoculum	Acetate-fed aerobic granules	Acetate-fed aerobic granules	Sodium acetate and phenol	COD and phenol	1000-1500	22-38	3.50[a]	-	7	-	Tay et al. (2005)
		MWTP	Sodium acetate and 4 -chlorophenol	Sodium acetate and 4 -chlorophenol	-	81.6± 5.3	-	14	89	-	Carucci et al. (2009)
	Sludge from an industry	BWTP	Glucose	COD, N and P	-	30	4.00[b]	7	35	3.0[c]	Song et al. (2010)
		RWTP	**Phenol**	**COD, Phenol and N**	**1123.60± 113.55**	**36.42± 1.85**	**2.00[a]/1.18[b]**	**10**	**40**	**1.99[c]/ 0.80[d]**	**Present study**
	Crushed granules	WTP and crushed granules	Abattoir wastewater	COD, N and P	900-1000	-	-	-	60	-	Verawaty et al. (2012)

	25% AGS	Activated sludge and 25% AGS	Sodium acetate	COD, N and P	1590	80	1.2-2.0[b]	17	19	3.20-3.60[c]	Long et al. (2014)
	Pyridine degrading strains	Pure culture	Synthetic sodium acetate and pyridine	TOC, pyridine and NH_4^+-N	200-500	-	3.33[a]	-	42	-	Liang et al. (2018)
	Stored granular sludge	Stored granular sludge	Glucose and sodium acetate	COD, N and P	3000-4000	37.21	2.17[b]	-	22	-	Wang et al. (2019)
Addition of carrier media / coagu-lant	GAC	STP	Glucose	Low strength COD	600	30	2.0[a]	40	100	0.8[c]	Li et al. (2011a)
	PAC	STP	Glucose	COD and N	>2500	<40	2.0[a]	7	30	-	Liu et al. (2016)
Modification in operating conditions	Shear force	MWTP	phenol	COD	1000-1500	35	3.0[a]	21	160	-	Adav et al. (2007)
	Aerobic starvation	MWTP	Glucose	COD and N	600	24	5.0[a]	16	75	0.75[c]	Gao et al. (2011)
	Settling time	MWTP	Glucose	COD and N	800	19	5.0[a]	11	54	0.75[c]	Gao et al. (2011)
	Stressed substrate loading	WTP	Sodium acetate	COD, N and P	1900± 200	<40	2.80[b]	10	28	10.2± 2.1[c]	Hamza et al. (2018)

[a]air flow rate (L min^{-1}); [b]superficial gas velocity (cm s^{-1}); [c]organic loading rate (kg COD $m^{-3}day^{-1}$); [d]organic loading rate (kg phenol $m^{-3}day^{-1}$)
MWTP: Municipal wastewater treatment plant; WTP: Wastewater Treatment Plant; DWRR: Domestic water resource recovery ; BWTP: Beer wastewater treatment plant; RWTP: Refinery wastewater treatment plant; AGS: Aerobic granular sludge; GAC: Granular activated carbon; PAC: Poly aluminum chloride; STP: Sewage treatment plant; TOC: Total organic carbon

time, granules were achieved in between 54-160 days (Adav et al., 2007; Gao et al., 2011), which was a longer time period for getting granulation. Liu and Tay (2015) and Hamza et al. (2018) achieved mature granulation within only 3 and 28 days, respectively, with a simple biodegradable carbon source sodium acetate at high loadings. Beer sludge was also used to develop granules rapidly within 35 days with simple glucose as a carbon source (Song et al., 2010). Therefore, it can be observed from Table 3.2 that all the strategies used for rapid granulation were either tedious, require supplementation, expensive, or fed with a simple carbon source. Therefore a simple approach is desirable for cultivating granules quickly to treat recalcitrant organics such as phenol in a single vessel without adding any extra supplementary materials. This study can be a possible approach to the above said.

3.4.4.2 Granular characteristics

The characteristics of granules are given in Table 3.3. The size distribution of granular biomass with D50 value in R1 and R2 with time is given in Fig. 3.3. The size of the inoculum sludge was 45.76±12.06 μm. The mean size increased from 35.55 to 889.58 μm in R1 and from 33.97 to 978.93 μm in R2 (day 1 to day 10) because of filamentous structure and then reduced to around 429 μm (day 28) and 228 μm (day 31) in R1 and R2, respectively. On day 1, the size of R1 and R2 biomass

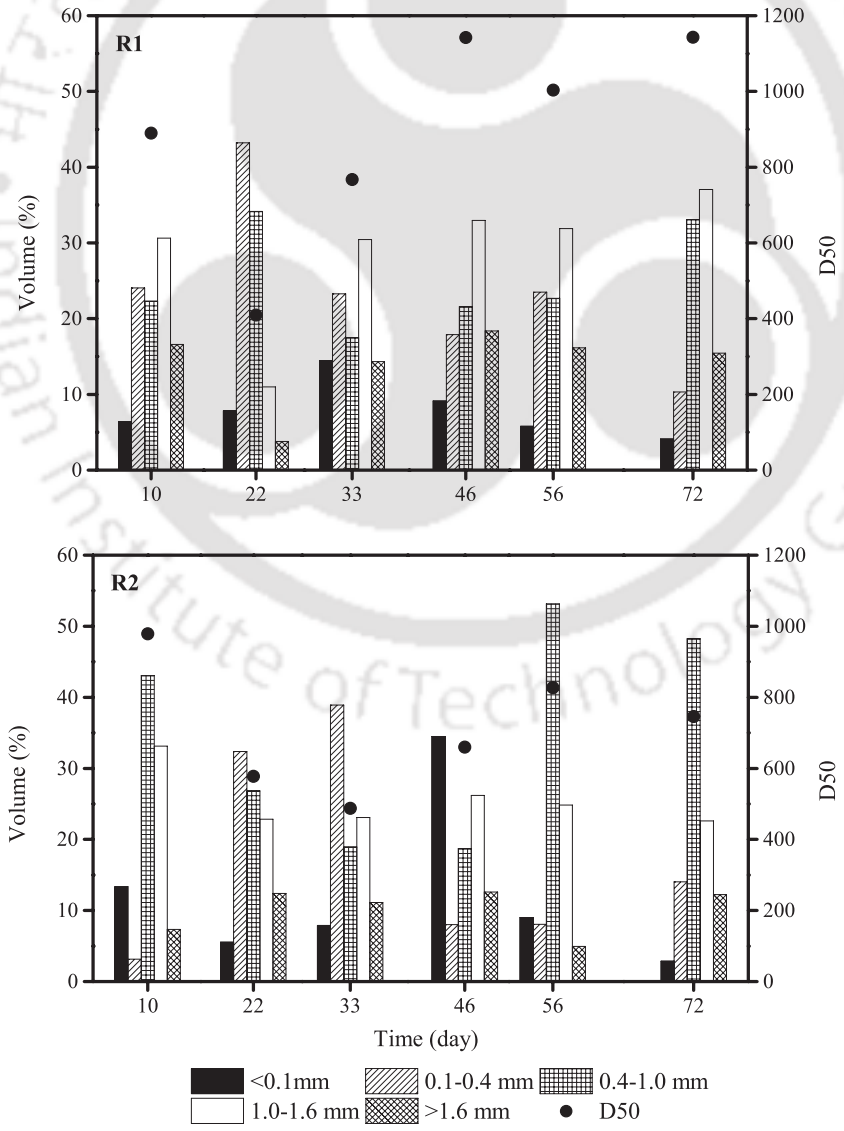

Fig. 3.3. Size distribution of granular biomass with time.

Table 3.3. Characteristics of granules of R1 and R2 during the steady-state.

Characteristics	R1	R2
VSS (g L^{-1})	3.65±0.09	2.30±0.08
SVI_{30} (mL g TSS^{-1})	36.42±1.85	55.60±2.15
GSV (m h^{-1})	38.02±1.58	29.88±1.03
Average granule size (μm)	1123.60±113.55	771.04±36.71
PN (mg $gVSS^{-1}$)	58.24±1.01	46.01±0.33
PS (mg $gVSS^{-1}$)	19.02±0.13	16.60±0.46
EPS (mg $gVSS^{-1}$)	77.26±1.13	62.62±0.68
F/M ratio (g COD $gVSS^{-1}$ day^{-1})	0.55	0.86

was smaller than the inoculum sludge, it might be because of the dilution made up to 6 L with tap water containing feed and aeration supplied. Since then, a rise in the granular size was noticed in both reactors and got stabilized to a value of around 1100 μm on day 40 and 700 μm on day 50, respectively, in R1 and R2. During the steady-state (days 45-74), the majority of the granular fraction (around 33%) was in the range of 1000-1600 μm in R1, while in R2, around 50% of granules were in the size range of 400-1000 μm (Fig. 3.3). The average granule size obtained during the steady-state was 1123.60±113.55 and 771.04±36.71 μm in R1 and R2, respectively (Table 3.3). The exposure of refinery sludge previously to phenol might result in the faster and larger granule formation by the rapid consumption of phenol, which was required for the growth, than the other substrate. This could be the possible reason for getting larger granules in R1 than R2.

The concentration profile of granular biomass (VSS) is illustrated in Fig. 3.4a. The inoculum sludge was having a VSS value of 1.60±0.11 g L^{-1}. VSS concentrations were found to be increased from 1.08 to 3.54 g L^{-1} in R1 and from 0.90 to 2.38 g L^{-1} in R2 after the acclimatization phase. The stable VSS values were 3.65±0.09 and 2.30±0.08 g L^{-1} in R1 and R2, respectively, during the steady-state (Table 3.3).

Settling properties were also found to be better for R1. The initial value of SVI_{30} for inoculum sludge was 51.26 mL $gTSS^{-1}$. Initially, a rise was observed in SVI_{30} values from a value of 61.05 and 65.76 mL $gTSS^{-1}$ (day 1) to 163.95 (day 13) and 294.84 mL $gTSS^{-1}$ (day 7) in R1 and R2, respectively (Fig. 3.4b). It might be due to the filamentous growth having lower settleability. Afterward, a gradual reduction was observed in th(Table 3.3). Analysis for GSV was carried out from day 22^{nd} onwards. On day 22, GSV values e SVI_{30} values in both of the reactors and got stabilized to the values of 36.42±1.85 and 55.60±2.15 mL $gTSS^{-1}$, respectively, in R1 and R2 during steady-state were 31.16±10.39 and 27.50±13.28 m h^{-1} in R1 and R2, respectively. As time progressed, GSV values increased and reached to 35.33±10.04 and 29.03±15.14 m h^{-1} in R1 and R2, respectively, at the end of the acclimatization phase (day 46) indicating the denser granule formation (Fig. 3.4b). In R1 and R2, the GSV values were 38.02±1.58 and 29.88±1.03 m h^{-1}, respectively, during steady-state (Table 3.3). From the results, it was observed that as time progressed, a reduction (except some initial days) and a rise were observed in SVI_{30} and GSV values, respectively, in both of the reactors confirming the granular development. It was also conferred from the lower SVI_{30} and higher GSV values of R1 (Fig. 3.4b) that R1 was depicting better settling behaviour than R2 resulting in the denser and compact granulation. R1 SVI_{30} value was found to be similar to many research works (Table 3.2).

Fig. 3.5 illustrates the EPS, PN and PS profiles of both the reactors. As the operation continued,

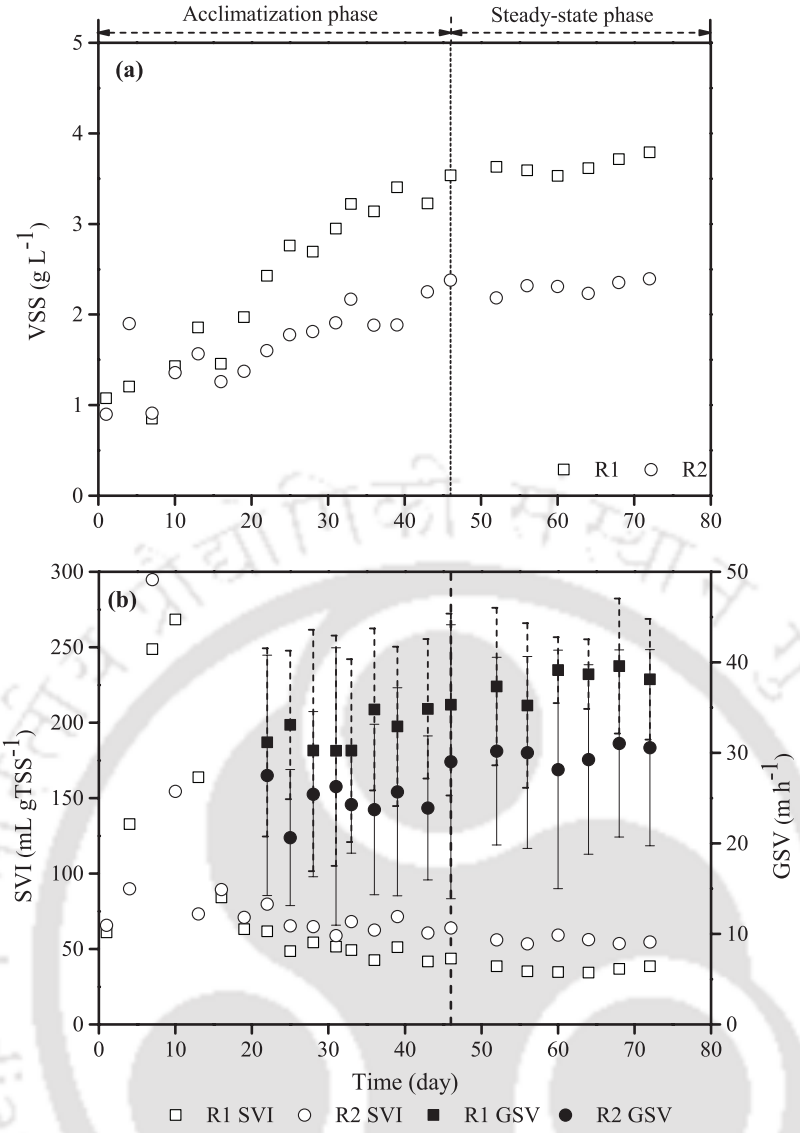

Fig. 3.4. Granular characteristics; (a) VSS, (b) SVI_{30} and GSV with time.

a distinct increment was observed in EPS, PN and PS contents of both the reactors and got stabilized during steady-state. Initial contents of EPS, PN and PS in R1 were 47.00, 36.32 and 12.88 mg $gVSS^{-1}$, whereas in R2, the values were 32.37, 23.43 and 8.94 mg $gVSS^{-1}$, respectively. During steady-state, in R1, the EPS, PN and PS values were 77.26±1.13, 58.24±1.01and 19.02±0.13 mg $gVSS^{-1}$, respectively (Table 3.3). On the other hand, in R2, the values were found to be 62.62±0.68, 46.01±0.33 and 16.60±0.46 mg $gVSS^{-1}$, respectively (Table 3.3). It was clear from the results that R1 was having more EPS, PN and PS content than R2. EPS, a sticky polysaccharide, promotes the binding of the cell by secreting a glue-like substance resulting in stable granule formation (Zhang et al., 2007). Toxic compounds enhanced the EPS secretion due to the toxic effects caused by them, thus encouraging the granule integrity (Chen et al., 2017). Higher EPS content in R1 could be due to the previous exposure of the toxic phenol to the refinery sludge. Another reason for higher EPS in R1 might be the higher VSS in R1 than R2. More EPS in R1 was supposed to be responsible for larger granules than R2 by forming a sticky network that was responsible for the aggregation of cells together.

Food to microorganism (F/M) ratios were 0.55 and 0.86 g COD $gVSS^{-1}$ day^{-1}, respectively, in R1 and R2. R1 F/M ratio was in the range required for aerobic granulation (0.3 to 6.0 g COD gSS^{-1} day^{-1}) (Li et al., 2008), thus resulting in excellent granular characteristics and pollutant removal

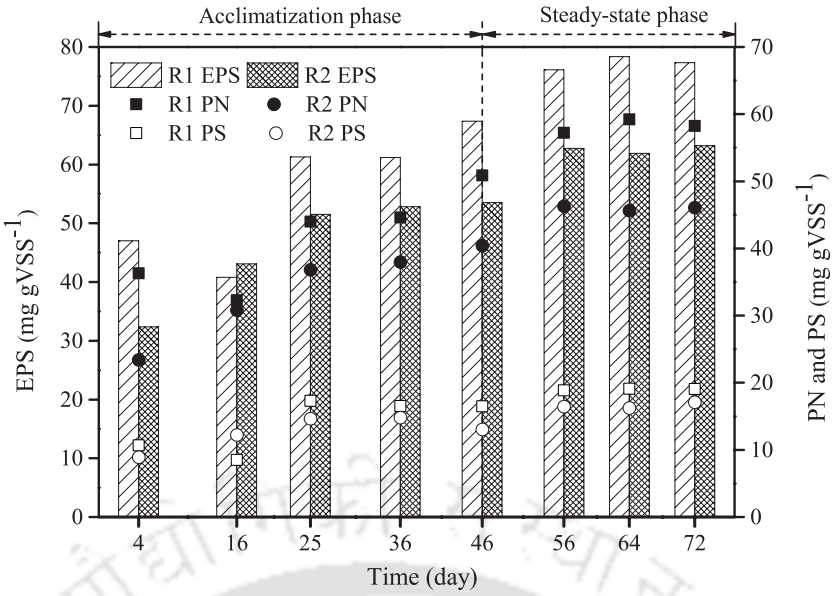

Fig. 3.5. EPS, PN and PS contents with time.

profiles. On the other hand, the reason for not having good granular characteristics in R2 might be the higher F/M ratio. It was reported that higher F/M ratio of 0.9±0.04 g COD gSS^{-1} day^{-1} resulted in a reduction in the settling behaviour of the granular sludge (Wu et al., 2018).

3.4.4.3 Pollutant removal profile

The OLR was almost the same in both of the SBRs; 2.00 kg COD m^{-3} day^{-1} (0.80 kg phenol m^{-3} day^{-1}) and 1.97 kg COD m^{-3} day^{-1} in R1 and R2, respectively. The pollutant removal performance during steady-state is provided in Table 3.4. Nearly complete phenol (>99%) was biodegraded in R1 throughout the study including both phases; acclimatization and steady-state (Fig. 3.6a). Almost negligible phenol was observed in the effluent (0.17±0.12 mg L^{-1}) of R1 from an influent phenol of 400 mg L^{-1} during steady-state. In R2, the source of COD was CH_3COONa. Therefore, COD removal was related to the degradation of CH_3COONa in R2. Around 94% COD removal was observed in R1 while it was around 91% in R2. Effluent COD values were 57.33±7.84 and 84.79±7.23 mg L^{-1} from the initial values of 996.62±24.48 and 984.36±16.83 mg L^{-1} in R1 and R2, respectively, during the period of steady-state (Fig. 3.6b). >99% and almost complete removal (94%) of phenol and COD, respectively, revealed the complete mineralization of phenol and intermediates formed during phenol biodegradation.

NLR of 0.20 kg NH_4^+-N m^{-3} day^{-1} was the same in both of the reactors. NH_4^+-N removal profile is given in Fig. 3.7a. For initial 13 (in R1) and 15 days (in R2), almost no NH_4^+-N along with the negligible amount of NO_2^--N and NO_3^--N (Fig. 3.7b) in the effluent were observed from the initial NH_4^+-N concentrations of 20 and 35 mg L^{-1} in R1 and R2, respectively. Hence, it was assumed that for the initial 13-15 days, NH_4^+-N was utilized by the microbes for their growth. Since then, a hike in effluent NH_4^+-N was noticed in both reactors indicating no nitrification. Later on, the partial nitrification was observed on days 41 and 37 in R1 and R2, respectively, with an influent ammonia-nitrogen concentration of around 100 mg L^{-1}. The longer time required by *Nitrosomonas* to develop in the reactors because of its slow growth might be the possible reason for achieving partial nitrification nearly at the end of the acclimatization stage. The majority of NH_4^+-N was converted into NO_2^--N (95.99±2.30 and 91.05±1.71 mg L^{-1}, respectively in R1 and R2) and a small amount to NO_3^--N

Table 3.4. Pollutant removal performance during steady-state.

Pollutant	R1			R2		
	Influent (mg L^{-1})	Effluent (mg L^{-1})	% removal	Influent (mg L^{-1})	Effluent (mg L^{-1})	% removal
Phenol	398.75±3.24	0.17±0.12	99.96±0.03	-	-	-
COD	996.62±24.48	57.33±7.84	94.25±0.77	984.36±16.83	84.79±7.23	91.39±0.73
NH_4^+-N	100.37±1.83	0.31±0.55	99.70±0.54	99.38±0.82	0.74±0.81	99.25±0.82

(13.04±2.60 and 16.46±1.57 mg L^{-1}, respectively, in R1 and R2) indicating the partial nitrification process. Effluent NH_4^+-N concentrations were 0.31±0.55 and 0.74±0.81 mg L^{-1}, respectively, in R1 and R2 from an influent NH_4^+-N of around 100 mg L^{-1}.

The likely explanation for the absence of complete nitrification and accumulation of NO_2^--N could be the free ammonia (FA). FA imposes an inhibitory effect on both *Nitrosomonas* and *Nitrobacter*. Susceptibility of *Nitrobacter* is more towards FA inhibition with a threshold value of 0.1-4.0 mg L^{-1}, whereas for *Nitrosomonas*, the threshold value was 10-150 mg L^{-1} (Yang et al., 2004). In R1 and R2, pH values were 7.77±0.11 and 7.83±0.14, respectively, with an average temperature of 31.8±1.14 °C

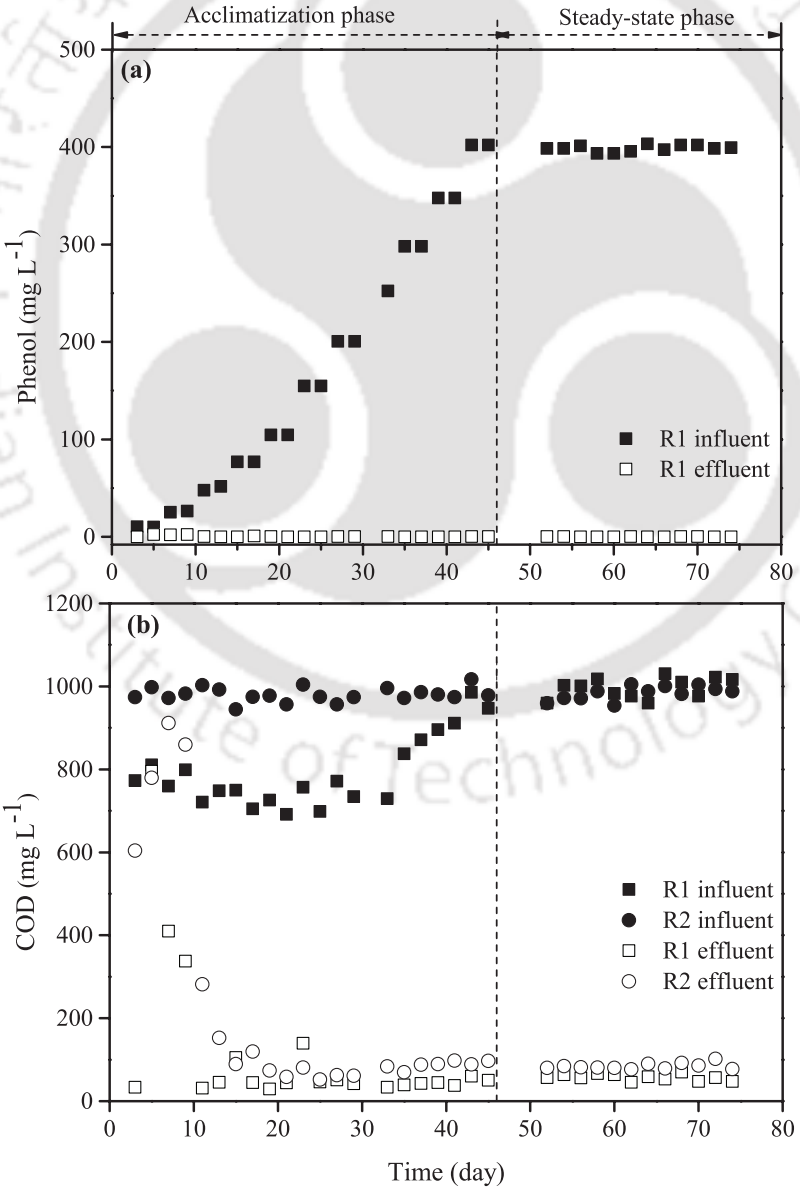

Fig. 3.6. Influent and effluent (a) phenol and (b) COD with time.

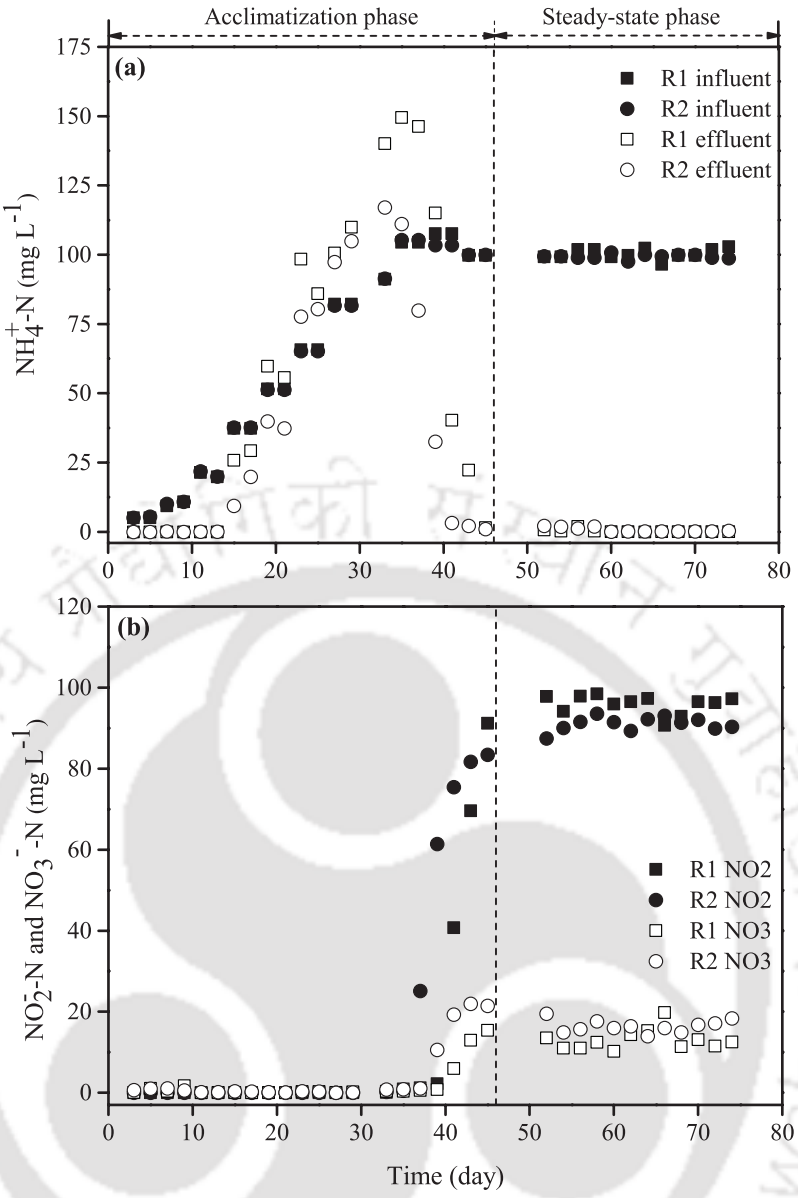

Fig. 3.7. (a) Influent and effluent NH_4^+-N and (b) effluent NO_2^--N and NO_3^--N with time.

during steady-state. FA concentrations for R1 and R2 were observed to be 5.44±1.62 and 6.12±1.53 mg L^{-1}, respectively, which were higher than the inhibition threshold for *Nitrobacter* in both the reactors. FA was calculated according to equation 3.1 (Yang et al., 2004).

$$FA\ (mgL^{-1}) = \frac{NH_4^+ - N \times 10^{pH}}{\exp[6334/(273+T)] + 10^{pH}} \tag{3.1}$$

The mass balance for NH_4^+-N is expressed as equation 3.2. Thereby, the total effluent nitrogen was around 109 and 108 mg L^{-1} in R1 and R2, respectively, from the influent value of 100 mg L^{-1}. The absence of denitrification was confirmed from the higher effluent value of nitrogen than that of influent in both reactors.

$$Influent\ NH_4^+ - N\ (mgL^{-1}) = Effluent\ NH_4^+ - N + effluent\ NO_2^- - N + effluent\ NO_2^- - N \tag{3.2}$$

In activated sludge system, nitrification was inhibited by phenol at a concentration of beyond 200 mg L^{-1} (Kim et al., 2008), whereas in aerobic granular system, nitrifying bacteria bearing NH_4^+-N

of 150 mg L^{-1} were able to tolerate up to 10 mg L^{-1} of phenol only (Liu et al., 2005). In this work, R1 granules with 100 mg L^{-1} of NH_4^+-N were able to perform nitrification without inhibition by phenol up to a concentration of 400 mg L^{-1}. The rapid start-up of partial nitrification granules were achieved in around 50 days with acetate and propionate as carbon sources (Wan et al., 2013). In the present work, the partial nitrification granules were developed in around 40 days with toxic phenol as a source of carbon. Therefore, the current research work was found to be better than the work of Wan et al. (2013) in terms of time required for achieving partial nitrification granules with a toxic substrate. It is clear from the results that contaminant removal was independent of inoculum sludge and substrate combination.

3.4.5 Conclusion of rapid granulation

The results illustrated that mature granules were rapidly developed only in 40 days with the combination of refinery sludge and phenol along with excellent granular characteristics (VSS, SVI_{30}, GSV, granule size and EPS content of 3.65±0.09 g L^{-1}, 36.42±1.85 mL $gTSS^{-1}$, 38.02±1.58 m h^{-1}, 1123.60±113.55 μm and 77.26±1.13 mg $gVSS^{-1}$, respectively) as compared to the granules generated from the combination of refinery sludge and sodium acetate. Therefore, rapid granulation was considered as a function of substrate and inoculum combination. The combination of inoculum sludge and substrate did not impose any impact on contaminants removal. More than 90% COD was removed along with almost 99% removal of NH_4^+-N in both reactors. Phenol was almost completely removed in R1. Therefore, the present study provides a rapid and reliable approach for AGS cultivation to treat recalcitrant organics, phenol, by selecting such a seed sludge that was previously exposed to the same recalcitrant contaminant (phenol in the present study) and also delivered an approach for obtaining rapid partial nitrification granules.

3.5 Reformation of aerobic granules

After 75 days of stable R1 operation with VSS, granule size and EPS of 3.67 g L^{-1}, 1202.03±487.78 μm and 78.23 mg $gVSS^{-1}$, respectively, the granules started to deteriorate and disintegration continued up to 84th day. The well-established mechanism of granule disintegration is still unknown. From the day 85, SCN^- was added to the feed to observe its impact on the granule reformation.

3.5.1 Feed characteristics

The influent feed composition is given in Table 3.5. Thiocyanate (SCN^- as KSCN) was added to the feed from 85th day onwards. In this current work, SCN^- was opted because of its simultaneous occurrence with phenol and ammonia-nitrogen in the wastewater generated from coal processing units (Jia et al., 2014) and also because of the documentation of EPS secretion due to environmental stress (McSwain et al., 2005). Thats why taking environmental stress (in the form of SCN^- addition) and simultaneous occurrence of above-mentioned pollutants into consideration, SCN^- was chosen for the current work.

3.5.2 Reactor operation

R1 was operated up to 84 days in similar manner as was up to 75 days with phenol and NH_4^+-N concentrations of 400 and 100 mg L^{-1}, respectively. From day 85, SCN^- concentration was gradually increased and was kept at 240 mg L^{-1} for 10 days (days 116-126). Afterward, it was again raised up to 340 mg L^{-1} and the R1 was operated for the next fifteen days at 340 mg L^{-1} for steady-state data (Table 3.5).

Table 3.5. Feed composition.

Days	75-84	85-115	116-126	133-146
Phenol[a]	400	400	400	400
NH_4^+-N[a]	100	100	100	100
SCN^-[a]	0	10-200	240	340
$NaHCO_3$[a]	added as required			
Phosphate buffer[b]	1 mL L^{-1}			
Trace metal solution[c]	1 mL L^{-1}			

[a]unit mg L^{-1}; [b]Phosphate buffer contained (g L^{-1}): 72.3 KH_2PO_4 and 104.5 K_2HPO_4; [c]Trace metal solution contained (mg L^{-1}): 10,000 $MgSO_4.7H_2O$, 10,000 $CaCl_2.2H_2O$, 5000 $FeCl_3.6H_2O$, 1000 $CuCl_2$, 1000 $ZnCl_2$, 500 $NiCl_2.6H_2O$ and 500 $CoCl_2$

3.5.3 Results and discussion

R1 was operated at steady-state for one month (days 45-74) with phenol and NH_4^+-N concentrations of 400 and 100 mg L^{-1}, respectively. R1 was stable in terms of granule size, VSS, SVI_{30}, GSV, EPS, COD, phenol and NH_4^+-N removals. On day 75, stable granule size, VSS, SVI_{30}, GSV and EPS values were 1202.03±487.78 μm, 3.67 g L^{-1}, 37.34 mL $gTSS^{-1}$, 36.85±9.73 m h^{-1} and 78.23 mg $gVSS^{-1}$, respectively, whereas COD, phenol and NH_4^+-N removal efficiencies were 94.57, 99.96 and 99.92%, respectively. After 75 days of reactor operation, granules started to deteriorate (possibly might be due to change in EPS content) and disintegration continued until the addition of SCN^-.

3.5.3.1 Effect of SCN^- on characteristics of granules

Granular characteristics at different SCN^- concentrations with operation time is provided in Table 3.6.

Granule size

Granule size has been considered as one of the most prominent factors responsible for granule formation (Liu et al., 2014). The day-wise progress in the granule reformation from the deteriorated one is given in Fig. 3.8 and morphology of granules before (day 84) and after (day 140) addition of SCN^- is illustrated in Fig. 3.9. From Fig. 3.8 and Fig. 3.9 (visual observation), it was clear that after 75 days of reactor operation, granules started to degenerate (day 84) at an OLR and NLR of 0.80 kg phenol m^{-3} day^{-1} and 0.20 kg NH_4^+-N m^{-3} day^{-1}, respectively, and regained structural integrity after

Table 3.6. Granular characteristics at different SCN^- concentrations with operation time.

Characteristics	Operation time (day/days)					
	75	80-84	85-115	116-126	127-132	133-146
SCN^- (mg L^{-1})	0	0	10-200	240	275-300	340
Average granule size (μm)	1202.03± 487.78	1007.10	1263.79± 174.26	1557.87± 27.07	1670.26	1819.87± 43.44
VSS (g L^{-1})	3.67	2.50	3.51±0.67	3.98±0.12	4.06	4.44±0.09
SVI_{30} (mL g TSS^{-1})	37.34	56.19	45.65±14.41	29.97±0.49	28.95	26.31±0.80
GSV (m h^{-1})	36.85±9.73	31.26	41.16±7.82	50.73 ±0.64	54.80	57.32±0.96
EPS (mg $gVSS^{-1}$)	78.23	53.83	64.81±13.22	87.94±0.92	93.21	101.45±1.06
SRT (days)	9.23	7.49	10.20	9.71	9.62	9.56
F/M ratio (g COD $gVSS^{-1}$ day^{-1})	0.54	0.80	0.57	0.50	0.50	0.45

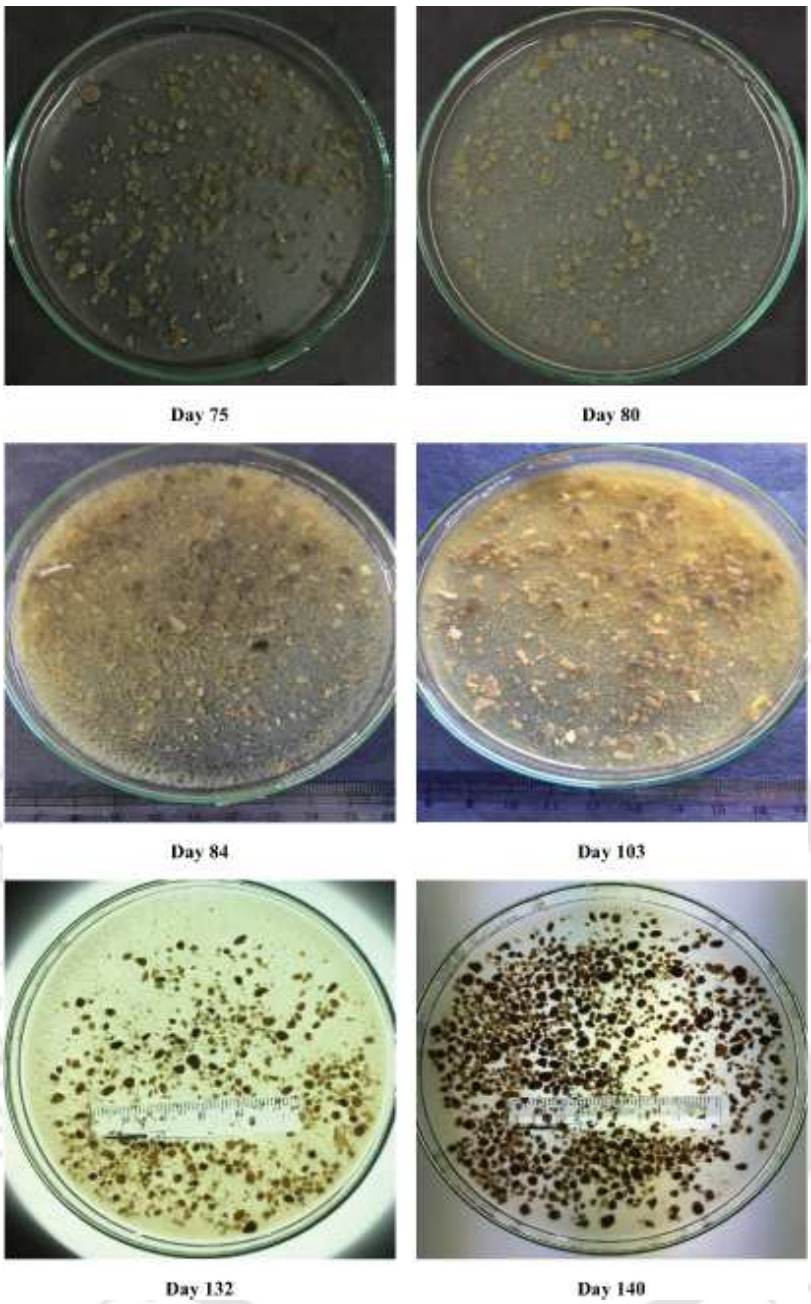

Fig. 3.8. Images of the granules before and after addition of SCN^-.

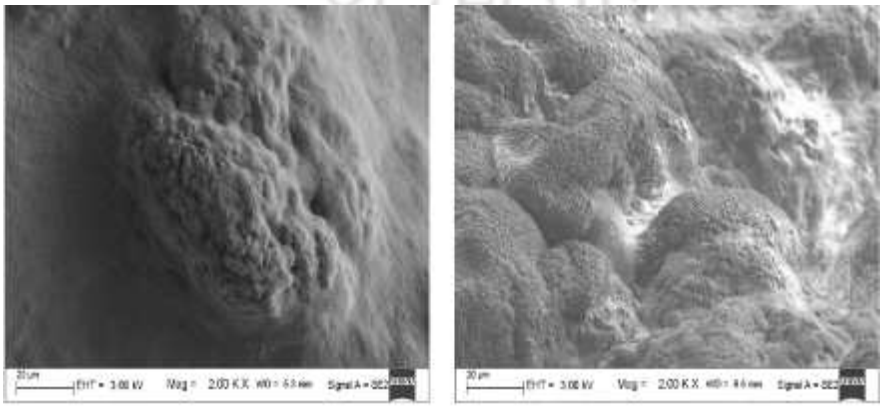

Fig. 3.9. FESEM images of the granules on day 84 and 140.

the addition of SCN^- (day 140). Liu et al. (2014) also observed granule disintegration after 86 days of reactor operation but with glucose as a carbon source, although the exact mechanism of granule rupture is still unknown. The change in granule size with operational time is given in Fig. 3.10a. The granule size was around 1202.03±487.78 μm on day 75, since then a reduction in granule size up to 87th day (911.19 μm) was observed indicating the rupture of the granules. Introduction of SCN^-

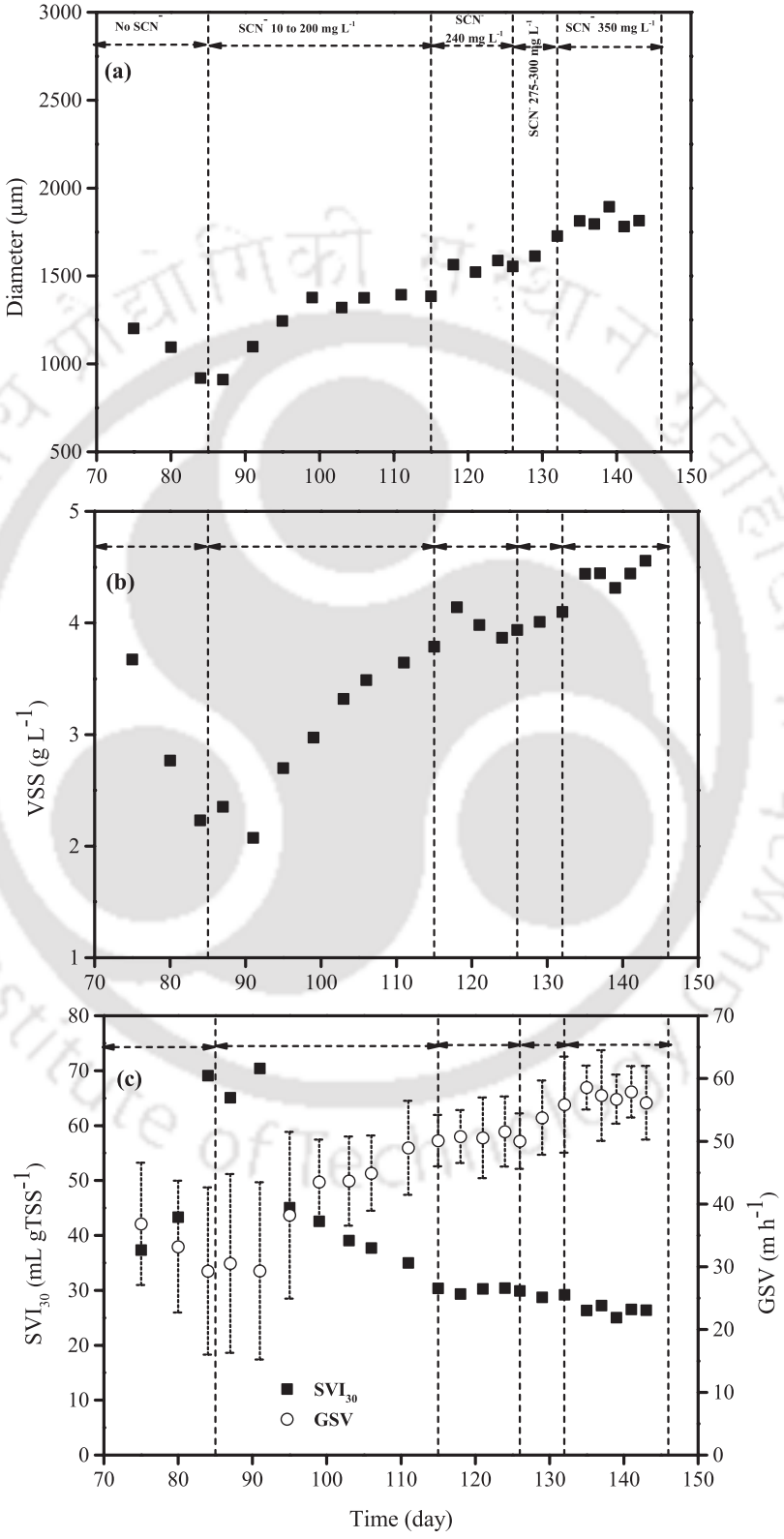

Fig. 3.10. Characteristics of granules (a) size, (b) VSS and (c) SVI and GSV during granule reformation study.

with a concentration of 10 mg L^{-1} didnt cause any positive impact on the size of granules, it might be because of time taken by AGS to cope up with the addition of toxic SCN^- (days 85-90). Nearly a week later (day 91), with the next dose of SCN^- (25 mg L^{-1}), an improvement in granule size was observed and it was continued up to day 146 of SBR operation. Granule reformulation was confirmed from the average granule size of 1819.87±43.44 μm formed after operating the reactor for 15 days (days 133-146) with SCN^- concentration of 340 mg L^{-1}.

VSS, SVI_{30} and GSV

VSS profile of the SBR is provided in Fig. 3.10b. VSS concentration decreased during the days 80-91 of reactor operation from the VSS value of 3.67 g L^{-1} (day 75) because of the deterioration of the granules. Granule disintegration was also supported through the solid retention time (SRT) values. On day 75, SRT was 9.23 days, whereas it was around 6.27 days on day 84 confirming the granule malfunctioning and biomass wash out. A rise in VSS was noticed after the addition of 75 mg L^{-1} of SCN^- and at 240 mg L^{-1} of SCN^- concentration (days 118-126), VSS reached to 3.98±0.12 g L^{-1}. During days 118-126, SRT was 9.71 days suggesting the granule reformation. The SCN^- concentration was again raised up to 340 mg L^{-1} to observe the impact of higher concentration of SCN^- on granular biomass and a higher average VSS of 4.44±0.09 g L^{-1} with 9.56 days SRT was observed during days 135-143. A rise in SVI_{30} value from 37.34 (day 75) to 70.42 mL $gTSS^{-1}$ (day 91) was observed indicating poor settling behaviour, it might be because of the granule dismantling (Fig. 3.10c). As SCN^- was increased, a reduction in SVI_{30} was noticed. SVI_{30} value decreased from 70.42 (day 91) to 29.97±0.49 mL $gTSS^{-1}$ (days 118-126) and further decreased to 26.31±0.80 mL $gTSS^{-1}$ after addition of 340 mg L^{-1} of SCN^- (days 135-143) (Fig. 3.10c). Lower SVI_{30} value confirmed the reformation of compact granular aggregate. An SVI value of 20-40 mL $gTSS^{-1}$ for the reformed granules after the addition of PAC was observed with glucose (Liu et al., 2014). The current research work was similar to the work of Liu et al. (2014) in terms of achieving SVI_{30} value (26.31±0.80 mL $gTSS^{-1}$) for the reformulated granules after the addition of toxic pollutant SCN^- and was advantageous in terms of getting reformed granules without the addition of any auxiliary materials. On the other hand, initially GSV was found to decrease from 36.85±9.73 (day 75) to 29.35±14.11 m h^{-1} (day 91). Later on, due to addition of SCN^-, a significant improvement was observed in the GSV value and got stabilized to 57.32±0.96 m h^{-1} (days 135-143) (Fig. 3.10c). From the Fig. 3.10c, it was concluded that as the SCN^- was continued to increase, a significant abatement in SVI_{30} and a rise in GSV values were observed indicating the granule reformulation. A week after addition of SCN^-, the granules showed adaptability towards SCN^- and afterward, a significant impact was observed on granule characteristics (Fig. 3.10) without any inhibitory effect of SCN^- up to a concentration of 340 mg L^{-1}.

F/M ratios with operation time are provided in Table 3.6. From the F/M ratio data, it was clear that during the operation time of 80-84 days (when no SCN^- was added to the feed), F/M ratio was quite higher with a value of 0.80 g COD $gVSS^{-1}$ day^{-1}. On the other hand, during the operation except for 80-84 days, F/M ratios were in the range required for aerobic granulation (0.3 to 6.0 g COD gSS^{-1} day^{-1}) (Li et al., 2008).

3.5.3.2 Effect of SCN^- on EPS

EPS is supposed to be a sticky substance that keeps the biofilms intact for maintaining its integrity and contains large number of functional groups such as hydroxyl and negatively charged carboxyl group. Due to the presence of these functional groups, ESP is to be considered as an excellent binding

polymer which could bind through many interactions like protein-polysaccharide, hydrophobic, ionic, H bonding, etc. (Zhang et al., 2007). Bacteria are negatively charged, which results in electrostatic repulsion between the cells (Pol et al., 2004). This repulsion must be reduced for the aggregation of bacteria. Since protein, the largest fraction of EPS, is comprised of the high amount of negatively charged amino acids which causes higher binding affinity of proteins than sugars with multivalent cations through electrostatic bonds resulting in the reduction in negative charge present on the surface of the bacterial cell, hence favouring the aerobic granulation by reducing the electrostatic repulsion between the cells (Zhang et al., 2007). Tsuneda et al. (2003) also stated that EPS covering on the surface of cells might reduce the negative surface charge around the cell surface, thus contributing in cell adhesion. Therefore, more secretion of EPS is desirable for the aerobic granulation. EPS content profile is illustrated in Fig. 3.11. Initially on day 75, EPS was around 78.23 mg $gVSS^{-1}$ and moved down to the lower value of 47.44 mg $gVSS^{-1}$ on day 91. Thereafter, a rise in EPS content was observed after the addition of toxic SCN^- and was continued throughout the study. During steady-state (days 133-146), the average value of EPS was 101.45±1.06 mg $gVSS^{-1}$. PN content was more eminent than PS content. From the EPS value, it was concluded that SCN^- was having a convincing impact on granule stability and also provoked the secretion of EPS for maintaining granular structure. Chen et al. (2017) also observed the higher EPS value after the addition of SCN^- in granule-based anammox process, where anammox granules secreted more EPS under adverse conditions caused by the addition of SCN^- to maintain the structure and activity of anammox granules. In the present study, aerobic granules also secreted more EPS because of toxic SCN^- addition and might have contributed to regaining the structural integrity of granules. The possible mechanism of granule reformulation after the addition of SCN^- is illustrated in Fig. 3.12. After 75 days of reactor operation, granules became unstable and started to deteriorate (confirmed by lower VSS and EPS values of 2.07 g L^{-1} and 47.44 mg $gVSS^{-1}$, respectively, on day 91). After the addition of toxic SCN^-, granules might have started to protect themselves against the toxic effect of SCN^- by secreting a gel-matrix of EPS (higher EPS values of 101.45±1.06 mg $gVSS^{-1}$ at SCN^- concentration of 340 mg L^{-1} during 133-146 days). Due to which broken granules agglomerated again in the trapping network of EPS. Because of the shear force caused due to air flow rate, the granules which were trapped in EPS gel network attained the regular structure. Thus, the addition of toxic SCN^- induced the granule reformulation by provoking more EPS secretion.

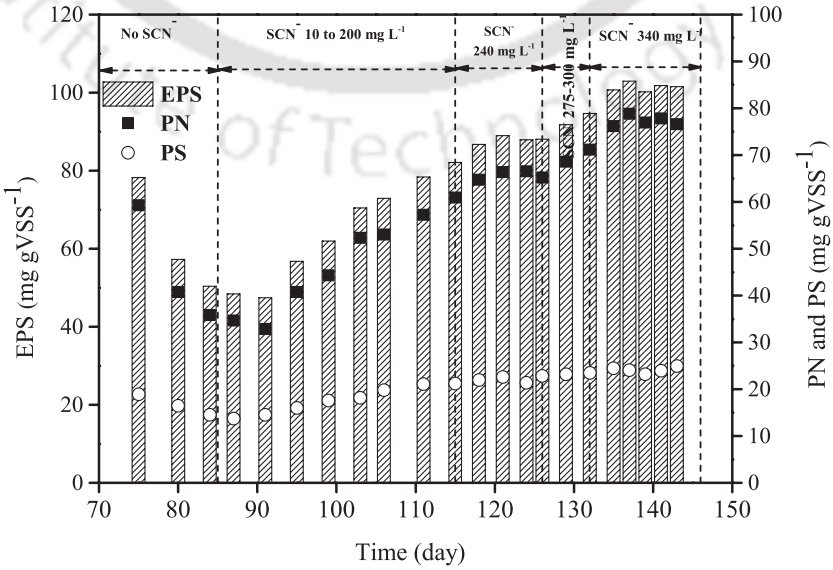

Fig. 3.11. Concentrations of total EPS, PN and PS contents during granule reformation.

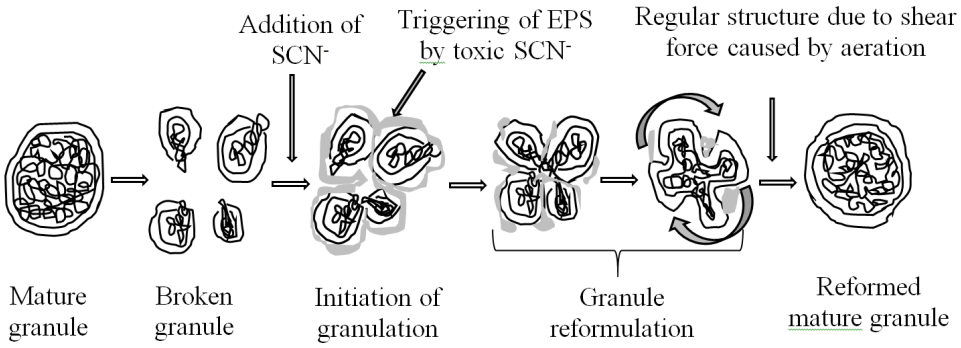

Fig. 3.12. A possible mechanism for the reformation of the granules.

3.5.3.3 Effect of SCN^- on reactor performance

R1 was operated with a constant OLR and NLR of 0.80 kg phenol m^{-3} day^{-1} (2.01±0.28 kg COD m^{-3} day^{-1}) and 0.20 kg NH_4^+-N m^{-3} day^{-1}, respectively, throughout the study. The pollutant removal profile at different SCN^- concentrations with operation time is given in Table 3.7. Phenol was almost completely biodegraded (⩾99%) from the influent phenol concentration of 400 mg L^{-1}. Granule disintegration did not show any impact on phenol biodegradation and biodegradation continued throughout the operation irrespective of granule deterioration and reformulation (Fig. 3.13a). It might be because of the presence of suspended solids in the SBR apart from AGS, which was supposed to contribute to phenol biodegradation. A little reduction was observed in COD removal efficiency from 94.57% (day 75) to 90.61% (day 92) because of the lower VSS resulted from the granule break down in SBR during those days (2.36±0.30 g L^{-1}). Once the granules began to reform after the addition of SCN^-, VSS started to increase (Fig. 3.10b), thus resulting in 94-97% COD removal efficiency (Fig. 3.13b). Complete mineralization of phenolic compound was confirmed from the higher COD removal efficiency.

Complete biotransformation of SCN^- was observed throughout the SBR operation (Fig. 3.13c). SCN^- did not show any adverse effect on granule reformulation up to a concentration of 340 mg L^{-1} along with around 99% removal efficiency and excellent granular characteristics (Fig. 3.13c and Fig. 3.10). Presence of sulphate in the reactor confirmed the SCN^- oxidation, even though it was not monitored.

Table 3.7. Pollutant removal profile at different SCN^- concentrations with operation time.

Pollutant		Operation time (day/days)					
		75	**80-84**	**85-115**	**116-126**	**127-132**	**133-146**
Phenol	**Influent (mg L^{-1})**	399.46	394.69	396.26±4.47	396.41±6.53	384.65	396.87±1.43
	Effluent (mg L^{-1})	0.16	0.25	0.28±0.29	0.61±0.47	0.03	0.17±0.15
	% removal	99.96	99.94	99.93±0.07	99.85±0.12	99.99	99.96±0.04
COD	**Influent (mg L^{-1})**	994.00	997.61	992.36±21.23	994.45±17.88	1012.01	1006.16±13.81
	Effluent (mg L^{-1})	53.96	135.58	60.15±40.96	40.03±13.62	36.98	43.56±10.19
	% removal	94.57	86.40	93.86±4.31	95.97±1.36	96.36	95.67±1.02
SCN^-	**Influent (mg L^{-1})**	-	-	94.73±60.56	235.77±2.00	282.46	339.29±4.05
	Effluent (mg L^{-1})	-	-	0.64±0.19	1.50±0.41	0.41	1.21±1.32
	% removal	-	-	98.29±2.73	99.36±0.17	99.85	99.65±0.38
NH_4^+-N	**Influent (mg L^{-1})**	99.76	98.30	100.34±3.01	99.07±1.69	98.30	96.54±1.93
	Effluent (mg L^{-1})	0.08	29.11	6.00±11.04	0.08±0.02	0.06	0.10±0.11
	% removal	99.92	70.38	93.88±11.28	99.92±0.02	99.94	99.89±0.11

Removal profile of NH_4^+-N is depicted in Fig. 3.14a. NH_4^+-N removal efficiency moved down from 99% (day 75) to 67% (day 86) from influent 100 mg L^{-1} of NH_4^+-N and again recovered to 99% soon after the addition of 75 mg L^{-1} of SCN^- (95^{th} day onwards) (Fig. 3.14a). It means nearly 10 days was taken by nitrifying bacteria to redevelop in the SBR. Additional NH_4^+-N also generated through the complete biotransformation of SCN^- (Equation 2.6). During steady-state (days 133-146),

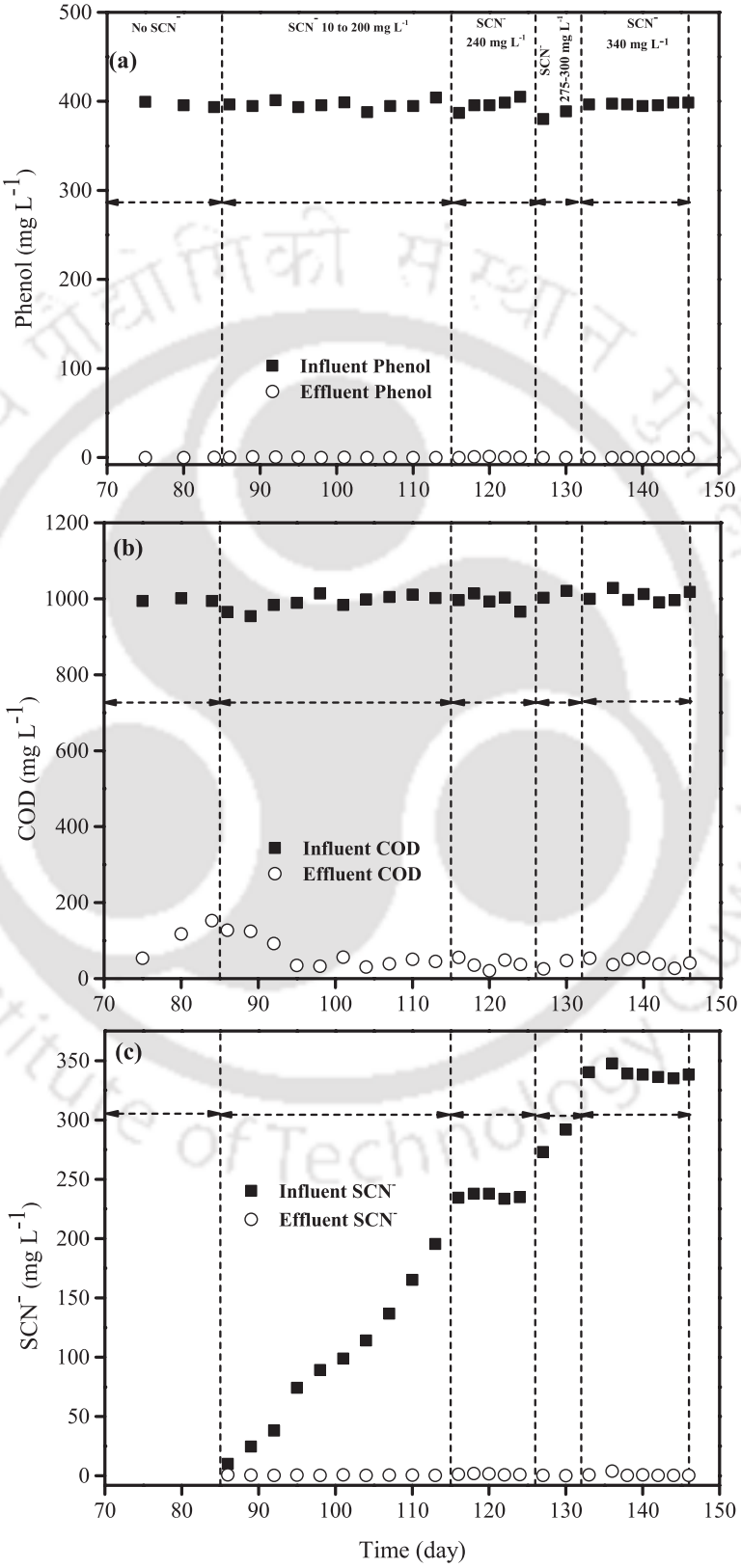

Fig. 3.13. Influent and effluent (a) phenol, (b) COD and (c) SCN^- during reformation.

the total influent nitrogen was around 180 mg L^{-1} out of which around 80 mg L^{-1} generated from the biotransformation of 340 mg L^{-1} of SCN^-. Therefore, around 180 mg L^{-1} of NH_4^+-N transformed in the present study. Effluent NO_2^--N and NO_3^--N followed a different trend during the SBR operation (Fig. 3.14b). On day 75, concentrations of NO_2^--N and NO_3^--N in the effluent were 93.45 and 13.89 mg L^{-1}, respectively, from 100 mg L^{-1} of influent NH_4^+-N. Higher amount of effluent NO_2^--N confirmed the nitritation process. On day 75, SRT was 9.23 days, which was lower than the required value for achieving complete nitrification (10-30 days) (Tchobanoglous et al., 2003), therefore most of NH_4^+-N transformed into NO_2^--N. After 75 days of SBR operation, loss in nitritation efficiency was observed because of the washout of the nitrifiers from the system due to granule disintegration (confirmed through the decline in VSS value; Fig. 3.10b) resulting in increased effluent NH_4^+-N (34.40 mg L^{-1}) and reduced effluent NO_2^--N and NO_3^--N concentrations up to 55.78 and 10.44 mg L^{-1}, respectively, (day 84) with a shorter SRT of 6.72 days. Afterward, as the granules started to reform after the addition of SCN^-, recovery in nitritation efficiency was observed (Fig. 3.14b). Effluent NO_2^--N concentration first increased to 91.72 mg L^{-1} (day 95) and further decreased to 59.35 mg L^{-1} (day

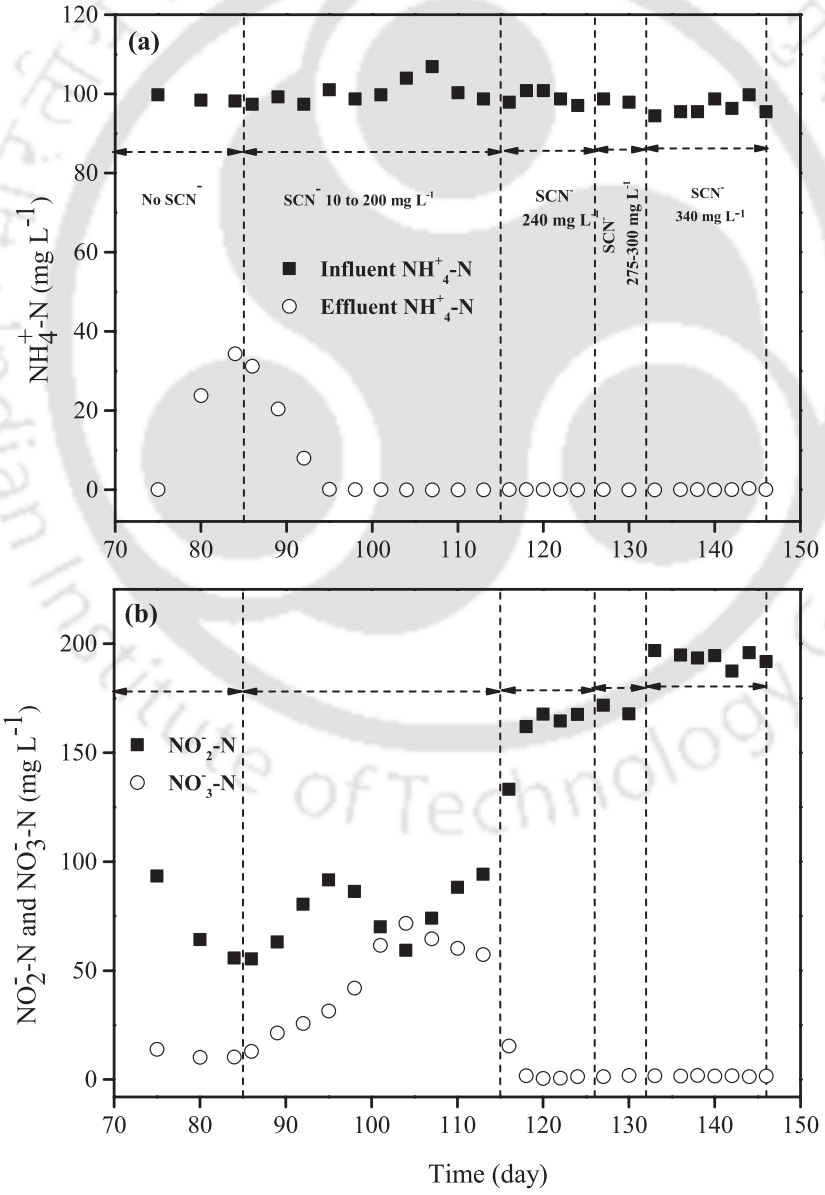

Fig. 3.14. (a) influent and effluent NH_4^+-N (b) effluent NO_2^--N and NO_3^--N during granule reformation.

104) at SCN^- concentration of 115 mg L^{-1} with an SRT of 10.93 days, at the same time effluent NO_3^--N concentration was on its maximum level (71.72 mg L^{-1}). It might be because of 10.93 days SRT, which was in the range of SRT values required for complete nitrification (10-30 days), therefore most of NH_4^+-N converted into NO_3^--N. As the SCN^- concentration was further increased (⩾240 mg L^{-1}), effluent NO_2^--N concentration increased, whereas effluent NO_3^--N and SRT values decreased because of the toxicity imparted by higher SCN^- (⩾240 mg L^{-1}) on the activity of nitrite-oxidizing bacteria (NOB) (116^{th} day onwards). At 240 mg L^{-1} of SCN^- (days116-126), effluent NO_2^--N concentration was around 159.05±14.59 mg L^{-1} from influent NH_4^+-N of around 156 mg L^{-1} (calculated from equation 2.6), whereas NO_3^--N was only 3.98±6.43 mg L^{-1} with an SRT of 9.71 days. During steady-state (days 133-146) at SCN^- concentration of 340 mg L^{-1}, effluent NO_2^--N and NO_3^--N concentrations were 193.58±3.13 and 1.73±0.16 mg L^{-1}, respectively, from the influent NH_4^+-N of around 180 mg L^{-1} (calculated from equation 2.6) with an SRT of 9.56 days. During days 133-146, effluent NH_4^+-N was almost negligible (around 0.10 mg L^{-1}). Nitritation efficiency was successfully recovered and indicated from the higher effluent NO_2^--N concentration (193.58±3.13 mg L^{-1}) confirming that ammonia-oxidizing bacteria (AOB) remained unaffected by the higher SCN^- concentration (⩾240 mg L^{-1}). The mass balance for nitrogen was calculated by equation 3.2. Total effluent nitrogen was around 195.41 mg L^{-1} from the influent NH_4^+-N of around 180 mg L^{-1}. Higher amount of effluent N than influent NH_4^+-N confirmed the absence of denitrification process. Li et al. (2011b) observed a slight inhibition on SCN^- removal at a phenol concentration of around 420 mg L^{-1} in a moving bed biofilm reactor. It was also observed that SCN^- and phenol concentrations beyond 200 mg L^{-1} seemed to inhibit nitrification (Kim et al., 2008). In the current work, no inhibition among the pollutants was observed up to the concentrations of 400, 180 and 340 mg L^{-1} for phenol, NH_4^+-N and SCN^-, respectively.

From the results, it was concluded that not only the addition of SCN^- induced the granule reformulation by provoking the EPS secretion but also reformed the granules with better characteristics than the granules formed before disintegration. The addition of SCN^- served two purposes; one was to reform the granules from the broken one along with the recovery of nitritation efficiency and second was the treatment of wastewater containing phenol, SCN^- and NH_4^+-N as well. To the author's best knowledge, this study is the first study in which broken aerobic granules again reformed by the addition of a toxic substance along with the recovery of the nitritation process.

3.5.4 Conclusion of granule reformation

The addition of toxic SCN^- showed a significant effect on the reformation of the aerobic granules by triggering the more EPS secretion, which was supposed to induce the granule agglomeration. Reformed granules also successfully regained their nitritation efficiency. Reformed granules were having better characteristics than the granules formed before deterioration. Granules with larger size (1819.87±43.44 μm), better settling behaviour (SVI_{30} and GSV of 26.31±0.80 mL $gTSS^{-1}$ and 57.32±0.96 m h^{-1}, respectively) and higher EPS (101.45±1.06 mg $gVSS^{-1}$) content were reformulated. Up to a concentration of 340 mg L^{-1}, SCN^- did not show any inhibitory effect on characteristics of reformed granules, phenol removal profile and nitritation efficiency.

References

Adav, S.S., Lee, D.J., Lai, J., 2007. Effects of aeration intensity on formation of phenol-fed aerobic granules and extracellular polymeric substances. Applied Microbiology and Biotechnology 77,

175-182.
Carucci, A., Milia, S., De Gioannis, G., Piredda, M., 2009. Acetate-fed aerobic granular sludge for the degradation of 4-chlorophenol. Journal of Hazardous Materials 166, 483-490.
Chen, Q.Q., Chen, H., Zhang, Z.Z., Guo, L.X., Jin, R.C., 2017. Effects of thiocyanate on granule-based anammox process and implications for regulation. Journal of Hazardous Materials 321, 81-91.
Gao, D., Liu, L., liang, H., Wu, W.M., 2011. Comparison of four enhancement strategies for aerobic granulation in sequencing batch reactors. Journal of Hazardous Materials 186, 320-327.
Hamza, R.A., Iorhemen, O.T., Zaghloul, M.S., Tay, J.H., 2018. Rapid formation and characterization of aerobic granules in pilot-scale sequential batch reactor for high-strength organic wastewater treatment. Journal of Water Process Engineering 22, 27-33.
Hu, J., Zhang, Q., Chen, Y.Y., Lee, D.J., 2016. Drying and recovery of aerobic granules. Bioresource Technology 218, 397-401.
Ivanov, V., Wang, X.H., Tay, S.T.L., Tay, J.H., 2006. Bioaugmentation and enhanced formation of microbial granules used in aerobic wastewater treatment. Applied Microbiology and Biotechnology 70, 374-381.
Jia, S., Han, H., Hou, B., Zhuang, H., Fang, F., Zhao, Q., 2014. Treatment of coal gasification wastewater by membrane bioreactor hybrid powdered activated carbon (MBRPAC) system. Chemosphere 117, 753-759.
Jiang, H.L., Tay, J.H., Tay, S.L., 2004. Changes in structure, activity and metabolism of aerobic granules as a microbial response to high phenol loading. Applied Microbiology and Biotechnology 63, 602-608.
Kim, Y.M., Park, D., Lee, D.S., Park, J.M., 2008. Inhibitory effects of toxic compounds on nitrification process for cokes wastewater treatment. Journal of Hazardous Materials 152, 915-921.
Kong, Q., Ngo, H.H., Shu, L., Fu, R.S., Jiang, C.H., Miao, M.S., 2014. Enhancement of aerobic granulation by zero-valent iron in sequencing batch airlift reactor. Journal of Hazardous Materials 279, 511-517.
Lee, D.J., Chen, Y.Y., Show, K.Y., Whiteley, C.G., Tay, J.H., 2010. Advances in aerobic granule formation and granule stability in the course of storage and reactor operation. Biotechnology Advances 28, 919-934.
Li, A.J., Li, X.Y., Yu, H.Q., 2011a. Granular activated carbon for aerobic sludge granulation in a bioreactor with a low-strength wastewater influent. Separation and Purification Technology 80, 276-283.
Li, A.J., Yang, S.F., Li, X.Y., Gu, J.D., 2008. Microbial population dynamics during aerobic sludge granulation at different organic loading rates. Water Research 42, 3552-3560.
Li, H.Q., Han, H.J., Du, M.A., Wang, W., 2011b. Removal of phenols, thiocyanate and ammonium from coal gasification wastewater using moving bed biofilm reactor. Bioresource Technology 102, 4667-4673.
Liang, J., Li, W., Zhang, H., Jiang, X., Wang, L., Liu, X., Shen, J., 2018. Coaggregation mechanism of pyridine-degrading strains for the acceleration of the aerobic granulation process. Chemical Engineering Journal 338, 176-183.
Liu, L., Gao, D.W., Zhang, M., Fu, Y., 2010. Comparison of Ca^{2+} and Mg^{2+} enhancing aerobic granulation in SBR. Journal of Hazardous Materials 181, 382-387.
Liu, S., Zhan, H., Xie, Y., Shi, W., Wang, S., 2018. Rapid cultivation of aerobic granular sludge by xanthan gum in SBR reactors. Water Science and Technology 2017, 360-369.
Liu, Y., Liu, Z., Wang, F., Chen, Y., Kuschk, P., Wang, X., 2014. Regulation of aerobic granular sludge reformulation after granular sludge broken: Effect of poly aluminum chloride (PAC). Bioresource Technology 158, 201-208.
Liu, Y.Q., Tay, J.H., 2015. Fast formation of aerobic granules by combining strong hydraulic selection pressure with overstressed organic loading rate. Water Research 80, 256-266.
Liu, Y.Q., Tay, J.H., Ivanov, V., Moy, B.Y.P., Yu, L., Tay, S.T.L., 2005. Influence of phenol on nitrification by microbial granules. Process Biochemistry 40, 3285-3289.
Liu, Z., Liu, Y., Kuschk, P., Wang, J., Chen, Y., Wang, X., 2016. Poly aluminum chloride (PAC) enhanced formation of aerobic granules: Coupling process between physicochemicalbiochemical effects.

Chemical Engineering Journal 284, 1127-1135.
Long, B., Xuan, X., Yang, C., Zhang, L., Cheng, Y., Wang, J., 2019. Stability of aerobic granular sludge in a pilot scale sequencing batch reactor enhanced by granular particle size control. Chemosphere 225, 460-469.
Long, B., Yang, C.Z., Pu, W.H., Yang, J.K., Jiang, G.S., Dan, J.F., Li, C.Y., Liu, F.B., 2014. Rapid cultivation of aerobic granular sludge in a pilot scale sequencing batch reactor. Bioresource Technology 166, 57-63.
McSwain, B., Irvine, R., Hausner, M., Wilderer, P., 2005. Composition and distribution of extracellular polymeric substances in aerobic flocs and granular sludge. Applied and Environmental Microbiology 71, 1051-1057.
Muñoz Palazon, B., Pesciaroli, C., Rodriguez Sanchez, A., Gonzalez Lopez, J., Gonzalez Martinez, A., 2018. Pollutants degradation performance and microbial community structure of aerobic granular sludge systems using inoculums adapted at mild and low temperature. Chemosphere 204, 431-441.
Ou, D., Li, W., Li, H., Wu, X., Li, C., Zhuge, Y., 2018. Enhancement of the removal and settling performance for aerobic granular sludge under hypersaline stress. Chemosphere 212, 400-407.
Pol, L.H., de Castro Lopes, S., Lettinga, G., Lens, P., 2004. Anaerobic sludge granulation. Water Research 38, 1376-1389.
Sahariah, B.P., Chakraborty, S., 2011. Kinetic analysis of phenol, thiocyanate and ammonia-nitrogen removals in an anaerobicanoxicaerobic moving bed bioreactor system. Journal of Hazardous Materials 190, 260-267.
Sheng, G.P., Yu, H.Q., Li, X.Y., 2010. Extracellular polymeric substances (EPS) of microbial aggregates in biological wastewater treatment systems: A review. Biotechnology Advances 28, 882-894.
Song, Z., Pan, Y., Zhang, K., Ren, N., Wang, A., 2010. Effect of seed sludge on characteristics and microbial community of aerobic granular sludge. Journal of Environmental Sciences 22, 1312-1318.
Tay, S.T.L., Moy, B.Y.P., Jiang, H.L., Tay, J.H., 2005. Rapid cultivation of stable aerobic phenol-degrading granules using acetate-fed granules as microbial seed. Journal of Biotechnology 115, 387-395.
Tchobanoglous, G., Burton, F.L., Stensel, H.D., Metcalf, Eddy, 2003. Wastewater Engineering: Treatment and Reuse, fourth ed. McGraw Hill Education, India.
Tsuneda, S., Jung, J., Hayashi, H., Aikawa, H., Hirata, A., Sasaki, H., 2003. Influence of extracellular polymers on electrokinetic properties of heterotrophic bacterial cells examined by soft particle electrophoresis theory. Colloids and Surfaces B: Biointerfaces 29, 181-188.
Verawaty, M., Pijuan, M., Yuan, Z., Bond, P., 2012. Determining the mechanisms for aerobic granulation from mixed seed of floccular and crushed granules in activated sludge wastewater treatment. Water Research 46, 761-771.
Wan, C., Sun, S., Lee, D.J., Liu, X., Wang, L., Yang, X., Pan, X., 2013. Partial nitrification using aerobic granules in continuous-flow reactor: Rapid startup. Bioresource Technology 142, 517-522.
Wang, S., Shi, W., Yu, S., Yi, X., Yang, X., 2012. Formation of aerobic granules by Mg^{2+} and Al^{3+} augmentation in sequencing batch airlift reactor at low temperature. Bioprocess and Biosystems engineering 35, 1049-1055.
Wang, X.C., Chen, Z.L., Kang, J., Zhao, X., Shen, J.M., Yang, L., 2019. The key role of inoculated sludge in fast start-up of sequencing batch reactor for the domestication of aerobic granular sludge. Journal of Environmental Sciences 78, 127-136.
Wang, X., Zhang, H., Yang, F., Wang, Y., Gao, M., 2008. Long-term storage and subsequent reactivation of aerobic granules. Bioresource Technology 99, 8304-8309.
Wei, D., Li, M., Wang, X., Han, F., Li, L., Guo, J., Ai, L., Fang, L., Liu, L., Du, B., 2016. Extracellular polymeric substances for Zn (II) binding during its sorption process onto aerobic granular sludge. Journal of Hazardous Materials 301, 407-415.
Wu, D., Zhang, Z., Yu, Z., Zhu, L., 2018. Optimization of F/M ratio for stability of aerobic granular process via quantitative sludge discharge. Bioresource Technology 252, 150-156.
Xu, J., He, J., Wang, M., Li, L., 2018. Cultivation and stable operation of aerobic granular sludge at

low temperature by sieving out the batt-like sludge. Chemosphere 211, 1219-1227.
Xu, X., Liu, J., Sun, H., 2019. Improving granular sludge stability via stimulation of extracellular polymeric substance production by adding layered double hydroxides. International Journal of Environmental Science and Technology 16, 987-994.
Yang, S.F., Tay, J.H., Liu, Y., 2004. Inhibition of free ammonia to the formation of aerobic granules. Biochemical Engineering Journal 17, 41-48.
Zhang, L., Feng, X., Zhu, N., Chen, J., 2007. Role of extracellular protein in the formation and stability of aerobic granules. Enzyme and Microbial Technology 41, 551-557.

Only the unknown frightens men. But once a man has faced the unknown, that terror becomes the known.

Antoine de Saint-Exupéry (1900-1944)
French writer and poet

4

Impact of High Phenol Loading on Aerobic Granulation

Impact of high loading of phenol developed from two different kinds of industrial sludge on aerobic granulation is discussed in this chapter along with the stability of aerobic granules.

4.1 Introduction

Phenol, a recalcitrant organics, is usually found in the wastewater generated from the many industries like pharmaceutical, petrochemical, pulp, coal refining industries, etc. (Ho et al., 2009). Biological treatment of phenol containing wastewater is difficult because of substrate inhibition at higher concentrations, which hinders the microbial activity and imposes an adverse impact on its phenol removal potential (Tay et al., 2005a). Phenol with other toxic inorganic compounds like thiocyanate (SCN^-) and ammonia-nitrogen (NH_4^+-N) is found in coal processing wastewater (coal gasification, coal liquefaction) (Vázquez et al., 2006). High levels of SCN^- and NH_4^+-N cause toxicity to the aquatic species and vertebrates (Li et al., 2011). Treatment of industrial wastewater containing organic and inorganic contaminants is a complex process that demands an efficient treatment approach for the concurrent removal of all the pollutants in a short time.

Aerobic granular sludge (AGS) technology is an inventive technology for treating complex wastewater because of its high tolerance potential to oxidize both organic and ammonium simultaneously in an economical way (Singh and Srivastava, 2011). AGS has been developed with a variety of benign substrates like glucose, acetate, molasses, ethanol, etc., with the organic loading rates (OLRs) ranging from 2.5 to 15.0 kg COD m^{-3} day^{-1} (Kim et al., 2008a; Moy et al., 2002; Winkler et al., 2018). Granules have also been cultivated with toxic recalcitrant phenol as a sole carbon source but with municipal activated sludge as an inoculum having the lower OLRs ranging from 1.5 to 3.0 kg COD m^{-3} day^{-1} (Jiang et al., 2002; Tay et al., 2004; Wosman et al., 2016). However, several bacterial strains isolated from phenol degrading aerobic granules were tested to degrade different concentrations of phenol in the batch tests (Adav et al., 2007a; Jiang et al., 2004a). On the other hand, pure strains capable of degrading upto 2000 mg L^{-1} phenol were also used to form aerobic granules and were tested for their potency to biologically oxidize phenol in batch tests (Ho et al., 2009). All the pure culture techniques for removal of phenol are tedious in nature in terms of cultivation and isolation of strains and require vigilance. Therefore, in perspective of onsite application of AGS, an efficient approach is needed to treat high phenolic wastewater with other toxic inorganic contaminants by aerobic granules without the use of pure strains.

The present study provides an alternate approach for treating toxic wastewater laden with high phenol along with SCN^- and NH_4^+-N by AGS technology without using pure strains in a comparative shorter HRT. This research work also demonstrates the comparison of aerobic granules developed from two different kinds of industrial sludge, refinery and brewery sludge, in terms of stability, granular biomass activity and characteristics of AGS along with the pollutants removal affinity.

4.2 Materials and methods

The sources of all the chemicals and reagents used in this study are given in *Chapter 2 (section 2.2.1)*.

4.2.1 Experimental set-up

Two identical transparent acrylic sequencing batch reactors (SBRs) (configuration is given in *Chapter 2; section 2.3.1*)seeded with two different kinds of industrial sludge, refinery (R1) and brewery sludge (R2), were operated in this work. The photographic image of reactor and schematic diagram are given in *Chapter 2* (Fig. 2.1 and Fig. 2.2, respectively). An oil free compressor was used to provide air as tiny air bubbles by the air diffuser placed at the bottom of the SBRs at a rate of 2.0 L min^{-1} (maintained through the rotameter). The feed was supplied in an up-flow mode through the peristaltic pumps.

4.2.2 Characteristics of seed sludge and synthetic wastewater

Refinery and brewery sludge were collected from the activated sludge unit of Indian Oil Corporation Limited, Guwahati and Master India Brewing Company, Guwahati, respectively. Refinery and brewery sludge characteristics are given in Table 4.1. R1 and R2 were inoculated with 3 L of refinery and brewery sludge, respectively. The synthetic wastewater composition is given in Table 4.2. The pH in both of the reactors was in between 7.5 to 8.0 and was maintained by phosphate buffer and $NaHCO_3$. The phosphorous required for the growth of the microorganisms was also provided by the phosphate buffer. The phosphate buffer and trace metal composition were adopted from Sahariah and Chakraborty (2011).

Table 4.1. Characteristics of refinery and brewery sludge.

Sludge	TSS (g L^{-1})	VSS (g L^{-1})	SVI_{30} (mL g TSS^{-1})	Average granule size (μm)	GBA
Refinery	3.08	1.98	44.00	35.54	8.01
Brewery	5.62	1.83	29.43	21.26	6.56

TSS: total suspended solids; VSS: volatile suspended solids; SVI_{30}: sludge volume index; GBA: granular biomass activity (mg COD removed $mgVSS^{-1}$ day^{-1})

4.2.3 Operational strategy

The operation stretegy in both reactors was the same as in *Chapter 3 (section 3.4.3)*. Initially, 1000 mg L^{-1} of sodium acetate was added as a benign carbon source in both of the SBRs. As the acclimatization progressed (First 38 days), the sodium acetate was gradually reduced and that of phenol, SCN^- and NH_4^+-N were increased. After 38 days of the acclimatization, sodium acetate was suspended and the concentrations were reached to 500, 100 and 100 mg L^{-1} for phenol, SCN^- and NH_4^+-N, respectively. Afterward, the concentrations of SCN^- and NH_4^+-N were kept constant at 100 mg L^{-1} for each throughout the work and only phenol concentration was varied in each SBRs. Based on the variation in phenol concentrations, the operation of the each SBR was divided into four phases:
Phase I (days 53-78) - 500 mg L^{-1} of phenol (2.41 kg COD m^{-3} day^{-1} or 1.00 kg phenol m^{-3} day^{-1});
Phase II (days 97-125) - 700 mg L^{-1} of phenol (3.32 kg COD m^{-3} day^{-1} or 1.40 kg phenol m^{-3} day^{-1});

Table 4.2. Synthetic wastewater composition.

Component	Concentration (mg L^{-1})				Component	Concentration (mL L^{-1})
Phenol (operation time in days)	500 (53-78)	700 (97-125)	1000 (149-181)	1200 (197-225)	**Phosphate buffer**[a]	1
SCN^- (SCN^- as KSCN)	100					
NH_4^+-N (NH_4^+-N as NH_4Cl)	100				**Trace metal solution**[b]	1
$NaHCO_3$	added as required					

[a]Phosphate buffer contained (g L^{-1}): 72.3 KH_2PO_4 and 104.5 K_2HPO_4; [b]Trace metal solution contained (mg L^{-1}): 10,000 $MgSO_4.7H_2O$, 10,000 $CaCl_2.2H_2O$, 5000 $FeCl_3.6H_2O$, 1000 $CuCl_2$, 1000 $ZnCl_2$, 500 $NiCl_2.6H_2O$ and 500 $CoCl_2$

Phase III (days 149-181) - 1000 mg L^{-1} of phenol (4.81 kg COD m^{-3} day^{-1} or 2.00 kg phenol m^{-3} day^{-1});

Phase IV (days 197-225) - 1200 mg L^{-1} of phenol (5.71 kg COD m^{-3} day^{-1} or 2.40 kg phenol m^{-3} day^{-1}).

A transition period of around 20 days after each phase was given to reach the next level of phenol concentration gradually and during that period, pollutant analysis were not performed. Both SBRs were operated at least for 25 days for each phase to obtain the steady-state data.

4.2.4 Analytical techniques

All the analytical methods used in this study have been mentioned in *Chapter 2 (section 2.2.2)* unless otherwise specified. The quantification of the granule strength in terms of integrity coefficient (IC) was measured according to Ghangrekar et al. (1996) and the detailed procedure was adopted from Xiao et al. (2008). 5 mL of granular sludge suspension was diluted to 30 mL with tap water in a 50 mL conical falcon tube and vortexed for 5 min by a vortex mixer (Spinix-vortex-shaker, Tarsons, India). After 1 min of settling, the suspended solids in both supernatant and settled sludge were measured. The granule strength in terms of IC can be determined by using equation 4.1.

$$IC = \left(1 - \frac{SS_t}{SS_0}\right) X 100 \tag{4.1}$$

Where, SS_0 represents the total amount of granular sludge and SS_t is the amount of solids present in the supernatant after t min of vortexing.

4.2.5 Granular biomass activity (GBA) test

GBA test was a little bit modified from the method as mentioned in *Chapter 2 (section 2.2.4)*. Sodium acetate, a simple carbon source, was used to perform the activity test to observe the efficacy of the granules to biodegrade a benign substrate after being exposed to a higher load of multiple toxic substrates. For the biomass activity analysis, the cumulative COD removal with time was assessed by taking the nearly same amount of granular biomass (VSS; 1.20-1.40 g L^{-1}) in two different 1 L beakers from each SBR. Each beaker volume was made up to 1 L by tap water after being fed with 1220 mg L^{-1} of sodium acetate (OLR of around 2.0 Kg COD m^{-3} day^{-1}) and was aerated at a rate of 2.0 L min^{-1}. Initially, COD was analysed at a shorter and later on at a longer time period up to 24-48 h of feeding. The activity test was operated in three cycles with the same feed concentration and the slope of the linear portion of the third cycle was considered to calculate the granular biomass activity.

Third cycle was considered only because up to 2nd cycle, acclimatization of granular biomass with the new substrate was considered. After each cycle completion, the supernatant was thrown after being settled for 5 min and fresh feed was given to the volume of 1 L in each beaker. VSS in each beaker was determined after the third cycle. The estimation of activity was done by the final VSS and slope of the linear portion of the third cycle of the cumulative COD removal with time and was determined by equation 2.1.

4.3 Results and discussion

4.3.1 Granule formation

The development of the granules in both of the SBRs is given in Fig. 4.1. Refinery and brewery sludge was like a suspension without any granules. After 9 days of inoculation with refinery sludge, fluffy and irregular granular structure was observed in R1, whereas in R2, the same structure was observed after 17 days of inoculation with brewery sludge. Adav et al. (2007b) observed granule initiation after 21 days of reactor operation with phenol as a carbon source by using activated sludge of municipal wastewater treatment plant as an inoculum. The possible reason for the less time taken in the initiation of granules in R1 might be the previous exposure of refinery sludge to the phenol. For the next 30 days, granules progressed to develop in both of the SBRs. Granules became matured after 40 days of reactor operation in R1 with a clear and regular structure (Fig. 4.1), whereas in R2, the granule maturation was still in progress and required more time to get matured (50 days).

The comparative results of granulation time along with OLR and granular characteristics are given in Table 4.3. Mature granules were developed from the municipal activated sludge in 33 days to treat phenol at a load of 1.50 kg phenol m^{-3} day^{-1} (Jiang et al., 2002). Jiang et al. (2004b) in another study observed mature granulation after 60 days for treating high phenolic wastewater (OLR of 1.00 -2.00 kg phenol m^{-3} day^{-1}) by using phenol degrading aerobic granules as an inoculum with phenol as a sole carbon source. Tay et al. (2004) achieved granulation from the municipal activated sludge (previously acclimatized with 50-500 mg L^{-1} of phenol concentrations in a batch study for two months) in 30 days only for degrading the high phenol with a load of 1.50-2.50 kg phenol m^{-3} day^{-1}. Granulation was also observed in just 7 days with phenol and sodium acetate as carbon sources for the treatment of phenol loading of 2.40 kg phenol m^{-3} day^{-1} (5.71 kg COD m^{-3} day^{-1}) by using acetate fed aerobic granules as a seed sludge having a precultivation period of four weeks (Tay et al., 2005b). In another study, Tay et al. (2005a) developed phenol degrading granules in 15 days from the acetate degrading granules for treating comparatively lower loading of phenol (1.80 kg phenol m^{-3} day^{-1}). Aerobic granules for tolerating much higher phenol loading (3.00 kg phenol m^{-3} day^{-1}) were also cultivated in quite a long time of 75 days from the domestic activated sludge at a much higher air flow rate of 5.0 L min^{-1} (Wosman et al., 2016). Therefore the present work is better than the studies given in Table 4.3 in terms of achieving granulation from the two different kinds of industrial sludge (refinery and brewery sludge) at a faster rate (40 and 50 days in R1 and R2, respectively) for treating high toxic loading of 2.40 kg phenol m^{-3} day^{-1} (5.71 kg COD m^{-3} day^{-1}) with phenol as a carbon source at a lower air flow rate of 2.0 L min^{-1} without using any precultivated granules or pre-acclimatized sludge.

Stable granules were observed in both R1 and R2 up to a load of 3.32 kg COD m^{-3} day^{-1} (Phase II) with a distinct form (Fig. 4.1; day 117). FESEM images also revealed the formation of a clear and smooth structure in Phase II (Fig. 4.2; 100 X and 5.00 KX resolution images of day 110). At a higher

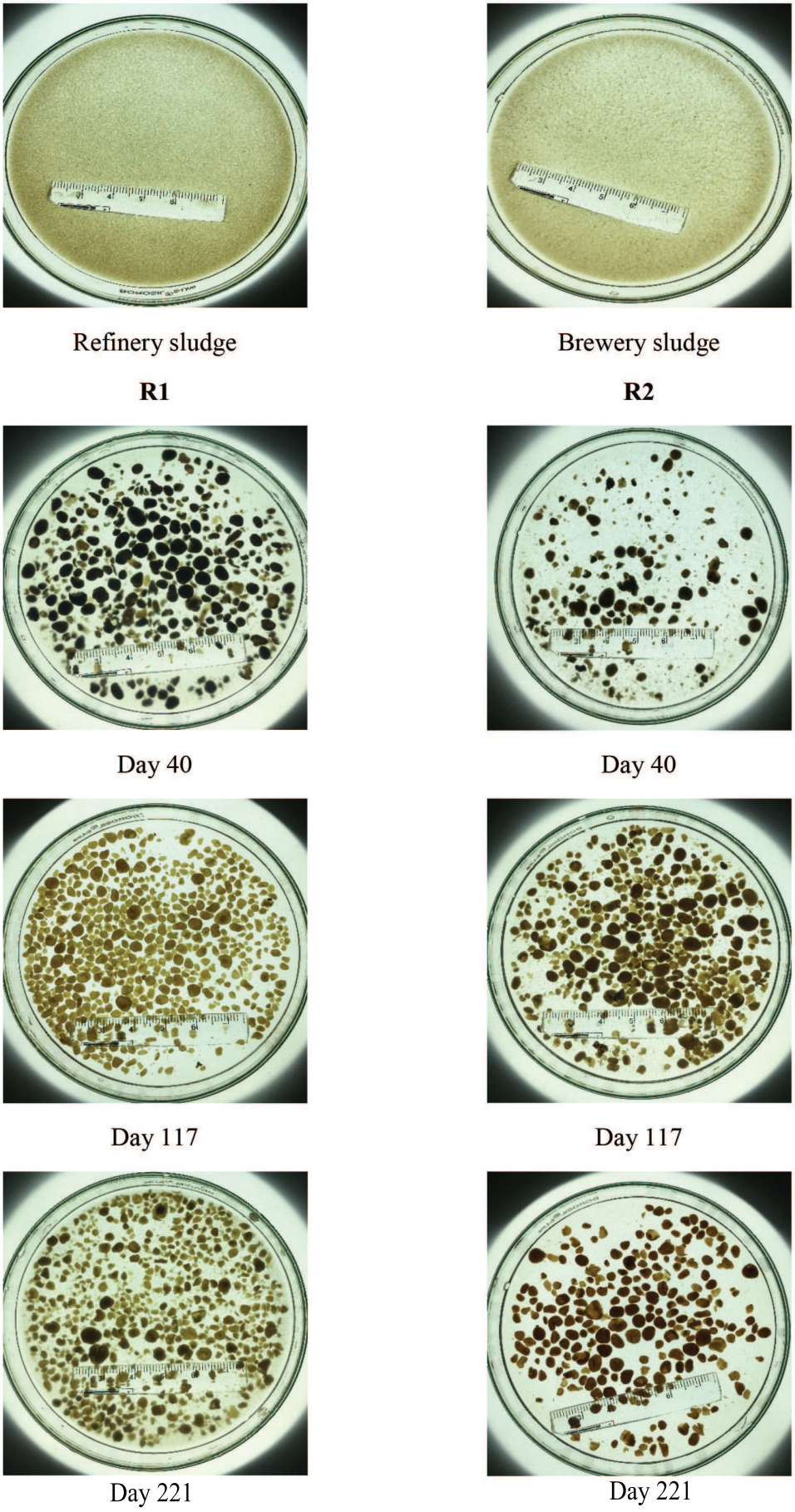

Fig. 4.1. Image of refinery and brewery sludge and granules with operation time.

Table 4.3. Comparison of granular characteristics.

Carbon source	Inoculum	Wastewater treatment	Average granule size (μm)	SVI (mL g TSS^{-1})	Air flow rate (L min^{-1})	Granulation time (days)	OLR[c/d]	References
Phenol	Municipal activated sludge	Phenol	350.00-600.00	40.00	3.5	33	1.50[d]	Jiang et al. (2002)
Phenol	Phenol degrading aerobic granules	Phenol	-	40.00-45.00	3.5	60	1.00-2.00[d]	Jiang et al. (2004b)
Phenol	Municipal activated sludge[a]	Phenol	520.00-1200.00	40.00-60.50	3.5	30	1.50-2.50[d]	Tay et al. (2004)
Phenol	Acetate fed aerobic granules	Phenol	-	<80.00	3.5	15	1.80[d]	Tay et al. (2005a)
Phenol and sodium acetate	Acetate fed aerobic granules[b]	Phenol and sodium acetate	-	22.00-38.00	3.5	7	5.71[c] /2.40[d]	Tay et al. (2005b)
Phenol	Domestic activated sludge	Phenol	-	-	5.0	75	3.00[d]	Wosman et al. (2016)
Phenol	**Refinery and brewery sludge**	**Phenol, thiocyanate and ammonia-nitrogen**	**2769.94±62.26**	**31.07±1.08**	**2.0**	**40-50**	**5.71[c] /2.40[d]**	**Present study**

[a]previously acclimatized with phenol concentration of 50-500 mg L^{-1} in batch study for two months; [b]precultivated for four weeks; [c]organic loading rate (kg COD m^{-3} day^{-1}); [d]organic loading rate (kg phenol m^{-3} day^{-1})

load of phenol with a concentration of more than 700 mg L^{-1} (>3.32 kg COD m^{-3} day^{-1}) (Phase III), R1 granules could not be able to cope up with the higher phenol load resulting in the granule deterioration with a shattered (Fig. 4.1; day 221) and disintegrated structure (Fig. 4.2; FESEM image of day 215 at 5.00 KX resolution). On the other hand, R2 granules were stable throughout the study with compact and smooth structure (Fig. 4.1 and 4.2) and were able to withstand with a phenol loading of 5.71 kg COD m^{-3} day^{-1}. Early disintegration of R1 granules at a lower load than R2 might have a correlation with the toxicity of phenol. Microbes often develop the aggregate like biofilm to serve as a hurdle against different kinds of toxicities when encountered with the environmental stresses such as toxic substances (Koechler et al., 2015). This could be the possible scenario for getting much stronger granules in R2 than that of R1. The microorganisms of R2 sludge (brewery sludge) were stressed to form a much stronger and stable granular structure after being repeatedly exposed to stepwise increment in toxic phenol loading which was naive to the brewery sludge microbes as compared to refinery sludge microorganisms having previous exposure of phenol. Threfore, R1 granules could not feel too much phenol toxicity to form a high phenol load-bearing stable and strong granules.

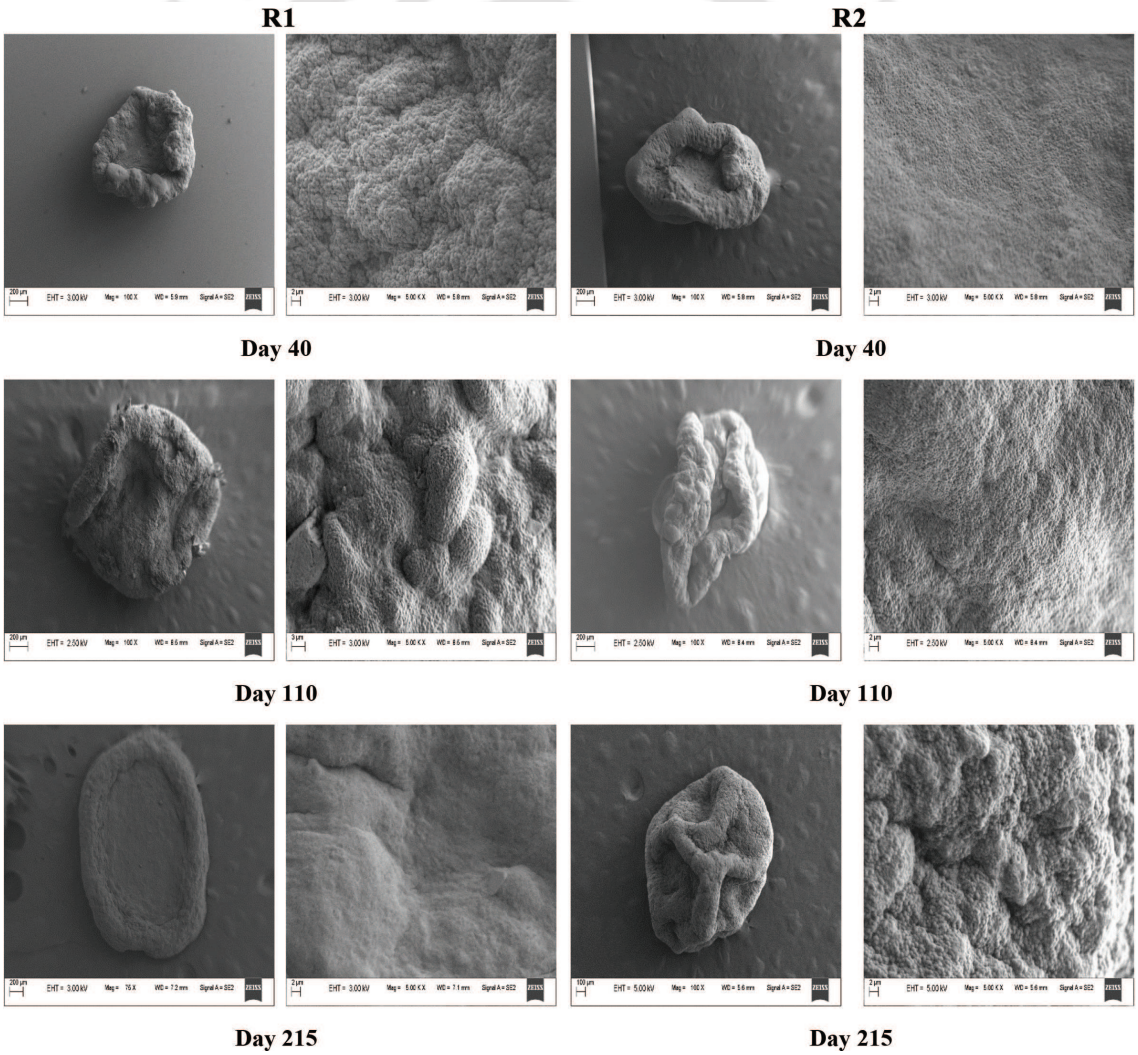

Fig. 4.2. FESEM images of granules with operation time.

4.3.2 Granular characteristics

The characteristics of the granules of R1 and R2 at different phenol concentrations are given in Table 4.4.

4.3.2.1 Granule size

The size of the granules with the operation for both of the SBRs are given in Fig. 4.3(a) and Table 4.4. 35.54 and 21.26 μm were the size of refinery and brewery sludge, respectively (Table 4.1). From Fig. 4.3 (a), it was observed that for initial 9 and 13 days, respectively, for R1 and R2, sludge size increased because of the filamentous growth and afterward, reduced for the next few days indicating the washout of the filamentous growth. Since days 21 and 25 in R1 and R2, respectively, a gradual increment in the size of granular sludge was observed and got stabilized to around 1600 μm on days 40 and 50 in R1 and R2, respectively. During Phase I (OLR of 2.41 kg COD m^{-3} day^{-1} or 1.00 kg phenol m^{-3} day^{-1}), the stabilized granules were having the mean size of 1600.67±69.81 and 1634.48±59.12 μm in R1 and R2, respectively. As the OLR increased to 3.32 kg COD m^{-3} day^{-1} or 1.40 kg phenol m^{-3} day^{-1} (Phase II), an increment in the diameter of the granules was noticed. R2 granules were found to be slightly larger than R1 granules with the mean sizes of 1870.62±69.56 and 2106.69±57.51 μm in R1 and R2, respectively. Up to a phenol loading of 3.32 kg COD m^{-3} day^{-1}, no toxic effect of phenol on granular size was observed in both of the SBRs. Further increment in phenol loading (>3.32 kg COD m^{-3} day^{-1}) imposed an adverse effect on the stability of R1 granules resulting in the reduction of size up to 1368.70±67.08 μm during Phase III (4.81 kg COD m^{-3} day^{-1} or 2.00 kg phenol m^{-3} day^{-1}) and further decreased to 1110.58±51.34 μm during Phase IV (5.71 kg COD m^{-3} day^{-1} or 2.40 kg phenol m^{-3} day^{-1}). R2 granules were remained unaffected with a rise in phenol loading and were continued to grow larger after every hike in phenol concentration because of the availability of more carbon source. During Phase IV, the mean size of the stable R2 granules were 2769.94±62.26 μm. It was evident from the results (Fig. 4.3(a)) that the granules of R2 were much stronger and stable in terms of tolerance potential towards high toxic phenol loading as compared to R1 granules.

4.3.2.2 Biomass (VSS) concentration

Biomass concentrations profiles of R1 and R2 are illustrated in Fig. 4.3 (b). The average VSS values for both of the SBRs for all the four phases are given in Table 4.4. The VSS values for refinery and brewery sludge were 1.98 and 1.83 g L^{-1}, respectively (Table 4.1). With little fluctuations during the initial days, the VSS values were tended to increase. At the time of granule maturation, R1 (day 40) and R2 (day 50) were having the VSS of 3.35 and 3.65 g L^{-1}, respectively. The stabilized average VSS values during Phase I in both of the SBRs were 3.34±0.08 and 3.75±0.06 g L^{-1} and further stabilized to 4.67±0.07 and 5.38±0.08 g L^{-1} in R1 and R2, respectively, during Phase II after an increment in phenol loading. A further rise in phenol loading caused toxicity to the R1 granules resulting in the deterioration of R1 VSS and finally reduced to an average value of 2.37±0.08 g L^{-1} during Phase IV. On the other hand, R2 granules were continued to grow with an increase in phenol loading and VSS got stabilized to the average value of 7.12±0.16 g L^{-1} at the highest phenol loading of 5.71 kg COD m^{-3} day^{-1} during Phase IV. Food to microorganism (F/M) ratio for each phase is provided in Table 4.4. From the data, it was clear that up to a phenol concentration of 700 mg L^{-1}, F/M ratios in both R1 and R2 were almost in the required range of F/M ratios for aerobic granulation (0.3 to 6.0 g COD gSS^{-1} day^{-1}) as mentioned by Li et al. (2008). Afterward, at phenol concentrations of more than 700 mg L^{-1}, the F/M ratio increased to more than 0.9 g COD $gVSS^{-1}$ day^{-1} in R1. Wu et al. (2018) reported that at high F/M ratio of 0.9±0.04 g COD gSS^{-1} day^{-1} caused a reduction in the settleability of the sludge, thus resulting in the washing out of various functional microbial strains from the system. Higher F/M ratio might be one of the possible reasons for the deteriorated granular characteristics and absence of the affinity of the granular sludge to degrade pollutants in R1.

Table 4.4. Characteristics of the granules of R1 and R2 at different phenol concentrations.

Phenol (days)	500 mg L^{-1}(53-78)		700 mg L^{-1}(97-125)		1000 mg L^{-1}(149-181)		1200 mg L^{-1}(197-225)	
Characteristics	**R1**	**R2**	**R1**	**R2**	**R1**	**R2**	**R1**	**R2**
Average granule size (μm)	1660.67±69.81	1634.48±59.12	1870.62±69.56	2106.69±57.51	1368.70 ±67.08	2554.47±53.23	1110.58±51.34	2769.94±62.26
VSS (g L^{-1})	3.34±0.08	3.75±0.06	4.67±0.07	5.38±0.08	2.88±0.21	5.85±0.08	2.37±0.08	7.12±0.16
SVI_{30} (mL g TSS^{-1})	37.09±0.78	35.63±0.53	35.90±0.72	34.34±0.83	66.47±1.44	32.80±1.04	77.05±1.49	31.07±1.08
GSV (m h^{-1})	37.10±1.25	42.84±1.22	48.66±0.79	49.17±1.12	43.18±0.86	52.09±1.05	41.86±1.10	55.86±1.08
PN (mg $gVSS^{-1}$)	38.41 ±0.92	40.61±0.92	50.97±1.39	60.02±1.11	44.44±0.91	74.05±0.73	40.98±0.95	80.72±1.09
PS (mg $gVSS^{-1}$)	23.58±0.62	24.29±0.57	30.91±1.07	30.87±0.55	28.83±0.56	33.22±0.58	26.65±0.70	34.11±0.71
EPS (mg $gVSS^{-1}$)	61.99±1.12	64.90±0.92	81.88±1.32	90.89±1.12	73.27±1.28	107.27±0.95	67.63±1.55	114.83±1.33
GBA (mg COD removed $mgVSS^{-1}day^{-1}$	12.71	13.59	14.73	15.27	-	-	3.43	16.35
SRT (days)	9.32	9.79	9.50	9.75	3.91	9.59	3.88	9.41
F/M ratio (g COD $gVSS^{-1}$ day^{-1})	0.72	0.64	0.71	0.62	1.66	0.82	2.41	0.80

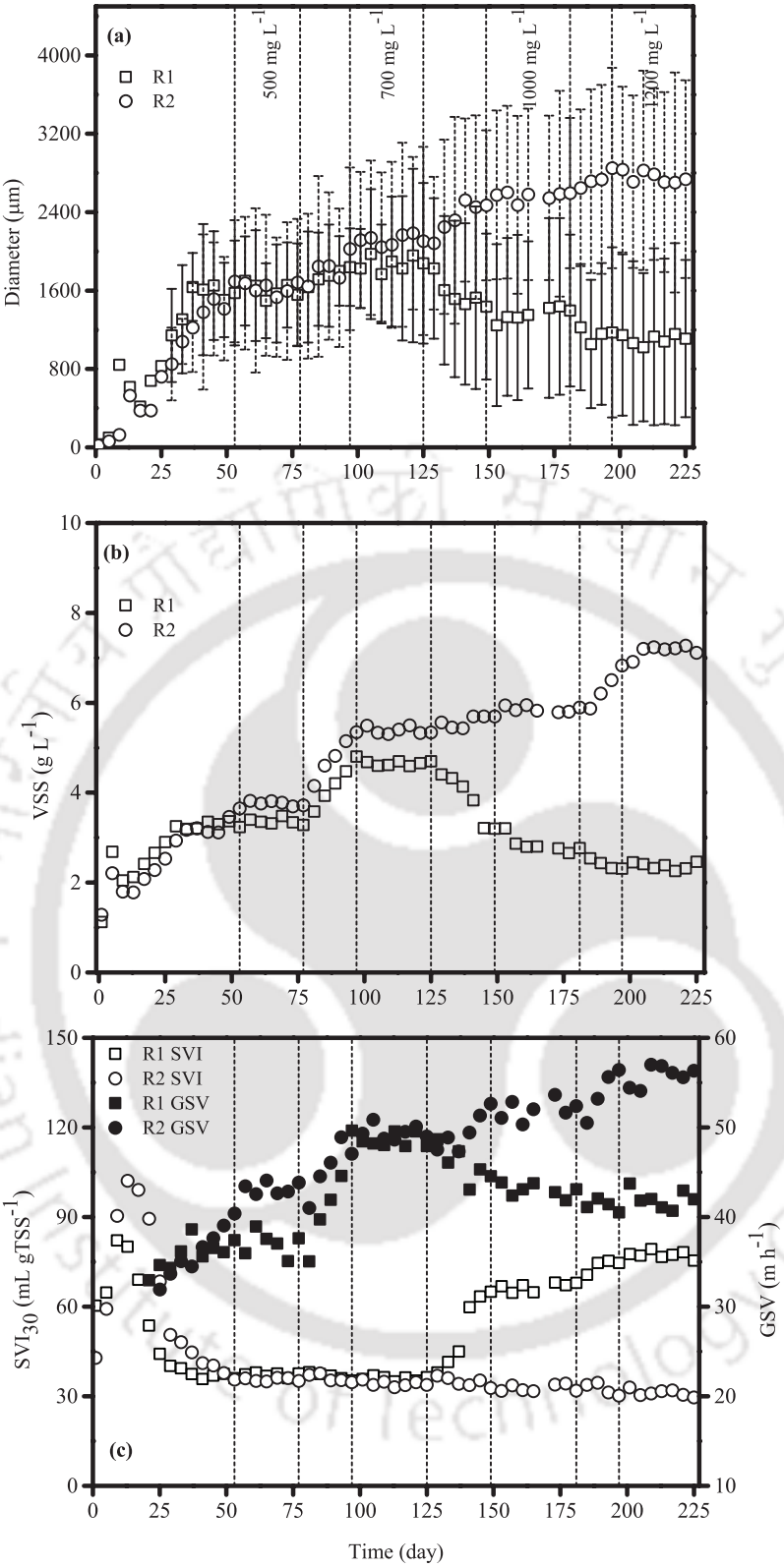

Fig. 4.3. Characteristics of granules: (a) diameter, (b) VSS and (c) SVI_{30} and GSV.

4.3.2.3 Settling characteristics of the granules

The settling behaviour (SVI_{30} and GSV) for the granules of R1 and R2 is given in Fig. 4.3 (c). The average values of both SVI_{30} and GSV at each phase for both of the SBRs are presented in Table 4.4. The SVI_{30} values were 44.00 and 29.43 mL $gTSS^{-1}$ for refinery and brewery sludge, respectively (Table 4.1). For the initial days, SVI_{30} values increased to 80.08 mL $gTSS^{-1}$ for R1 (day 13) and 102.16

mL $gTSS^{-1}$ for R2 (day 13) indicating the filamentous growth with the poor settling property. In the progression of the granule development, SVI_{30} values dropped to 35-37 mL $gTSS^{-1}$ for both of the reactors at the time of granule maturation. The stabilized average SVI_{30} values of 37.09±0.78 and 35.63±0.53 mL $gTSS^{-1}$ for R1 and R2, respectively were observed during Phase I. During Phase II, the average SVI_{30} values were 35.90±0.72 and 34.34±0.83 mL $gTSS^{-1}$ in R1 and R2, respectively. As the loading of phenol was increased beyond 3.32 kg COD m^{-3} day^{-1}, a reduction in the R1 SVI_{30} value was observed. R1 SVI_{30} value continued to deteriorate after every next level of phenol loading indicating the disturbance in the settling behaviour of R1 granules caused due to the high toxic phenol loading with an average value of 77.05±1.49 mL $gTSS^{-1}$ during Phase IV. No negative impact of high phenol loading was observed on SVI_{30} in R2 with an average value of 31.07±1.08 mL $gTSS^{-1}$ (Phase IV). The R2 SVI_{30} value obtained in the present work was quite comparable with other research works described in Table 4.3.

The analysis of GSV was started from days 21 and 25 onwards with the values of 32.94 and 31.93 m h^{-1} in R1 and R2, respectively, and are provided in Fig. 4.3 (c). GSV values followed a rising pattern as the granulation progressed and reached the values of 35.62 and 40.40 m h^{-1} in R1 and R2, respectively, at the time of granule maturation. The stabilized GSV values during Phase I were 37.10±1.25 and 42.84±1.22 m h^{-1} in R1 and R2, respectively. R2 possessed a little higher GSV than R1 during Phase I. During Phase II, the GSV values for R1 and R2 were 48.66±0.79 and 49.17±1.12 m h^{-1}, respectively. Like other characteristics, R1 GSV got worsened at higher phenol loading of more than 3.32 kg COD m^{-3} day^{-1} with an average GSV of 41.86±1.10 m h^{-1} during Phase IV. R2 GSV progressed to increase with a rise in phenol loading and stabilized to an average GSV of 55.86±1.08 m h^{-1} during Phase IV. From the results of settling characteristics (Fig. 4.3c), it was noticed that the granules of R1 turned into a weaker and loose structure resulting in poor settleability because of high phenol load. On the contrary, R2 granules did not lose their compactness (concluded from the lower SVI_{30} and higher GSV) even after being exposed to higher toxic phenol loading and exhibited good settling behaviour throughout the study.

4.3.2.4 Extracellular polymeric substances (EPS)

EPS, a glue-like sticky microbial secretion, plays a vital role in the formation of the granules and in maintaining the structural integrity of the granules by forming a gel-like structure (Zhang et al., 2007). Fig. 4.4 illustrates the compositions of EPS, proteins (PN) and polysaccharides (PS). EPS values, along with PN and PS for each phase, are given in Table 4.4. On day 1, EPS was around 25 mg $gVSS^{-1}$ and reached to a value of around 60 mg $gVSS^{-1}$ in both of the SBRs, whereas PS and PN values were around 23 and 40 mg $gVSS^{-1}$ in both indicating the more profoundness of PN content than PS. An increment in EPS value suggested the granular development. The stabilized values of EPS during Phase I were 61.99±1.12 and 64.90±0.92 mg $gVSS^{-1}$ in R1 and R2, respectively. As the toxicity level of phenol was increased, a rise in EPS (major rise in PN content) was noticed. Toxic substances provoke the bacterial EPS secretion for promoting the granular integrity (Chen et al., 2017). This might be the possible reason for achieving a high level of EPS. During Phase II, EPS (PN) values were 81.88±1.32 (50.97±1.39) and 90.89±1.12 (60.02±1.11) mg $gVSS^{-1}$ in R1 and R2, respectively. A further rise in phenol loading caused a negative impact on the EPS content (mainly on PN content) of R1 with the EPS and PN values of 67.63±1.55 and 40.98±0.95 mg $gVSS^{-1}$, respectively, resulting in a disturbance in the granular stability. On the other hand, R2 EPS values followed a rising trend with the rise in phenol concentration to the next level. During Phase IV, EPS and PN values were

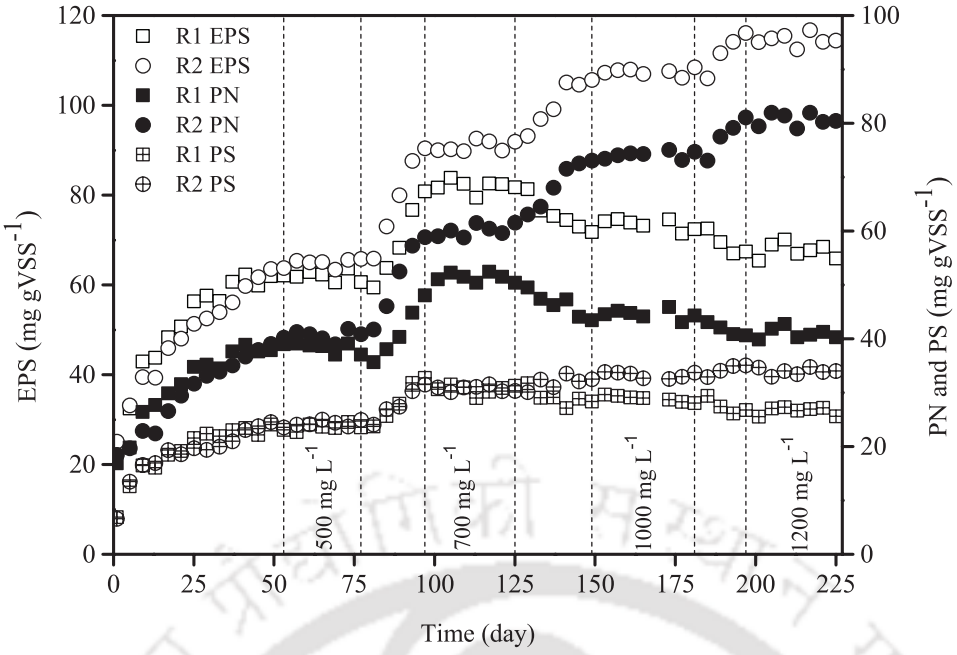

Fig. 4.4. Total EPS, PN and PS contents.

114.83±1.33 and 80.72±1.09 mg $gVSS^{-1}$, respectively. Higher EPS in R2 might be the possible reason for granular stability at higher phenol loading.

On day 210, the distribution pattern of total cells, dead cells, proteins and polysaccharides was analysed through CLSM imaging (Fig. 4.5). Higher fluorescence for SYTOX Blue was observed in R1 indicating the more dead portion in R1 than R2. Fluorescence for proteins and polysaccharides was detected in extended form for the granules of R2 than R1 granules.

4.3.2.5 Strength of the granules

The granular strength is the ability of the granules to resist against the deterioration imposed by the exalted shear stress (Xiao et al., 2008). Direct measurement of the strength of the individual granules is quite difficult. Integrity coefficient can be an indirect index for measuring the granular strength qualitatively. Even though it does not provide the exact measure of granular strength, it gives practical information about the strength of the granules against the shear force on to the granules during the reactor operation (Ghangrekar et al., 1996). A higher percentage of integrity coefficient represents greater granular strength (Chen et al., 2007). The integrity coefficient values were 85.6 and 99.0%, respectively, for R1 and R2 on day 220 (during Phase IV) representing a higher strength of R2 granules than R1 at higher phenol loading.

4.3.3 GBA of the AGS

The activity test was performed to evaluate the ability of AGS to degrade a simple carbon source, sodium acetate, in terms of COD removal after being subjected to recalcitrant organic and inorganic compounds for a long time. Fig. 4.6 illustrates the cumulative COD removal with time for seed sludge and AGS exposed to 700 and 1200 mg L^{-1} in both of the reactors and also depicts the biomass activity for seed sludge and AGS with three phenol concentrations (500, 700 and 1200 mg L^{-1}) in both R1 and R2. The compilation of GBA data is given in Table 4.4. It was clear from the results that granules of R1 and R2 were more active than their parent sludge after feeding with phenol. In R1, activity value increased to its maximum value (14.73 mg COD removed $mgVSS^{-1}$ day^{-1}) at a phenol concentration of 700 mg L^{-1} and reduced to 3.43 mg COD removed $mgVSS^{-1}$ day^{-1} at 1200 mg L^{-1} of

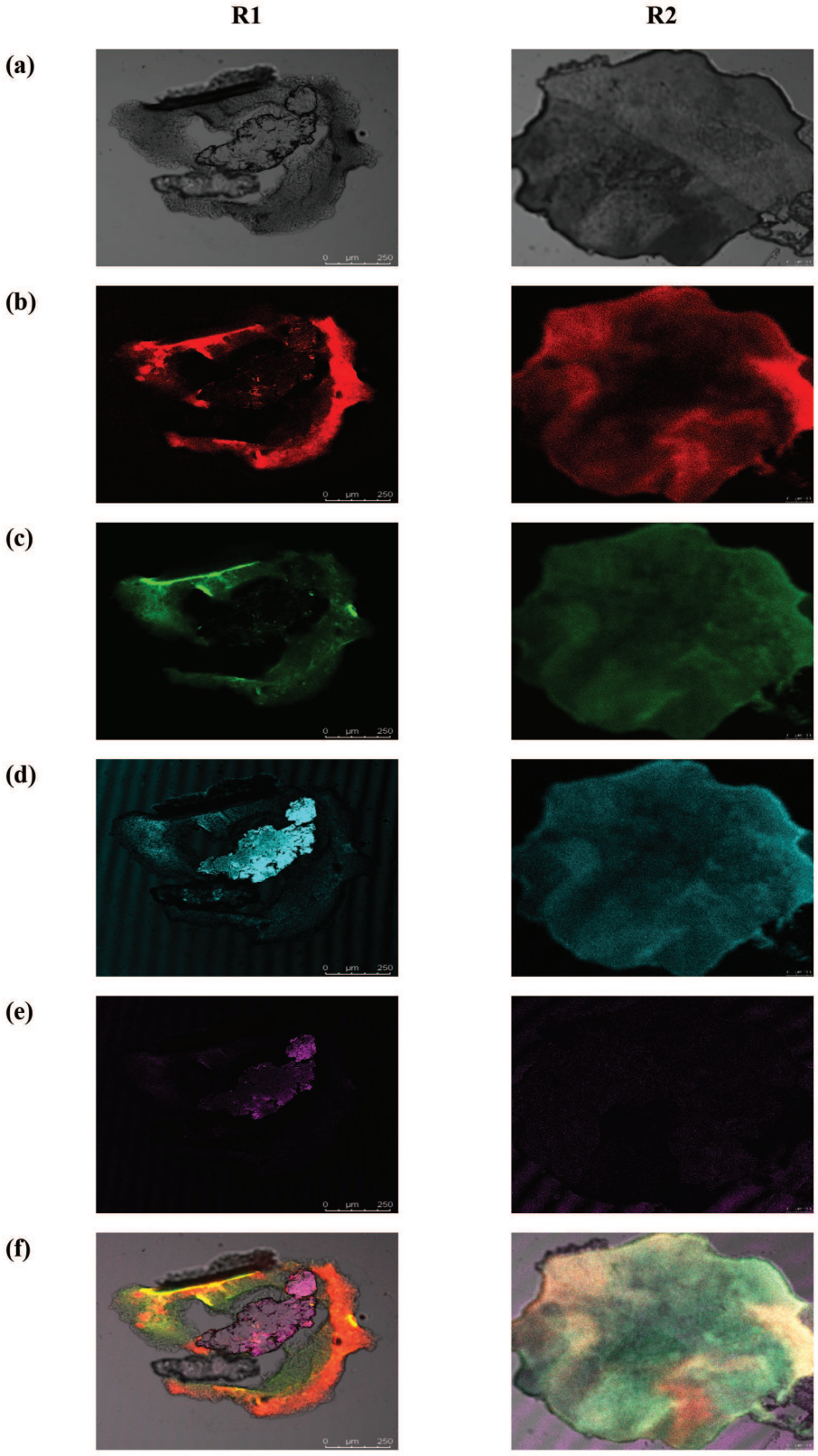

Fig. 4.5. CLSM images of R1 (Bar=250µm) and R2 (Bar=100µm) on 210th day: (a) optical microscopy photograph; (b) total cells (SYTO 63); (c) proteins (FITC); (d) polysaccharides (Con A); (e) dead cells (SYTOX Blue); (f) combined image of (b)-(e).

phenol indicating the more inactive AGS in R1 at high phenol load which was not able to degrade even a simple carbon source. On the other hand, R2 AGS followed an ascending pattern after each level of phenol concentration and reached to a maximum value of 16.35 mg COD removed mgVSS^{-1}

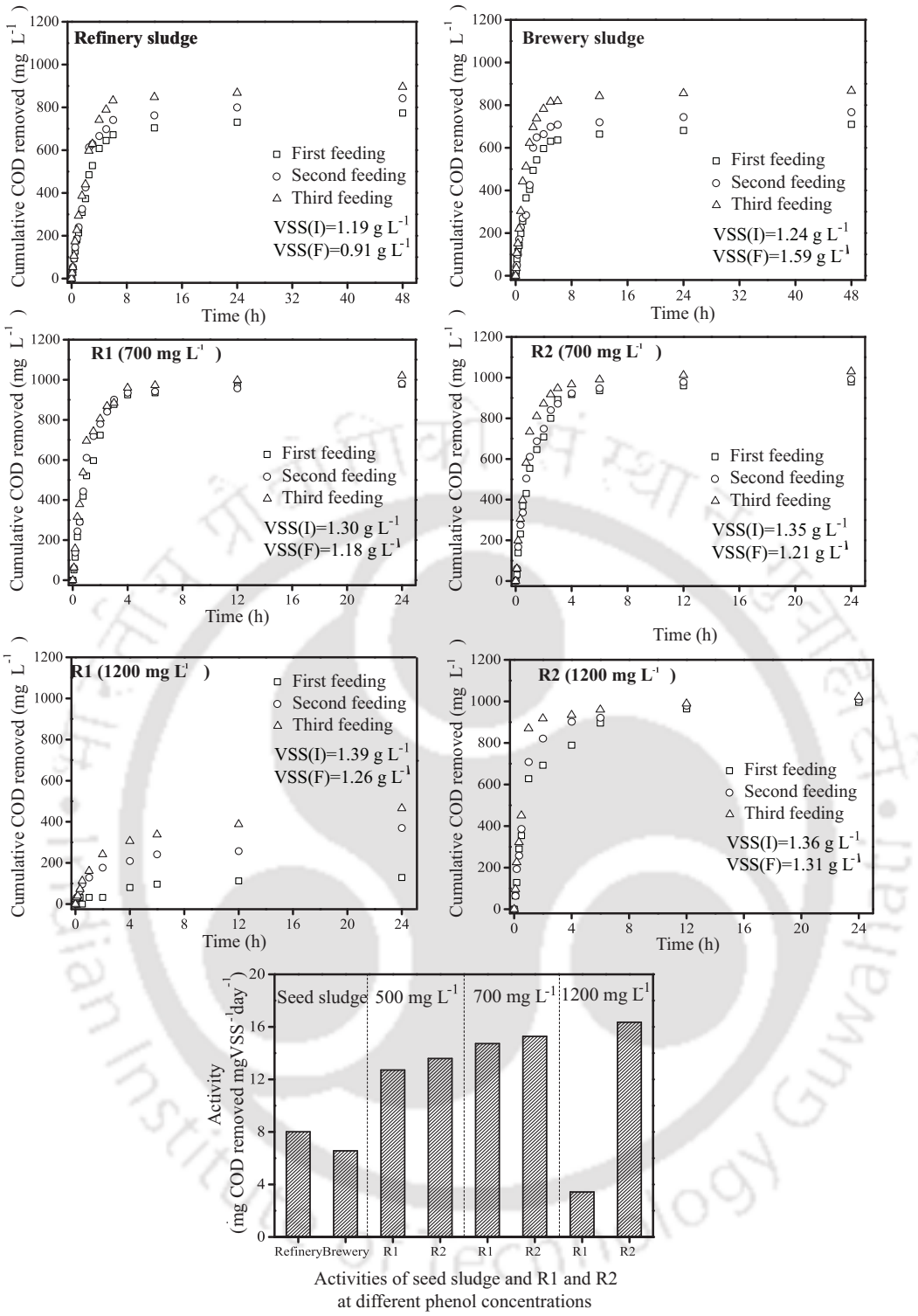

Fig. 4.6. Cumulative COD removal (mg L^{-1}) with time for seed sludge and for different phenol concentrations and biomass activity for all.

day^{-1} at 1200 mg L^{-1} of phenol indicating that the phenol loading up to 5.71 kg COD m^{-3} day^{-1} (1200 mg L^{-1} of phenol) did not impose any adverse effect on the effectiveness of R2 AGS towards toxic recalcitrant organics.

4.3.4 Pollutants removal profile

The pollutant removal profile at different phenol concentrations with operation time is provided in Table 4.5. The biodegradation of phenol is given in Fig. 4.7(a). Both reactors granules were able to

remove all the phenol (>99% removal efficiencies) since the start of the reactor and continued to do the same till the concentration of phenol reached to 700 mg L^{-1} (3.32 kg COD m^{-3} day^{-1}). Phenol loading more than 3.32 kg COD m^{-3} day^{-1} in R1 imposed a significant inhibitory effect on phenol degradation resulting in the loss of phenol removal efficiency of R1 granules. On the other hand, granules of R2 successfully removed phenol (>99% removal efficiency) without any adverse effect on phenol removal up to a phenol loading of 5.71 kg COD m^{-3} day^{-1}. It might be because of the compactness of granules (see *section 4.3.2.3*), which provided adequate stability towards the high toxicity of phenol. The same phenomenon was observed for COD removal as the phenol was the only carbon source during all phases (Fig. 4.7(b)). COD removal efficiencies for R1 and R2 were observed to be around 94% up to a phenol loading of 3.32 kg COD m^{-3} day^{-1}. Afterward, no COD removal was observed in R1, whereas R2 continued to remove COD (around 94% removal) throughout the study.

The biodegradation of SCN^- is given in Fig 4.7(c). The maximum concentration was used in this work for SCN^- was 100 mg L^{-1} in both of the reactors. In R1, SCN^- removal was more than 95% up to 40 mg L^{-1} of influent SCN^- except for day 3. Afterward, removal reduced to around 40% with 80 mg L^{-1} of influent SCN^- in the reactor. Since then, a rise in SCN^- removal efficiency was observed in R1 and removal efficiency got stabilized to around 99% with 100 mg L^{-1} of influent SCN^- (maximum concentration of influent SCN^- used in this study) up to Phase II. After Phase II, no SCN^- removal was observed in R1. Instability of R1 granules due to high phenol loadings might be the reason for not achieving SCN^- removal at higher concentrations of phenol. Whereas, a slight longer lag in ability of R2 granules to biodegrade SCN^- was observed and required around 27 days to start degradation of SCN^-. Once SCN^- degradation got initiated, it was continued to the last with around 99% removal efficiency irrespective of the increment in phenol loadings after each phase. A slight inhibition on SCN^- removal was observed with 420.4 mg L^{-1} of phenol in a moving bed biofilm reactor treating phenol, SCN^- and ammonium simultaneously (Li et al., 2011). Presence of 110-350 mg L^{-1} of phenol resulted in late biodegradation of SCN^- requiring 60 and 82 h when 50 mg L^{-1} of NO_2^- was present in the wastewater of aerobic reactor removing phenol, SCN^- and ammonium concurrently (Vázquez et al., 2006). In the current work (R2), SCN^- biodegradation was attained in a quick time of 12 h without any inhibition up to 1200 and 119.21±1.95 mg L^{-1} of phenol and NO_2^--N (discussed later), respectively.

Profiles of NH_4^+-N transformation in both of the reactors for all the phases are illustrated in Fig. 4.8. NH_4^+-N concentration was kept constant (100 mg L^{-1}) in both R1 and R2 after gradual increment to 100 mg L^{-1}. For the first 6 days (20 mg L^{-1} of NH_4^+-N), no NH_4^+-N was observed in the effluents of R1 and R2 along with no NO_2^--N and NO_3^--N in the effluent. Since then, up to days 24 and 30 in R1 and R2, respectively, the effluent NH_4^+-N was higher than the influent in each SBR suggesting no NH_4^+-N transformation. The conclusion was also made that the time required for cultivating nitrifying bacteria in R1 and R2 was 24 and 30 days, respectively. As the study progressed, almost complete NH_4^+-N removal (99%) was observed in R1 and R2 up to a phenol loading of 3.32 kg COD m^{-3} day^{-1} (Phase II). Inhibitory effect of phenol with a loading of higher than 3.32 kg COD m^{-3} day^{-1} was observed on nitrification in R1 resulting in the absence of nitrification with a quite higher effluent values (194.27±3.83 mg L^{-1} of NH_4^+-N) from an influent value of 124 mg L^{-1} of NH_4^+-N (comprising feed NH_4^+-N and NH_4^+-N generated from the biotransformation of SCN^-; *Chapter 2, section 2.3.4.2)* during Phase IV (phenol loading of 5.71 kg COD m^3 day^{-1}). Higher effluent value of NH_4^+-N than the influent might be because of the accumulation of NH_4^+-N from the previous cycles during Phase III

Table 4.5. Pollutant removal profile at different phenol concentrations with operation time.

Pollutant		Operation time (day/days)							
		53-78		97-125		149-181		197-225	
		R1	R2	R1	R2	R1	R2	R1	R2
Phenol	Influent (mg L^{-1})	498.92±3.35	498.69±1.04	697.26±2.40	696.87±1.22	1000.80±3.35	998.77±3.00	1197.36±4.49	1202.65±3.11
	Effluent (mg L^{-1})	1.00±0.69	0.66±0.27	0.93±0.84	0.78±0.60	2052.29±149.15	1.06±1.15	2649.11±125.96	0.72±0.23
	% removal	99.80±0.14	99.87±0.05	99.87±0.12	99.89±0.09	-105.06±14.84	99.89±0.12	-121.96±10.76	99.94±0.02
COD	Influent (mg L^{-1})	1205.96±26.86	1207.58±14.73	1658.86±42.68	1679.45±44.40	2395.07±47.33	2405.96±31.75	2805.59±43.54	2854.04±44.72
	Effluent (mg L^{-1})	68.02±5.62	71.01±9.05	89.28±11.41	84.91±6.70	4666.69±185.34	128.12±14.14	5523.43±150.56	154.45±37.38
	% removal	94.36±0.47	94.12±0.71	94.61±0.73	94.94±0.39	-94.89±8.35	94.67±0.61	-93.83±6.75	94.58±1.32
SCN^-	Influent (mg L^{-1})	99.08±0.64	99.61±1.00	99.38±2.74	99.39±0.51	99.07±1.27	99.58±1.23	98.26±1.06	99.42±0.63
	Effluent (mg L^{-1})	0.36±0.15	0.67±0.33	0.78±0.39	0.56±0.27	204.00±5.53	0.86±0.44	204.23±5.40	0.59±0.39
	% removal	99.63±0.15	99.33±0.33	99.21±0.41	99.43±0.28	-105.95±6.32	99.14±0.44	-107.88±6.16	99.41±0.39
NH_4^+-N	Influent (mg L^{-1})	98.00±0.80	100.14±0.36	99.60±1.20	100.42±1.91	98.61±0.92	100.11±0.90	99.29±0.53	100.06±1.28
	Effluent (mg L^{-1})	0.49±0.25	0.32±0.25	0.45±0.28	0.48±0.29	188.02±10.61	0.44±0.27	194.27±3.83	0.39±0.28
	% removal	99.50±0.26	99.68±0.25	99.55±0.28	99.52±0.29	-90.63±9.82	99.56±0.27	-95.66±4.04	99.61±0.28

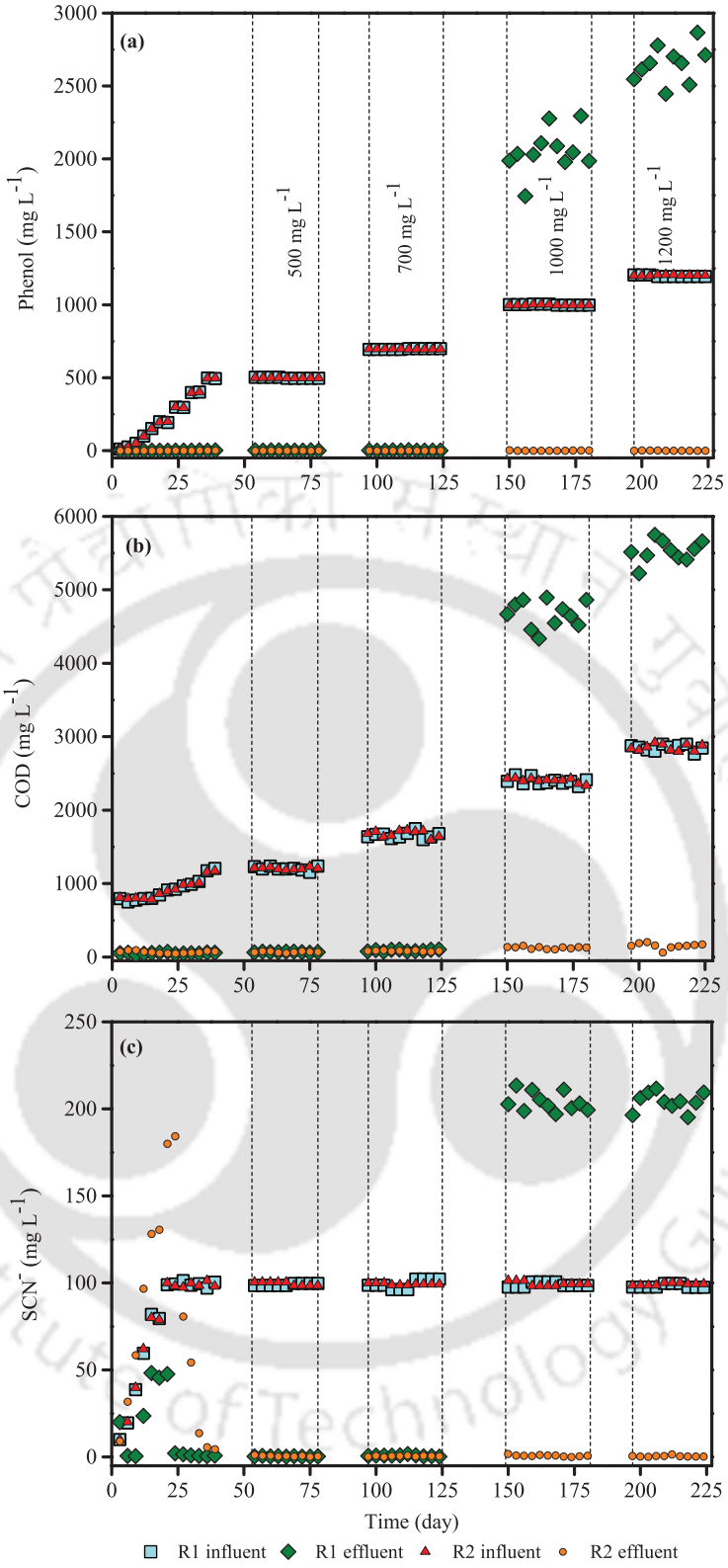

Fig. 4.7. Concentration profiles of (a) phenol, (b) COD and (c) SCN^-.

and IV in R1. R2 granules continued to transform NH_4^+-N (>99%) up to phenol loading of 5.71 kg COD m^{-3} day^{-1} (Phase IV) without any inhibitory effect of higher phenol loading with the effluent 0.39±0.28 mg L^{-1} of NH_4^+-N during Phase IV. Effluent NO_2^--N concentrations were 127.63±1.56 and 119.32±1.18 mg L^{-1} in R1 and R2, respectively, during Phase II (phenol loading of 3.32 kg COD m^{-3} day^{-1}). So far, no inhibition on the nitritation due to phenol loading was observed in both of the reactors. Beyond 3.32 kg COD m^{-3} day^{-1} of phenol loading, the toxic effect of phenol was

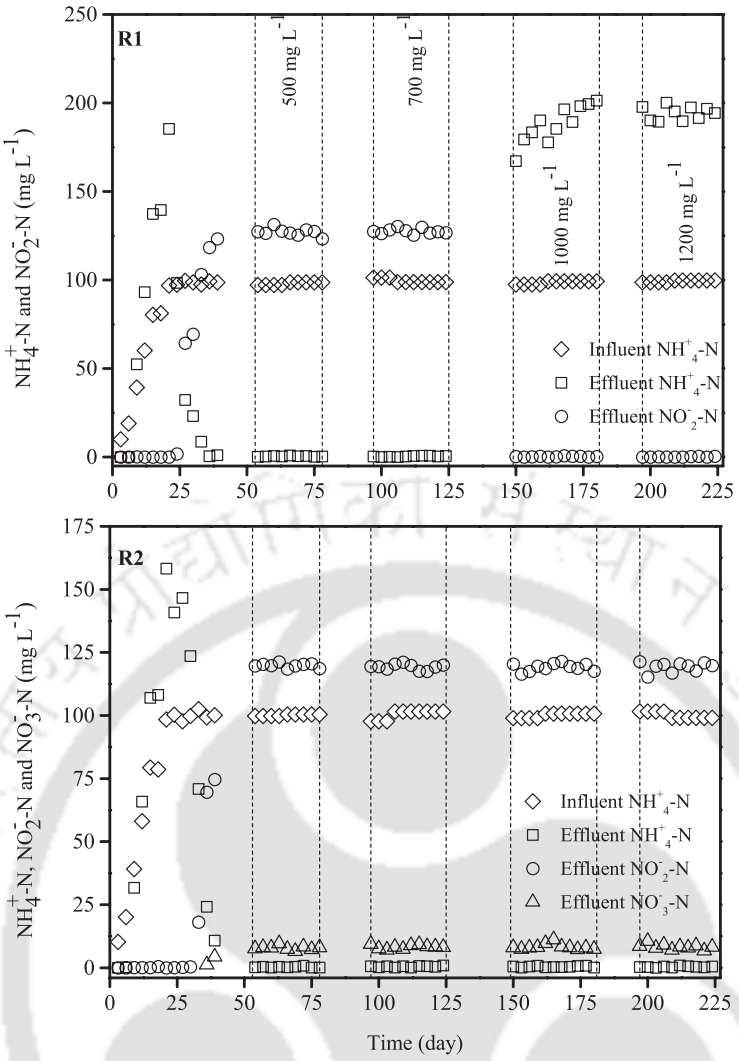

Fig. 4.8. Concentration profiles of NH_4^+-N, NO_2^--N and NO_3^--N.

observed in R1 resulting in the absence of nitritation (Phase III and IV). R2 granules continued to exhibit an excellent nitritation efficiency throughout the study and did not undergo any inhibition because of higher phenol load. During Phase IV, effluent NO_2^--N concentrations were 0.22±0.20 and 119.21±1.95 mg L^{-1} in R1 and R2, respectively. NO_3^--N was not detected in R1 effluent throughout the work, on the other hand, an average concentration of 8.22±0.96 mg L^{-1} of NO_3^--N was observed in the effluent of R2 from Phase I to IV. Partial nitrification was observed in R1 (up to an OLR of 3.32 kg COD m^{-3} day^{-1}; Phase II) and R2 (all phases) concluding the absence of nitrite-oxidizing bacteria (NOB) and the possible reason for getting nitritation might be shorter SRT than the values required for complete nitrification 10-30 days (Tchobanoglous et al., 2003). The importance of SRT on nitrification is discussed in *Chapter 2 (section 2.3.4.2)*. SRT values during Phase II were around 9.50 and 9.75 days, respectively, in R1 and R2. In R1, SRT values reduced to around 3.88 days during Phase IV, whereas in R2, SRT of around 9.41 days was observed. Therefore, SRT lower than 10 days was supposed to the possible reason for the inhibition of NOB growth and for the accumulation of NO_2^--N in R1 (up to Phase II) and R2 (all phases) as well. Phenol concentration beyond 200 mg L^{-1} imposed an adverse effect on nitrification in activated sludge system (Kim et al., 2008b). Inhibition on the nitrifying activity of aerobic granules beyond 10 mg L^{-1} of phenol in batch tests was observed (Liu et al., 2005). The current work was found to be strategic for achieving nitrification in an SBR without any inhibition of phenol up to 1200 mg L^{-1} on AGS (R2).

4.4 Conclusion

It was concluded from the present work that the stability of granules were independent of rapid granulation. Granulation from brewery sludge (R2) required 50 days and showed a stable and distinct potential towards the higher phenol toxicity (phenol loading of 5.71 kg COD m^{-3} day^{-1}) without any inhibition among all the toxic pollutants. On the other hand, granules developed from the refinery sludge (R1) were not able to tolerate phenol loading beyond 3.32 kg COD m^{-3} day^{-1} resulting in the deteriorated R1 performance, even though developed in only 40 days. R2 granules were more stable and compact supported by the higher GSV, lower SVI_{30} and higher EPS content at a phenol loading of 5.71 kg COD m^{-3} day^{-1}, whereas R1 granules started to deteriorate and even lost their ability to degrade benign substrate, sodium acetate, after being exposed to higher phenol loading (>3.32 kg COD m^{-3} day^{-1}).

References

Adav, S.S., Chen, M.Y., Lee, D.J., Ren, N.Q., 2007a. Degradation of phenol by *Acinetobacter* strain isolated from aerobic granules. Chemosphere 67, 1566-1572.

Adav, S.S., Lee, D.J., Lai, J., 2007b. Effects of aeration intensity on formation of phenol-fed aerobic granules and extracellular polymeric substances. Applied Microbiology and Biotechnology 77, 175-182.

Chen, Q.Q., Chen, H., Zhang, Z.Z., Guo, L.X., Jin, R.C., 2017. Effects of thiocyanate on granule-based anammox process and implications for regulation. Journal of Hazardous Materials 321, 81-91.

Chen, Y., Jiang, W., Liang, D.T., Tay, J.H., 2007. Structure and stability of aerobic granules cultivated under different shear force in sequencing batch reactors. Applied Microbiology and Biotechnology 76, 1199-1208.

Ghangrekar, M., Asolekar, S., Ranganathan, K., Joshi, S., 1996. Experience with UASB reactor start-up under different operating conditions. Water Science and Technology 34, 421-428.

Ho, K.L., Lin, B., Chen, Y.Y., Lee, D.J., 2009. Biodegradation of phenol using *Corynebacterium* sp. DJ1 aerobic granules. Bioresource Technology 100, 5051-5055.

Jiang, H.L., Tay, J.H., Maszenan, A.M., Tay, S.T.L., 2004a. Bacterial diversity and function of aerobic granules engineered in a sequencing batch reactor for phenol degradation. Applied and Environmental Microbiology 70, 6767-6775.

Jiang, H.L., Tay, J.H., Tay, S.L., 2004b. Changes in structure, activity and metabolism of aerobic granules as a microbial response to high phenol loading. Applied Microbiology and Biotechnology 63, 602-608.

Jiang, H.L., Tay, J.H., Tay, S.T.L., 2002. Aggregation of immobilized activated sludge cells into aerobically grown microbial granules for the aerobic biodegradation of phenol. Letters in Applied Microbiology 35, 439-445.

Kim, I.S., Kim, S.M., Jang, A., 2008a. Characterization of aerobic granules by microbial density at different COD loading rates. Bioresource Technology 99, 18-25.

Kim, Y.M., Park, D., Lee, D.S., Park, J.M., 2008b. Inhibitory effects of toxic compounds on nitrification process for cokes wastewater treatment. Journal of Hazardous Materials 152, 915-921.

Koechler, S., Farasin, J., Cleiss Arnold, J., Arsène Ploetze, F., 2015. Toxic metal resistance in biofilms: diversity of microbial responses and their evolution. Research in Microbiology 166, 764-773.

Li, A.J., Yang, S.F., Li, X.Y., Gu, J.D., 2008. Microbial population dynamics during aerobic sludge granulation at different organic loading rates. Water Research 42, 3552-3560.

Li, H.Q., Han, H.J., Du, M.A., Wang, W., 2011. Removal of phenols, thiocyanate and ammonium from coal gasification wastewater using moving bed biofilm reactor. Bioresource Technology 102, 4667-4673.

Liu, Y.Q., Tay, J.H., Ivanov, V., Moy, B.Y.P., Yu, L., Tay, S.T.L., 2005. Influence of phenol on nitrification by microbial granules. Process Biochemistry 40, 3285-3289.

Moy, B., Tay, J., Toh, S., Liu, Y., Tay, S., 2002. High organic loading influences the physical characteristics of aerobic sludge granules. Letters in Applied Microbiology 34, 407-412.

Sahariah, B.P., Chakraborty, S., 2011. Kinetic analysis of phenol, thiocyanate and ammonia-nitrogen removals in an anaerobic-anoxic-aerobic moving bed bioreactor system. Journal of Hazardous Materials 190, 260-267.

Singh, M., Srivastava, R., 2011. Sequencing batch reactor technology for biological wastewater treatment: a review. AsiaPacific Journal of Chemical Engineering 6, 3-13.

Tay, J.H., Jiang, H.L., Tay, S.T.L., 2004. High-rate biodegradation of phenol by aerobically grown microbial granules. Journal of Environmental Engineering 130, 1415-1423.

Tay, S.T.L., Moy, B.Y.P., Maszenan, A.M., Tay, J.H., 2005a. Comparing activated sludge and aerobic granules as microbial inocula for phenol biodegradation. Applied Microbiology and Biotechnology 67, 708-713.

Tay, S.T.L., Moy, B.Y.P., Jiang, H.L., Tay, J.H., 2005b. Rapid cultivation of stable aerobic phenol-degrading granules using acetate-fed granules as microbial seed. Journal of Biotechnology 115, 387-395.

Tchobanoglous, G., Burton, F.L., Stensel, H.D., Metcalf, Eddy, 2003. Wastewater Engineering: Treatment and Reuse, fourth ed. McGraw Hill Education, India.

Vázquez, I., Rodríguez, J., Marañón, E., Castrillón, L., Fernández, Y., 2006. Simultaneous removal of phenol, ammonium and thiocyanate from coke wastewater by aerobic biodegradation. Journal of Hazardous Materials 137, 1773-1780.

Winkler, M.K.H., Meunier, C., Henriet, O., Mahillon, J., Suárez Ojeda, M.E., Del Moro, G., De Sanctis, M., Di Iaconi, C., Weissbrodt, D.G., 2018. An integrative review of granular sludge for the biological removal of nutrients and recalcitrant organic matter from wastewater. Chemical Engineering Journal 336, 489-502.

Wosman, A., Lu, Y., Sun, S., Liu, X., Wan, C., Zhang, Y., Lee, D.J., Tay, J., 2016. Effect of operational strategies on activated sludges acclimation to phenol, subsequent aerobic granulation, and accumulation of polyhydoxyalkanoates. Journal of Hazardous Materials 317, 221-228.

Wu, D., Zhang, Z., Yu, Z., Zhu, L., 2018. Optimization of F/M ratio for stability of aerobic granular process via quantitative sludge discharge. Bioresource Technology 252, 150-156.

Xiao, F., Yang, S.F., Li, X.Y., 2008. Physical and hydrodynamic properties of aerobic granules produced in sequencing batch reactors. Separation and Purification Technology 63, 634-641.

Zhang, L., Feng, X., Zhu, N., Chen, J., 2007. Role of extracellular protein in the formation and stability of aerobic granules. Enzyme and Microbial Technology 41, 551-557.

What is important is not what you hear said, it's what you observe.

Michael Connelly (1956-)
American author

5

Treatment of Aromatic, Inorganics and Nitrogenous Heterocyclic Compounds by Aerobic Granules

This chapter deals with the potential of aerobic granular sludge to treat pyridine, indole and ammonia-nitrogen along with phenol and thiocynate concurrently.

5.1 Introduction

Sustainable treatment technology for industrial wastewater like for coal gasification is a challenging task because of containing toxic and refractory organic compounds such as phenol, polycyclic aromatic hydrocarbons and nitrogenous heterocyclic compounds (NHCs) along with inorganic compounds like thiocyanate (SCN^-) and ammonia-nitrogen (NH_4^+-N) (Shi et al., 2019; Wei et al., 2012). Being toxic, mutagenic and carcinogenic in nature, NHCs such as pyridine and indole impart an adverse effect on human health and ecosystem (Shi et al., 2019). In addition, increasing public attentiveness on the environmental aspect has led to the establishment of stringent discharge limits of pollutants present in industrial wastewater (Pillai and Gupta, 2016). Therefore, a viable approach is required for the treatment of complex toxic wastewater before being discharged to the surface water bodies.

Various treatment technologies have been adopted for treating pyridine and indole rich wastewater, such as Fenton oxidation (Hammouda et al., 2016; Li et al., 2014), adsorption (Sarker et al., 2018; Zhu et al., 2016), catalytic ozonation (Zhu et al., 2017), etc. High energy ingestion and high cost limit the implementation of various physicochemical processes (Wang et al., 2018). However, biological process provides an efficient and cost-effective approach to treat toxic and recalcitrant pollutants such as NHCs (Wang et al., 2011). Though, the application of the biological method for removing pyridine and indole is limited because of the microbial growth inhibition imparted by high toxicity of pyridine and indole (Chen et al., 2013; Wang et al., 2018). In addition, because of the presence of various toxic and refractory compounds, the simultaneous removal of all the pollutants is difficult because of the inhibition episode among the pollutants (Vázquez et al., 2006). For example, SCN^- and phenol inhibit nitrification when present with NH_4^+-N (Kim et al., 2008) and the presence of phenol affects the pyridine biodegradation as well (Sun et al., 2011). Hence, a sustainable treatment methodology is desired to attain the simultaneous removal of multiple toxic and refractory pollutants without any inhibition phenomenon among them.

Aerobic granular sludge (AGS) technology has been appeared as an invention in the field of wastewater treatment technology because of having good settling property, distinct outline, denser,

regular and compact structure and potential to treat high toxic loading (Jiang et al., 2017; Liang et al., 2019; Sguanci et al., 2019). Because of the above addressed unique properties, AGS has been adopted to treat high loading wastewater containing organics and nitrogen (Moy et al., 2002; Yang et al., 2003). Furthermore, the ability of AGS to treat recalcitrant contaminants like phenol, *p*-nitrophenol, aniline, pyridine, etc., has been addressed in many literature works (Adav et al., 2007a; Adav et al., 2008; Jiang et al., 2017; Liu et al., 2015). Studies for concurrent nitritation with *p*-nitrophenol or *o*-cresol removal, simultaneous removal of aromatic compounds (phenol, *o*-cresol and *p*-nitrophenol) and concurrent pyridine and nitrogen removal by aerobic granules are also well documented in the literature (Jemaat et al., 2013; Jemaat et al., 2014; Liu et al., 2018; Ramos et al., 2015). But so far, no study addresses the concurrent removal of multiple toxic pollutants such as NHCs (pyridine and indole), aromatic compound (phenol) and inorganic compounds (SCN^- and NH_4^+-N) (coexist in the coal gasification wastewater) by AGS.

Therefore, based on the lacunae in the literature, the objective of the present study is to investigate the potential of AGS to biodegrade pyridine, indole and NH_4^+-N along with phenol and SCN^- concurrently. The granular biomass activity (before and after exposure of AGS to pyridine and/or indole) in terms of mg COD removed $mgVSS^{-1}$ day^{-1} was also analyzed.

5.2 Materials and methods

5.2.1 Experimental setup

The source of the chemicals and reagents used in this study is given in *Chapter 2 (section 2.2.1)*. Pyridine and indole was puchased from Merck (India) and Hi-media (India) Three identical transparent acrylic sequencing batch reactors (SBRs) with same configuration as given in *Chapter 2 (section 2.3.1)* were used to cultivate AGS. In all SBRs, air was supplied by an air compressor and diffused through the air bubblers positioned at the bottom of SBRs with an airflow rate of 2.0 L min^{-1} maintained by rotameter. The photographic image and schematic representation of the SBR is given in *Chapter 2* (Fig. 2.1 and Fig. 2.2, respectively). The influent feed was provided by the peristaltic pumps from the bottom of the SBRs.

5.2.2 Characteristics of seed sludge and influent feed

All SBRs were inoculated with the refinery sludge collected from the wastewater treatment plant of Indian Oil Corporation Limited, Guwahati. The total and volatile suspended solids (TSS and VSS) in the refinery sludge were 3.31 and 2.22 g L^{-1}, respectively. The size and sludge volume index (SVI_{30}) value of seed sludge were 49.40 μm and 49.20 mL $gTSS^{-1}$, respectively. All three 6 L SBRs were inoculated with 3 L refinery sludge. The influent synthetic wastewater composition for all SBRs is given in Table 5.1. Phenol (500 mg L^{-1}), NH_4^+-N as NH_4Cl (100 mg L^{-1}) and SCN^- as KSCN (100 mg L^{-1}) were the common constituents in all SBRs. R1, R2 and R3 were operated with pyridine, indole and an equimolar mixture of pyridine and indole, respectively (Table 5.1). Indole was dissolved in hot water before being mixed with the influent feed because of its poor solubility in cold water (Higashio and Shoji, 2004). pH was maintained between 7.5-8.0 using phosphate buffer and $NaHCO_3$ in all SBRs. Phosphate buffer was also a source of phosphorus required for the growth of microbes. Trace metals composition was adopted from Sahariah and Chakraborty (2011).

5.2.3 Reactor operation

The same operational approach for all SBRs was used as given in *Chapter 3 (section 3.4.3)*. During

Table 5.1. Influent feed composition.

Reactor	R1					R2					R3				
Operation time (days)	1-39	39-46	54-72	82-100	110-128	1-39	39-46	54-72	82-100	110-128	1-39	39-46	54-72	82-100	110-128
Phenol[a]	10-500		500			10-500		500			10-500		500		
NH_4^+-N[a]	10-100		100			10-100		100			10-100		100		
SCN^-[a]	10-100		100			10-100		100			10-100		100		
Sodium acetate[a]	1000-0		0			1000-0		0			1000-0		0		
Pyridine[a]	0	0	80.70± 2.08 (1.0mM[d])	201.03± 4.22 (2.5mM[d])	402.93± 6.29 (5.0mM[d])	0	0	0	0	0	0	0	41.31± 1.23 (0.5mM[d])	103.45± 2.63 (1.25mM[d])	204.78± 3.76 (2.5mM[d])
Indole[a]	0	0	0	0	0	0	0	120.65± 4.84 (1.0mM[d])	304.38± 9.50 (2.5mM[d])	596.94± 9.44 (5.0mM[d])	0	0	61.54± 2.69 (0.5mM[d])	155.36± 6.48 (1.25mM[d])	295.42± 2.38 (2.5mM[d])
$NaHCO_3$[a]	added as required					added as required					added as required				
Phosphate buffer[b]	1 mL L^{-1}					1 mL L^{-1}					1 mL L^{-1}				
Trace metal solution[c]	1 mL L^{-1}					1 mL L^{-1}					1 mL L^{-1}				

[a]unit mg L^{-1}; [b]Phosphate buffer contained (g L^{-1}): 72.3 $KHiouPO_4$ and 104.5 K_2HPO_4; [c]Trace metal solution contained (mg L^{-1}): 10,000 $MgSO_4.7H_2O$, 10,000 $CaCl_2.2H_2O$, 5000 $FeCl_3.6H_2O$, 1000 $CuCl_2$, 1000 $ZnCl_2$, 500 $NiCl_2.6H_2O$ and 500 $CoCl_2$; [d]millimolar concentration

acclimatization (first 39 days), a simple carbon source sodium acetate (1000 mg L^{-1}) was added in all SBRs to facilitate the biomass growth. As the operation proceeded, the concentration of sodium acetate was gradually reduced and that of phenol, SCN^- and NH_4^+-N concentrations were increased in the feed (Table 5.1). At the end of 39th day, sodium acetate was suspended, while concentrations of phenol, SCN^- and NH_4^+-N were reached to the desired levels of 500, 100 and 100 mg L^{-1}, respectively, and kept constant throughout the study (Table 5.1). A period of 7 days (days 39-46) was given to all SBRs to get acclimatized with 500 mg L^{-1} of phenol, 100 mg L^{-1} of SCN^- and 100 mg L^{-1} of NH_4^+-N before pyridine and/or indole exposure. Since then (days 46-53), concentrations of NHCs were gradually increased to reach 1.0 mM. R1 and R2 were operated with pyridine and indole respectively, whereas R3 was operated with a mixture of an equimolar concentrations of both pyridine and indole (Table 5.1). Three concentrations of pyridine and/or indole (1.0, 2.5 and 5.0 mM) (Table 5.1) were analyzed to observe the impact of NHCs on AGS. A transition period of 10 days was kept for a gradual rise in pyridine and/or indole concentrations to the next desired level after each increment. During the transition period, only granular characteristics were analyzed. All SBRs were operated for at least 18 days with each pyridine and/or indole concentration to obtain steady-state data.

5.2.4 Analytical procedures

All the analytical methods used in this study have been mentioned in *Chapter 2 (section 2.2.2)*) and unless otherwise specified. Granular biomass activity (GBA) determination is given in *Chapter 4 (section 4.2.5)*. Concentrations of pyridine and indole were quantified by using a high performance liquid chromatography (HPLC) (Prostar 210, Varian, USA). Pyridine analysis was performed using an Agilent 5 TC-C18 column (dimensions 250 mm x 4.6 mm) with a mobile phase consisting of methanol and milli-Q water in the ratio of 80:20 at a flow rate of 1 mL min^{-1} (Bai et al., 2011). However, indole was analyzed using C-18 Thermo hypersil column (dimensions 100 mm x 4.6 mm) with a mobile phase comprising 70% acetonitrile and 30% milli-Q water pumped at 1 mL min^{-1} flow rate (Goswami et al., 2017). Both pyridine and indole were detected with a UV- detector set at 254 nm.

5.3 Results and discussion

5.3.1 Granule formation

The granular development with time is illustrated in Fig. 5.1. The refinery sludge was a brown colour suspension without any granular structure (Fig. 5.1). Granular structure appeared in all SBRs on 13th day and took around 40 days to get matured in all SBRs. Granulation time of 42 days was taken to accelerate the granulation process using pure pyridine degrading strains in SBRs (Liang et al., 2018). The current work was similar to the previously addressed work in terms of achieving granulation but with mixed culture. Addition of 1.0 mM (80.70±2.08 mg L^{-1}) of pyridine in R1, 1.0 mM (120.65±4.84 mg L^{-1}) of indole in R2 and an equimolar mixture of pyridine (0.5 mM) and indole (0.5 mM) (41.31±1.23 and 61.54±2.69 mg L^{-1}, respectively) in R3, did not affect the granulation process (Fig. 5.1; day 65) and granules were of round in shape with a distinct and clear outline (visual observation). FESEM images of day 65 (Fig. 5.2) also revealed the clear and compact structure (visual observation) in all SBRs. R1 granules continued to exhibit clear, distinct and compact structure even after addition of pyridine up to a concentration of 5.0 mM (402.93±6.29), whereas concentrations of indole (R2) and an equimolar mixture of pyridine and indole (R3) beyond 1.0 mM imposed an adverse effect on granulation resulting in the deteriorated structure (Fig. 5.1 and Fig. 5.2; day 120). It was confirmed from the results that indole was more toxic than pyridine for the granules at a concentration

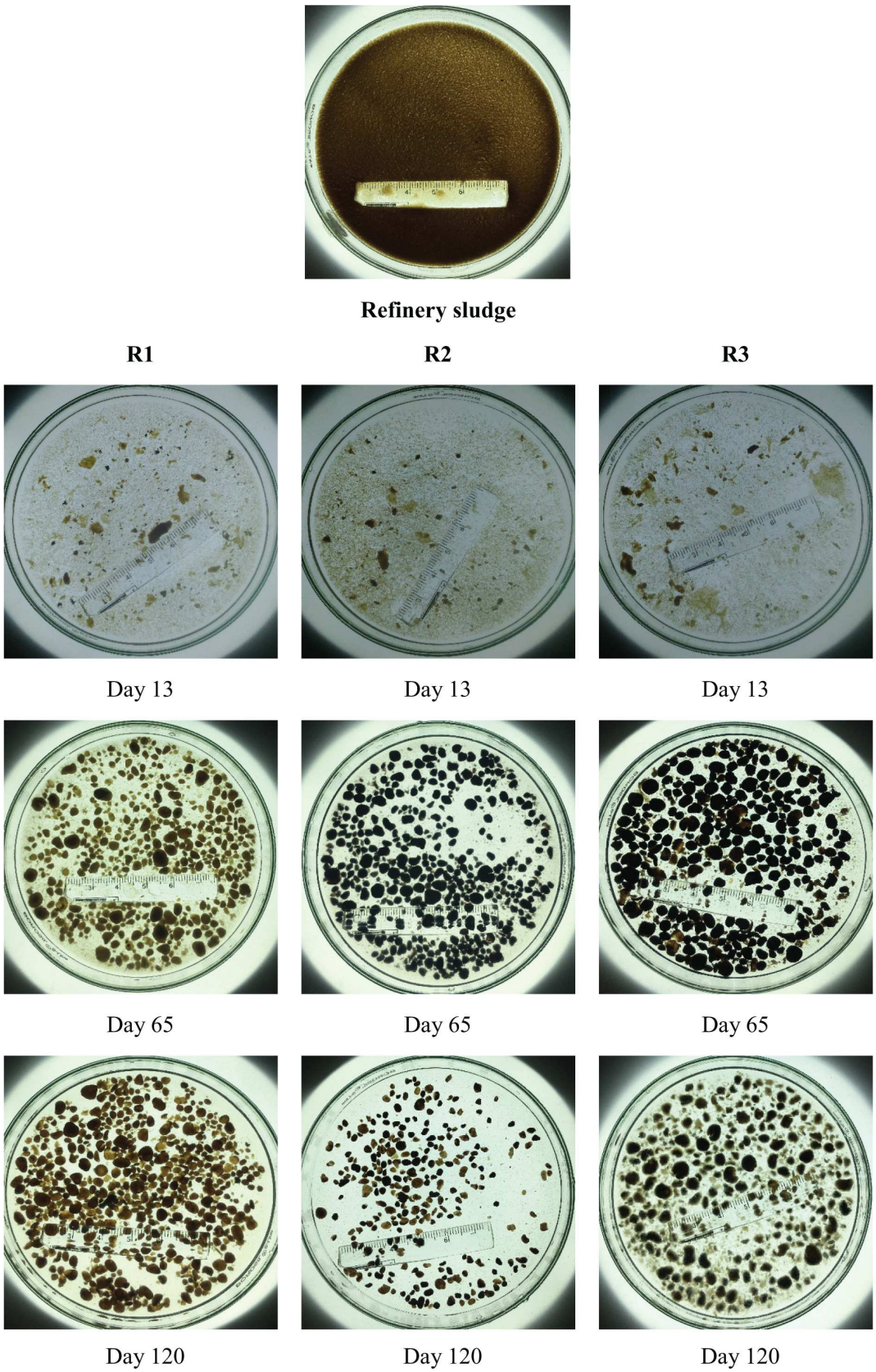

Fig. 5.1. Images of refinery sludge and granules at 1.0 mM (day 65) and 5.0 mM (day 120) of NHCs concentrations.

beyond 1.0 mM (2.5 and 5.0 mM in R2 and 1.25 and 2.50 mM in R3) because pyridine did not show any inhibitory effect on granulation up to 5.0 mM concentration. In the current work, granulation was achieved with a combination of multiple toxic pollutants comprising pyridine, indole, phenol,

SCN^- and NH_4^+-N using refinery sludge, a mixed population, as an inoculum.

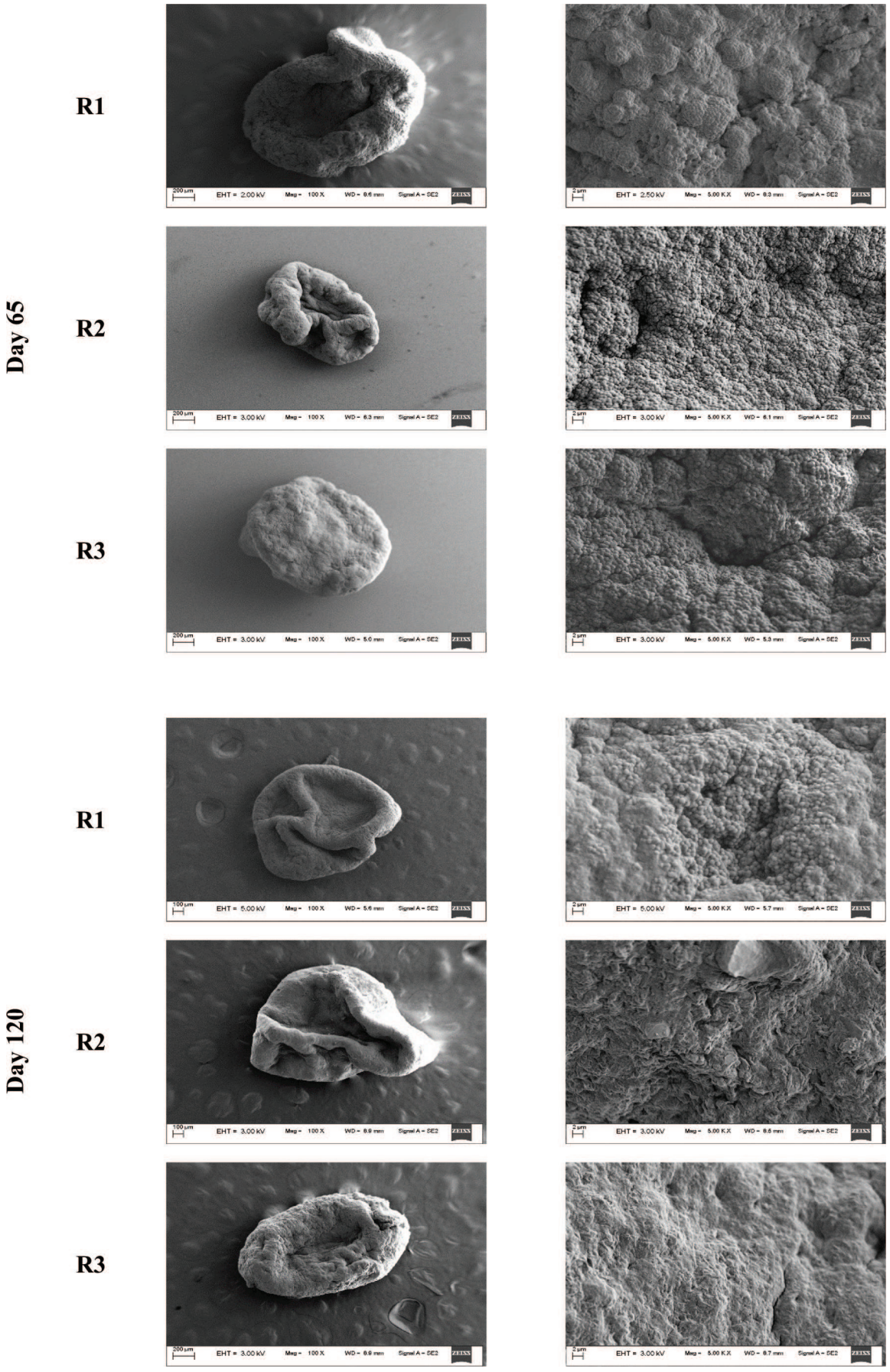

Fig. 5.2. FESEM images of granules at 1.0 mM (day 65) and 5.0 mM (day 120) of NHCs concentrations.

5.3.2 Granular Characteristics

Granular characteristics are given in Table 5.2.

5.3.2.1 Granule size

Fig. 5.3a and Table 5.2 provide information about the average granule size (diameter) in all SBRs. During first the 10 days, fluctuation in granule size was observed and since then, an increasing pattern was reported in all SBRs. At the time of maturation (day 40), the size of the mature granules was 900.91±374.69, 956.05±401.85, 977.69±673.08 μm in R1, R2 and R3, respectively, with 500 mg L^{-1} of phenol as a carbon source. After acclimatization with 500, 100 and 100 mg L^{-1} of phenol, SCN^- and NH_4^+-N, respectively, for 7 days (days 39-46), the average size of the stabilized granules (before exposure of NHCs) was 1038.69, 1021.74 and 1200.13 μm, respectively, in R1, R2 and R3. Since 54th day onwards after addition of NHCs (pyridine and/or indole) with 1.0 mM concentration, the size of the granules increased and reached to the stabilized values of 1329.83±48.72, 1195.45±52.20 and 1261.81±40.77 μm in R1, R2 and R3, respectively, during 54-72 days. Afterward, as the concentrations of pyridine and/or indole were raised, the size of the granules followed different trends in R1, R2 and R3. R1 granules exhibited a rising trend in size after each increment in pyridine concentration with the average values of 1796.10±13.95 (days 82-100) and 2144.40±54.85 μm (days 110-130) with 2.5 mM (201.03±4.22) and 5.0 mM (402.93±6.29 mg L^{-1}) of pyridine, respectively, indicating no inhibitory effect of sole pyridine on the granular size. On the other hand, the size of the granules decreased in R2 and R3 as the concentrations of indole and an equimolar mixture of pyridine and indole were increased. At 5.0 mM concentration in R2 and R3, the average size was 969.62±44.71 and 953.54±59.24 μm, respectively, reporting the toxic effect of indole on granules beyond 1.0 mM concentration.

5.3.2.2 Biomass concentration

Biomass concentration (VSS) is provided in Fig. 5.3b and Table 5.2. At the beginning of start-up period (day 1), the VSS values were 1.53, 1.33 and 1.35 g L^{-1} in R1, R2 and R3, respectively. As the concentrations of phenol, SCN^- and NH_4^+-N were increased, an increment in VSS values was observed in all SBRs and stabilized to 3.64, 3.52 and 3.65 g L^{-1} in R1, R2 and R3, respectively, with 500, 100 and 100 mg L^{-1} of phenol, SCN^- and NH_4^+-N, respectively, during 39-46 days. As the addition of NHCs was implemented with 1.0 mM concentration, VSS values increased because of the supply of the additional carbon sources and stabilized to 4.57±0.08, 4.14±0.05 and 4.33±0.07 g L^{-1} in R1, R2 and R3, respectively, without exhibiting any toxic effect of NHCs up to 1.0 mM concentration. R1 AGS appeared to increase in concentration with an increase in pyridine concentration and did not undergo any inhibition up to a higher pyridine concentration of 5.0 mM (402.93±6.29 mg L^{-1}) with an average VSS value of 6.00±0.08 g L^{-1} (days 110-130). Whereas a reducing trend was observed in the VSS values with rise in concentrations beyond 1.0 mM for indole and an equimolar mixture of pyridine and indole, respectively, in R2 and R3. At 5.0 mM concentration of indole and an equimolar mixture of pyridine and indole, the reduced average VSS values were 3.26±0.11 and 3.55±0.07 g L^{-1} in R2 and R3, respectively. From the lower VSS values in R2 and R3, it was confirmed that higher concentrations of indole and an equimolar mixture of indole with pyridine beyond 1.0 mM caused the granule disintegration resulting in biomass washout (also supported by lower solid retention time (SRT) values of 4.96 and 5.32 days, respectively, in R2 and R3; discussed in later section).

Food to microorganism (F/M) ratios with operation time for all the reactors are provided in

Table 5.2. Characteristics of AGS with operation time.

Reactor	R1				R2				R3			
Operation time (days)	39-46	54-72	82-100	110-130	39-46	54-72	82-100	110-130	39-46	54-72	82-100	110-130
Average granule size (μm)	1038.69	1329.83± 48.72	1796.10± 13.95	2144.40± 54.85	1021.74	1195.45± 52.20	1024.13± 41.05	969.62± 44.71	1200.13	1261.81± 40.77	1038.05± 47.33	953.54± 59.24
VSS (g L^{-1})	3.64	4.57± 0.08	5.64± 0.09	6.00± 0.08	3.52	4.14± 0.05	3.40± 0.04	3.26± .011	3.65	4.33± 0.07	3.97± 0.06	3.55± 0.07
SVI_{30} (mL $gTSS^{-1}$)	37.75	36.46± 0.95.	37.58± 0.68	37.98± 0.84	37.09	39.13± 0.61	59.66± 0.88	73.21± 0.70	38.15	37.68± 0.69	57.05± 2.25	68.99± 0.80
GSV (m h^{-1})	43.14	49.63± 0.86	54.28± 0.56	56.44± 0.64	41.49	48.81± 0.82	46.18± 0.59	43.86± 0.62	42.99	50.16± 0.78	47.21± 0.61	45.74± 0.86
PS (mg $gVSS^{-1}$)	24.95	24.85± 0.62	26.64± 0.43	27.50± 0.56	23.72	24.86± 0.42	24.23± 0.71	23.57± 0.41	24.54	24.55± 0.51	23.91± 0.49	24.22± 0.53
PN (mg $gVSS^{-1}$)	73.83	77.60± .068	80.08± 0.65	83.71± 0.90	74.57	74.72± 0.43	64.64± 0.92	61.07± 0.84	73.19	74.02± 0.57	67.30± 0.24	64.08± 0.27
EPS (mg $gVSS^{-1}$)	98.78	102.45± 0.91	106.72± 0.52	111.21± 1.11	98.29	99.59± 0.43	88.87± 1.49	84.63± 1.16	97.73	98.57± 0.76	91.210± 0.28	88.29± 0.43
SRT (days)	-	8.96	9.18	9.16	-	9.51	5.41	4.96	-	9.43	4.81	5.32
F/M ratio (g COD $gVSS^{-1}$ day^{-1})	0.59	0.63	0.63	0.80	0.62	0.74	1.22	1.80	0.59	0.67	0.98	1.50

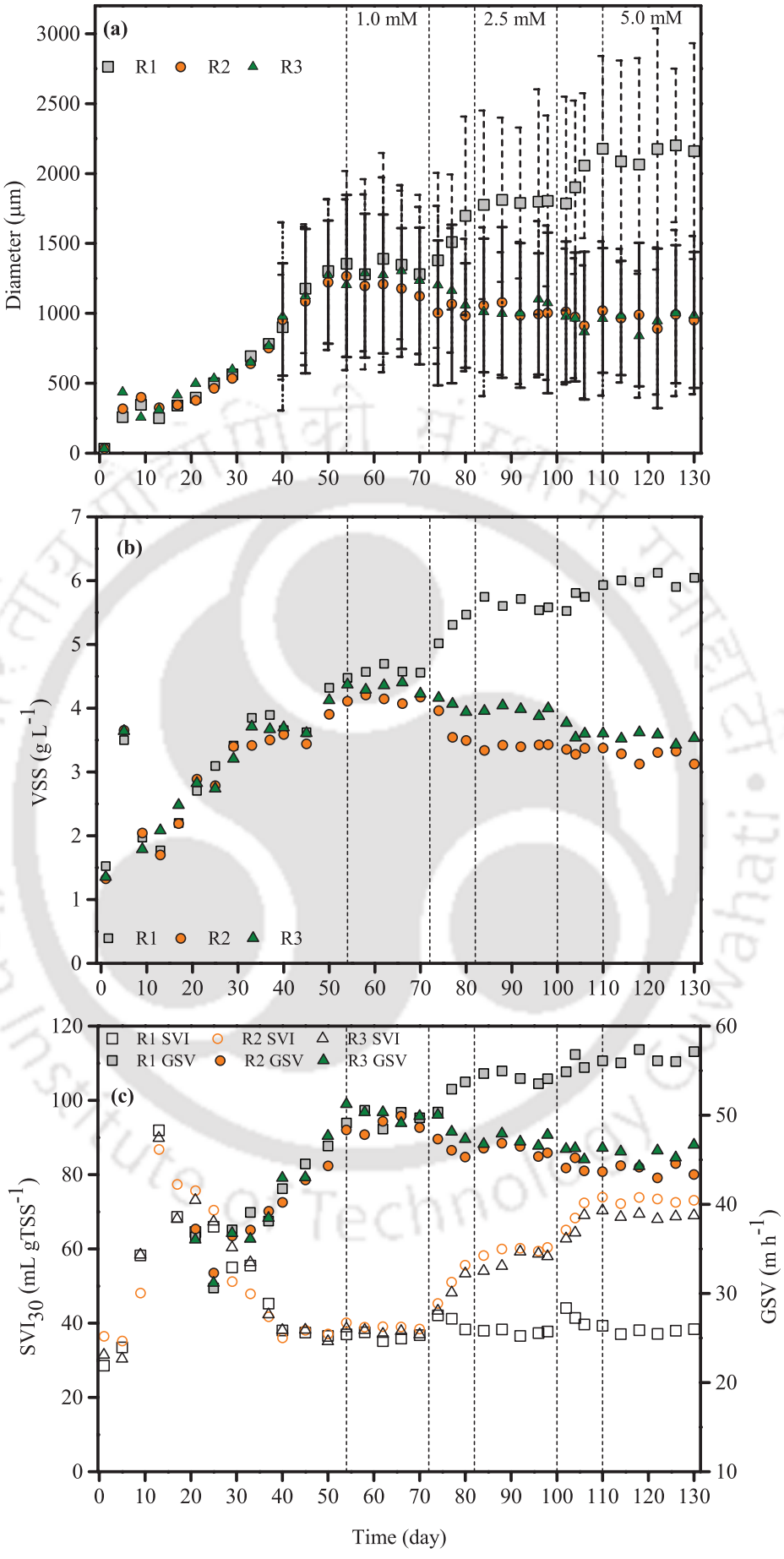

Fig. 5.3. Characteristics of granules: (a) diameter, (b) VSS and (c) SVI_{30} and GSV.

Table 5.2. From the data, it was clear that after NHCs concentrations beyond 1mM in R2 and R3, F/M ratios were more than 0.9 g COD $gVSS^{-1}$ day^{-1}. Wu et al. (2018) reported that washing out of functional microbial strains occurred due to the reduction in the settling property of the sludge at a high F/M ratio of 0.9±0.04 g COD gSS^{-1} day^{-1}. Therefore, F/M ratio beyond 0.9 g COD $gVSS^{-1}$ day^{-1} might be one of the possible reasons for worsened granular characteristics and absence of the potential of aerobic granules to degrade pollutants in R2 and R3.

5.3.2.3 Settling behaviour

Settling behaviour was determined in terms of SVI_{30} and GSV and is given in Fig. 5.3c and Table 5.2. The same phenomenon was observed with settling characteristics as was observed with granule size and VSS in all SBRs. During start-up of SBRs (day 1), the SVI_{30} values were 28.57, 36.51 and 31.42 mL $gTSS^{-1}$ in R1, R2 and R3, respectively. SVI_{30} values increased during first 15-17 days and since then, a reduction in SVI_{30} values was observed in all SBRs indicating the granulation. During 36-45 days, the SVI_{30} values were 37.75, 37.09 and 38.15 mL $gTSS^{-1}$ in R1, R2 and R3, respectively. As NHCs with a concentration of 1.0 mM were supplied to the SBRs (days 54-72), no appreciable impact on SVI_{30} was observed with values of 36.46±0.95, 39.13±0.61 and 37.68±0.69 mL $gTSS^{-1}$ in R1, R2 and R3, respectively. No significant impact on R1 SVI_{30} was observed with increase in pyridine concentrations up to 2.5 (days 82-100) and 5.0 mM (days 110-130) with SVI_{30} values of 37.58±0.68 and 37.98±0.84 mL $gTSS^{-1}$, respectively. However, AGS of R2 and R3 went under serious detrimental effect caused by the higher concentrations of indole and indole with pyridine beyond 1.0 mM and confirmed from the higher SVI_{30} values of 73.21±0.70 and 68.99±0.80 mL $gTSS^{-1}$ in R2 and R3 at 5.0 mM of indole and an equimolar mixture of pyridine and indole during 110-130 days. SVI_{30} value of R1 was quite similar to the SVI value of 35.00 mL $gTSS^{-1}$ obtained with phenol in other research work (Adav et al., 2007b).

Analysis of GSV was started from day 21 with values of 36.35, 37.24 and 36.02 m h^{-1} and increased to 43.14, 41.49 and 42.99 m h^{-1} during 39-46 days in R1, R2 and R3, respectively. With addition of 1.0 mM NHCs, GSV increased to the stable values of 49.63±0.86, 48.81±0.82 and 50.16±0.78 m h^{-1} in R1, R2 and R3, respectively, during 54-72 days. GSV values increased with an increase in pyridine concentration in R1 and reached the maximum stable value of 56.44±0.64 m h^{-1} at 5.0 mM pyridine during 110-130 days. Whereas like SVI_{30} adverse effect of indole on GSV was also observed in R2 and R3 with the concentrations beyond 1.0 mM of indole and an equimolar mixture of indole with pyridine resulting in the reduced values. At 5.0 mM concentration of indole and an equimolar mixture of indole with pyridine, the decreased values of GSV were 43.86±0.62 and 45.74±0.86 m h^{-1}, respectively, during 110-130 days. GSV values were quite higher in the current work (R1) from the study of Liu et al. (2015), who observed a GSV of 37.20±2.70 m h^{-1} with pyridine and quite similar to the work of Juang et al. (2010), who obtained a GSV of around 54.00 m h^{-1} with acetate.

Because of good settling behaviour, granular biomass could be able to retain in R1 resulting in the higher biomass concentration in R1, whereas poor settling in R2 and R3 caused the biomass washout resulting in the lower VSS.

5.3.2.4 Extracellular polymeric substances (EPS)

EPS, a sticky microbial secretion, is an important factor for entrapping bacteria together in the biofilms by making a gel-like matrix governing granule formation and stability (Zhang et al., 2007). EPS,

proteins (PN) and polysaccharides (PS) contents are given in Fig. 5.4 and Table 5.2. EPS, PN and PS contents increased from day 1 values of 21.73, 15.35 and 6.38 mg $gVSS^{-1}$ in R1, 25.52, 17.26 and 8.26 mg $gVSS^{-1}$ in R2 and 27.32, 18.59 and 8.72 mg $gVSS^{-1}$ in R3, respectively, with an increase in phenol, SCN^- and NH_4^+-N concentrations and reached to 98.78, 73.83 and 24.95 mg $gVSS^{-1}$ in R1, 98.29,

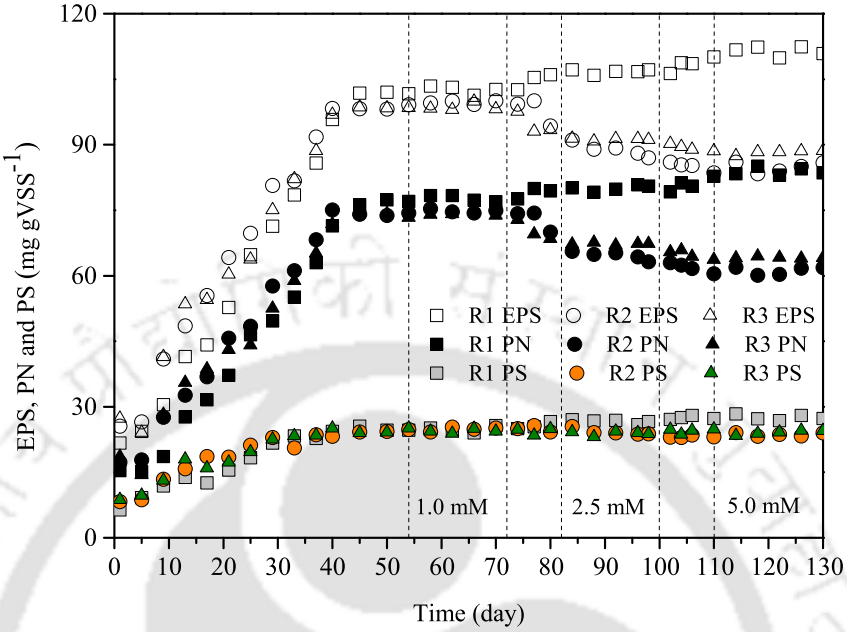

Fig. 5.4. Total EPS, PN and PS contents.

74.57 and 23.72 mg $gVSS^{-1}$ in R2 and 97.73, 73.19 and 24.54 mg $gVSS^{-1}$ in R3, respectively (days 39-46), as the concentrations of phenol, SCN^- and NH_4^+-N were increased up to the desired levels of 500,100 and 100 mg L^{-1}, respectively. Since then till the end of the study, no significant impact on PS content was observed even after the addition of NHCs up to 5.0 mM concentration in all SBRs suggesting that PS content did not play any appreciable role in maintaining granular stability. However, PN content was having a prominent impact on granulation confirmed from its value as the operation progressed in all SBRs. After the addition of 1.0 mM pyridine, indole and an equimolar mixture of pyridine and indole in R1, R2 and R3, respectively, the stabilized EPS values were 102.45±0.91, 99.59±0.43 and 98.57±0.76 mg $gVSS^{-1}$, respectively. Further increment in NHCs concentrations imparted a significant impact on EPS profiles (especially PN content) of all SBRs. As the concentration of pyridine was raised further, a slight rise in EPS concentration was observed without any inhibitory effect of pyridine up to 5.0 mM concentration on EPS. Whereas the concentrations of indole and an equimolar mixture of pyridine and indole beyond 1.0 mM imposed an inhibitory effect on EPS secretion in R2 and R3, respectively. At 5.0 mM concentration of pyridine (R1), indole (R2) and an equimolar mixture of pyridine and indole (R3), the EPS (PN) values were 111.21±1.11 (83.71±0.90), 84.63±1.49 (61.07±0.84) and 88.29±0.43 (64.08±0.27) mg $gVSS^{-1}$, respectively (days 110-130). From the results, it was clear that indole imposed a toxic effect on EPS secretion beyond 1.0 mM concentration irrespective of its presence, whether it was present alone (R2) or present with pyridine (R3).

The confocal laser scanning microscopic (CLSM) observation was done before (day 50) (Fig.5.5) and after the addition of 0.5 mM NHCs (day 120) (Fig. 5.6) to observe the distribution of total cells, dead cells, PN and PS contents. Extended fluorescence for PN and PS contents and lower fluorescence

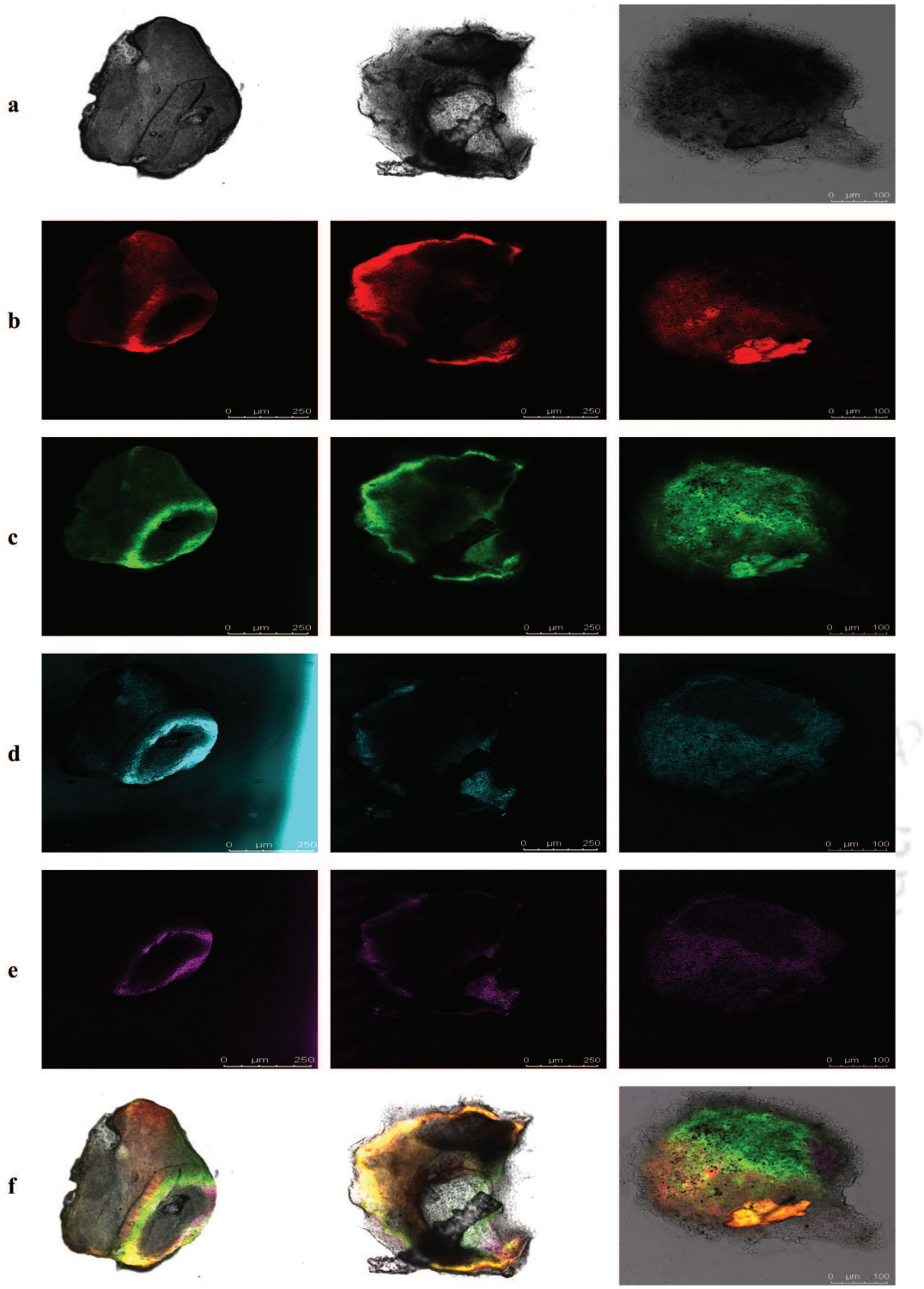

Fig. 5.5. CLSM images of R1 (Bar=100μm) and R2 and R3 (Bar=250μm) on 50th day: (a) optical microscopy photograph; (b) total cells (SYTO 63); (c) proteins (FITC); (d) polysaccharides (Con A); (e) dead cells (SYTOX Blue); (f) combined image of (b)(e).

for dead cells were detected in the granules collected from all SBRs before exposure of NHCs (day 50; Fig. 5.5). However, after the addition of NHCs, different patterns for dead cells, PN and PS contents were observed in R1, R2 and R3 (day 120; Fig. 5.6). R1 still showed an extended fluorescence for PN and PS contents, whereas reduced fluorescence for PN and PS contents was observed in R2 and R3 (Fig. 5.6).

From the granular characteristics, it was concluded that granule continued to show good

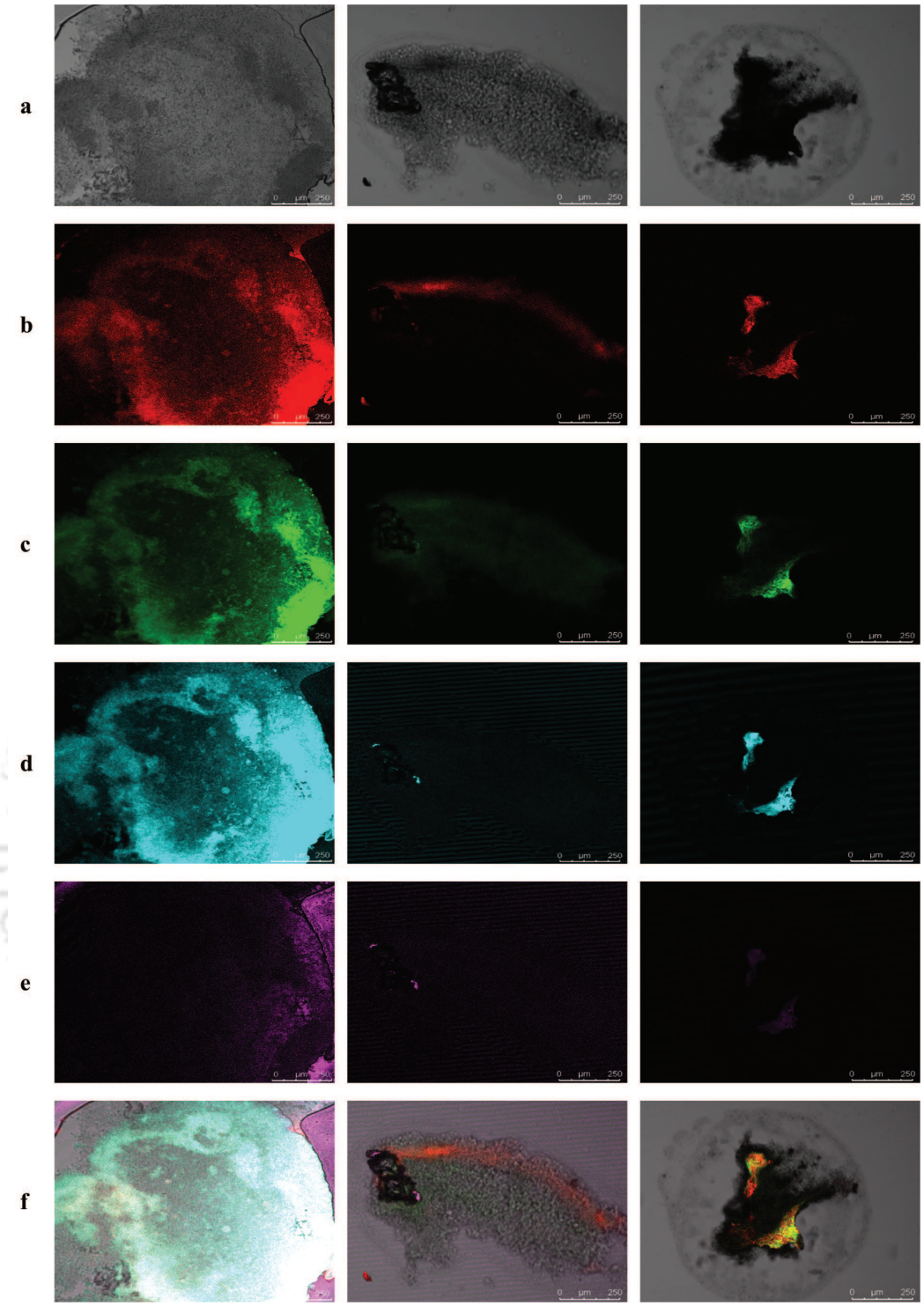

Fig. 5.6. CLSM images of R1, R2 and R3 (Bar = 250µm) on 120th day: (a) optical microscopy photograph; (b) total cells (SYTO 63); (c) proteins (FITC); (d) polysaccharides (Con A); (e) dead cells (SYTOX Blue); (f) combined image of (b)(e).

characteristics after the addition of pyridine up to 5.0 mM concentration (R1) without any inhibition. However, indole beyond 1.0 mM concentration imposed inhibitory effect on granular characteristics in R2 (alone) and R3 (present with pyridine).

5.3.3 GBA test

The basis of performing GBA was to analyze the AGS ability to biodegrade a benign substrate before and after being exposed to NHCs. GBA at different pyridine and /or indole concentrations is provided

in Table 5.3. Fig. 5.7 depicts the cumulative COD removal with time with (5.0 mM) and without addition of pyridine and/or indole. The biomass activity of refinery sludge was 6.99 mg COD removed $mgVSS^{-1}$ day^{-1}. On 50^{th} day, GBA was increased to 11.66, 13.10 and 12.23 mg COD removed $mgVSS^{-1}$ day^{-1}, in R1, R2 and R3, respectively (at this point of time, all SBRs were operated with 500 mg L^{-1} of phenol, 100 mg L^{-1} of SCN^- and 100 mg L^{-1} of NH_4^+-N). After the addition of 1.0 mM NHCs in

Table 5.3. Granular biomass activity at different pyridine and /or indole concentrations.

Pyridine and /or indole concentrations	Granular biomass activity (mg COD removed $mgVSS^{-1}$ day^{-1})		
	R1	R2	R3
0 (day 50)	11.66	13.10	12.23
1.0 mM (day 62)	14.32	13.65	13.04
5.0 mM (day 122)	15.62	4.00	4.66

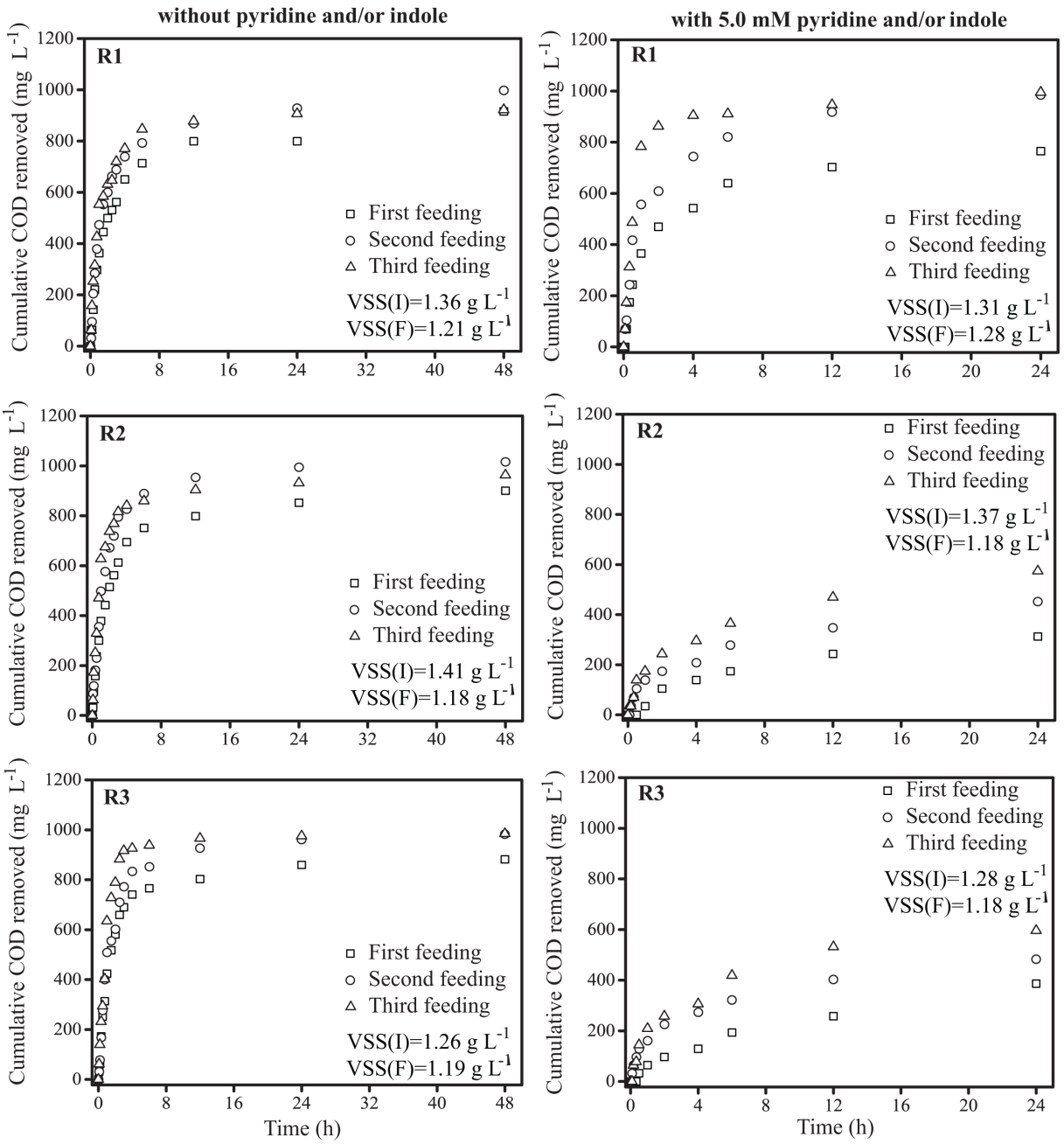

Fig. 5.7. Cumulative COD removal (mg L^{-1}) with and without pyridine and/or indole.

SBRs, an increment in GBA (Table 5.3, day 62) was observed with values of 14.32, 13.65 and 13.04 mg COD removed $mgVSS^{-1}$ day^{-1}, in R1, R2 and R3, respectively, indicating that at 1.0 mM NHCs concentration, AGS became more active than that of without NHCs (day 50). GBA of R1 AGS followed a rising trend after each increment in pyridine concentration and reached a maximum value of 15.62 mg COD removed $mgVSS^{-1}$ day^{-1} at 5.0 mM pyridine concentration indicating the enhancement in the granular activity. However, in R2 and R3, GBA decreased to 4.00 and 4.66 mg COD removed $mgVSS^{-1}$ day^{-1} (at 5.0 mM) with increase in NHCs concentration beyond 1.0 mM indicating the more inactive biomass in R2 and R3. It was also suggested from the GBA test results that indole imparted a significant inhibitory effect on the activity of granules at a concentration beyond 1.0 mM.

5.3.4 Pollutants removal profile

Pollutant removal profile with operation time is given in Table 5.4. Phenol biodegradation is given in Fig. 5.8a. Phenol biodegradation started from day 1 and continued up to a phenol concentration of 500 mg L^{-1} with ⩾99% removal efficiencies in all SBRs. During 39-46 days when influent phenol concentration was stabilized to 500 mg L^{-1}, the effluent phenol concentrations were 1.69, 1.49 and 1.03 mg L^{-1} in R1, R2 and R3, respectively. Afterward, phenol concentration was kept constant to 500 mg L^{-1} in all SBRs throughout the study. Addition of pyridine in R1, indole in R2 and an equimolar mixture of pyridine and indole in R3 with a concentration of 1.0 mM did not impose any inhibition on phenol biodegradation and all SBRs continued to exhibit phenol biodegradation with more than 99% removal efficiencies. R1 AGS exhibited its potency to biodegrade phenol (⩾99% removal efficiency) in the presence of pyridine up to a concentration of 5.0 mM (402.93±6.29 mg L^{-1}) with effluent concentration of 0.73±0.41 mg L^{-1} from the influent 500 mg L^{-1} of phenol during 110-130 days. Whereas no phenol biodegradation was observed with an increase in concentration of indole and an equimolar mixture of pyridine and indole beyond 1.0 mM in R2 and R3, respectively, with effluent values of 753.40±38.47 and 827.91±47.07 mg L^{-1} from the influent 500 mg L^{-1} of phenol (days 110-130). Higher effluent values than the influent phenol in R2 and R3 were because of the accumulation of phenol from the previous cycles. From the results (Fig. 5.8a), it was clear that sole pyridine up to 5.0 mM concentration did not cause any inhibition on phenol biodegradation (R1), whereas indole with a concentration of more than 1.0 mM inhibited the phenol biodegradation (R2) even when was present with pyridine (R3) concluding more toxicity of indole on phenol biodegradation than pyridine.

COD removal profiles for all SBRs are given in Fig.5.8b. During 39-46 days with influent 500 mg L^{-1} of phenol, COD removal was 92-94% in all SBRs from the influent COD values of 1068.79, 1084.42 and 1076.68 mg L^{-1} in R1, R2 and R3, respectively. After the addition of 1.0 mM concentration of pyridine in R1, indole in R2 and an equimolar mixture of pyridine and indole in R3 (days 54-72), the COD removal was around 93% from the influent COD values of 1430.06±33.64, 1538.49±46.13 and 1453.74±24.51 mg L^{-1} in R1, R2, and R3, respectively, indicating no inhibition on COD removal up to 1.0 mM concentration of NHCs in all SBRs. Pyridine up to a concentration of 5.0 mM did not inhibit the COD removal with around 93% COD removal efficiency from the influent COD value of 2391.37±34.50 mg L^{-1} in R1 (days 110-130). With an increase in indole concentration beyond 1.0 mM in R2 and R3, inhibition on COD removal was observed in R2 and R3 from the influent COD values of 2938.62±58.65 and 2661.10±26.40 mg L^{-1}, respectively (days 110-130). The increase in influent COD values was due to the additional COD supplied by the pyridine and indole.

The maximum desired concentration of SCN^- was 100 mg L^{-1} in all SBRs. Except first few days, complete biotransformation of SCN^- was achieved in all reactors until the addition of NHCs beyond

Table 5.4. Pollutant removal profile with operation time.

Pollutant		Operation time (day/days)											
		39-46			54-72			82-100			110-130		
		R1	R2	R3	R1	R2	R3	R1	R2	R3	R1	R2	R3
Phenol	Influent (mg L^{-1})	498.78	498.72	498.82	499.86±1.28	499.39±2.43	499.08±2.77	496.29±2.03	496.96±1.57	501.34±0.92	500.59±1.01	498.16±0.90	497.01±0.09
	Effluent (mg L^{-1})	1.69	1.49	1.03	0.73±0.81	0.56±0.35	0.57±0.31	0.81±0.66	772.43±27.62	831.19±42.07	0.73±0.41	753.40±38.47	827.91±47.07
	% removal	99.66	99.70	99.79	99.85±0.16	99.89±0.07	99.89±0.06	99.84±0.13	-55.44±5.77	-65.79±8.36	99.85±0.08	-51.23±7.64	-66.58±9.47
COD	Influent (mg L^{-1})	1068.79	1084.42	1076.68	1430.06±33.64	1538.49±46.13	1453.74±24.51	1787.50±32.81	2077.35±32.59	1953.69±42.53	2391.37±34.50	2938.62±58.65	2661.10±26.40
	Effluent (mg L^{-1})	78.11	67.59	75.75	96.02±4.05	99.85±4.09	100.13±5.88	130.40±13.59	3141.94±109.54	2622.14±142.74	166.29±14.09	4542.93±152.36	3889.93±96.52
	% removal	92.68	93.77	92.97	93.28±0.32	93.50±0.35	93.11±0.46	92.70±0.78	-51.27±5.47	-34.32±8.57	93.04±0.60	-54.68±6.87	-46.20±4.14
SCN^-	Influent (mg L^{-1})	99.83	101.39	98.47	99.16±0.31	98.48±0.96	99.07±0.21	98.40±0.54	99.75±0.85	99.21±0.02	99.77±0.60	98.42±0.40	99.02±1.03
	Effluent (mg L^{-1})	0.70	0.45	0.54	0.70±0.26	0.71±0.39	0.50±0.13	0.53±0.25	178.18±4.37	177.26±3.32	0.60±0.20	178.73±4.38	176.16±7.19
	% removal	99.3	99.56	99.45	99.30±0.26	99.28±0.40	99.49±0.13	99.46±0.25	-78.65±4.92	-78.67±3.34	99.40±0.20	-81.61±4.39	-77.90±7.05
Pyridine	Influent (mg L^{-1})	-	-	-	80.70±2.08	-	41.31±1.23	201.03±4.22	-	103.45±2.63	402.93±6.29	-	204.78±3.76
	Effluent (mg L^{-1})	-	-	-	15.14±2.27	-	5.73±1.51	33.18±1.45	-	96.01±3.12	103.62±2.40	-	267.28±9.40
	% removal	-	-	-	81.22±2.96	-	86.14±3.49	83.89±0.71	-	7.18±2.40	74.28±0.59	-	-30.57±5.50
Indole	Influent (mg L^{-1})	-	-	-	-	120.65±4.84	61.54±2.69	-	304.38±9.50	155.36±6.48	-	596.94±9.44	295.42±2.38
	Effluent (mg L^{-1})	-	-	-	-	35.72±2.25	18.21±1.80	-	336.14±8.70	185.20±11.68	-	949.71±37.41	335.48±2.97
	% removal	-	-	-	-	70.36±1.98	70.36±3.08	-	-10.48±2.67	-19.20±5.40	-	-59.11±6.24	-13.56±1.15
NH_4^+-N	Influent (mg L^{-1})	98.40	99.10	97.86	99.10±0.37	100.33±1.06	100.09±1.32	100.33±1.11	99.44±0.34	98.34±0.67	98.65±0.27	100.50±2.53	100.66±1.23
	Effluent (mg L^{-1})	15.41	12.08	14.51	0.79±0.40	0.55±0.23	0.54±0.23	0.83±0.30	168.06±11.73	176.42±11.68	1.93±0.49	173.67±11.87	172.80±13.27
	% removal	84.39	87.82	85.20	99.21±0.40	99.46±0.23	99.46±0.22	99.17±0.30	-69.00±11.68	-79.41±11.84	98.04±0.50	-72.72±9.41	-71.68±13.18

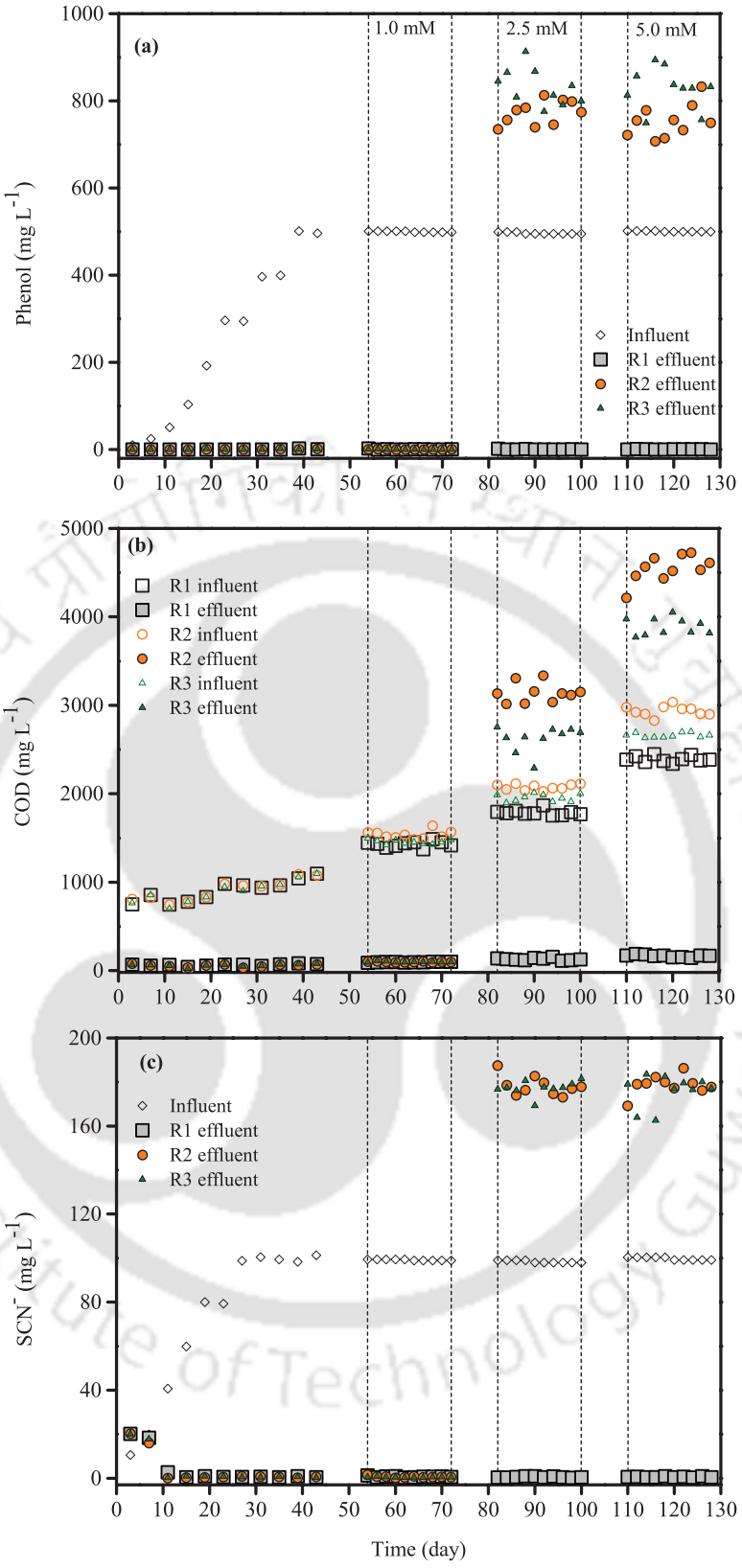

Fig. 5.8. Concentration profiles of (a) phenol, (b) COD and (c) SCN^-.

1.0 mM concentration (Fig. 5.8c). Pyridine up to 5.0 mM concentration did not inhibit the SCN^- biotransformation with more than 99% SCN^- removal efficiency (days 54-72) in R1. Presence of SO_4^{2-} was confirmed from the ion chromatogram and assured the complete biotransformation of SCN^-, though SO_4^{2-} was not monitored quantitatively. Like phenol and COD removals (Fig. 5.8a&b), the toxic effect of indole at a concentration of more than 1.0 mM on SCN^- removal was observed in

R2 and R3. During 110-130 days, at 5.0 mM concentration of indole and an equimolar mixture of pyridine and indole, effluent SCN^- values were 178.73±4.38 and 176.16±7.19 mg L^{-1} in R2 and R3, respectively, which were higher than the influent SCN^- of 100 mg L^{-1} because of the accumulation from the previous cycles. Li et al. (2011) observed a slight inhibitory effect of phenol with a concentration of 420.4 mg L^{-1} on SCN^- removal in a moving bed biofilm reactor for concurrent treatment of phenol, SCN^- and ammonium. In the current work, no inhibition on SCN^- removal was observed with a phenol concentration of 500 mg L^{-1} along with 5.0 and 1.0 mM of pyridine and indole, respectively (Fig. 5.8c) .

NHCs removal profiles are given in Fig. 5.9. Introduction of gradual addition of pyridine, indole and an equimolar mixture of both started from the 46th day onwards and reached to a concentration of 1.0 mM on day 54th in R1, R2 and R3, respectively. After addition of indole in R2 and R3, colour of R2 and R3 granules changed to the dark purple colour from the brown colour. Zhang et al. (2015) reported a purple colour product after reaction of indole with phenol hydroxylase, this might be the possible reason for the purple colour of R2 and R3 granules. Since then for next the 18 days (days 54-72), all SBRs were operated with 1.0 mM of NHCs. With a concentration of 1.0 mM, Pyridine (R1) and indole (R2) removal efficiencies were 81.22±2.96 and 70.36±1.98% from the influent pyridine (R1) and indole (R2) values of 80.70±2.08 and 120.65±4.85 mg L^{-1}, respectively. No inhibitory effect between two NHCs (R3), pyridine and indole, was observed at an equimolar concentration of 1.0 mM with removal efficiencies of 86.14±3.49 and 70.36±3.08% from the influent values of 41.31±1.23 and 61.54±2.69 mg L^{-1} for pyridine and indole, respectively. At a pyridine concentration of 2.5 mM in R1, pyridine removal was around 83% from the influent pyridine of 201.03±4.22 mg L^{-1} (days 82-100), further increment in pyridine concentration up to 5.0 mM resulted in the slight reduction in pyridine removal efficiency (74%) from the influent pyridine value of 402.93±6.29 mg L^{-1} (days 110-130). On the other hand, in R2, indole was not degraded at a concentration beyond 1.0 mM i.e., higher concentration of indole imposed inhibitory effect on its removal. At 2.5 and 5.0 mM concentrations, the effluent indole values were 336.14±8.70 and 949.71±37.41 mg L^{-1} from the influent indole values of 304.38±9.50 and 596.94±9.44 mg L^{-1}, respectively. At a concentration higher than 1.0 mM, indole not only imposed an inhibitory effect on its removal but also hampered the removal of other substrates like pyridine, phenol, SCN^- and NH_4^+-N (R3).

One possible reason for higher indole toxicity could be the nitrogenous heterocyclic and benzene ring making the indole less accessible to enzymes; however, pyridine was readily accessible because of the single ring structure (Li et al., 2001). With a concentration of 5.0 mM of an equimolar mixture of pyridine (2.5 mM; 204.78±3.76 mg L^{-1}) and indole (2.5 mM; 295.42±2.38 mg L^{-1}) in R3 (days 110-130), the effluent concentrations of pyridine and indole were 267.28±9.40 and 335.48±2.97 mg L^{-1}, respectively, which were higher than the influent because of the accumulation from the previous cycles.

The concentration profile of NH_4^+-N, NO_2^--N and NO_3^--N is given in Fig. 5.10. The maximum desired concentration of NH_4^+-N was 100 mg L^{-1} in all SBRs. Nitrifiers took around 35 days to appear in all SBRs as NH_4^+-N removal and rise in NO_2^--N were observed after 35 days of operation in all SBRs except few initial days. At 1.0 mM concentration of pyridine, indole and an equimolar mixture of pyridine and indole in R1, R2 and R3, respectively, around 99% NH_4^+-N removal was observed with effluent NO_2^--N values of 138.12±2.91, 138.55±2.61 and 138.67±1.69 mg L^{-1} in R1, R2 and R3, respectively (days 54-72). Effluent NO_3^--N values were almost negligible throughout the study in all

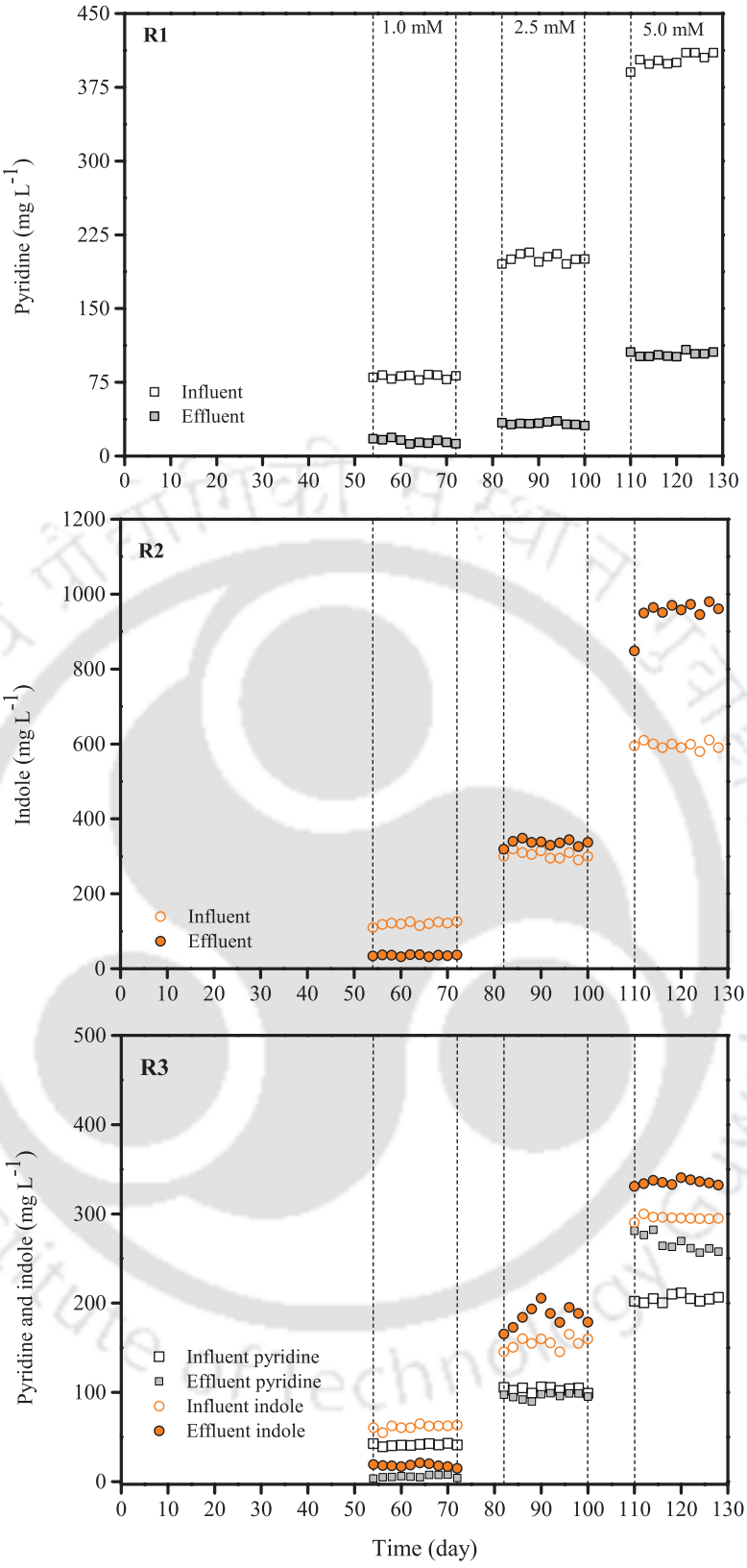

Fig. 5.9. Pyridine and/or indole concentrations in R1, R2 and R3.

SBRs, therefore were not taken into consideration. The possible reason for the absence of complete nitrification was SRT. During 54-72 days, SRT values were 8.96, 9.51 and 9.43 days in R1, R2 and R3, respectively, which were less than the values required for achieving complete nitrification (10-30 days) (Tchobanoglous et al., 2003). Hence, only nitritation process was observed in all SBRs during 54-72 days. Transformation of SCN^- also provided additional NH_4^+-N to the SBRs (Equation 2.6). In

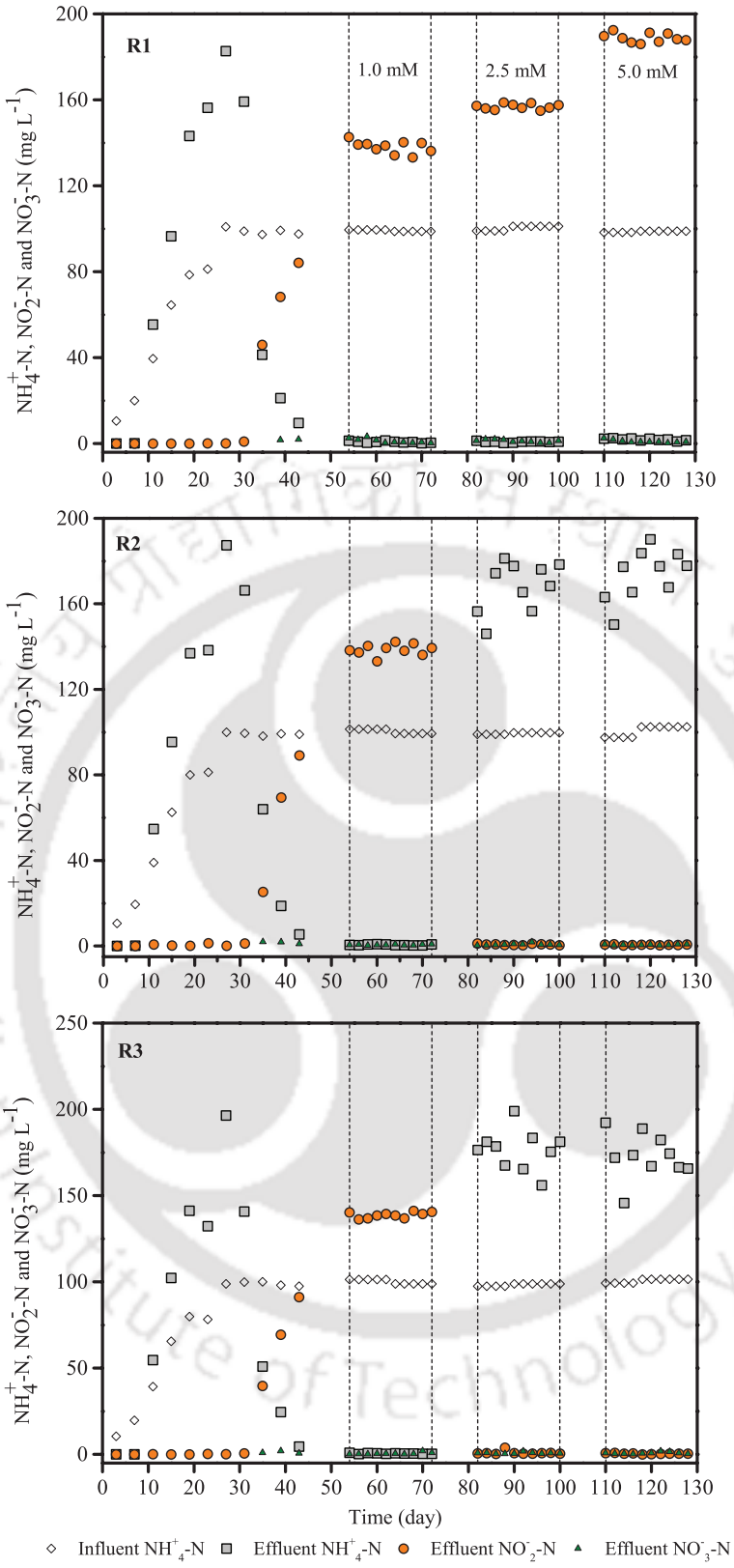

Fig. 5.10. Concentration profiles of NH_4^+-N, NO_2^--N and NO_3^--N.

addition, NHCs biodegradation was accompanied by the ammonium generation (Liu et al., 2018), though ammonia generation through the biodegradation of NHCs was not quantified. Therefore, both SCN^- biotransformation and NHCs biodegradation contributed to NH_4^+-N along with 100 mg L^{-1} of influent NH_4^+-N. NH_4^+-N generated from SCN^- biotransformation and NHCs biodegradation also transformed into NO_2^--N, this might be the possible reason for getting around 138 mg L^{-1} of NO_2^--N

from influent 100 mg L- of NH_4^+-N. R1 granules continued to transform NH_4^+-N into NO_2^--N with the increase in pyridine concentration up to 5.0 mM with around 98% NH_4^+-N removal efficiency (1.93±0.49 mg L^{-1} of effluent NH_4^+-N). During 110-130 days in R1, the effluent NO_2^--N value was 188.93±2.13 mg L^{-1} with an SRT value of 9.16 days. The possible reason for higher effluent NO_2^--N in R1 was the transformation of NH_4^+-N generated from SCN^- biotransformation and pyridine biodegradation into NO_2^--N and also could be due to the accumulation from the previous cycles. Inhibition on NH_4^+-N removal was observed in R2 and R3, as the concentrations of indole and an equimolar mixture of pyridine and indole were raised to beyond 1.0 mM. During days 110-130 days at 5.0 mM concentration of indole and an equimolar mixture of pyridine and indole, effluent NO_2^--N values were 0.63±0.17 and 0.52±0.25 mg L^{-1} with SRT values of 4.96 and 5.32 days in R2 and R3, respectively, indicating the absence of nitrification. During those days (days 110-130), effluent NH_4^+-N values were 173.67±11.87 and 172.80±13.27 mg L^{-1} in R2 and R3, respectively, which were higher from the influent value of 100 mg L^{-1} because of the accumulation of NH_4^+-N from the previous cycles. Like other pollutants, indole beyond 1.0 mM concentration inhibited NH_4^+-N removal irrespective of its presence (alone or with other substrates).

Liu et al. (2015) observed granulation with a pyridine concentration of 500-4000 mg L^{-1} in an SBR using pure bacterial culture capable of degrading pyridine as an inoculum. Pyridine degradation up to a concentration of 3000 mg L^{-1} was also reported using pyridine-degrading strains in an SBR (Liang et al., 2018). Liu et al. (2018) achieved aerobic granulation for treating 1500 mg L^{-1} of pyridine and nitrogen simultaneously in an SBR. No study on indole removal by AGS is reported so far. In current work, R1 AGS showed the potential to degrade pyridine up to concentration of 402.93±6.29 mg L^{-1} along with phenol, SCN^- and NH_4^+-N. In addition, degradation of 120.65±4.84 mg L^{-1} of indole (R2) and simultaneous degradation of pyridine (41.31±1.23 mg L^{-1}) and indole (61.54±2.69 mg L^{-1}) along with 500 mg L^{-1} of phenol, 100 mg L^{-1} of SCN^- and 100 mg L^{-1} of NH_4^+-N (R3) was also achieved by mixed culture. No inhibition phenomenon among all the pollutants was observed up to the NHCs concentration of 1.0 mM.

5.4 Conclusion

R1 AGS demonstrated a significant potential to biodegrade pyridine up to a concentration of 5.0 mM (402.93±6.29 mg L^{-1}) along with 500 mg L^{-1} of phenol, 100 mg L^{-1} of SCN^- and 100 mg L^{-1} of NH_4^+-N without any inhibition phenomenon among the pollutants and exhibited good granular characteristics as well. However, indole beyond 1.0 mM concentration imposed a toxic and inhibitory effect on granular characteristics and other pollutant removals (R2). Simultaneous removal of pyridine and indole was achieved with 1.0 mM concentration of an equimolar mixture of pyridine and indole along with phenol, SCN^- and NH_4^+-N in R3. Therefore, the current study provides an alternative approach to treat wastewater in which pyridine, indole, ammonium, phenol and thiocyanate coexist.

References

Adav, S.S., Lee, D.J., Ren, N., 2007a. Biodegradation of pyridine using aerobic granules in the presence of phenol. Water Research 41, 2903-2910.

Adav, S.S., Lee, D.J., Show, K.Y., Tay, J.H., 2008. Aerobic granular sludge: Recent advances. Biotechnology Advances 26, 411-423.

Adav, S.S., Lee, D.J., Lai, J., 2007b. Effects of aeration intensity on formation of phenol-fed aerobic granules and extracellular polymeric substances. Applied Microbiology and Biotechnology 77,

175-182.
Bai, Y., Sun, Q., Sun, R., Wen, D., Tang, X., 2011. Bioaugmentation and adsorption treatment of coking wastewater containing pyridine and quinoline using zeolite-biological aerated filters. Environmental Science & Technology 45, 1940-1948.
Chen, Y., Xie, X.G., Ren, C.G., Dai, C.C., 2013. Degradation of N-heterocyclic indole by a novel endophytic fungus *Phomopsis liquidambari*. Bioresource Technology 129, 568-574.
Goswami, L., Kumar, R.V., Manikandan, N.A., Pakshirajan, K., Pugazhenthi, G., 2017. Simultaneous polycyclic aromatic hydrocarbon degradation and lipid accumulation by *Rhodococcus opacus* for potential biodiesel production. Journal of Water Process Engineering 17, 1-10.
Hammouda, S.B., Adhoum, N., Monser, L., 2016. Chemical oxidation of a malodorous compound, indole, using iron entrapped in calcium alginate beads. Journal of Hazardous Materials 301, 350-361.
Higashio, Y., Shoji, T., 2004. Heterocyclic compounds such as pyrrole, pyridines, pyrrolidine, piperidine, indole, imidazol and pyrazines. Applied Catalysis A: General 260, 251-259.
Jemaat, Z., Suárez Ojeda, M.E., Pérez, J., Carrera, J., 2013. Simultaneous nitritation and *p*-nitrophenol removal using aerobic granular biomass in a continuous airlift reactor. Bioresource Technology 150, 307-313.
Jemaat, Z., Suárez Ojeda, M.E., Pérez, J., Carrera, J., 2014. Partial nitritation and *o*-cresol removal with aerobic granular biomass in a continuous airlift reactor. Water Research 48, 354-362.
Jiang, Y., Wei, L., Yang, K., Shi, X., Wang, H., 2017. Rapid formation of aniline-degrading aerobic granular sludge and investigation of its microbial community succession. Journal of Cleaner Production 166, 1235-1243.
Juang, Y.C., Adav, S.S., Lee, D.J., Tay, J.H., 2010. Stable aerobic granules for continuous-flow reactors: Precipitating calcium and iron salts in granular interiors. Bioresource Technology 101, 8051-8057.
Kim, Y.M., Park, D., Lee, D.S., Park, J.M., 2008. Inhibitory effects of toxic compounds on nitrification process for cokes wastewater treatment. Journal of Hazardous Materials 152, 915-921.
Li, H.Q., Han, H.J., Du, M.A., Wang, W., 2011. Removal of phenols, thiocyanate and ammonium from coal gasification wastewater using moving bed biofilm reactor. Bioresource Technology 102, 4667-4673.
Li, N., Lu, X., Zhang, S., 2014. A novel reuse method for waste printed circuit boards as catalyst for wastewater bearing pyridine degradation. Chemical Engineering Journal 257, 253-261.
Li, Y., Gu, G., Zhao, J., Yu, H., 2001. Anoxic degradation of nitrogenous heterocyclic compounds by acclimated activated sludge. Process Biochemistry 37, 81-86.
Liang, J., Li, W., Zhang, H., Jiang, X., Wang, L., Liu, X., Shen, J., 2018. Coaggregation mechanism of pyridine-degrading strains for the acceleration of the aerobic granulation process. Chemical Engineering Journal 338, 176-183.
Liang, Z., Tu, Q., Su, X., Yang, X., Chen, J., Chen, Y., Liu, C., Li, H., He, Q., 2019. Formation, extracellular polymeric substances and microbial community of aerobic granules enhanced by microbial flocculant compared with poly-aluminum chloride. Journal of Cleaner Production 220, 544-552.
Liu, X., Chen, Y., Zhang, X., Jiang, X., Wu, S., Shen, J., Sun, X., Li, J., Lu, L., Wang, L., 2015. Aerobic granulation strategy for bioaugmentation of a sequencing batch reactor (SBR) treating high strength pyridine wastewater. Journal of Hazardous Materials 295, 153-160.
Liu, X., Wu, S., Zhang, D., Shen, J., Han, W., Sun, X., Li, J., Wang, L., 2018. Simultaneous pyridine biodegradation and nitrogen removal in an aerobic granular system. Journal of Environmental Sciences 67, 318-329.
Moy, B., Tay, J., Toh, S., Liu, Y., Tay, S., 2002. High organic loading influences the physical characteristics of aerobic sludge granules. Letters in Applied Microbiology 34, 407-412.
Pillai, I.M.S., Gupta, A.K., 2016. Anodic oxidation of coke oven wastewater: Multiparameter optimization for simultaneous removal of cyanide, COD and phenol. Journal of Environmental Management 176, 45-53.
Ramos, C., Suárez Ojeda, M.E., Carrera, J., 2015. Long-term impact of salinity on the performance and microbial population of an aerobic granular reactor treating a high-strength aromatic wastewater.

Bioresource Technology 198, 844-851.
Sahariah, B.P., Chakraborty, S., 2011. Kinetic analysis of phenol, thiocyanate and ammonia-nitrogen removals in an anaerobicanoxicaerobic moving bed bioreactor system. Journal of Hazardous Materials 190, 260-267.
Sarker, M., Song, J.Y., Jeong, A.R., Min, K.S., Jhung, S.H., 2018. Adsorptive removal of indole and quinoline from model fuel using adenine-grafted metal-organic frameworks. Journal of Hazardous Materials 344, 593-601.
Sguanci, S., Lubello, C., Caffaz, S., Lotti, T., 2019. Long-term stability of aerobic granular sludge for the treatment of very low-strength real domestic wastewater. Journal of Cleaner Production 222, 882-890.
Shi, J., Xu, C., Han, Y., Han, H., 2019. Enhanced anaerobic biodegradation efficiency and mechanism of quinoline, pyridine, and indole in coal gasification wastewater. Chemical Engineering Journal 361, 1019-1029.
Sun, J.Q., Xu, L., Tang, Y.Q., Chen, F.M., Liu, W.Q., Wu, X.L., 2011. Degradation of pyridine by one *Rhodococcus* strain in the presence of chromium (VI) or phenol. Journal of Hazardous Materials 191, 62-68.
Tchobanoglous, G., Burton, F.L., Stensel, H.D., Metcalf, Eddy, 2003. Wastewater Engineering: Treatment and Reuse, fourth ed. McGraw Hill Education, India.
Vázquez, I., Rodríguez, J., Marañón, E., Castrillón, L., Fernández, Y., 2006. Simultaneous removal of phenol, ammonium and thiocyanate from coke wastewater by aerobic biodegradation. Journal of Hazardous Materials 137, 1773-1780.
Wang, J., Jiang, X., Liu, X., Sun, X., Han, W., Li, J., Wang, L., Shen, J., 2018. Microbial degradation mechanism of pyridine by *Paracoccus* sp. NJUST30 newly isolated from aerobic granules. Chemical Engineering Journal 344, 86-94.
Wang, W., Han, H., Yuan, M., Li, H., Fang, F., Wang, K., 2011. Treatment of coal gasification wastewater by a two-continuous UASB system with step-feed for COD and phenols removal. Bioresource Technology 102, 5454-5460.
Wei, X.X., Zhang, Z.Y., Fan, Q.L., Yuan, X.Y., Guo, D.S., 2012. The effect of treatment stages on the coking wastewater hazardous compounds and their toxicity. Journal of Hazardous Materials 239, 135-141.
Wu, D., Zhang, Z., Yu, Z., Zhu, L., 2018. Optimization of F/M ratio for stability of aerobic granular process via quantitative sludge discharge. Bioresource Technology 252, 150-156.
Yang, S.F., Tay, J.H., Liu, Y., 2003. A novel granular sludge sequencing batch reactor for removal of organic and nitrogen from wastewater. Journal of Biotechnology 106, 77-86.
Zhang, L., Feng, X., Zhu, N., Chen, J., 2007. Role of extracellular protein in the formation and stability of aerobic granules. Enzyme and Microbial Technology 41, 551-557.
Zhang, X., Qu, Y., Ma, Q., Zhang, Z., Li, D., Wang, J., Shen, W., Shen, E., Zhou, J., 2015. Illumina MiSeq sequencing reveals diverse microbial communities of activated sludge systems stimulated by different aromatics for indigo biosynthesis from indole. PLoS One 10, e0125732.
Zhu, H., Han, Y., Ma, W., Han, H., Ma, W., 2017. Removal of selected nitrogenous heterocyclic compounds in biologically pretreated coal gasification wastewater (BPCGW) using the catalytic ozonation process combined with the two-stage membrane bioreactor (MBR). Bioresource Technology 245, 786-793.
Zhu, Q., Moggridge, G.D., DAgostino, C., 2016. Adsorption of pyridine from aqueous solutions by polymeric adsorbents MN 200 and MN 500. Part 2: Kinetics and diffusion analysis. Chemical Engineering Journal 306, 1223-1233.

The environmental crisis is a global problem, and only global action will resolve it.

Barry Commoner (1917-2012)
American cellular biologist

6

Conclusions and Future Scope

This chapter summarizes the major conclusions of the research work and key findings of all objectives accomplished along with the limitations associated with the current study. The current chapter also provides recommendations for future research.

6.1 Major conclusions

Aerobic granules were successfully developed during all phases and major conclusions from the study are mentioned below.

- Large granules (D50 of 1334.24±30.56 µm) with higher biomass concentration (4.31±0.40 g L^{-1}) were observed at 6 h cycle time (OLR of 2.03 kg COD m^{-3} day^{-1}).
- Air flow rate of 2.5 L min^{-1} was found to be best in terms of both reactor performance and granular characteristics.
- Mature granules were rapidly developed only in 40 days with the combination of refinery sludge and phenol along with excellent granular characteristics.
- Rapid granulation was considered as a function of substrate and inoculum combination.
- Addition of SCN^- showed a significant effect on the reformation of the granules by triggering the more EPS secretion, which induced the granule agglomeration by forming a gel-like network.
- Reformation by SCN^- addition provided a strategy to reduce the start-up time required for the formation of granules after disintegration from scratch.
- Granules obtained from brewery sludge showed better granular characteristics and were able to tolerate higher OLR of 5.71 kg COD m^{-3} day^{-1} than the granules developed from refinery sludge.
- Pollutant tolerance was independent of rapid granulation.
- A negative impact of indole on AGS with a concentration of more than 1.0 mM was observed. On the other hand, AGS was able to treat sole pyridine up to a concentration of 5.0 mM.

6.2 Key findings

Key findings of each objective are given below.

Chapter 2

- *Cycle time*
  - Excellent granular characteristics were observed at a cycle time of 6 h, whereas an increase

in cycle time (12 and 24 h) caused the granule deterioration resulting in the smaller granule size (520.94±343.18 and 97.93±4.21 μm, respectively).

- SVI could not be a sole crucial factor in determining the settleability of aerobic granules.
- Almost two-fold increment in EPS content (44.36 to 79.65 mg $gVSS^{-1}$) was observed with four times reduction in cycle time (24 to 6 h).
- Independence of pollutant removals from the aerobic granulation was observed.
- Up-flow liquid velocity of 2.5 m h^{-1} was found suitable for achieving better granulation.

❋ *Air flow rate*

- Larger granules (2938.67±64.91 μm) with higher biomass concentration (4.17±0.09 g L^{-1}) were observed at 2.5 L min^{-1} air flow rate (R2).
- With a decrease (1.5 L min^{-1}) and an increase (3.5 L min^{-1}) in the air flow rate, both granule characteristics and reactor performance deteriorated.
- Loose and porous granules were detected at lower air flow rate (R1, 1.5 L min^{-1}), whereas higher air flow rate (R3, 3.5 L min^{-1}) triggered the biomass washout.
- CLSM imaging illustrated the extended fluorescence for active biomass, proteins and polysaccharides in R2 granules; however, a higher portion of dead cells in R3 granules.
- Removal efficiencies of 99, 98 and 95% were observed for phenol, thiocyanate and COD, respectively, at 2.5 L min^{-1} air flow rate.
- R2 granules showed partial nitrification, while R1 and R3 granules did not exhibit any NH_4^+-N removal.

Chapter 3

❋ *Rapid granulation*

- Rapid granulation with a combination of refinery sludge as an inoculum and phenol as a substrate (R1) was achieved only in just 40 days, whereas the combination of refinery sludge and sodium acetate (R2) required around 50 days for the maturation of granules.
- R1 granules showed better granular characteristics (average granule size, biomass concentration and EPS content of 1123.60±113.55 μm, 3.65±0.09 g L^{-1} and 77.26±1.13 mg $gVSS^{-1}$, respectively) as compared to R2 granules.
- No impact of the combination of seed sludge with different substrates on phenol and ammonia-nitrogen removal was observed.

❋ *Granule reformation*

- Reformulation of granules from the deteriorated one was observed after the addition of toxic pollutant (SCN^-), not by the addition of any supplementary material.
- Reformed granules illustrated better characteristics (average granule size and EPS content of 1819.87±43.44 μm and 101.45±1.06 mg $gVSS^{-1}$, respectively) than the granules formed before disintegration (average granule size and EPS content of 1202.03±487.78 μm and 78.23 mg $gVSS^{-1}$, respectively).

- The addition of toxic SCN^- provoked the EPS secretion, thus promoting the granular integrity.
- Phenol removal remained unaffected from the granule disintegration with around 99% removal efficiency throughout the study.
- Nitritation efficiency of aerobic granules recovered after the reformation.
- No inhibitory effect of SCN^- up to 340 mg L^{-1} was observed on granular characteristic and reactor performance.

Chapter 4

- R2 granules, developed from the brewery sludge, showed better granular characteristics (average granule size, biomass concentration and EPS content of 2769.94±62.26 μm, 7.12±0.16 g L^{-1} and 114.83±1.33 mg $gVSS^{-1}$, respectively) for treating high phenol load of 5.71 kg COD m^{-3} day^{-1} despite being matured in 50 days as compared to granules developed from the refinery sludge (R1) in 40 days.
- R1 granules started to deteriorate at an OLR of more than 3.32 kg COD m^{-3} day^{-1}, whereas granules of R2 were able to withstand up to an OLR of 5.71 kg COD m^{-3} day^{-1}.
- OLR of more than 3.32 kg COD m^{-3} day^{-1} limited the pollutant removal profiles in R1; however, R2 granules continued to demonstrate better removal profiles for phenol, COD, SCN^- and NH_4^+-N up to 5.71 kg COD m^{-3} day^{-1} loading.
- At higher load of 5.71 kg COD m^{-3} day^{-1}, R1 granules became inactive with granular biomass activity value of 3.43 mg COD removed $mgVSS^{-1}$ day^{-1}, whereas R2 granules were at their maximum activity value of 16.35 mg COD removed $mgVSS^{-1}$ day^{-1}.
- CLSM imaging also revealed a more dead portion in R1 at higher phenol loading.

Chapter 5

- Granules were successfully cultivated with 1.0 mM concentration of pyridine and/or indole along with phenol (500 mg L^{-1}), SCN^- (100 mg L^{-1}) and NH_4^+-N (100 mg L^{-1}) and exhibited good granular properties and reactor performance in terms of pollutant removal.
- Indole was found more toxic to the granules because of the toxicity imparted by indole on granules at a concentration beyond 1.0 mM irrespective of its presence (only NHC or with pyridine) resulting in the deterioration of granular characteristics and reactor performance (R2 and R3).
- Pyridine, when was the only NHC in the reactor (R1), continued to exhibit better granular characteristics and pollutant removal efficiencies up to 5.0 mM concentration.
- Granular biomass activity data revealed more inactivity of granular biomass at 5.0 mM concentration of indole (R2) and an equimolar mixture of pyridine and indole (R3) with values of 4.00 and 4.66 mg COD removed $mgVSS^{-1}$ day^{-1}, respectively, as compared to more active biomass at 5.0 mM pyridine (R1) with activity value of 15.62 mg COD removed $mgVSS^{-1}$ day^{-1}.

6.3 Limitations

- SBRs require frequent cleaning during start-up time because of the microbial growth on the walls of the SBRs. Therefore operation is labor intensive during starting phase.
- Air stones need to be replaced once in a month to maintain uniform air bubbling throughout the reactor as they get clogged by biomass, which may cause a slight increase in maintenance cost.
- Long start-up period for granule maturation.

6.4 Scope for future work

- Treatment of wastewater containing a high amount of ammonia-nitrogen along with other recalcitrant compounds.
- Identification of microbial community of aerobic granules developed for treating refractory compounds.
- Treatment of real coal gasification wastewater by aerobic granulation.
- Effect of pollutant shock loadings on aerobic granulation.
- Concurrent removal of aromatic, inorganics and NHCs by aerobic granulation in continuous flow reactor.

Appendix-I

List of instruments used in the present study

Instruments	Parameters tested/ measured	Model/ manufacturer/specification
Air compressor	To provide aeration into the reactor	Tarsons Rockwac 420
Centrifuge	Separation of suspended solids	Remi CM-8 plus, India
COD digester	COD	HACH, USA
Confocal laser scanning microscopy (CLSM)	CLSM imaging	Leica TCS SP8, Leica, Germany
Digital pH meter	pH	Systronics, India
DO meter	DO	LBOD101, Hach, USA
Electronic balance	Weight of chemicals	KERN, USA
Field emission scanning electron microscopy	Granule morphology	Zeiss, Sigma, Germany
High performance liquid chromatography (HPLC)	Pyridine and indole	Prostar 210, Varian, USA
Hot air blower	To maintain temperature	Usha, India
Hot air oven	TSS and drying	ICT, India
Ion chromatography	NO_3^-- N analysis	792 Basic IC, Metrohm, Switzerland
Laser particle size analyser	Measuring granule size	Mastersizer 2000, Malvern instruments, UK
Microtome	Granule sectioning	RM 2245, Leica, Germany
Muffle furnace	VSS	Multispan, India
Peristaltic pumps	Feeding of media to the reactor	Miclins, India
Refrigerator	Sample storage at 4 řC	Labocon LMR-102
Rotameter	To control the airflow in the reactor	CVG technocrafts, Mumbai, India
Spinix-vortex-shaker	To break the granules or to homogenize the samples	Tarsons, India
Visible spectrophotometer	Phenol, NH_4^+-N, NO_2^--N, SCN^-, PN and PS	Systronics, India
Water bath	Heat treatment to granules and protein analysis	ICT, India
Water purification system	To provide Millipore and milli-Q water	Merck, Germany

Appendix-II

Linear calibration curves

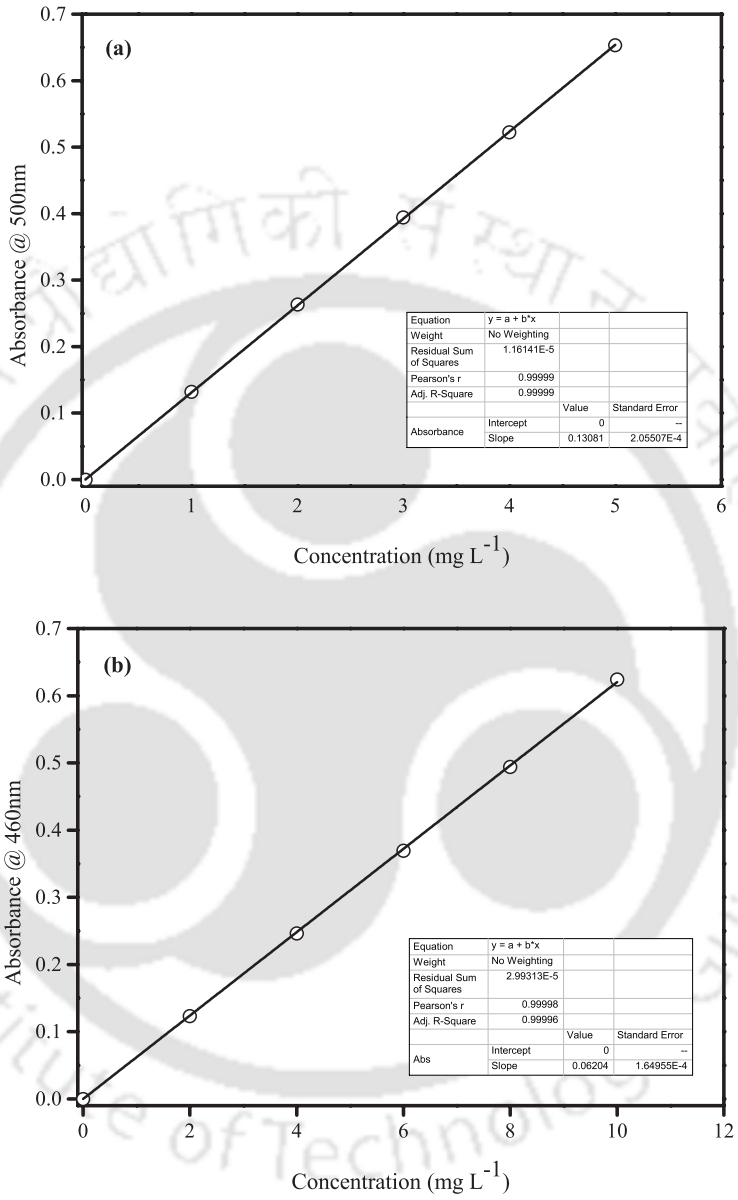

Fig. AII.1. Linear calibration curves for the analysis of (a) Phenol and (b) Thiocyanate

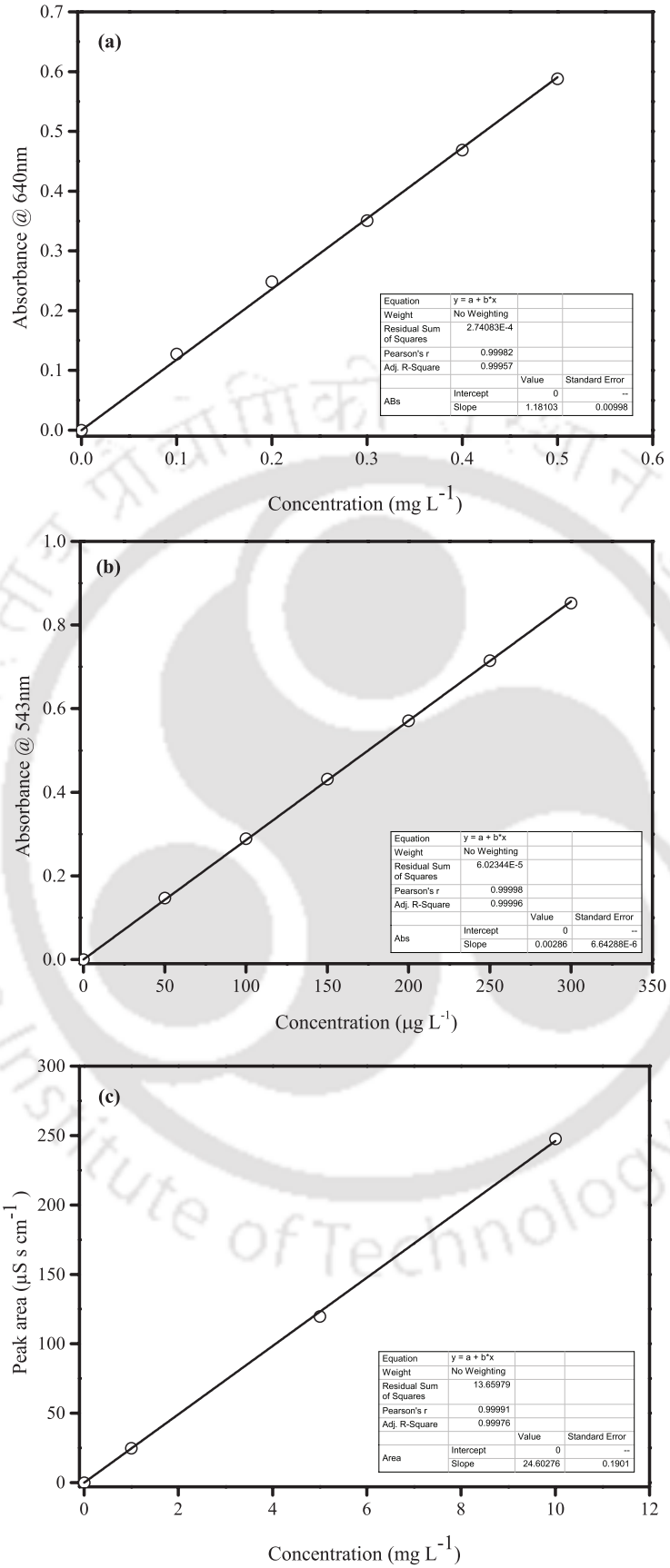

Fig. AII.2. Linear calibration curves for the analysis of (a) Ammonia-nitrogen (b) Nitrite-nitrogen and (c) Nitrate-nitrogen.

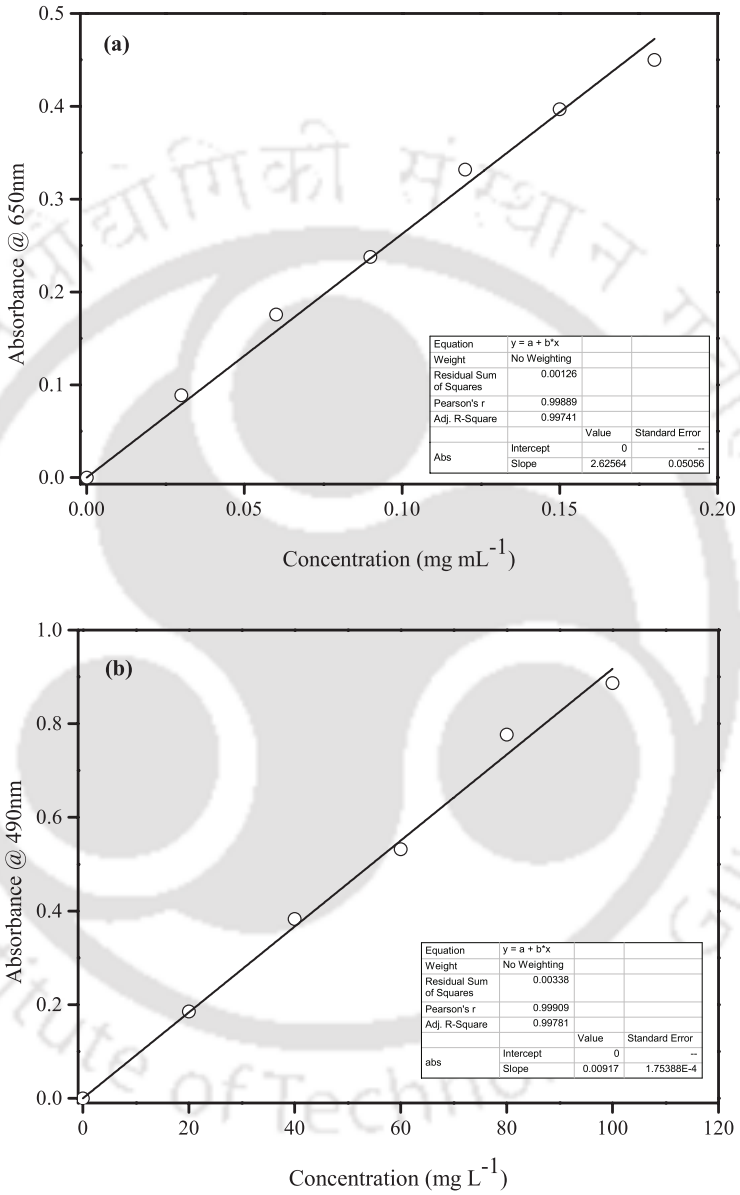

Fig. AII.3. Linear calibration curves for the analysis of (a) Proteins and (b) Polysaccharides.

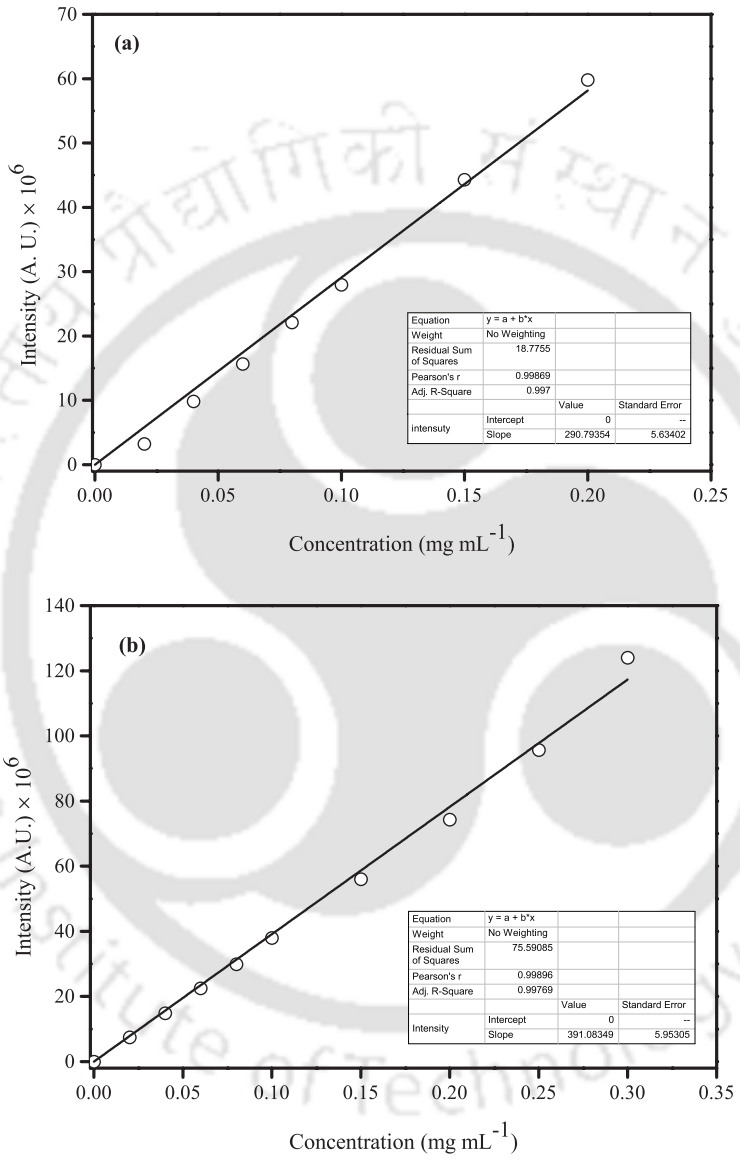

Fig. AII.4. Linear calibration curves for the analysis of (a) Pyridine and (b) Indole.

List of Publications

Published articles

- **Tomar, S. K.**, Chakraborty, S., 2020. Impact of high phenol loading on aerobic granules from two different kinds of industrial sludge along with thiocyanate and ammonium. Bioresource Technology 315, 123824.
- **Tomar, S. K.**, Chakraborty, S., 2020. Impact of thiocyanate on the reformation of aerobic granules from the disintegrated granules treating phenol-contained wastewater along with the recovery of nitritation efficiency. Journal of Water Process Engineering 36, 101260.
- **Tomar, S. K.**, Chakraborty, S., 2019. Comparison of rapid granulation developed from the same industrial sludge with two different substrates. International Biodeterioration & Biodegradation 142, 218-226.
- **Tomar, S. K.**, Chakraborty, S., 2018. Effect of air flow rate on development of aerobic granules, biomass activity and nitrification efficiency for treating phenol, thiocyanate and ammonium. Journal of Environmental Management 219, 178-188.
- **Tomar, S. K.**, Chakraborty, S., 2018. Characteristics of aerobic granules treating phenol and ammonium at different cycle time and up flow liquid velocity. International Biodeterioration & Biodegradation 127, 113-123

Articles (submitted/under preparation)

- **Tomar, S. K.**, Kumar, R., Chakraborty, S., 2020. Simultaneous biodegradation of pyridine, indole and ammonium along with phenol and thiocyanate by aerobic granular sludge. (submitted in Chemosphere)
- **Tomar, S. K.**, Chakraborty, S. A review on aerobic granulation. (under preparation)

Book chapter

- **Tomar, S. K.**, Chakraborty, S., 2019. Performance of an Aerobic Granular Reactor Treating Organics and Ammonia Nitrogen with Time. Wastewater Reuse and Watershed Management: Engineering Implications for Agriculture, Industry, and the Environment, 13, Apple Academic Press.

Conferences

- **Tomar, S.K.**, Chakraborty, S., 2018. Impact of thiocyanate (SCN^-) on granular characteristics after disintegration of granules. Third International Conference on Sustainable Energy and Environmental Challenges (3rd SEEC), December 18-21, Indian Institute of Technology Roorkee, India. (Oral presentation)
- **Tomar, S.K.**, Chakraborty, S., 2018. Comparison of granule characteristics developed from same inoculum sludge with two different substrates in sequencing batch rectors. International Conference on Bioprocess for Sustainable Environment and Energy (ICBSEE-2018), December

6-7, National Institute of Technology Rourkela, Odisha, India. (Poster presentation) ***(Most Innovative Technology Award)***

- **Tomar, S.K.**, Chakraborty, S., 2018. Impact of low concentration of phenol on aerobic granular sludge. Recycle 2018, International Conference on Waste Management, February 22-24, Indian Institute of Technology Guwahati, Guwahati, India. (Oral presentation)
- **Tomar, S.K.**, Chakraborty, S., 2018. Performance of aerobic granular reactor treating organics and ammonia nitrogen with time. International Conference on Water and Wastewater Management and Modelling, January 16-17, Central University of Jharkhand, Ranchi, India. (Oral presentation)
- **Tomar, S.K.**, Chakraborty, S., 2017. Profile sampling of aerobic granular reactor treating organics and ammonia nitrogen. Bioprocessing India 2017, Recent Trends in Bioprocessing for Healthcare, Energy and Environment, December 9-11, Indian Institute of Technology Guwahati, Guwahati, India. (Oral presentation)
- **Tomar, S.K.**, Chakraborty, S., 2016. Effect of thiocyanate (SCN^-) on aerobic granulation for treating phenol and ammonia nitrogen rich wastewater in a sequential batch reactor (SBR). International Conference on Current Trends in Biotechnology (ICCB-2016), December 8-10, VIT University, Vellore, India. (Poster presentation)
- **Tomar, S.K.**, Chakraborty, S., 2016. Aerobic granulation: An encouraging environmental technology for wastewater treatment. Recycle 2016, International Conference on Waste Management, April 1-2, Indian Institute of Technology Guwahati, Guwahati, India. (Poster presentation)